N 70 16465

NASA CR-72606

# INVESTIGATION OF DEEP FLAWS IN THIN WALLED TANKS



By

J. N. Masters, W. P. Haese and R. W. Finger

Prepared for

NATIONAL AERONAUTICS & SPACE ADMINISTRATION

Contract NAS 3-10290

THE BOEING COMPANY

Requests for copies of this report should be referred to

National Aeronautics and Space Administration
Office of Scientific and Technical Information
Attention: AFSS-A
Washington, D.C. 20546

NASA CR-72606
D2-121696-1

# FINAL REPORT
# INVESTIGATION OF DEEP FLAWS IN THIN WALLED TANKS

By
J. N. Masters, W. P. Haese, and R. W. Finger

Prepared for
NATIONAL AERONAUTICS AND SPACE ADMINISTRATION

December 1969

Contract NAS 3-10290

Technical Management
NASA Lewis Research Center
Cleveland, Ohio

Liquid Rocket Technology Branch
Gordon T. Smith

THE BOEING COMPANY
Aerospace Systems Division
Seattle, Washington

# PREFACE

This report describes an investigation of static and cyclic flaw growth characteristics of deep flaws in thin walled cryogenic tank materials performed by The Boeing Company from June 1967 to March 1969 under Contract NAS3-10290. The work was administered by Mr. Gordon T. Smith of the NASA Lewis Research Center.

Boeing personnel who participated in the investigation include C. F. Tiffany; J. N. Masters, project supervisor; W. P. Haese, Principal investigator; and R. W. Finger and R. C. Shah, research engineers. Program support was provided by A. A. Ottlyk and H. M. Olden, specimen testing; F. D. Walsh, fracture surface photography; and D. G. Good, technical illustrations and art work.

The information contained in this report is also released as Boeing Dcoument D2-121696-1.

# INVESTIGATION OF DEEP FLAWS IN THIN WALL TANKS

By

J. N. Masters, W. P. Haese, and R. W. Finger

## ABSTRACT

The conditions controlling fracture instability and subcritical flaw growth in relatively thin sections containing deep surface flaws were experimentally investigated for 2219-T87 aluminum and 5Al-2.5Sn titanium base metal and weldments. The program consisted primarily of testing uniaxially loaded surface flawed specimens in ambient, liquid nitrogen, and liquid hydrogen environments. It was concluded that for test conditions in which the plastic zone size is relatively small with respect to the thickness, well ordered static and cyclic data is generated, and experimentally determined deep flaw magnification factors adequately describe the fracturing process. As relative thickness is reduced, combinations of stable flaw growth and plasticity effects control, and cyclic flaw growth rates increase rapidly. In the extreme case, (very thin gages with respect to the plastic zone size) the surface flaw grows through the thickness, under rising load, and ultimately fails as a through-the-thickness crack.

CONTENTS

## ILLUSTRATIONS

ILLUSTRATIONS (Continued)

ILLUSTRATIONS (Continued)

ILLUSTRATIONS (Continued)

## TABLES

TABLES (Continued)

TABLES (Continued)

TABLES (Continued)

TABLES (Continued)

TABLES (Continued)

TABLES (Continued)

## SYMBOLS

| | |
|---|---|
| $K$ | Stress intensity factor defined by linear elastic fracture mechanics. |
| $K_I$ | Stress intensity factor under condition of plane strain. |
| $K_{Ic}$ | Plane-strain fracture toughness of a material. |
| $a$ | Depth of semielliptical surface flaw or semiminor axis of the ellipse $X^2/a^2+y^2/e^2 = 1$. |
| $2c$ | Effective width of semielliptical surface flaw. |
| $\phi$ | Elliptical angle measured for semi-major axis of ellipse. |
| $\Phi$ | Complete elliptical integral of the second kind having modules K defined as $K = (1 - a^2/c^2)^{1/2}$ |
| $Q$ | Flaw shape parameter $=\Phi^2 - 0.212\,(\sigma/\sigma_{ys})^2$ |
| $\sigma$ | Uniform tensile stress applied perpendicularly to plane of crack or peak cyclic value thereof. |
| $\sigma_{ys}$ | Uniaxial tensile yield strength. |
| $\sigma_{ult}$ | Uniaxial tensile ultimate strength. |
| $E$ | Young's modulus. |
| $N$ | Number of loading cycles. |
| $\nu$ | Poisson's ratio. |

Subscripts

| | |
|---|---|
| i | at initial conditions |
| F | at finial conditions |

## SUMMARY

The experimental work described herein was undertaken to investigate the conditions controlling fracture instability and subcritical flaw growth of thin sections containing deep, part-through flaws. Two materials were tested: 2219-T87 aluminum and 5Al-2.5Sn titanium base metal and weldments. Uniaxially stressed surface flawed specimens were tested in ambient, liquid nitrogen, and liquid hydrogen environments. Tests performed were either static tests to failure or cyclic tests with zero-to-tension loading profiles. Additionally, center cracked panels were tested statically for each material, thickness, and test temperature. Each material was tested in two thicknesses. The aluminum base metal was tested in gages of 0.625 and 0.063-inch thickness; the aluminum weldments in 1.00 and 0.125-inch thicknesses; and the titanium base metal and weldments both in 0.200 and 0.020-inch thicknesses.

By comparing the data from the various types of tests it was concluded that the behavior of surface flaws subjected to a rising load to failure can be placed into two distinct categories:

1. In one case, the flaw remains stable until a stress intensity is reached at which point the flaw growth occurs very rapidly, resulting in complete fracture; the flaw is critical before it reaches the back surface.

2. In the second case, significant slow flaw growth occurs prior to reaching maximum load. In some cases, the flaw actually grows slowly completely through the thickness. Upon a further rise in load, the flaw can then become critical as a through-crack.

The parameters controlling these behaviors are not fully understood; however, it appears that the size of the plastic zone at the bottom tip of the flaw, relative to the specimen thickness or to the size of the remaining ligament (i.e., the net thickness, $t_n$), plays an important part. For plane strain conditions, the plastic zone size can be estimated by $\rho \simeq \frac{\pi}{16}\left(K_{Ic}/\sigma_{ys}\right)^2$. From the data generated, it appears that for values of $\rho/t_n$ up to about 1.00, the flaw will become critical before growing through-the-thickness. In this category, well ordered data was generated, describing the effects of flaw shapes and $a/t$ values for thick 2219-T87 aluminum base metal at all test temperatures and for thick 5Al-2.5Sn titanium base metal and weldments at cryogenic temperatures. In this same category, it was found that cyclic flaw growth rates were relatively low, and the cyclic specimens (cycled at stress levels just less than that at which comparable static specimens fail) failed before the flaw grew through the thickness.

In the second category the static test results were characterized by an absence of deep flawed effects (i.e., Irwin's apparent $K_{Ic}$ did not decrease with increasing flaw depth). In the extreme case, where the flaw did grow through-the-thickness before failure, the failure stress was , as expected, relatable to the through-the-thickness crack tests, even though the initial defect was a surface flaw. In this category cyclic flaw growth rates are much higher than in item (1) above, and the flaws were also found to grow through-the-thickness before failure.

# 1.0 INTRODUCTION

Previous investigations of failure modes of structure loaded in tension and containing crack-like defects have been directed primarily to the problems of either embedded or surface flaws which are relatively small with respect to the thickness, or to through-cracks. Relatively thin walled structure fabricated from materials of moderate toughness can involve the problem of part-through flaws which either initially or during service, may extend to depths which are quite large with respect to the thickness. Prior to initiation of this program, some analytical efforts had been directed toward the problem of fracture instability of deep flaws, experimental data on fracture, and on subcritical growth of such flaws was very limited.

This experimental investigation was thus undertaken to investigate the conditions controlling fracture instability and subcritical flaw growth characteristics of tension loaded structures containing deep, part-through flaws. Two materials in base metal and weld metal form were investigated: 2219-T87 aluminum and 5Al-2.5 Sn titanium. Uniaxially stressed surface flawed specimens were tested in ambient, liquid nitrogen, and liquid hydrogen environments, under conditions of either loading directly to failure or under zero-tension loading profiles. Thickness, flaw shapes, and flaw depth-to-thickness ratios were systematically varied. With these variables, several combinations of strength and plastic zone sizes were investigated.

## 2.0 TECHNICAL BACKGROUND

Relationships between stress intensity, flaw size, and nominal stress field have been derived for a number of crack geometries and loading conditions. In order to predict pressure vessel performance, solutions for the semi-elliptical surface flaws have proved to be the most useful. To date several approximate solutions are available.

Irwin (Ref. 1) first obtained a solution for a semi-elliptical surface flaw in a plate and estimated that the solution may be valid for flaws with depth up to about one-half the material thickness. As part of the Boeing research and development program (IR&D), Kobayashi (Ref. 2) arrived at an approximate stress intensity solution for deep flaws having small depth-to-length ratios, i.e., small a/2c values. Smith derived a solution for the semi-circular flaw in a semi-infinite body (Ref. 3). This solution provided further refinement of the free surface correction Irwin used in his equation. As part of the Boeing IR&D program, Smith estimated what the free surface corrections should be for the semi-elliptical surface flaws in a semi-infinite space (Ref. 4). He also obtained an approximation of the stress intensity for the semi-circular surface flaws which become very deep with respect to the thickness (Ref. 4). Using the single-edge-notch solution, i.e., a/2c = 0 of Gross, et al., (Ref. 5) and his solution for the deep semi-circular flaw, Smith roughly estimated stress intensity factors for deep surface flaws of intermediate shape, i.e., a/2c ratios between 0 and 0.5 (Ref. 4). Kobayashi and Moss (Ref. 6) have derived an approximate solution for the surface flaw that accounts for the effects of the stress-free surfaces and the ductility of the material.

The limited experimental evidence obtained before this program suggested that:

(1) Irwin's estimated flaw depth limitation of 0.5t for his solution is approximately correct;

(2) The stress intensity for deep semi-circular flaws can be reasonably approximated using Smith's solution;

(3) The Kobayashi solution for deep flaws provides a reasonable approximation of the stress intensities for flaws with a/2c ratios of approximately .30, but may tend slightly to underestimate the values for very small a/2c ratios;

(4) The Smith estimates for deep semi-elliptical flaws will overestimate the stress intensities for flaws with small a/2c ratios, i.e., a/2c less than .20.

The stress intensity relationships for the surface flaw obtained by Irwin, Kobayashi, Smith and Kobayashi and Moss are summarized below.

## 2.1 Irwin Analysis

Utilizing Green and Sneddon (Ref. 7) solution for the distribution of stresses near a flat elliptical crack in an elastic solid subjected to uniform tension in a direction perpendicular to the plane of the crack at infinity, Irwin (Ref. 1) derived the expression for the stress intensity factor.

$$K_I^* = \frac{\sigma \sqrt{\pi a}}{\Phi} \left[ \frac{1}{c^2} (a^2 \cos^2\phi + c^2 \sin^2\phi \right]^{1/4} \qquad (1)$$

Irwin estimated the stress intensity factor for a semi-elliptical surface flaw in a finite thickness plate as

$$K_I = 1.1 \sigma (\pi a/Q)^{1/2} \left[ \frac{1}{c^2} (a^2 \cos^2\phi + c^2 \sin^2\phi) \right]^{1/4} \qquad (2)$$

where he introduced the constant 1.1 to account for the effect on stress intensity of the stress-free plate surfaces and replaced Q for $\Phi$ to account for the effect on the stress intensity of the plastic yielding around the flaw periphery. Figure 1 describes Q for varying flaw shapes and stress ratios. Expression (2) was considered valid for surface flaws for flaw depths up to one-half the plate thickness and for stress levels not exceeding yield stress.

The maximum value of $K_I$ occurs at the end of the semi-minor axis of the ellipse and has the value:

$$K_I = 1.1 \ \sigma \ (\pi a/Q)^{1/2} \qquad (3)$$

## 2.2 Kobayashi Analysis

For surface flaws that have a small depth to length ratio, but are deep with respect to the plate thickness, Kobayashi assumed the following form for the stress intensity:

$$K_I = 1.1 \, M_K \, \frac{\sigma \sqrt{\pi a}}{\Phi} \qquad (4)$$

where: $M_K = M_{kf} \times M_{kp}$

Following Irwin (Ref. 1) the multiplying constant, 1.1, is taken to account for the effect of the free surface on the stress intensity factor.

$M_{kf}$, the elastic stress intensity magnification due to deep flaw, was estimated from an infinite strip with a central through-the-thickness crack under the conditions of plane strain.

$M_{kp}$ is the stress intensity magnification due to plastic yielding in an infinite plate with a central through-the-thickness crack under the conditions of plane strain.

* See List of Symbols for Definition of Terms.

A Plot of $M_K$, i.e., $M_{kf} \times M_{kp}$, versus a/t is given in Figure 2 for $(\sigma / \sigma_{ys}) = 0.4$ and 0.8 for $\nu = 1/3$.

Based on the experimental data, Tiffany et al., (Ref. 8) extended the plot of $M_K$ up to a/t = 1 as shown in Figure 3. They represented the stress intensity equation as

$$K_I = 1.1\, M_K\, \sigma \sqrt{\frac{\pi a}{Q}} \qquad (5)$$

## 2.3 Smith Analysis

Smith's (Ref. 3) linear elastic analysis of a semi-circular surface flaw in a semi-infinite body resulted in the following stress intensity relationship:

$$K_I = M_I \frac{2\sigma\sqrt{a}}{\sqrt{\pi}}$$

This result corresponds to that shown in equations (2) and (3) except that the 1.1 free surface correction assumed by Irwin is replaced by the $M_I$ coefficient, which is dependent upon location on the flaw periphery (Figure 4) and plasticity correction is not incorporated.

For semi-elliptical flaws in semi-infinite bodies Smith (Ref. 4) estimated the free surface coefficient, $M_I'$. This result is shown in Figure 5. The stress intensity relation thus becomes:

$$K_I = M_I'\ \sigma\ (\pi a/Q)^{1/2}$$

where:

$$M_I' = M_I \left[\left(\frac{a}{c}\right)^2 \cos^2\phi + \sin^2\phi\right]^{1/4} \left[\frac{1.1}{M_I} - \left(\frac{1.1}{M_I} - 1\right)\frac{a}{c}\right] \qquad (6)$$

As seen in Figure 5 the point of maximum stress intensity occurs at the point of maximum flaw depth for all flaws with a/2c ratios less than about .35 to .40. This is consistent with Irwin's analysis; however, the magnitude of the free surface corrections are slightly less than the 1.1 he estimated. Smith (Ref. 4) obtained the stress intensity factors for semi-circular flaws in a finite thickness plate and using it and Gross's single-edge-notch solution he estimated the stress intensity factors for semi-elliptical surface flaws in a plate as a function of a/2c and a/t ratios. The resulting relationship is:

$$K_I = M_I'\ M_K'\ \sigma\,(\pi\, a/Q)^{1/2}$$

$M_K'$ is the finite thickness (or deep flaw stress intensity magnification) correction. The $M_K'$ versus a/t curve for the semi-circular flaw and the estimated curves for semi-elliptical flaws with a/2c ratios of .10, .15, .20, .25 and .30 are shown in Figure 6.

## 2.4 Kobayashi-Moss Analysis

Kobayashi and Moss (Ref. 6) assumed that the stress intensity magnification factor in surface-flawed tension plates is decomposable in three parts. They, then, represented the stress intensity at the minor axis of surface flaw as

$$K_1 = M_F M_B M_P \frac{\sigma (\pi a)^{1/2}}{\Phi} \tag{8}$$

The first part of the magnification factor, $M_F$, is due to the stress free front surface. Utilizing the results of previous investigations (Ref. 3 and 9) $M_F$ was represented as

$$M_F = 1 + 0.12 (1 - a/2c)^2$$

The second part of magnification factor, $M_B$, is caused by the stress free back surface. This was estimated from the approximate solution by Kobayashi, et al., of two coplanar elliptical flaws in an infinite solid subjected to uniaxial tension (Ref. 10). Assuming no coupling between $M_F$ and $M_B$, the elastic part of the magnification factor $M_e = M_F M_B$ is given for the surface flaw in Figure 7. The free surfaces effect $M_e$ was truncated at the particular values of a/t for given $\sigma/\sigma_{ys}$ when the modified Dugdale yield zone penetrated the thickness of the specimen.

The plasticity magnification, Mp, was based on a modified Dugdale yield zone surrounding a penny-shaped crack of radius, b, in an infinite solid composed of strain hardening material. The normal stress component in the modified Dugdale model of extended yield zone was assumed to vary linearly from a maximum value of $\sigma_o$ at the edge of physical crack of radius b to a minimum value of $\sigma_{ys}$ at the edge of extended crack of radius d as shown in Figure 8. The pasticity magnification is obtained by comparing the crack opening displacement at the center of this modified Dugdale crack to that of the physical crack. Values of Mp for various values of m ($m = 1 - \sigma_{ys}/\sigma_o$) are shown in Figure 8.

This is the only approximate solution for surface flaws which shows the effect of strain hardening on stress intensity. It should be noted that the solution is still preliminary and needs refinements in the elastic and plastic magnification factors. General usage of this approximate solution is discouraged until it is refined. It should be used only to gain the intuition of the magnitude of corrections and the effect of strain hardening.

# 3.0 MATERIAL AND FABRICATION PROCEDURES

## 3.1 Materials

The 5Al-2.5Sn (ELI) titanium plate, 0.04 x 24.0 x 72.0-inches and 0.20 x 36.0 72.0-inches was purchased in the annealed condition per MIL-T-9046E, Type II, composition B. Composition of the heats used on the program is given in Appendix A.

The 5Al-2.5Sn (ELI) specimens were fabricated and tested in the annealed condition. Two of the plates used for fabricating base metal specimens and most of the plates used to fabricate weld panels required a hot flattening cycle before they could be used to fabricate parts since they were received from the vendor with considerable waviness. The thermal cycle used for flattening, 1250°F for one-half hour would not be expected to affect material properties significantly.

5Al-2.5Sn (ELI) titanium filler wire used for making the titanium welds was purchased per AMS 4953 except composition was to be:

| | |
|---|---|
| Aluminum | 4.7 - 5.6% |
| Tin | 2.0 - 3.0% |
| Iron | 0.15% Max |
| Carbon | 0.035% Max |
| Oxygen | 0.09% Max |
| Nitrogen | 0.009% Max |
| Hydrogen | 0.005% Max |
| Other Elements | 0.10% Max |
| Titanium | Remainder |

Ultimate tensile strength was set at 100 ksi. Actual compositions of the spools used on the program are given in Appendix A.

2219-T87 aluminum plate, 0.125 x 36 x 96-inches, 0.625 x 36 x 96-inches, and 1.0 x 36 x 96-inches was purchased per BMS 7-105C. All sheets of the same gage were from the same heat lot. Compositions for each gage are given in Appendix A.

The aluminum base metal specimens were fabricated in the T87 condition. Welded aluminum specimens were made by welding T87 material with the GTA process, leaving the weld in the as-welded condition.

Filler wire was used to weld 0.125-inch thick panels only. Filler wire was 2319 aluminum alloy purchased per BMS 7-75 Type III. Actual composition of spools used for welding is given in Appendix A.

## 3.2 Welding

The welds on the program were made to be typical of welds used on space program tankage. Consequently, both aluminum and titanium were welded with the GTA (Tungsten Inert Gas Process). All panels welded on the program had square butt edge preparations.

### 5A1-2.5Sn Titanium

Titanium panels were welded in two thicknesses, 0.04-inch and 0.20-inch. The panels and filler wire were chemically cleaned before welding per BAC 5753. Immediately prior to welding, the parts were hand scraped for a distance of 1/2-inch back from the abutting edges, and the faying surfaces were draw filed. Special tooling was used to weld the panels and shield the welds from oxidation. Figure 9 shows an end view of the tooling setup.

On the 0.040-inch thick welds a single weld pass was used with 0.045-inch diameter filler wire. On the 0.20-inch thick welds two passes were made from one side and 0.062-inch diameter filler wire was used. Weld quality in both gages was comparable with the quality of space program flight tankage as determined by X-ray and visual inspection. Actual weld parameters used on the titanium are included in Appendix B.

### 2219-T87 Aluminum

Aluminum panels were welded in two thicknesses, 0.125-inch and 1.00-inch. Panels and filler wire were cleaned before welding per BAC 5765. Just prior to welding, parts were hand scraped for a distance of 1/2-inch back from the abutting edges and the faying surfaces were draw filed.

The 0.125-inch thick welds were welded with one pass using 0.063-inch diameter 2319 aluminum filler wire. The 1.00-inch thick aluminum welds were made with four passes and no filler wire. One seal pass and one penetration pass was made from each side. Weld quality was comparable with the quality of space program tankage as determined by X ray and visual inspection. Actual welding parameters are shown in Appendix B.

## 3.3 Straightening of Welded Panels

Significant weld distortion occurred during welding specimen panels with the exception of 0.040-inch thick 5A1-2.5Sn titanium.

Figure 10 shows weld distortion in a 0.125-inch thick aluminum panel. The distortion is shown being removed by impacting the area adjacent to the weld with a magnetic hammer in Figure 11. Final contour of the straightened part is shown in Figure 12.

A large press was used to straighten the 1.00-inch thick welded specimens. X ray and penetrant checks were made on the straightened aluminum parts to assure that they were not damaged during straightening.

Weld distortion of 0.20-inch thick 5Al-2.5Sn titanium welded panel was removed by hot flattening the parts at 1250°F for 30 minutes in a hot sizing press.

## 3.4 Specimen Fabrication Procedure

Three different types of test specimens were fabricated on the program. Smooth tensile specimens used for determining mechanical properties are shown in Figure 13 and 14. Surface flaw specimens used to evaluate the static and cyclic flaw growth characteristics for surface flaws are shown in Figures 15 through 25. Center crack specimens used to determine failure stresses for through the thickness crack specimens of the plate and weld thicknesses tested on the program are shown in Figures 26 through 28.

All specimens were machined from plate and weldments of the same thickness as the specimen to minimize machining except for the thin flawed titanium specimens that were machined from 0.040-inch thick titanium sheet and the thin base metal aluminum specimens that were machined from 0.125-inch thick plate. Loading holes were drilled and reamed using drill jigs to assure uniform loading of the specimen. Figure 29 shows hole drilling on a one-inch thick welded aluminum specimen.

Specimens were oriented per the requirement of the contract instrument i.e., the major axis of the surface flaw and the length dimension of the through-flaw were perpendicular to the minimum tensile strength direction established from the mechanical property tests. This requirement resulted in the axis of the flaw being oriented parallel to rolling direction in the titanium specimens and perpendicular to rolling direction in the aluminum specimens.

All initial flaws were prepared by using an electric discharge machine (EDM) to introduce an initial flaw with a terminating radius of less than 0.003-inch. The EDM flaw was then extended using low stress fatigue. Maximum cyclic stress levels for surface flaw specimens for the 5Al-2.5Sn (ELI) titanium varied from 16 to 40 ksi. For the 2219 aluminum surface flaw specimens maximum cyclic stress levels ranged from 10 to 16 ksi. The number of cycles required to extend the initial flaw varied from specimen to specimen, depending on initial flaw size. Because the weld center is the weakest part of the weld, flaws were placed in the center of the weld for all welded specimens. Figure 30 shows the setup for fatigue sharpening the flaw on a 0.020-inch thick titanium specimen. The microscope was used to determine when the flaw had been sharpened by tension fatigue.

## 4.0 EXPERIMENTAL PROCEDURE

All room temperature test specimens were tested in ambient atmosphere in an enclosed building with temperatures ranging between 65 and 75°F. A strain rate of 0.005 in/in/minute was used on all smooth tensile specimens until the material yield strength was reached. A strain rate of 0.02 in/in/minutes was then used for the remaining portion of the loading sequence until failure. Static fracture toughness specimens were pulled at a rate needed to precipitate complete fracture within 1 to 3 minutes after initial application of load.

Cyclically tested specimens were subjected to trapezoidal loading profile with a maximum frequency of 20 cycles per minute. Figure 31 shows the test machine used to cycle test many of the larger specimens on the program at room temperature and -320°F. This machine was also used for static tests and flaw sharpening. Minimum stress of the trapezoidal loading profile was approximately 10 per cent of the maximum load. The trapezoidal loading profile was generated by dividing each cyclic period into four equal parts. The first part was spent in going from minimum load to maximum load, the second in holding the specimen at maximum load; the third in unloading; and the fourth part at minimum load.

The -320°F and -423°F tests were conducted in the environments of liquid nitrogen and liquid hydrogen, respectively. The liquid nitrogen was introduced into a wrap-around open can cryostat to keep the gage area of each specimen completely submerged. The -423°F tests were conducted in a similar manner except that to keep the specimen completely immersed in hydrogen, double walled vacuum insulated cryostats were used. Figure 32 shows the double walled cryostat that was used for the majority of hydrogen specimens on the program. Thermocouples were attached to control specimens to check temperature during each series of tests.

The point at which the flaw grew through the thickness during cycle testing of the thinner specimens on the program was detected by strain gages bonded to the back side of the specimen. A typical trace of one of these strain gages is shown schematically in Figure 33.

## 5.0 DESCRIPTION AND INTERPRETATION OF RESULTS

### 5.1 Mechanical Property Tests

Results of mechanical properties tests of the plates and weldments used on the program are given in Tables 1 through 6. Tests were conducted at room temperature in air, at -320°F in liquid nitrogen, and at -423°F in liquid hydrogen; the effect of temperature on ultimate tensile strength, yield strength, elongation, and Poisson's ratio is illustrated in Figures 34 through 41.

Uniaxial yield strengths were calculated using loads corresponding to a 0.2-percent offset on load-strain curves. For all tests at room temperature and at -320°F, longitudinal strains were measured using 2.0-inch gage length extensometers; at -423°F, strains were measured using longitudinally oriented back-to-back strain gages.

Poisson's ratio measurements were made from continuous strain gage recordings of load (P) versus longitudinal strain ($E_L$) and transverse strain ($E_T$). The elastic Poisson's ratio was then computed from the formula

$$\mu = \frac{d_{E_T}}{dP} \div \frac{d_{E_L}}{dP}$$

where: $\mu$ is the elastic Poisson's ratio;

$\frac{d_{E_T}}{dP}$ and $\frac{d_{E_L}}{dP}$ are the average slopes of the elastic portions of the load-versus-transverse-strain and load-versus-longitudinal-strain recordings respectively.

### 5.2 Static Tests of Surface Flawed Specimens

Results of surface flawed specimens tested statically are summarized in Tables 7 through 55. The data is presented in the following sequence:

0.200-inch titanium base metal --- Tables 7 through 13.
0.200-inch titanium weld metal --- Tables 14 through 20.
0.020-inch titanium base metal --- Tables 21 through 25.
0.020-inch titanium weld metal --- Tables 26 through 30.
0.625-inch aluminum base metal--- Tables 31 through 37.
0.063-inch aluminum base metal--- Tables 38 through 43.
1.00 -inch aluminum weld metal--- Tables 44 through 49.
0.125-inch aluminum weld metal--- Tables 50 through 55.

In each of the above-noted tables, specimen dimensions, test conditions, and gross and net area stresses at maximum load are shown in the first columns, followed by initial flaw dimensions as measured after fracture. For reference purposes, the apparent $K_{Ic}$ is shown as calculated from equation 3, using initial flaw sizes and gross stress at maximum load. Where applicable, the last column shows apparent $M_K$ values obtained by dividing the estimated true $K_{Ic}$ value by the apparent value listed in the preceding column. The true or baseline $K_{Ic}$ values were estimated as follows. First, all the data points were grouped by material, thickness, and test temperature. Each group was then plotted in terms of apparent $K_{Ic}$ value versus flaw depth-to-thickness ratio (a/t), noting net stress-to-yield strength ratios and nominal flaw shapes (a/2c values) on each plot.

A preliminary review of the data of tables 7 through 55, when plotted as noted above led to the following general observations and comments:

(1) For comparable flaw shapes and a/t values, the titanium weld metal data points exhibited a slightly greater scatter than that of base metal. Fracture faces of the weld specimens were very coarse.

(2) The majority of 0.200-inch base metal specimens came from heat #G-7622. A very few specimens were machined from heat #303268. This latter heat was considerably tougher than normal. Because of this, and since only a few specimens of the tougher heat were involved, they were not included in subsequent studies of the data trends.

(3) Several of the 0.625-inch aluminum base metal specimens exhibited rather severe delaminations at the flaw bottom. This was most predominant at room temperature in the longest flaws (lowest a/2c ratios) and was not evident in any of the specimens tested at -423°F. In almost all cases, the apparent calculated toughness was higher for those specimens in which a delamination was observed. Accordingly, these specimens (noted in Tables 31 through 35) were also not included in subsequent studies of data trends.

From observation of the remaining data (i.e., after eliminating points from titanium heat #303268, and from delaminated aluminum base metal specimens) it became apparent that the fracture behavior for the various materials, thicknesses, and test temperatures could be grouped into one of two general categories, as follows:

(1) In one case, the plots showed a trend of gradually decreasing apparent $K_{Ic}$ with increasing a/t value. Additionally, this $K_{Ic}$ decrease became more pronounced as the flaw depth-to-length value decreased and as the a/t values increased above values of about 0.30. These trends, in these material/temperature combinations appeared to prevail for net-to-yield stress ratios ($\sigma_n/\sigma_y$) of up to about 0.90 for the

aluminum, and for possibly somewhat higher ratios for the titanium. Above these values of $\sigma_n/\sigma_y$, the trend was reversed (i.e., apparent $K_{Ic}$ values were depressed with increasing $\sigma_n/\sigma_y$ values even as a/t values decreased). The trends noted above applied to the 0.625-inch thick 2219-T87 aluminum base metal at all test temperatures, and to both base metal and weldments in 0.200-inch 5Al-2.5 Sn titanium at -320°F and -423°F. Examples of this behavior are shown in Figures 42 and 43. Through the use of such plots, by visually extending scatter band curves to intersect the ordinate (at a/t of zero), baseline $K_{Ic}$ values were selected for the above-noted combinations. The $K_{Ic}$ values selected are summarized below.

| MATERIAL | THICKNESS INCHES | TEMPERATURE | BASELINE $K_{Ic}$ KSI $\sqrt{IN}$ |
|---|---|---|---|
| 2219-T87 Base Metal | 0.625 | Room | 47.0 |
| 2219-T87 Base Metal | 0.625 | -320°F | 50.0 |
| 2219-T87 Base Metal | 0.625 | -423°F | 50.0 |
| 5Al-2.5 Sn Base Metal | 0.200 | -320°F | 75.0 |
| 5Al-2.5 Sn Base Metal | 0.200 | -423°F | 60.0 |
| 5Al-2.5 Sn Weld Metal | 0.200 | -320°F | 85.0 |
| 5Al-2.5 Sn Weld Metal | 0.200 | -423°F | 75.0 |

These toughness values are plotted in Figure 44 as a function of test temperature.

(2) In the second group of material/thickness/temperature combinations apparent $K_{Ic}$ values did not decrease with increasing a/t values. This held true for the 0.125 and 1.00-inch aluminum welds, the 0.063-inch aluminum base metal, the 0.020-inch titanium base metal and weldments at all test temperatures, as well as the 0.200-inch titanium base metal and weldments at room temperature. Examples of these data are shown in Figures 45 through 50. Figures 45, 46, and 47 include the 1.00-inch aluminum welds at room temperature, -320°F, and -423°F, respectively, and in order, represent $\sigma_n/\sigma_y$ values well above 1.00 at room temperature, to elastic failures at -423°F. Figures 48, 49 and 50 show representative thin gage data. Note that in each of these figures, data points are included for specimens which were machined down from the thick gage stock. For example, Figure 48, which illustrates the 0.063-inch thick aluminum base metal, includes two data points of 0.063-inch specimens machined from 0.625-inch

stock. These additional tests were performed in an attempt to resolve differences observed (in both static and cyclic behavior) between the thick and thin tests. It can be seen that the data from the specimens milled down from the thicker stock generally fall quite close to that of the thin wrought specimens, and thus possible metallurgical differences resulting from the amount of rolling can be ruled out as a major contributor to the observed differences of fracture behavior of the varied gages.

Returning to the data in item (1) above, the next step involved the determination of apparent magnification factors. This was done by dividing the respective baseline $K_{Ic}$ value (as shown in Figure 44) by the corresponding apparent $K_{Ic}$ value (calculated from Equation 3, and included in Tables 9 through 35). The magnification factors were then plotted against a/t values for each flaw shape, material, and test temperature. The resulting plots are shown in Figures 51 through 53 for the 0.200-inch titanium and in Figures 54 through 56 for the 0.625-inch aluminum. For reference purposes, Kobayashi's approximate $M_K$ curve is scribed on all plots. Note first, that for a given flaw shape, both the titanium weldments and base metal data are shown together. Except for the slightly greater scatter in the weld data, the points do generally fall in the same pattern. Secondly, it can be seen that, for a given material and flaw shape, data from all test temperatures are in good agreement. On the other hand, the magnification factors for the titanium are somewhat higher than those of aluminum at corresponding flaw shapes. This is shown more clearly in Figures 57 and 58. These curves were constructed by visually fairing a curve through each family of data and then linearly interpolating to the a/2c values shown. Note that the family of curves are extended only to a/t values of 0.80 for the titanium which represents the limit of those specimens tested. The curves for the aluminum are extended to an a/t value of 0.85, even though some specimens were tested at larger depth ratios. From examination of the actual data (see Figures 54, 55, and 56) it appears that magnification reaches a maximum at about this depth ratio, and then tends to level off or even drop again at greater depths. As a/2c values decrease, this drop in apparent magnification appears to be more pronounced. Not very many specimens were tested in this range; however, there are data points for -320°F test specimens representing each of the three flaw shapes in the noted figures. The magnification reaches a maximum at approximately the same depth (a/t = 0.85) for each shape. It is interesting to note that the calculated plastic zone size just envelopes the remaining unbroken ligament ($t_n$) at about this depth for -320°F properties. This and the following may explain the observed behavior.

Once the remaining ligament is completely yielded, fracture may initiate at some angle, $\alpha$, around the flaw periphery from the bottom of the flaw. As longer flaws (lower a/2c values) are tested, the angle at which fracture initiates must become larger in order for fracture initiation to take place outside of the yielded region. The larger the angle, the lower is the applied stress intensity as compared to that at

$\alpha = 0$, and as calculated by equation 3. Thus, a higher load is required to cause failure. This behavior then would be characterized by magnification curves which drop rapidly after reaching a maximum.

For shorter flaws, $\alpha$ need not be as large. Secondly, the applied stress intensity does not vary rapidly as $\alpha$ increases. Thus, the expected behavior for short flaws is for the magnification to reach a maximum, but not to drop off as rapidly with further increase in flaw depth. Observation of the -320°F data in Figures 54, 55, and 56 suggests that this may be occurring. However, since there are only a few data points in this range, the curves in Figures 57 and 58 were limited in a/t values of 0.80 and 0.85, respectively. By comparing these curves to corresponding data points of Figures 51 through 56, it is seen that with very few exceptions, the data falls within a band of about plus or minus ten percent. This spread is not substantially greater than that observed in static fracture testing of identical specimens.

When comparing the experimentally developed magnification curves with the approximate solutions developed earlier by Kobayashi and by Smith, the following conclusions can be drawn:

(1) When comparing the titanium data (Figure 57) with that of Smith's work (Figure 6) it appears that for low a/2c values, Smith's curves greatly overestimate the magnification, and for high a/2c values, they underestimate the magnification. The magnification factors are in very good agreement at an a/2c value of 0.20.

(2) For the aluminum data (Figure 58), it is seen that Smith's curves greatly overestimate the magnification at all flaw shapes except possibly those approaching a semicircular shape.

(3) Kobayashi's magnification curve (Figure 3) compares well with the experimental data at intermediate flaw shapes (i.e., for a/2c values of about 0.35 in titanium and about 0.20 in aluminum).

## 5.3 Static Tests of Center Crack Panels

Tables 56 through 59 give data from 5A1-2.5 Sn titanium base metal and weld metal tested at room temperature, -320°F, and -423°F. Tables 60 through 63 contain results of 2219-T87 aluminum base metal and weld metal tested at room temperature, -320°F, and -423°F. $K_{CN}$ values shown in these tables were calculated using the expression below:

$$K_{CN} = Y \sigma_G \sqrt{a}$$

where: a = 1/2 the initial crack length (no crack growth measurements were taken)

$Y$ = parameter obtained from Figure 59

$\sigma_G$ = gross area stress

## 5.4 Cyclic Flaw Growth Tests

Results of surface flawed specimens tested under cyclic loading conditions are summarized in Tables 64 through 88. The data is presented in the following sequence:

0.200-inch titanium base metal --- Tables 64 through 66.
0.200-inch titanium weld metal --- Tables 67 through 69.
0.020-inch titanium base metal --- Tables 70 through 72.
0.020-inch titanium weld metal --- Tables 73 through 75.
0.625-inch aluminum base metal--- Tables 76 through 78.
0.063 and 0.100-inch aluminum base metal --- Tables 79 through 82.
1.00 -inch aluminum weld metal--- Tables 83 through 85.
0.125-inch aluminum weld metal--- Tables 86 through 87.

Make-up of these tables is similar to that of the static tests except that gross stress column represents maximum cyclic stress and the last column represents either total number of cycles to failure (for specimens which became critical before the flaw grew through-the-thickness) or cycles to grow the flaw through-the-thickness. Note that some specimens were cycled a predetermined number of cycles, and then were marked and pulled to failure. In this case, flaw dimensions at the end of the first cyclic run (as measured after failure) are noted at the bottom of the respective tables.

Review of the data contained in Tables 64 through 88 reveals that failure occurred prior to the time that the flaw grew through-the-thickness in only two groups of tests. This behavior occurred in the 0.625-inch 2219-T87 aluminum base metal at all test temperatures, and in the 0.200-inch 5A1-2.5 Sn titanium (base metal and weldments) at test temperatures of -320°F and -423°F. In all other cases (except, of course, where only incremental growth tests were performed) the flaw grew through-the-thickness prior to failure. These two types of behavior were not unexpected: if the critical flaw depth at the maximum cyclic stress is less than the thickness, failure before growing through will result. Conversely, if the critical flaw size is greater than the thickness, then breakthrough before failure results. The cyclic failure mode of the following combinations were thus unexpected:

1.00 -inch aluminum welds at -423°F.
0.063-inch aluminum base metal at -320°F and -423°F.
0.020-inch titanium at -423°F.

In each of these cases, the prior static tests had produced failures at stresses well below yield strength. Failure before breakthrough would then have been predicted at similar cyclic stresses and flaw shapes, yet, the flaws grew through the thickness prior to failure in each instance. For example, compare the static and cyclic behavior of the 1.00-inch aluminum welds at -423°F. Static specimen 3AW90H-3 (see Table 49) contained an initial flaw 0.835 inches deep by 2.895 inches long, and failed statically at a gross stress of 18.8 KSI. Cyclic specimen AWC65H-4 (see Table 84) contained a smaller initial flaw (0.645 by 2.080-inch), and was cycled at a slightly higher maximum stress, 20.0 KSI. Instead of failing, the flaw grew through in 148 cycles. Final flaw length was slightly greater than 3.0 inches. The bottom of the flaw had penetrated the thickness for a length of about an inch. Similar comparisons between static and cyclic behavior can be made for the other combinations noted above. This is discussed in more detail in Section 5.5.

Regardless of the fracture mode, cyclic growth rates can be calculated by differentiating cyclic life curves of the various sets of data. Where test conditions resulted in cyclic failure, this involved first making a plot of applied initial stress intensity (including appropriate magnification from Figures 57 and 58) versus cycles-to-failure for all specimens of a given thickness and test temperature. Where the flaws grew through-the-thickness before failure, the rate data were obtained by first plotting the initial flaw size versus cycles-to-leak. Note here, though, that for any test condition, different cyclic stress levels result in a different curve of ($a_i$) versus cycles-to-leak. Thus, only one stress level was used for each of these cases.

From the resulting plots (of either $K_I$ versus cycles-to-fail or $a_i$ versus cycles-to-leak) curves were faired through the data points, and these curves were then differentiated. The resulting rate curves are shown in Figures 60 through 62 for the titanium base metal and welds, Figures 63 through 65 for the aluminum base metal, and Figures 66 through 68 for the aluminum weldments. Note that on several of these curves average rates from incremental growth tests are included. These points usually involved tests of thick stock incrementally cycled at lower-than-normal stress levels (and thus lower K levels) so that rough comparisons between "thick" and "thin" growth rates could be compared at a fixed K level. Additionally, where growth rates had been established earlier for similar materials (Ref. 11), these rates are included for direct comparison.

Observation of the data in Figures 60 through 68 leads to the following general comments:

(1) For the titanium (Figures 60 through 62) at a given thickness, test temperature, and stress intensity, the base metal growth rates are comparable to weldment growth rates. Growth rates are significantly higher at room temperature than at either -320°F or -423°F. At all temperatures, growth rates at a given calculated stress intensity of the

0.020-inch stock are higher (by a factor of about 100) than that of the thicker material. Minor differences in rates exist at reduced temperatures between the 0.200-inch material tested herein and similar gages of Reference 11; however, this appears to be attributable to inclusion of magnification factors for the 0.200-inch data.

(2) For the aluminum base metal (Figures 63 through 65) it is seen that growth rates are essentially unaffected by test temperature. Rates for the 0.063-inch stock are consistently much higher than for the 0.625-inch specimen tests. Note in Figure 64 that two additional series of tests were performed. The first involved testing of 0.063-inch specimens machined from 0.625-inch stock. The resulting rates fall on the same curve as the 0.063-inch wrought specimens. Secondly, the series of intermediate thickness tests (0.100-inch thick) are seen to be at rates between the two extremes of thicknesses. As with the titanium data, growth rates of the 0.625-inch (longitudinal) are somewhat lower than that of similar gages reported in Reference 11 (note transverse grain). Some, but not all, of this difference can be attributed to inclusion of magnification factors in the K values of the 0.625-inch data (these factors reached a maximum of about 1.05). The remaining differences probably represent the effect of grain direction: the more pronounced delamination tendencies in the longitudinal direction may tend to retard flaw growth.

(3) For the aluminum weldments (Figures 66 through 68) it is seen that, while growth rates are higher, trends similar to that of the aluminum base metal exist. That is, rates are relatively unaffected by test temperature and rates for the thin (0.125-inch) stock are much higher than that of the thick (1.00-inch) stock.

The most significant of the above-noted observations is that of the large differences in growth rates of the thin stock with respect to that of the thick specimen tests. Recall that for the titanium at cryogenic test temperatures and for the aluminum base metal at all test temperatures, magnification was included in the thick specimen stress intensity values and was not included in the thin specimen stress intensity values. This procedure was adopted to maintain consistency with observed static test behavior. Note in Figure 61 that rate curves are shown for the 0.020-inch base metal tests, both with and without magnified stress intensities. The result, of course, forces better agreement in the right-hand portion of the curve (note that increasing initial flaw depths are involved in this area) but has a decreasing effect for the shallower flaws which make up the left-hand portion of the curve. It is concluded that differences in magnification alone cannot account for the observed differences in behavior.

Additionally, as noted by Hall (Ref. 12), there is reason to believe that flaw growth rates should vary between specimens of widely different flaw shapes. It was estimated that the growth rate of long flaws ($a/2c \approx 0$) should be between two and five times higher than that of semicircular flaws. Note that for the data described in Figures 60 through 68, all of the thinner stock involved a/2c values of about 0.05; the thick stock contained flaws with a/2c values of about 0.30 to 0.40. It appears that this variable could account for some of the difference in observed rates between the thick and thin data, but certainly not all of it.

## 5.5 Comparison of Static and Cyclic Data

As a result of the observations noted in the previous paragraphs, the major areas of concern involve: (1) large variations in the effect of flaw depths on static fracture behavior of the various materials and test conditions; and (2) large differences in cyclic flaw growth rates with variations in thickness. Possibly, a better understanding of these phenomena can be provided by additional study of the results of the different types of tests performed, but with an eye toward discovering possible factors common to the flaw growth or fracturing behavior involved in the different types of tests.

For example, review of the thin stock cyclic data reveals that in two series of tests, flaw growth through the thickness occurred on the first cycle. These involved the 0.063-inch and the 0.100-inch 2219-T87 base metal tests at -320°F. The cyclic life curves associated with these tests are shown in Figure 69. As seen, the curves are plotted in terms of initial flaw depth versus cycles-to-leak. Incidentally, these are the same type of curves which were drawn and differentiated to obtain the growth rate curves presented in Section 5.4. Note that the curves faired through the points would intersect the ordinate (the one-cycle line) at a flaw size less than the thickness. In fact, two 0.063 specimens (one cycled to 51 KSI gross stress and one to 61 KSI) did grow completely through on the first cycle. Of the 0.100-inch data, it is seen also that two specimens grew through on the first cycle. In terms relatable to the growth rate curves shown earlier, these four specimens represent average rates ranging from 16,000 to above 30,000 micro-inches per cycle (in other words, rates more than another order of magnitude greater than plotted in Figures 63 through 65). This observation leads to the following:

(1) First, rough approximations for these thin specimens show that on the last cycle before flaw breakthrough, the plastic zone ahead of the flaw occupies most if not all of the remaining unbroken ligament. In other words, in the flaw depth direction, there is little if any elastic material between the flaw and the back surface. Therefore, even though the nominal applied stress is elastic, the flaw front is effectively subjected to a completely plastic field. The result might not be unlike the problem of cyclic behavior of shallow flaws in thick-walled structure cycled to very high cross-section stresses. An example of this was

published in Reference 11. Figure 70, reprinted from Reference 11, illustrates the point for 5Al-2.5 Sn base metal, 0.188-inches thick, and cycled at various stress levels in liquid nitrogen. Note that at maximum gross cyclic stresses from about 115 to 160 KSI, the cyclic lives are in excellent agreement with predictions based on end-point data. However, at cyclic stresses of 175 KSI (approaching 98 percent of yield strength) the cyclic growth increased by a factor of from seven to forty times above that expected.

(2) Secondly, consider the implication of the one-cycle-to-breakthrough in terms of static fracture behavior. Recall that one of the 0.063-inch thick cyclic specimens (specimen ABC48N-5 in Table 80) contained an initial flaw which was 0.048 inches deep. The flaw grew through the thickness on the first 51-KSI cycle. Additionally, from Table 40, it is seen that all corresponding static specimens failed at stress levels above 53 KSI. The actual range of fracture stresses was 53.1 to 56.7 KSI. The range of initial flaw depths was 0.046 to 0.057 inches. It is suggested that in some, if not in all, of these fracture tests, the flaw grew through the thickness (without becoming critical) well before the time that the maximum failure load was reached. If this is true, then fracture would be controlled by through-crack considerations, and, obviously, surface crack solutions would not be meaningful. To check this possibility, the thin stock static data was again reviewed in an attempt to see if a correlation existed between the static surface flaw test results and the static center crack test results. The assumption was made that if the surface flaw grew through the thickness (under stable conditions) prior to rapid failure, then the failure stress should be predictable by considering the $K_{CN}$ value and a through-crack length (2a) comparable to the initial surface flaw length (2c). Unfortunately, for most of the materials involved, this would result in net section stresses too close to (or even exceeding) the yield strength, and thus not within the realm of applicability of the $K_{CN}$ values. However, the thin-gage titanium tested at -423°F failed at low enough stress levels to provide a comparison. Figure 71 shows the results. The solid curve represents the conventional stress-flaw size relationship for through cracks of initial lengths (2a) and the experimentally determined $K_{CN}$ value of 104.7 KSI $\sqrt{IN}$. The curve is computed based upon a finite width specimen equal in width to the surface flaw specimens (i.e., 4.00 inches). Superimposed on the figure are corresponding surface flaw data points (from Tables 24 and 25). The points now are plotted in terms of gross area failing stress versus initial surface crack length (2c). The striking correspondence observed in the thru-crack and surface flaw data strongly suggests that these surface flaws did break through, under stable conditions and, indeed, did fail as through cracks. Similar checks were made on the other groups of thick

specimens, but, as expected, no good correspondence was noted except possibly that noted in the next item.

(3) The above-noted studies lead to the belief that large amounts of stable growth can occur during the rising load portion of either cyclic or static fracture tests. It is believed that this occurred, to some extent in all the static tests performed on the series of "thin" stock (i.e., at all temperatures for the 0.020 titanium, the 0.063 aluminum base metal, and the 0.125 aluminum weldments). At the one extreme, this growth can result in the flaw completely penetrating the back side well before reaching critical stress intensities. The material/thickness combinations noted above are, in each case, those in which deep flaw magnification was not observed. The only other series of tests in which elastic failures prevailed, but in which no deep flaw magnification was apparent, were the 1.00-inch aluminum weldments tested at cryogenic temperatures and the 0.200-inch (long flaws) titanium at room temperature. This fact led to another review of the cyclic test specimens for the corresponding materials. Close examination of the fracture faces of the 1.00-inch aluminum weldments revealed, in most cases, signs of two slightly different textures occupying the area between the initial and the final flaw size. Figure 72 is a fractagraph of one of these specimens. Based on the prior discussions, it might be assumed that these differences in texture actually represent the differences resulting from stable growth on the first cycle, as opposed to a more uniform growth on subsequent cycles. Accordingly, the fracture faces of each of the 1.00-inch weldment cyclic specimen was reviewed, and the assumed first cycle growth was measured and recorded. Study of this data resulted in the conclusion that this "first-cycle" growth appeared to be related to the applied stress intensity. This is illustrated in Figure 73. As noted, at $K_I$ values below about 15 KSI $\sqrt{IN}$, no growth is seen, but at higher K levels, at all test temperatures, this growth increased rapidly.

(4) As noted above, the only other set of static data which did not display a deep flaw effect was the 0.200-inch titanium tested at room temperature. Observation of the fracture faces of the cyclic specimens in this series of tests failed to reveal distinct markings which might be considered to be evidence of large first cycle growth. One specimen (number TBC12R-5) contained a faint line between the initial and final flaw, but certainly not conclusive.

While there remains a question regarding the growth characteristics of the 0.200-inch titanium tested at room temperature, there is considerable evidence to suggest that relatively large amounts of stable growth can occur during the rising load portion of either static or cyclic tests. The factors controlling this occurrence are not

fully understood. However, it is significant that it is not necessarily limited to the thin section, deep flawed tests (e.g., the 0.063 inch aluminum and the 0.020-inch titanium). Large amounts of growth apparently occurred in fifty percent deep flaws in the one-inch aluminum welds. Thus, neither thickness, nor a/t values alone are responsible. Rather, it appears that this phenomenon may be related to the plastic zone size ($\rho$) in relation to the thickness of the remaining ligament ($t_n$) below the flaw. If this is true, one can speculate on the effect of varying $\rho/t_n$ or $\rho/t$ values on fracture and flaw growth behavior. A schematic model is shown in Figure 74. Assume that for a given material and test temperature, specimens of different thicknesses ($t_1 > t_2 > t_3 > t_4$) are tested statically with identical flaw shapes but with several a/t values for each thickness. The data is then plotted in terms of $K_{Ic}$ (from equation 3, and using initial flaw size and maximum load). The resultant set of data might plot as shown in the figure. For the largest thickness, $t_1$, the calculated toughness value would first increase with increasing a/t values until the net section stresses are below the yield strength. With further increase in a/t, the calculated toughness would drop, to reach a minimum when the plastic zone engulfs the remaining ligament (as discussed in Section 5.2). With increased thickness, the curve of $t_1$ in Figure 74 would not change materially. However, with reduced thickness ($t_2$), the test results are such that there is a lessened effect of increasing a/t. With another decrease in thickness ($t_3$), the curve flattens out because of combinations of plasticity and stable flaw growth effects; that is, the actual critical flaw size is larger than estimated and thus the actual maximum $K_{Ic}$ value is not calculated. Finally, as the thickness is further reduced ($t_4$) growth through the thickness occurs prior to reaching maximum load, and the resulting calculated K is (though fictitious) completely unaffected by a/t value. It is speculated that each of these behaviors occurred in the program, as follows:

| | |
|---|---|
| 0.200-inch titanium at -320°F and -423°F | --- equivalent to $t_1$ |
| 0.625-inch aluminum at all temperatures | --- equivalent to $t_2$ |
| 0.200-inch titanium at room temperature | --- equivalent to $t_3$ |
| 1.00 -inch aluminum weld at all temperatures | --- equivalent to $t_3$ |
| All other combinations | --- equivalent to $t_4$ |

With regard to static tests, then, the above is offered as a possible explanation of the behavior experienced as to whether deep flaw magnification was observed or not. The difference in behavior of thicknesses $t_1$ and $t_2$ may explain some of the differences in apparent $M_K$ values noted in Figure 57 as opposed to those of Figure 58.

With regard to cyclic behavior, for a given material, growth rates at moderate stress levels increase with decreasing thickness. For thicknesses $t_1$ and $t_2$, the flaw would not grow through the thickness prior to failure. For thicknesses $t_3$ and

$t_4$, flaw growth through the thickness would occur prior to failure, even at cyclic stresses approaching the materials yield strength.

## 5.6 Design and Analysis Implications

Several past studies (Ref. 8, 11, and 12) have dealt with the problem of applying fracture data and analytical methods in the areas of (1) material selection; (2) the estimation of failure modes and structural life; and (3) the determination of non-destructive inspection acceptance limits. At first, these studies involved structures in which initial and critical flaws were small with respect to the thickness. In such cases, analytical methods were shown to be adequate. With time, though, several instances arose which involved deep flaws in thinner gages. Because sufficient experimental data was not usually available, certain analytical assumptions were required to be made. Primarily, these involved (1) the use of Kobayashi's magnification (Figure 3), and (2) it was assumed that cyclic flaw growth rates from thick walled tests could be used if adjusted for the magnified stress intensities. It was a major objective of the program reported herein to assess the adequacy of these assumptions. Based upon the findings of this program, it is seen that deep flaw magnification levels can be somewhat higher than assumed by Kobayashi. In certain cases, this would result in an error in failure mode predictions for a given vessel. Where the plastic zone size is relatively small, cyclic flaw growth rates do not vary significantly with increased flaw depth to thickness ratio. On the other hand, it is seen that cyclic life can be greatly underestimated for the thinnest cases. Fortunately, in this category, the failure mode is leakage, not catastrophic failure.

Additional experimental work is required to resolve the above noted shortcomings. In the interim the following suggestions are made:

(1) Where sufficient data is not available, assume that deep flaw magnifications are as shown in Figure 57.

(2) Where the calculated plastic zone size is small (e.g., less than ten percent of the thickness) cyclic flaw growth rates can be predicted by using thick walled data adjusted by the above noted magnifications.

(3) For thinner stock, experimental cyclic growth rate data obtained by maintaining strict similitude between test specimen and vessel gages is considered mandatory.

## 6.0 OBSERVATIONS AND CONCLUSIONS

Some observations and conclusions relative to the 5Al-2.5 Sn titanium and 2219-T87 aluminum tested herein are applicable to most metallic materials. These are as follows:

(1) For a given material, if the thickness is relatively large with respect to the surface flaw plastic zone size, a deep flaw stress intensity magnification exists which increases with increased flaw depth and decreased a/2c values. This behavior was observed in the 0.200-inch titanium base metal and weldments tested at -320°F and -423°F, and the 0.625-inch aluminum base metal tested at all temperatures.

(2) For somewhat thinner gages (relative to the plastic zone size) stable flaw growth and increased plasticity effects result in an effect which makes it appear that deep flaw magnification does not exist (i.e., a curve resulting from a plot of Irwin's K versus a/t is approximately horizontal). Rather, it is believed that $K_{IC}$ values are underestimated at low a/t values, even though failure might occur at net section stresses well below yield strength. This behavior was observed in the 1.00-inch aluminum weldments at reduced test temperatures, and probably in the 0.200-inch titanium base metal and weldments at room temperature.

(3) With an additional reduction in relative thickness/plastic zone size, fracture occurs after the surface flaw penetrates the back surface. In this case the failure mode is actually that of a through-the-thickness crack. It is believed that this behavior occurrred in the 0.020-inch titanium base metal and weldments at all test temperatures, in the 0.063 inch aluminum base metal at all test temperatures, and in the 0.125-inch aluminum weldments at all test temperatures.

(4) As thickness decreases per the above items, cyclic flaw growth rates increase much more rapidly than previously expected.

## REFERENCES


1. Irwin, G. R., "Crack Extension Force for a Part-Through Crack in a Plate," Journal of App. Mech., Vol. 29, Trans. ASME, Vol. 84, Series E, December 1962.

2. Kobayashi, A. S., "On the Magnification Factors of Deep Surface Flaws," Structural Development Research Memorandum No. 16, The Boeing Company, December 1965.

3. Smith, F. W., "Stresses Near a Semi-Circular Edge Crack, "Ph. D. Dissertation, University of Washington, 1966.

4. Smith, F. W., "Stress Intensity Factor for a Semi-Elliptical Flaw," Structural Development Research Memorandum No. 17, The Boeing Company, August 1966.

5. Gross, B., Srawley, J. E., and Brown, W. F., "Stress Intensity Factors for a Single Edge Notch Tension Specimen by Boundary Collocation of a Stress Function," NASA TND-2395, 1964.

6. Kobayashi, A. S., and Moss, W. L., "Stress Intensity Magnification Factors for Surface-Flawed Tension Plate and Notched Round Tension Box," presented at the Second International Conference on Fracture, Brighton, England, 1969.

7. Green, A. E., and Sneddon, I. N., "The Distribution of Stress in the Neighborhood of a Flat Elliptical Crack in an Elastic Solid," Proc. Cambridge.

8. Tiffany, C. F., Masters, J. N., and Pall, F. A., "Some Fracture Considerations in the Design and Analysis of Spacecraft Pressure Vessels," presented at the ASM National Metals Congress, Chicago, October 1966.

9. Wiggleworth, L. A., "Stress Distribution in a Notched Plate," Mathematika, Vol. 4, 1957.

10. Kobayashi, A. S., Ziv, M., and Hall, L. R., "Approximate Stress Intensity Factor for an Embedded Elliptical Crack Near Two Parallel Free Surfaces," International Journal of Fracture Mechanics, Vol. 1, No. 2, 1965.

11. Tiffany, C. F., Lorenz, P. M., and Hall, L. R., "Investigation of Plane-Strain Flaw Growth in Thick-Walled Tanks," NASA CR-54837, Final Report on Contract NAS3-4194, February 1966.

12. Hall, L. R., "Plane-Strain Cyclic Flaw Growth in 2014-T62 Aluminum and 6Al-4V(ELI) Titanium," NASA CR-72396, Final Report on Contract NAS 3-7993, November 1968.

# APPENDIX A

## MATERIAL COMPOSITION
(% By Weight)

### 5Al-2.5 Sn Titanium Plate

| Thick-ness | Heat No. | C | Fe | N | Al | H | Sn | Mn | $O_2$ | Remarks |
|---|---|---|---|---|---|---|---|---|---|---|
| .20 | G-7622 | .022 | .15 | .008 | 5.0 | .005 | 2.6 | .003 | .060 | Used for most static base metal tests |
| .20 | 303268 | .020 | .06 | .007 | 5.5 | .007 | 2.6 | .010 | .109 | Used for most cycle base metal tests and five base metal tests |
| .20 | 293622 | .020 | .07 | .009 | 5.2 | .005 | 2.6 | .010 | .103 | Used only for weld specimens |
| .20 | 7909 | .023 | .14 | .014 | 5.0 | .005 | 2.6 | .001 | .080 | Used only for weld specimens |
| .20 | G-8818 | .025 | .16 | .013 | 5.2 | .005 | 2.4 | .001 | .090 | Used only for weld specimens |
| .04 | G-1207 | .015 | .07 | .012 | 5.5 | .011 | 2.7 | .003 | .080 | Used for both base metal and weld metal |

### 2219-T87 Aluminum Plate

| Thick-ness | Heat No. | Mn | Si | Cu | Mg | Zn | Ti | Fe | V | Zr |
|---|---|---|---|---|---|---|---|---|---|---|
| 0.125<br>0.625<br>1.00 | 720471<br>720891<br>719511 | .40 Max<br>.20 Min | .20 Max | 6.8 Max<br>5.8 Min | .02 Max | .10 Max | .10 Max<br>.02 Min | .30 Max | .15 Max<br>.05 Min | .25 Max<br>.10 Min |

### 5Al-2.5 Sn Titanium Weld Wire

| C | Fe | Mn | N | $O_2$ | H | Al | Zn |
|---|---|---|---|---|---|---|---|
| .014 | .063 | .05 | .009 | .100 | .0050 | 5.58 | 2.56 |

### 2319 Aluminum Weld Wire

| Cu | Fe | Si | Mn | Mg | Zi | Ti | V | Zr&Be |
|---|---|---|---|---|---|---|---|---|
| 6.00 | 0.18 | 0.15 | 0.25 | 0.02 | 0.05 | 0.14 | 0.07 | 0.17 |

## APPENDIX B

## WELDING PARAMETERS

### Welding Parameters: 0.040-inch Titanium

Single Pass Weld

Filler Alloy: 5Al-2.5Sn-Ti
Torch Gas: 90 CFH 100% He
Back-up Gas: 15 CFH 100% AR
Electrode Size: -3/32" 2% Thoriated Tungsten
Electrode Configuration: -Start Point
Hold-Down Finger Spacing: -5/32"
Filler Wire Diameter: -0.045
Amperage: 85-90
Voltage: 11.5
Travel Speed: 20-IPM
Wire Speed: 10-IPM

Weld Position: Downhand
Weld Process: DCSP-GTA
Gas Cup Orfice: 1/2 inch-ID
No trailer was used for these welds.

### Welding Parameters: 0.200-inch Titanium

Two Pass Weld from One Side

Filler Alloy: 5Al-2.5Sn-Ti
Torch-Gas: 100 CFH - He
Back-up Gas: 45 CFH - He
Trailer Gas: 70 CFH - He
Edge Groove Gas: 10 CFH - He
Electrode: 1/8 inch 2% Thoriated Tungsten
Electrode Configuration: 0.040 Blunt End
Electrode Stickout: 1/4 inch
Hold Down Finger Spacing: 0.400 inch
Filler Wire Diameter: 0.062

Weld Position: - Down Hand
Weld Process: - DCSP-GTA
Gas Cup Orfice: 1/2 inch I.D.
Back-up Groove: 0.400 inch

| Penetration Pass: - | | Filler Pass: | |
|---|---|---|---|
| AMPS | 230-250 | AMPS | 185-200 |
| Volts | 9.5-10 | Volts | 11 |
| Travel Speed | 6-IPM | Travel Speed | 6-IPM |
| Wire Speed | None | Wire Speed | 23-IPM |

Variations in amperage and voltage on the above weld setting were due primarily to moving from one power supply to another, midway through this phase of the program.

Welding Parameters: 0.125-inch aluminum

One and Two Pass Weld from One Side

Filler Alloy: 2319 Aluminum-.063
Torch Gas: 90 CFH 100% He
Electrode Configuration: Sharp Point
Electrode Stick-Out 1/2 inch
Electrode: 1/8" 2% thoriated tungsten
Finger spacing 1/2 inch on each side of joint
Pass #1
Amps - 90
Volts - 13.5
Travel Speed - 8-IPM
Wire Speed - 20-IPM

Joint Thickness - 0.125 inch
Weld Position: Down Hand
Weld Process: DCSP-GTA
Gas Cup Orifice 5/8 inch

Pass #2 if needed for fill
Amps - 90
Volts - 14
Travel Speed - 10-IPM
Wire Speed - 10-IPM

Welding Parameters: 1.00-inch aluminum

Filler Alloy - None
Torch Gas: 110 CFH 100% He
Electrode: 3/16 2% Thoriated Tungsten
Electrode Configuration: Rounded tapered point, blunt end
Electrode stick-out: 1/2 inch
Fusion Pass:
Amps - 200
Volts - 12.1
Travel Speed - 15-IPM
Wire Speed - None

Weld Position - Down Hand
Weld Process - DCSP-GTA
Gas Cup Orifice 5/8 inch

1st Penetration Pass: Side #1
Amps - 400
Volts - 12
Travel Speed - 3-IPM
Wire Speed - None

Side #2 parameters were the same as above used for side #1.

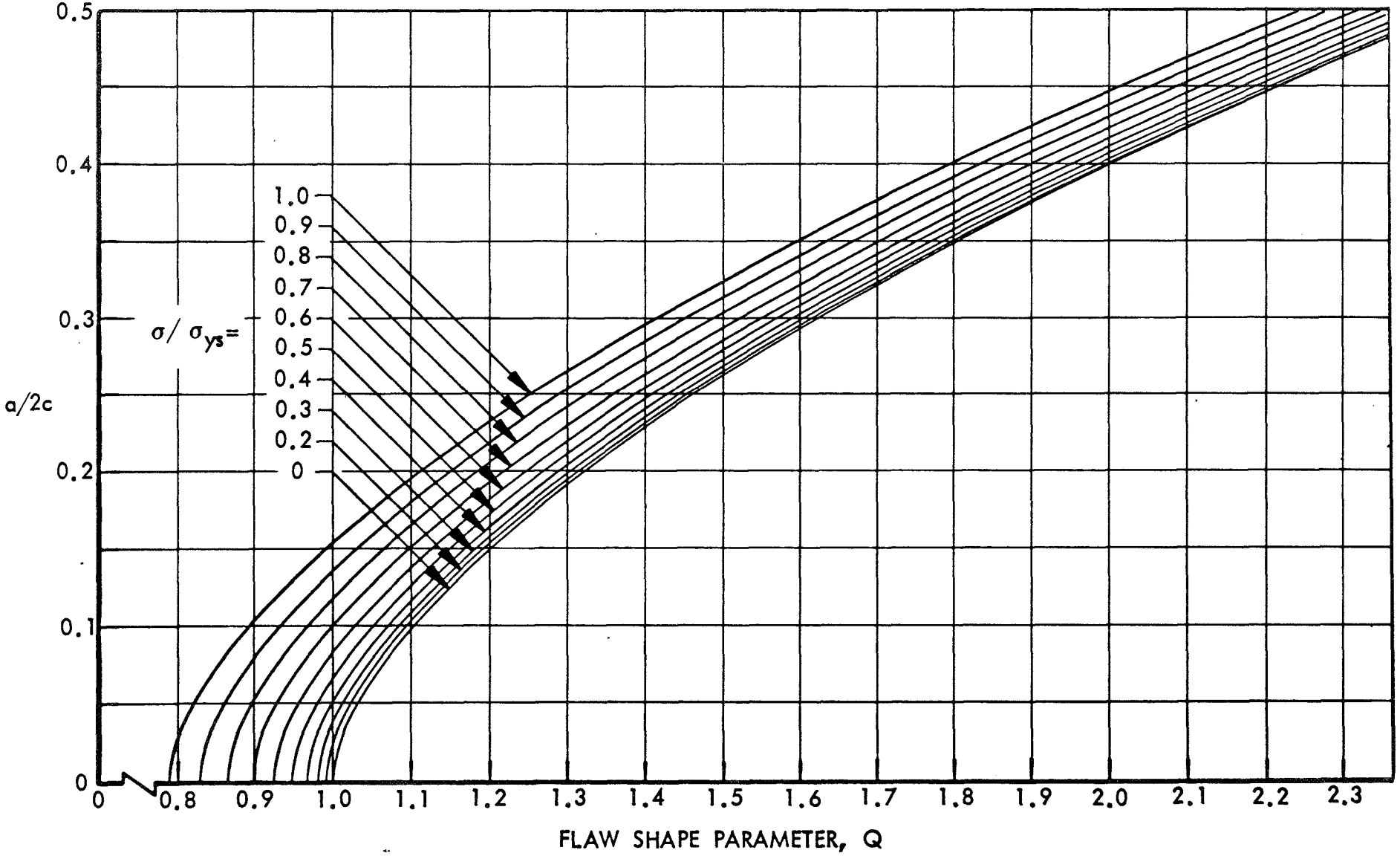


Figure 1: SHAPE PARAMETER CURVES FOR SURFACE AND INTERNAL FLAWS

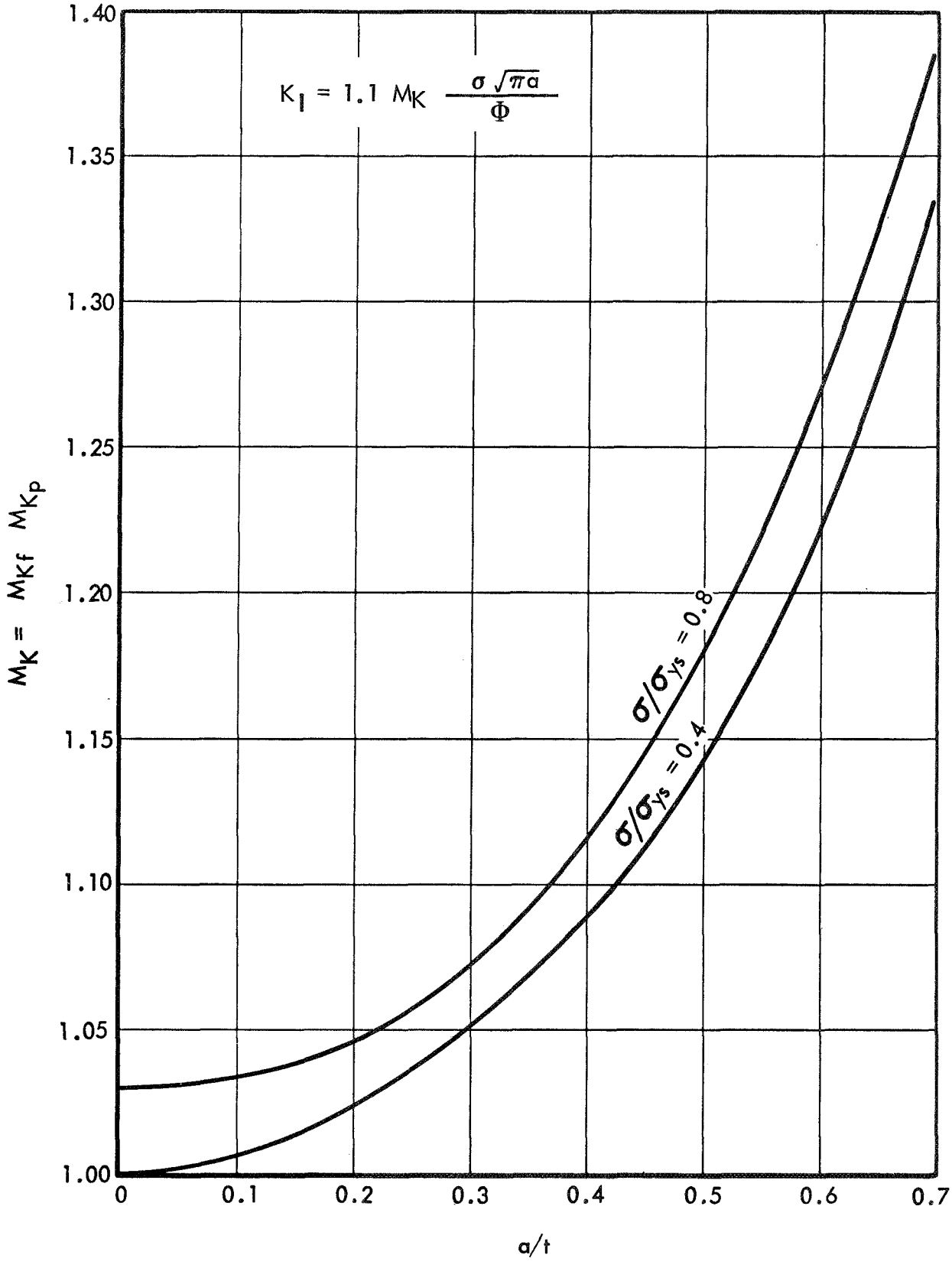


Figure 2 : STRESS INTENSITY MAGNIFICATION FACTOR DUE TO DEEP FLAW AND PLASTIC YIELDING FOR PLANE STRAIN
$\nu = 1/3,\ a/2c < 0.3$

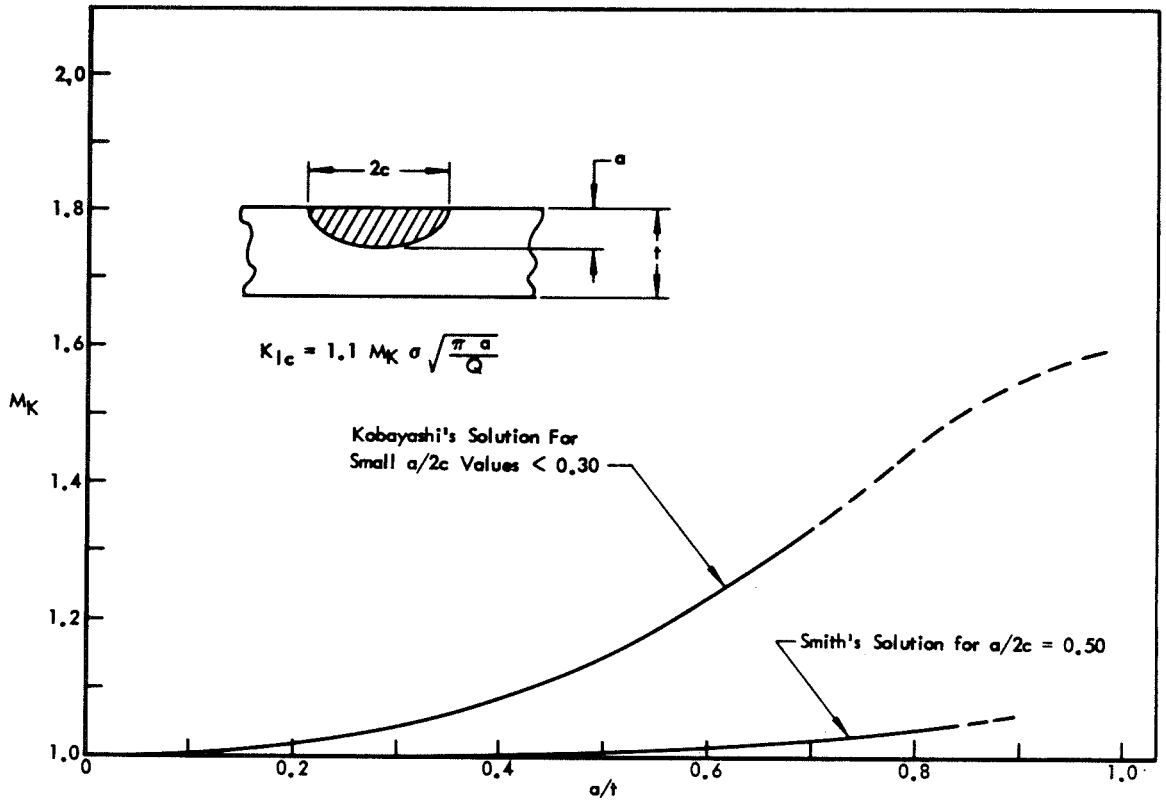


Figure 3: STRESS INTENSITY MAGNIFICATION FACTORS FOR DEEP SURFACE FLAWS

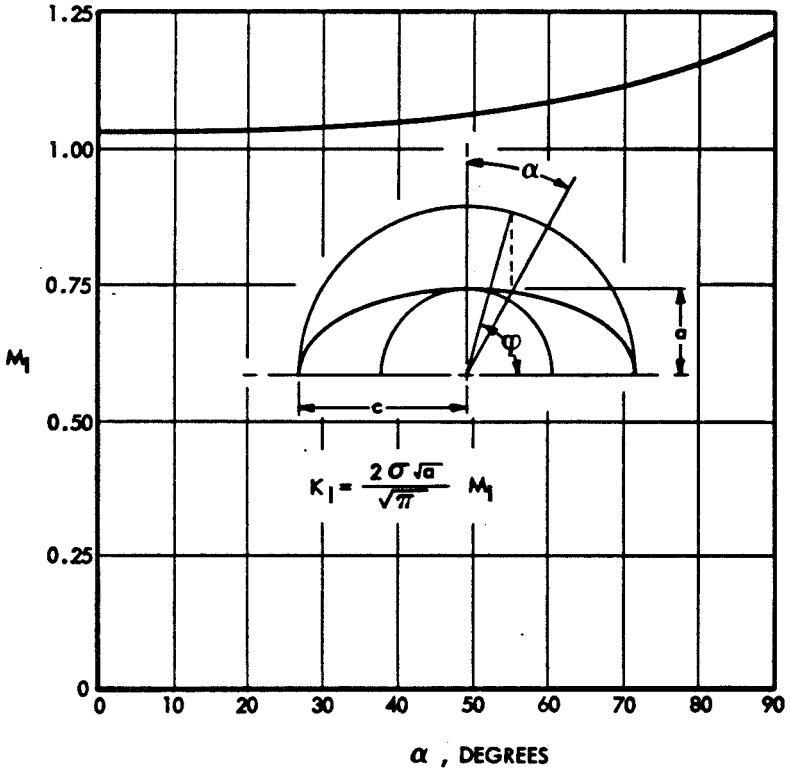


Figure 4: STRESS INTENSITY FACTOR FOR A SEMI-CIRCULAR SURFACE FLAW

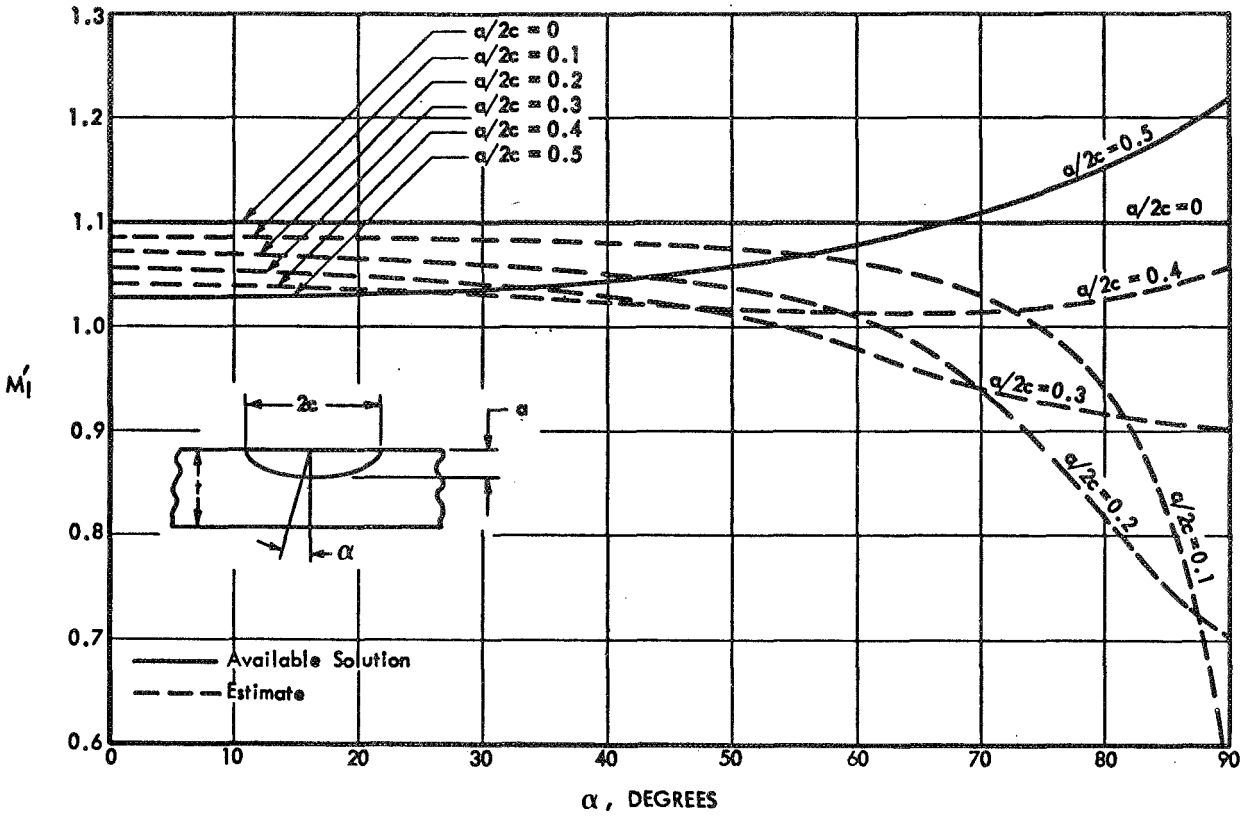


Figure 5: STRESS INTENSITY FACTOR FOR A SEMI-ELLIPTICAL SURFACE FLAW

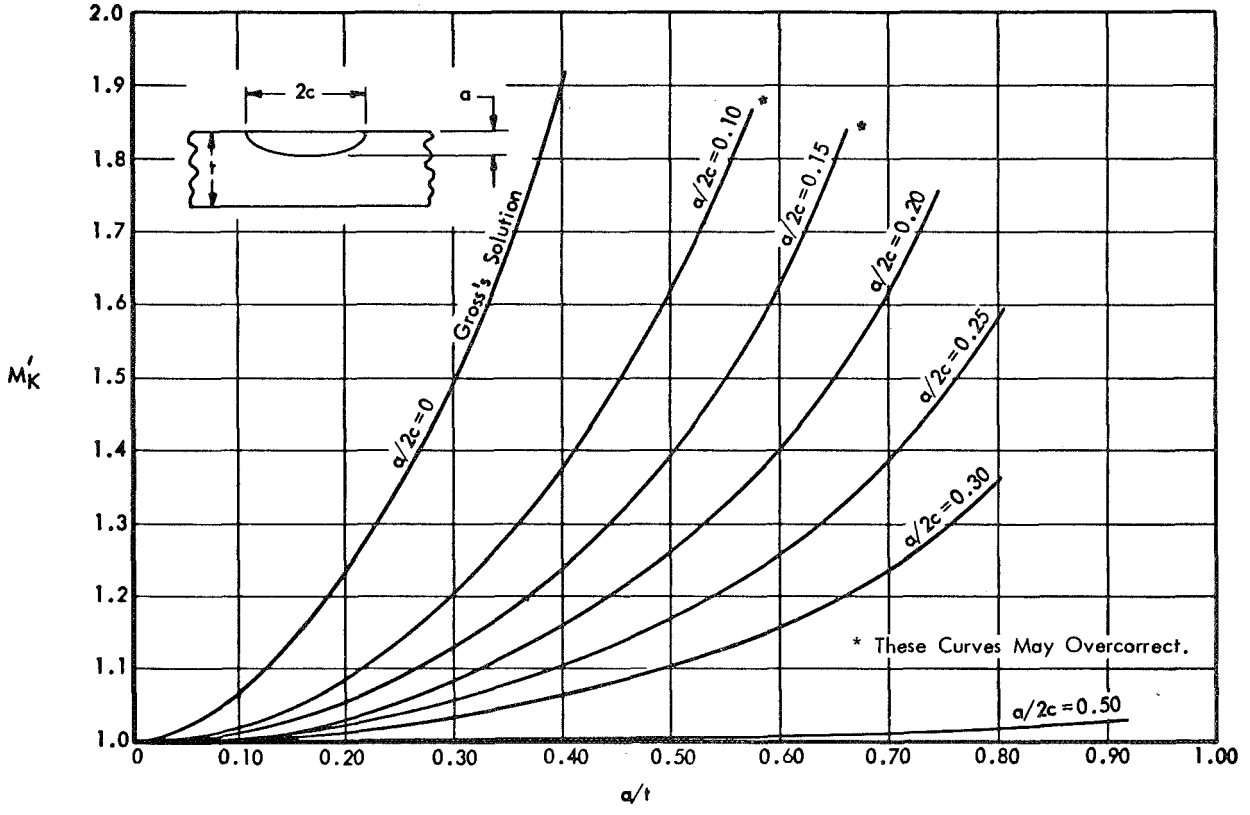


Figure 6: ELASTIC STRESS INTENSITY MAGNIFICATION FACTORS FOR DEEP SURFACE FLAWS (Estimations by F. Smith)

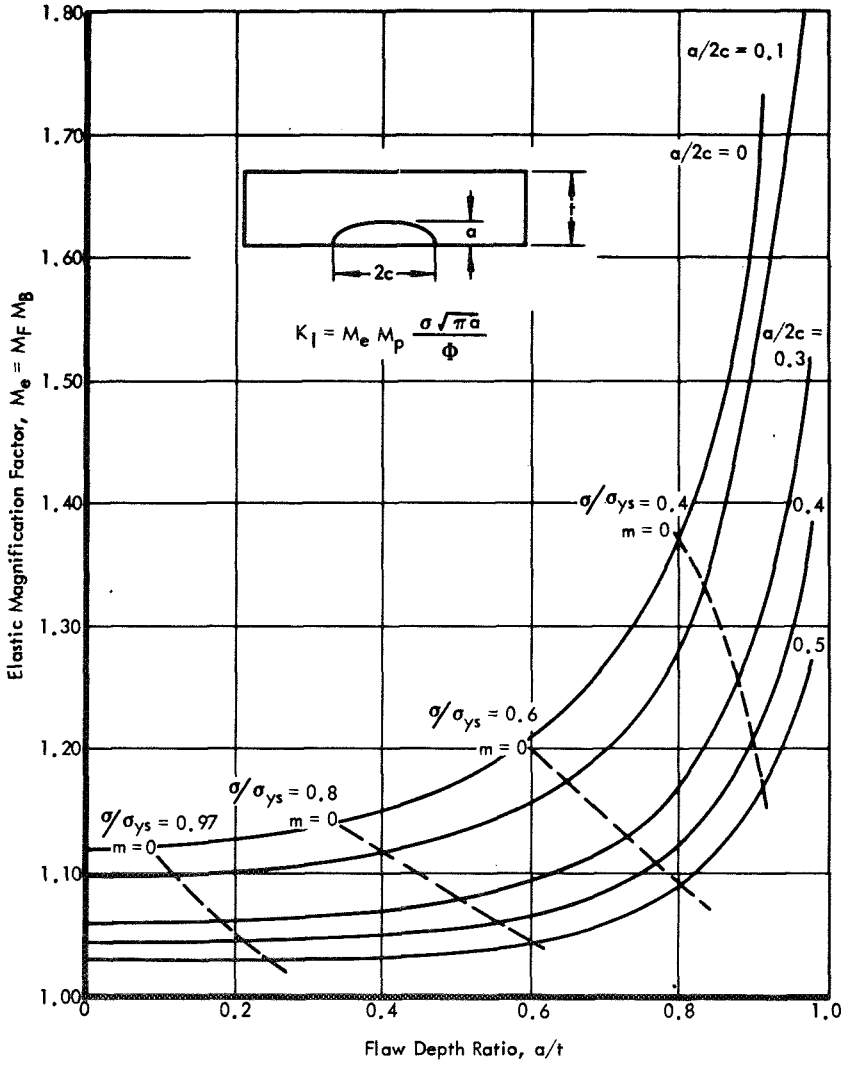


Figure 7: ELASTIC STRESS INTENSITY MAGNIFICATION FACTOR, $M_e$, FOR A SURFACE-FLAWED TENSION PLATE

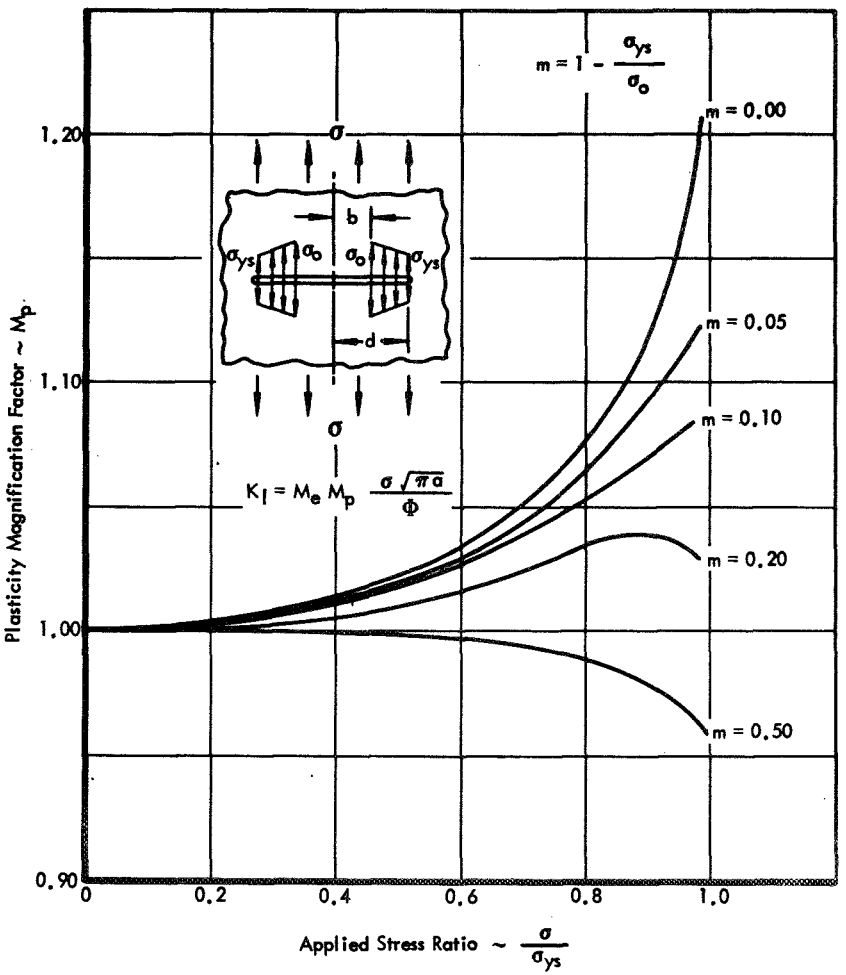


Figure 8: PLASTIC STRESS INTENSITY MAGNIFICATION FACTOR FOR PENNY-SHAPED CRACK IN AN INFINITE SOLID SUBJECTED TO UNIAXIAL TENSION

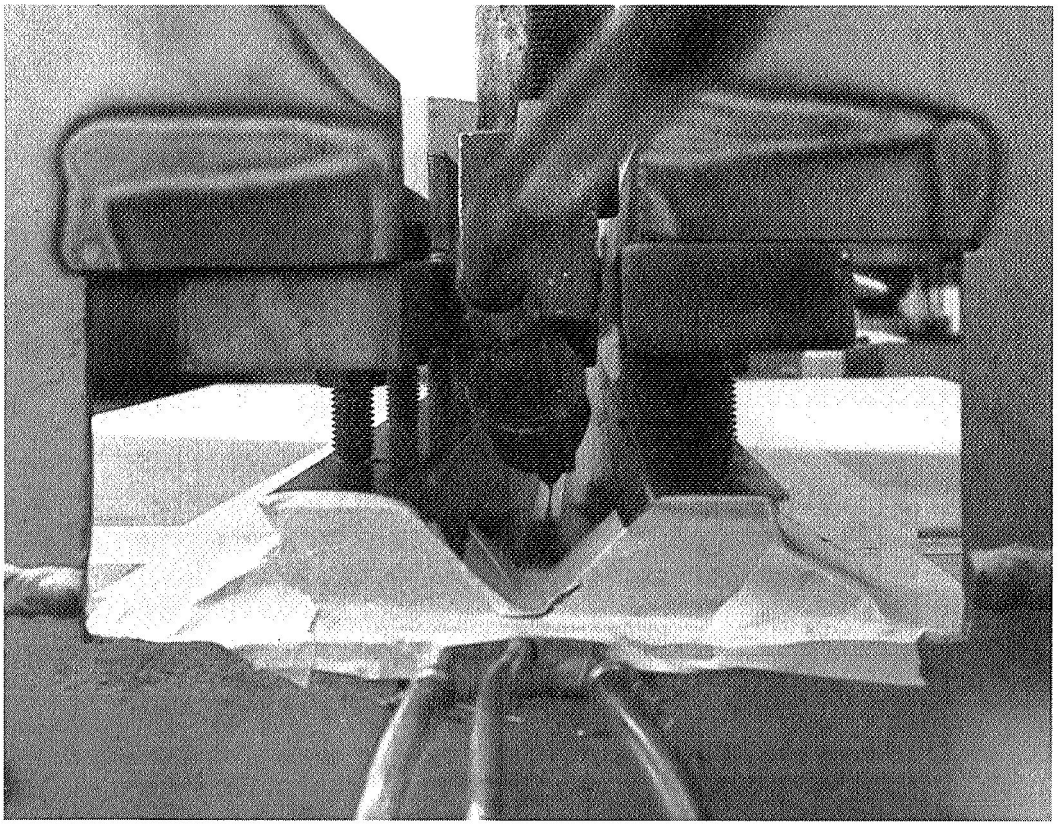

Figure 9: END VIEW OF WELD TOOLING USED FOR TITANIUM WELDING

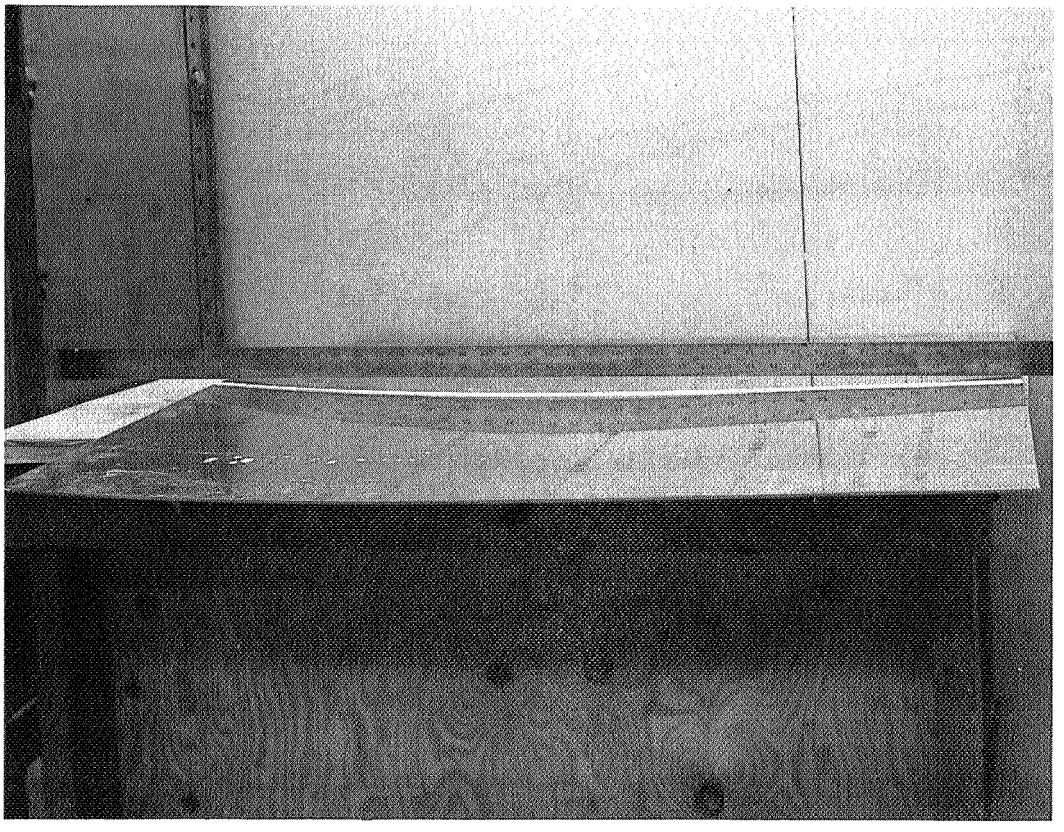

Figure 10: WELD DISTORTION IN 0.125 INCH THICK 2219-T87 ALUMINUM PANEL

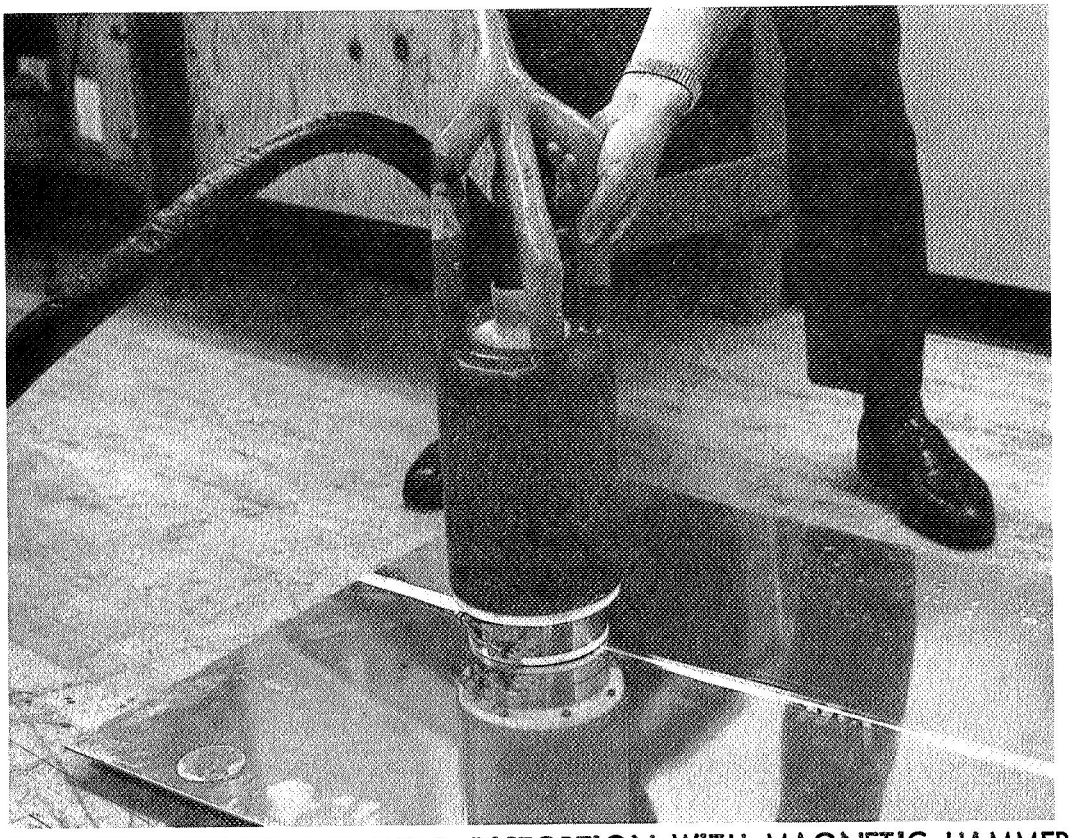

Figure 11: REMOVING WELD DISTORTION WITH MAGNETIC HAMMER

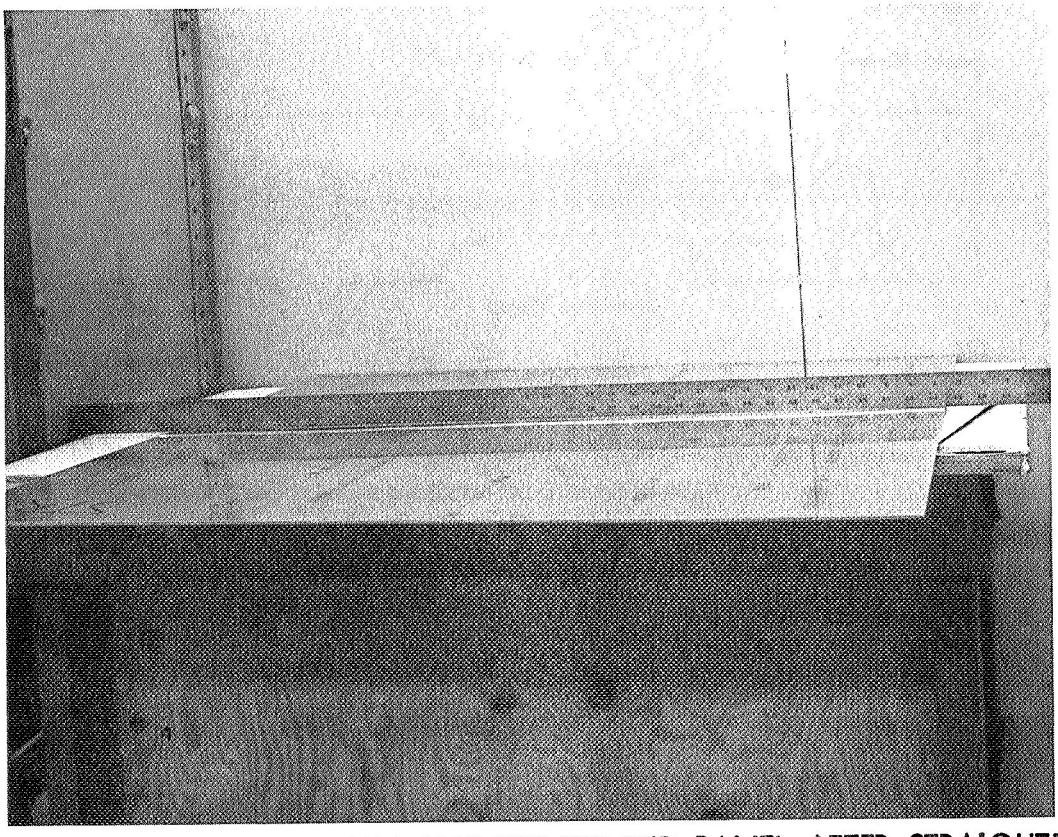

Figure 12: 0.125 INCH THICK 2219-T87 WELDED PANEL AFTER STRAIGHTENING

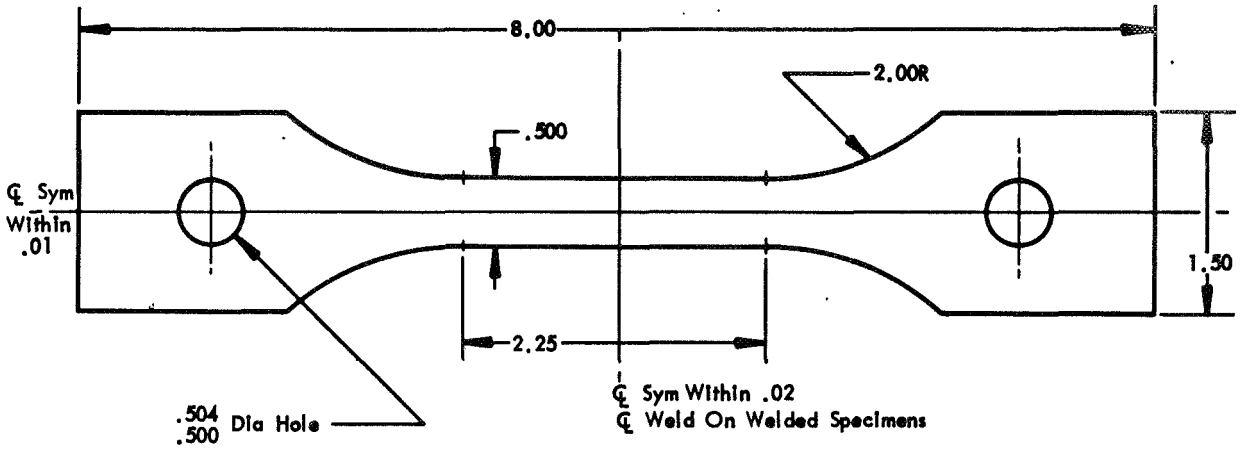


On Welded Specimens Grind Weld Bead Flush Within ±.01 On Both Sides

Weld Metal Specimens For 5Al-2.5 Sn (ELI) Titanium & 2219-T87 Aluminum All Thicknesses

Base Metal Specimens For 5Al-2.5 Sn (ELI) Titanium & 2219-T87 Aluminum All Thicknesses Except 1.00 (See Figure )

All Dimensions In Inches

Figure 13: MECHANICAL PROPERTY SPECIMEN FOR 5AL-2.5Sn (ELI) TITANIUM AND 2219-T87 ALUMINUM (Base and Weld Metal)

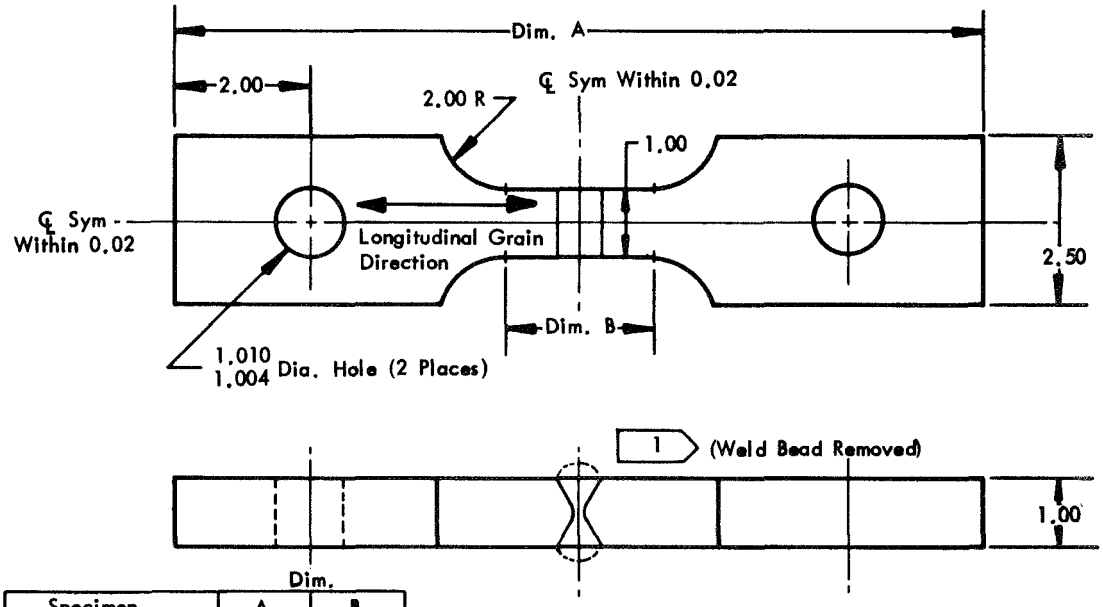


| Specimen | | A | B |
|---|---|---|---|
| -1 | R.T. & -320°F | 12.00 | 2.25 |
| -2 | -423°F | 22.00 | 12.25 |

All Dimensions In Inches

1 Thickness In Reduced Section Must Not Be Less Than The Plate Thickness After Removing The Weld Bead

Figure 14: MECHANICAL PROPERTY SPECIMEN FOR 1.00 THICK 2219 ALUMINUM WELD

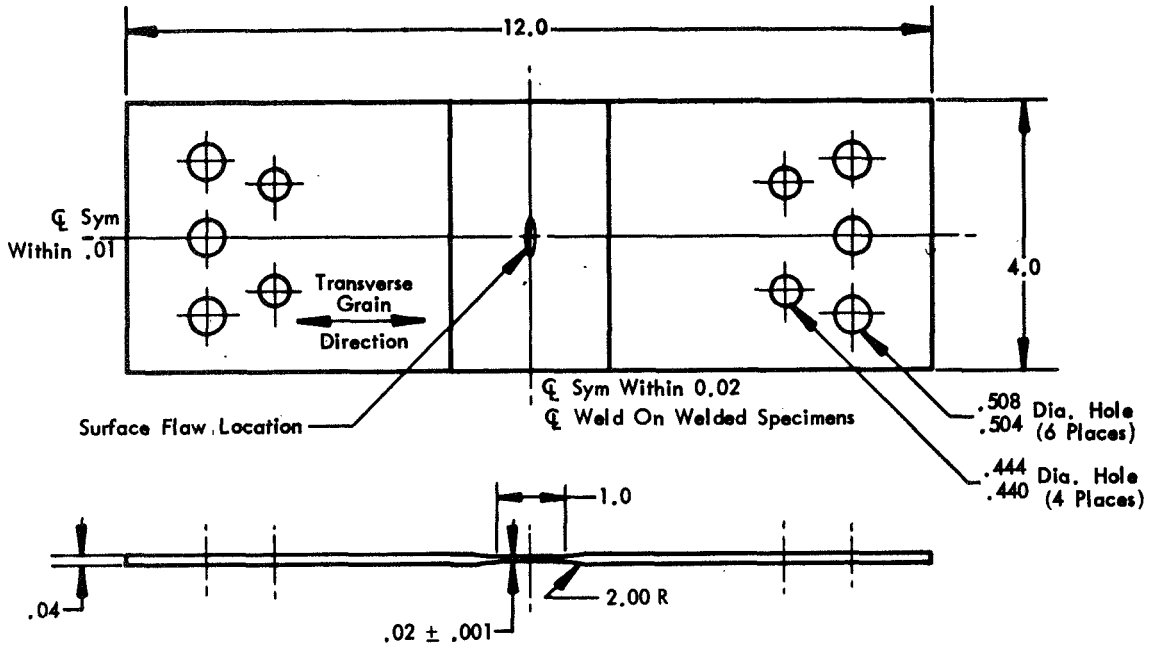


Weld & Base Metal
All Dimensions In Inches
On Welded Specimens Grind Weld Bead Flush Within ± .01 On Both Sides
Specimen No. 4

Figure 15: SURFACE FLAW SPECIMEN FOR 5AL-2.5Sn (ELI) TITANIUM

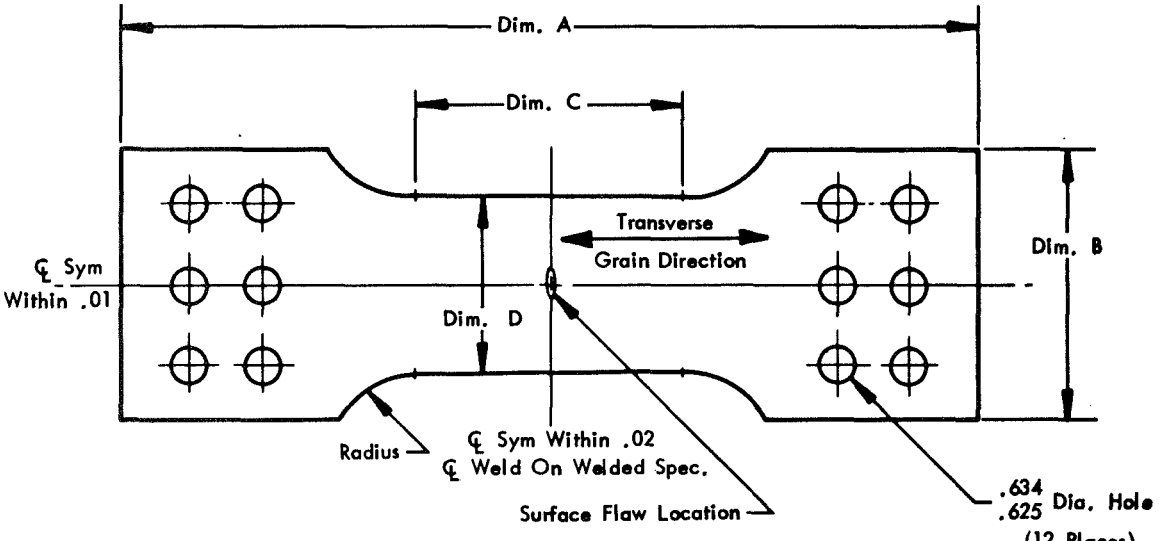


| Specimen No. | Dim. A | Dim. B | Dim. C | Dim. D | Radius | |
|---|---|---|---|---|---|---|
| 3-2 | 16.00 | 4.75 | 5.00 | 3.25 | 3.00 | Base Metal Only |
| 3-3A | 19.00 | 6.00 | 8.00 | 4.75 | 3.00 | Base Metal Only |
| 3-12 | 16.00 | 4.75 | 5.00 | 2.75 | 3.00 | Base & Weld Metal |
| 3-13 | 15.00 | 6.00 | 5.00 | 4.00 | 2.00 | Base & Weld Metal |

All Dimensions In Inches Specimen Made From 0.20" Thick Plate
On Welded Specimens Grind Weld Bead Flush Within ± .01 On Both Sides

Figure 16: SURFACE FLAW SPECIMEN FOR 5AL-2.5Sn (ELI) TITANIUM

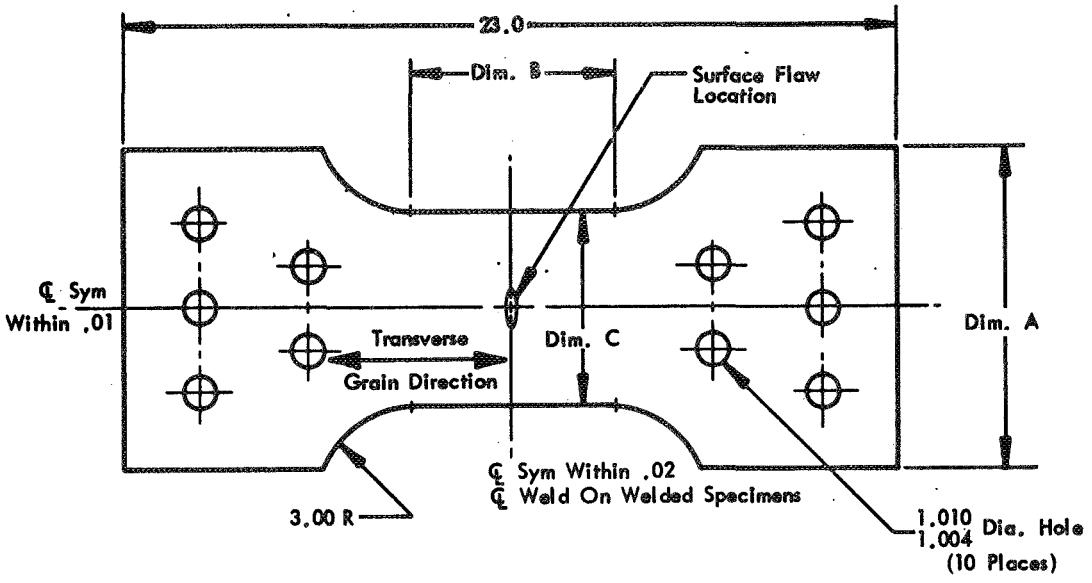


| Specimen No. | Dim. A | Dim. B | Dim. C | |
|---|---|---|---|---|
| 3-4 | 9.00 | 7.00 | 7.00 | Base Metal Only |
| 3-14 | 8.75 | 6.00 | 5.75 | Weld Metal Only |
| 3-16 | 8.75 | 6.00 | 6.00 | Base Metal Only |

Specimens Made From 0.20" Thick Plate

All Dimensions In Inches

On Welded Specimens Grind Weld Bead Flush Within ± .01 On Both Sides

Figure 17: SURFACE FLAW SPECIMEN FOR 5AL-2.5Sn (ELI) TITANIUM

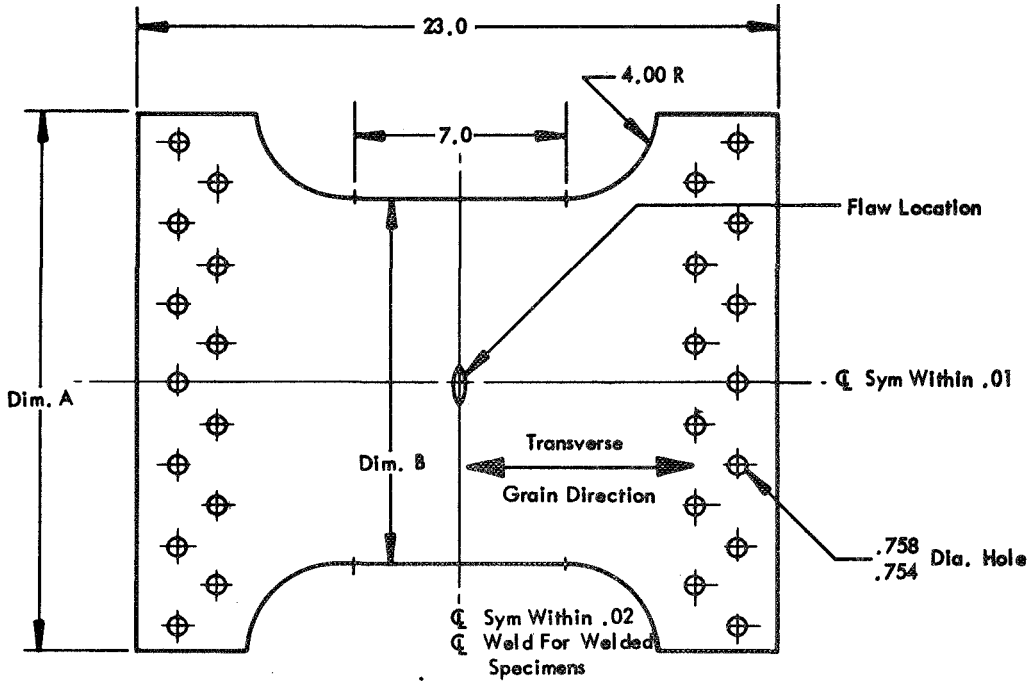


| Specimen No. | Dim. A | Dim. B | No. Holes | |
|---|---|---|---|---|
| 3-5 | 20.00 | 13.5 | 26 | Base Metal Only |
| 3-15 | 17.50 | 11.00 | 22 | Weld Metal Only |

Specimen Made From .20 Thick Plate All Dimensions In Inches

On Welded Specimens Grind Weld Bead Flush Within ± .01 On Both Sides

Figure 18: SURFACE FLAW SPECIMEN FOR 5AL-2.5Sn (ELI) TITANIUM

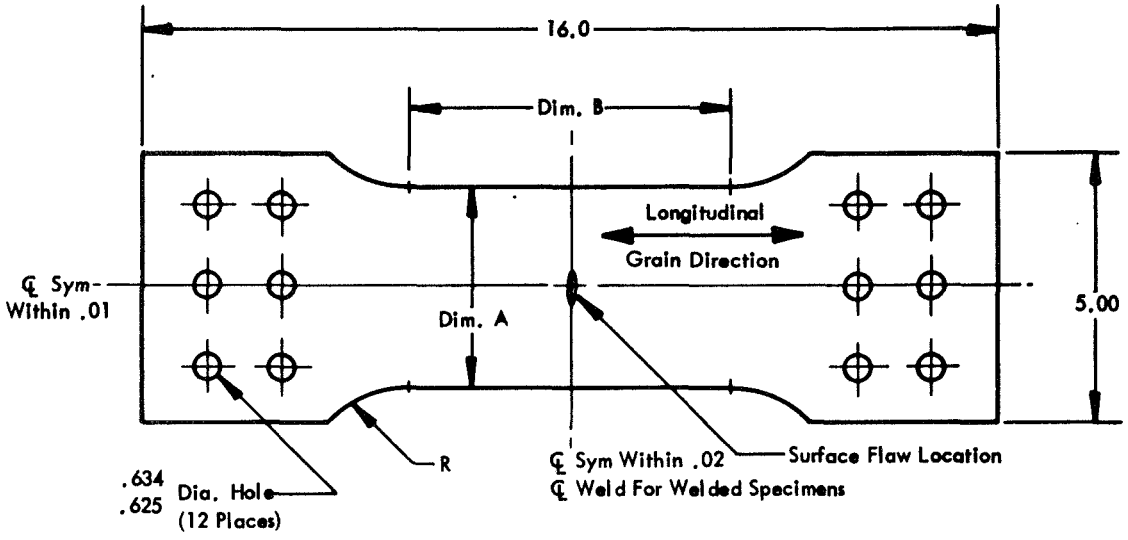


| Specimen No. | Dim. A | Dim. B | Radius | Thickness | |
|---|---|---|---|---|---|
| 5-1 | 2.50 | 4.50 | 3.00 | .063 | Base Metal |
| 7-1 | 3.75 | 6.00 | 2.00 | .125 | Weld Metal |

All Dimensions In Inches

Figure 19: SURFACE FLAW SPECIMEN FOR 2219-T87 ALUMINUM

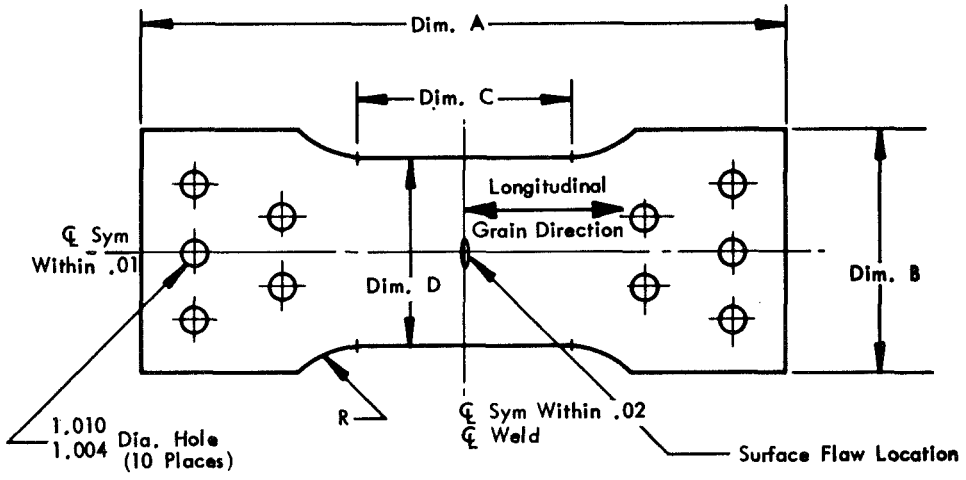


All Dimensions In Inches

| Specimen No. | Dim. A | Dim. B | Dim. C | Dim. D | Radius | Thickness | |
|---|---|---|---|---|---|---|---|
| 7-3 | 24.00 | 8.50 | 8.00 | 7.50 | 1.5 | .125 | Weld Metal Only |
| 5-2 | 27.00 | 8.90 | 10.00 | 5.50 | 3.0 | .063 | Base Metal Only |
| 5-3 | 27.00 | 8.90 | 10.00 | 6.75 | 3.0 | .063 | Base Metal Only |
| 5-2A | 27.00 | 8.90 | 10.00 | 5.50 | 3.0 | .625 | Base Metal Only |
| 5-3A | 27.00 | 8.90 | 10.00 | 5.50 | 3.0 | .625 | Base Metal Only |

On Welded Specimens Grind Weld Bead Flush Within ± .01 On Both Sides

Figure 20: SURFACE FLAW SPECIMEN FOR 2219-T87 ALUMINUM

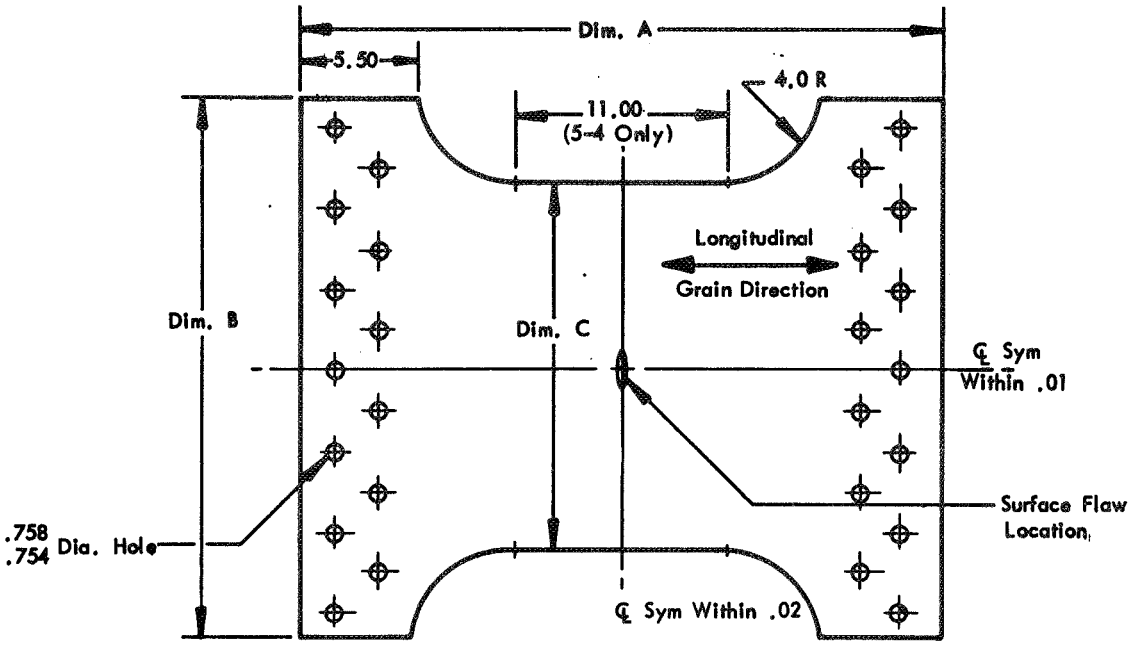


All Dimensions in Inches

| Specimen No. | Dim. A | Dim. B | Dim. C | Thickness | No. Holes | |
|---|---|---|---|---|---|---|
| 10-1 | 36.00 | 18.00 | 11.00 | .625 | 22 | Base Metal |
| 10-2 | 36.00 | 22.5 | 14.5 | .625 | 26 | Base Metal |
| 10-3 | 36.00 | 30.00 | 22.00 | .625 | 38 | Base Metal |
| 5-4 | 27.00 | 20.00 | 12.0 | .063 | 26 | Base Metal |

Figure 21: SURFACE FLAW SPECIMEN FOR 2219-T87 ALUMINUM

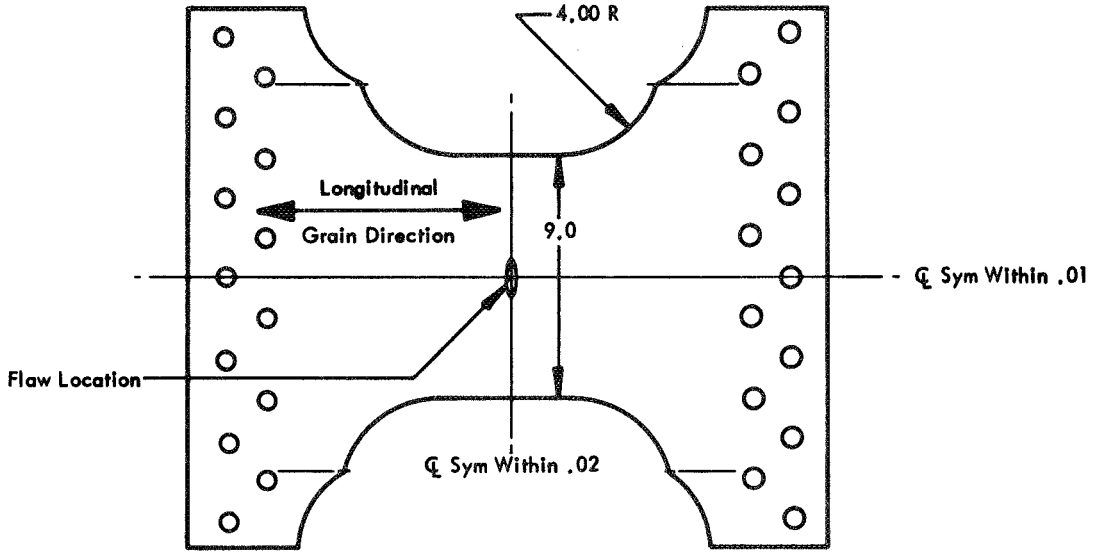


Make From 5-4 Specimen
All Dimensions in Inches

Figure 22: SURFACE FLAW SPECIMEN FOR 2219-T87 ALUMINUM

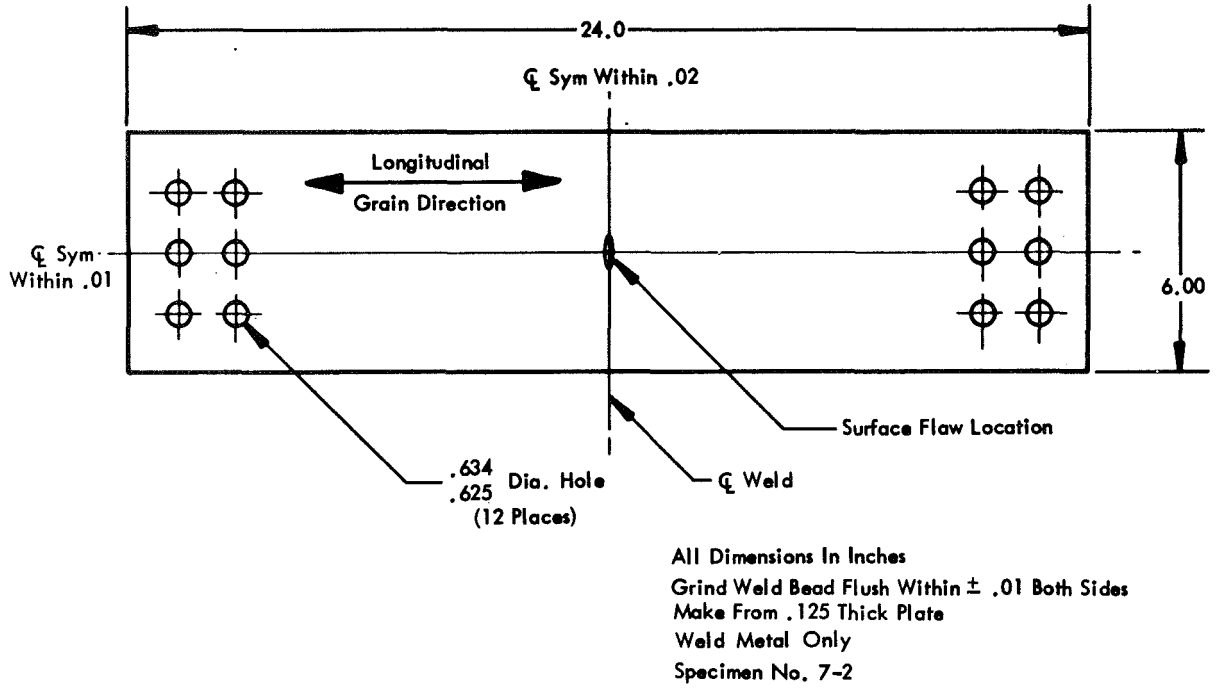


Figure 23: SURFACE FLAW SPECIMEN FOR 2219 ALUMINUM WELD

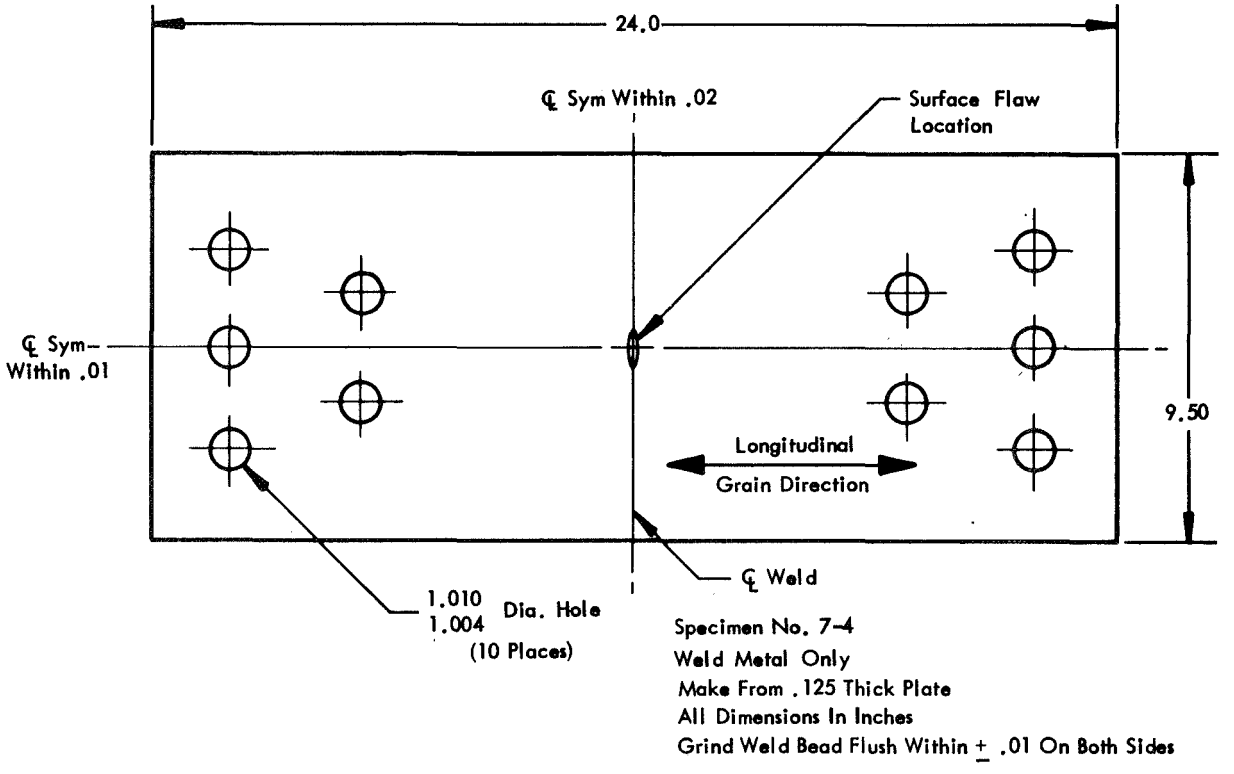


Figure 24: SURFACE FLAW SPECIMEN FOR 2219 ALUMINUM WELD

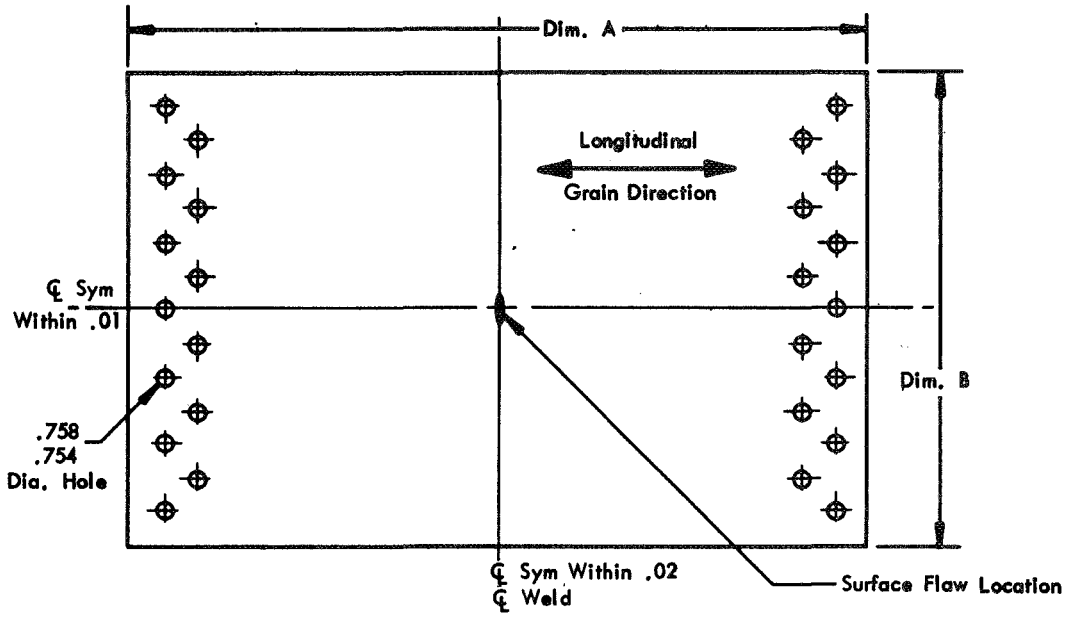


All Dimensions In Inches
Grind Weld Flush Within ± .01
On Both Sides Of Weld Metal
Specimens

| Specimen No. | Dim. A | Dim. B | Thickness | No. Holes | |
|---|---|---|---|---|---|
| 7-5 | 30.00 | 12.00 | .125 | 14 | Weld Metal Only |
| 7-6 | 30.00 | 13.50 | 1.00 | 14 | Weld Metal Only |
| 7-7 | 30.00 | 16.00 | 1.00 | 18 | Weld Metal Only |
| 7-8 | 36.00 | 24.00 | 1.00 | 30 | Weld Metal Only |
| 7-9 | 36.00 | 30.00 | 1.00 | 38 | Weld Metal Only |
| 7-11 | 36.00 | 20.00 | 1.00 | 22 | Weld Metal Only |

Figure 25: SURFACE FLAW SPECIMEN FOR 2219-T87 ALUMINUM

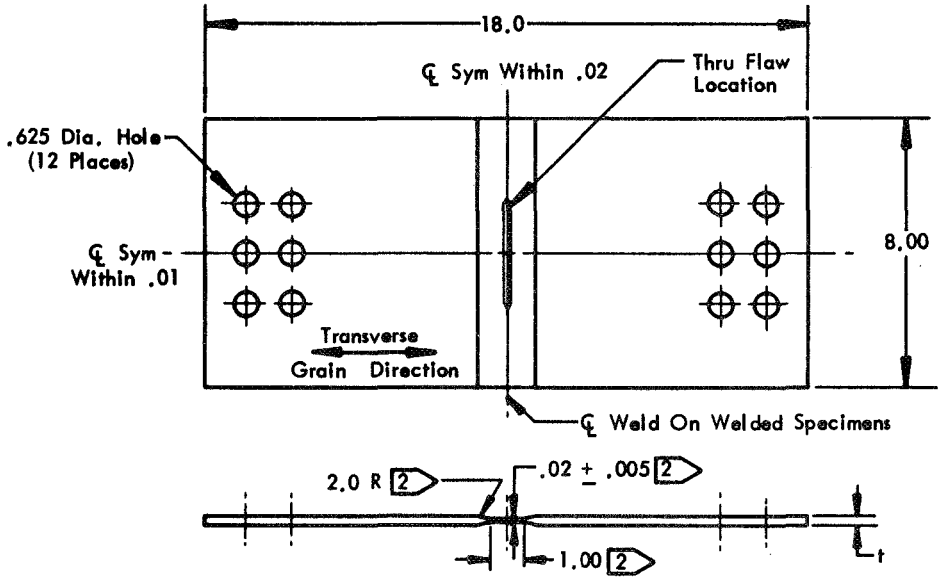


[2] This Dimension Applies Only To Specimens Made From .040 Sheet

On Welded Specimens Grind Weld Bead Flush Within ± .01 On Both Sides

| Specimen No. | Thickness |
|---|---|
| 8-1 | .040 |
| 8-1A | .200 |

All Dimensions In Inches
Weld & Base Metal

Figure 26: CENTER CRACK FLAW SPECIMEN FOR 5AL-2.5Sn (ELI) TITANIUM

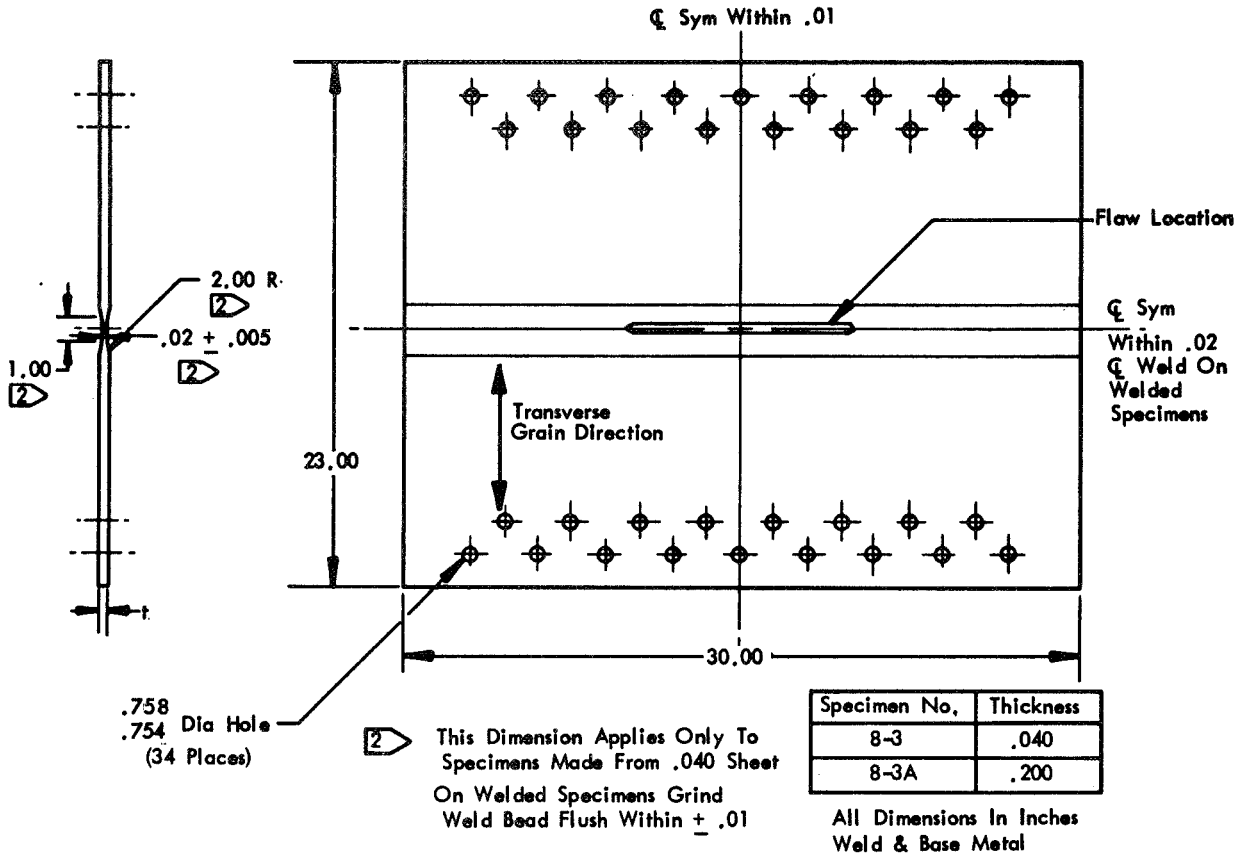


| Specimen No. | Thickness |
|---|---|
| 8-3 | .040 |
| 8-3A | .200 |

Figure 27: CENTER CRACK FLAW SPECIMEN FOR 5AL-2.5Sn (ELI) TITANIUM

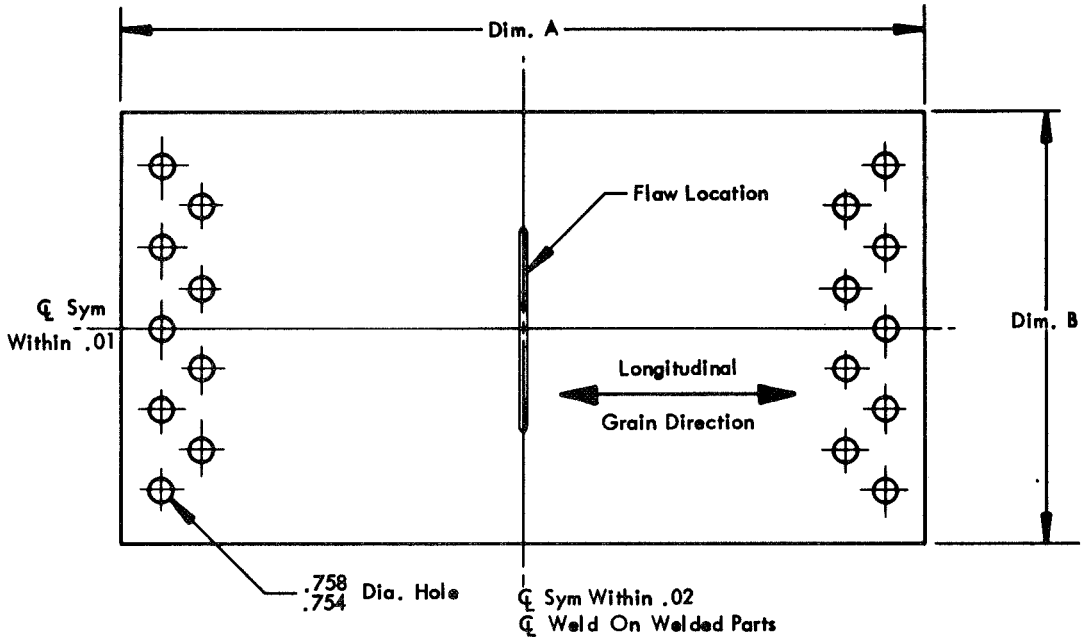


| Specimen No. | Dim. A | Dim. B | Thickness | No. Holes | |
|---|---|---|---|---|---|
| 8-2 | 36.00 | 16.00 | .063 & .625 | 18 | Base Metal Only |
| 8-4 | 36.00 | 36.00 | .125 & 1.00 | 22 | Weld Metal Only |
| 8-5 | 24.00 | 12.00 | .063, .625 & 1.00 | 14 | Base & Weld Metal |
| 8-6 | 36.00 | 30.00 | .125 | 38 | Weld Metal Only |

All Dimensions In Inches
On Welded Specimens Grind Weld Bead Flush Within ± .01 On Both Sides.

Figure 28: CENTER CRACK FLAW SPECIMEN FOR 2219-T87 ALUMINUM

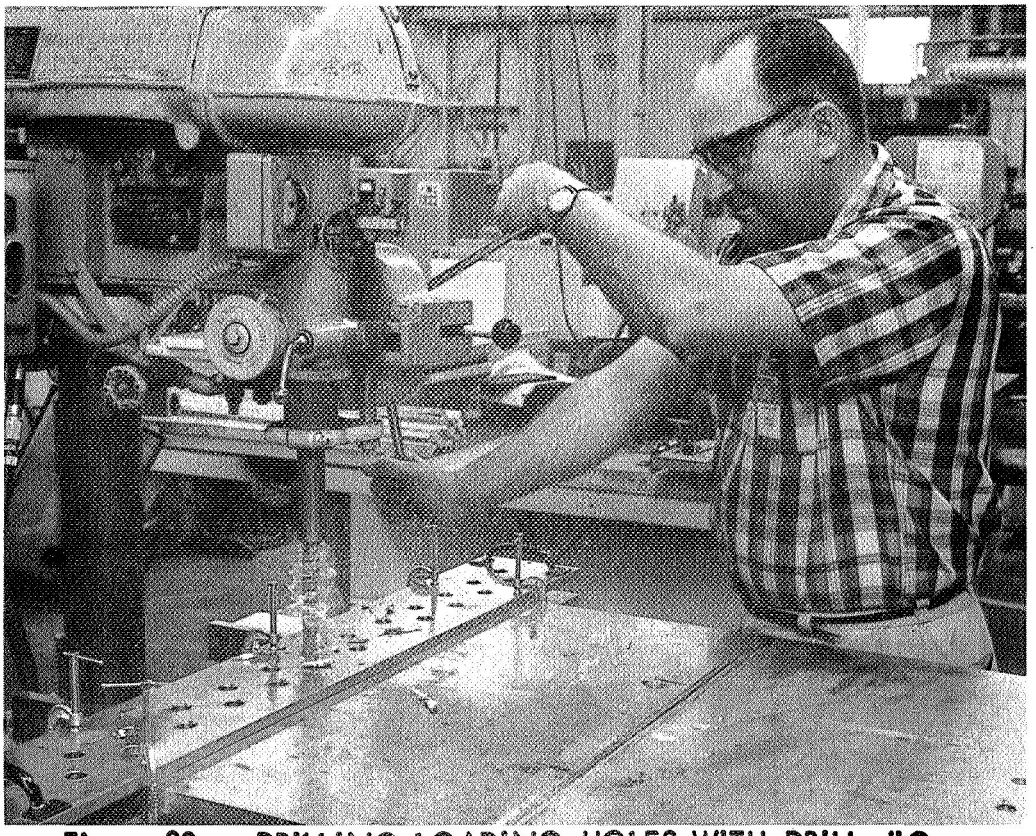

Figure 29: DRILLING LOADING HOLES WITH DRILL JIG IN 1.00 INCH THICK SPECIMEN

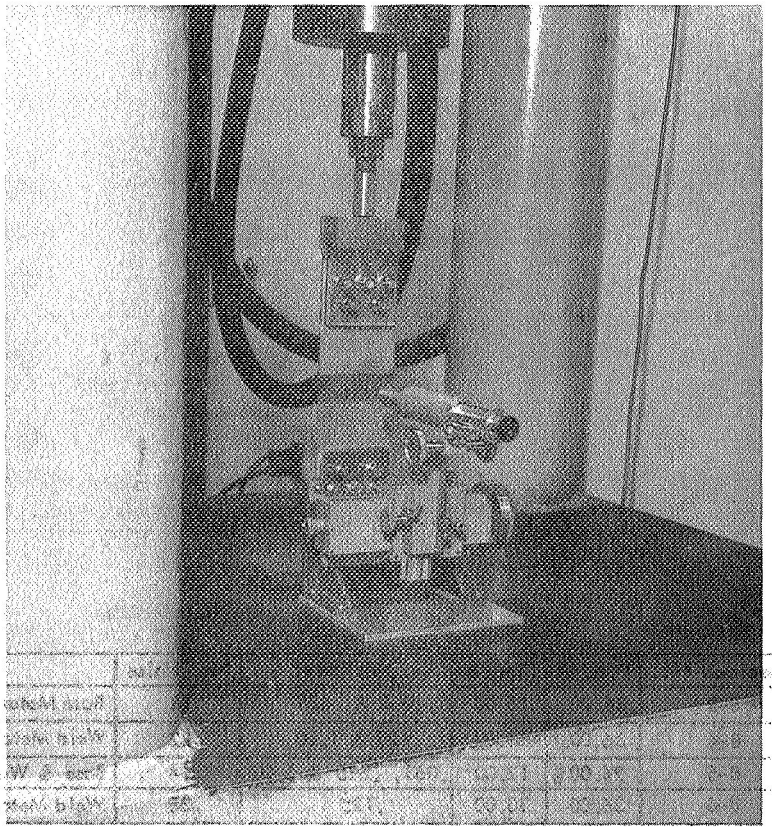

Figure 30: TEST SETUP FOR FATIGUE SHARPENING FLAW IN 0.020 INCH THICK TITANIUM SPECIMEN

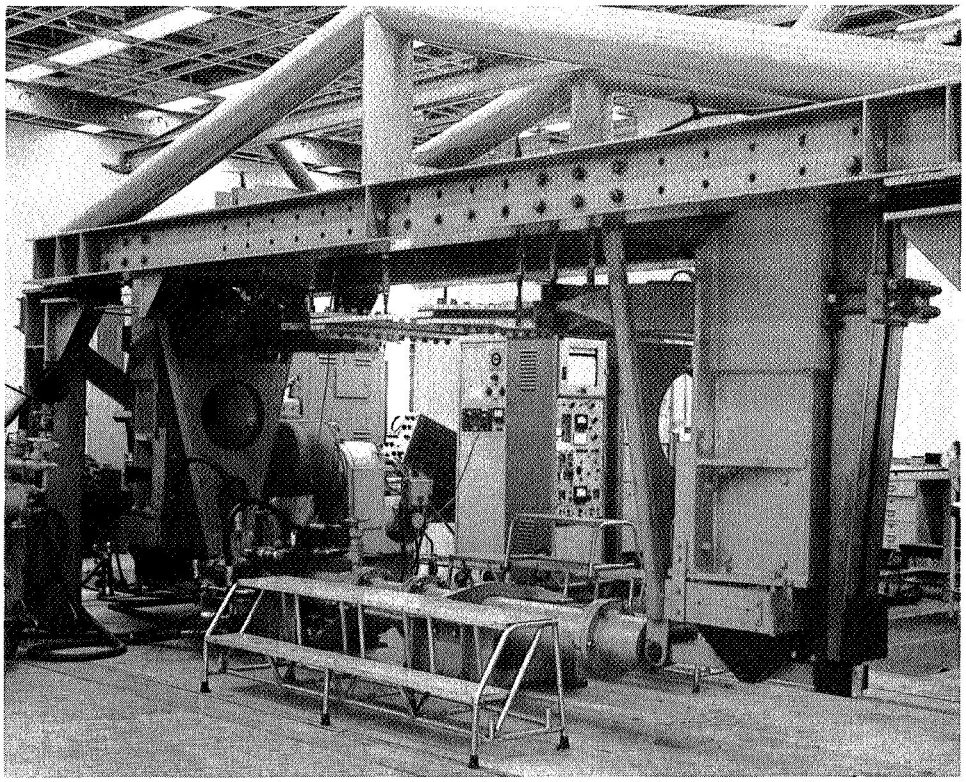

Figure 31: HORIZONTAL 350 KIP TEST MACHINE USED TO CYCLE AND STATIC TEST LARGER ROOM TEMPERATURE AND -320°F SPECIMENS

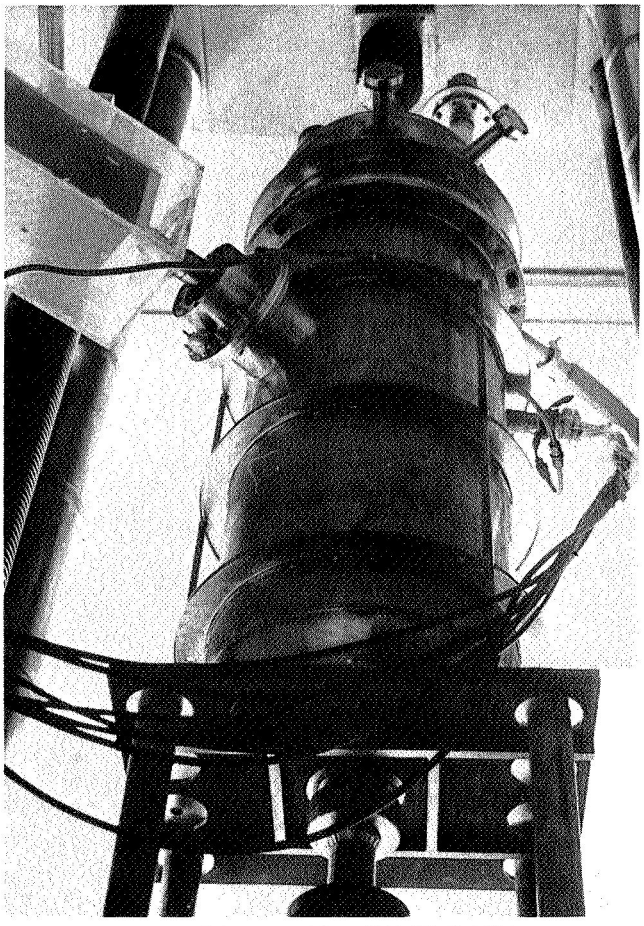

Figure 32: $LH_2$ CRYOSTAT

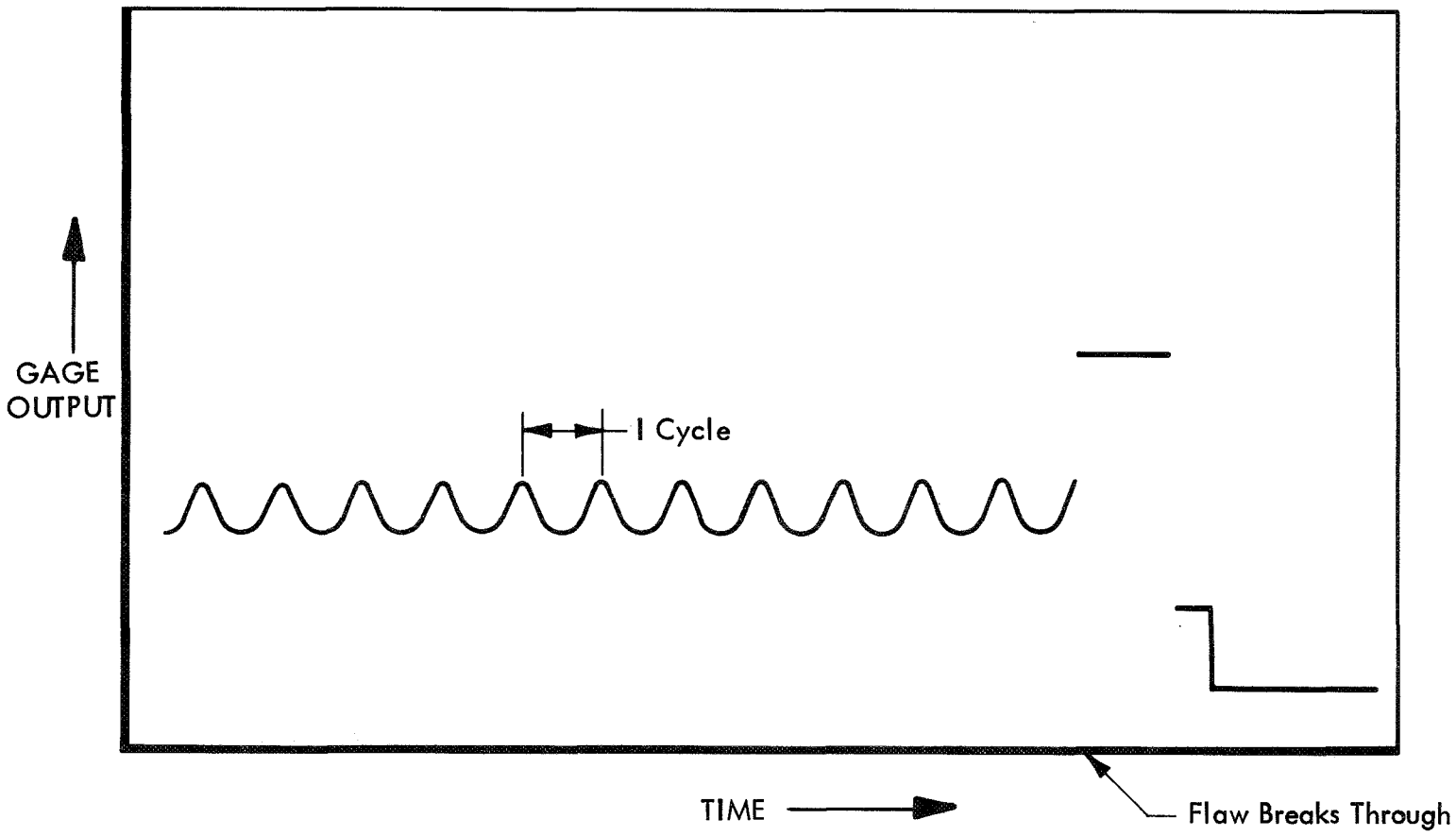


Figure 33: TRACE OF STRAIN GAGE BONDED TO BACK OF SPECIMEN TO DETECT BREAK THROUGH OF FLAW

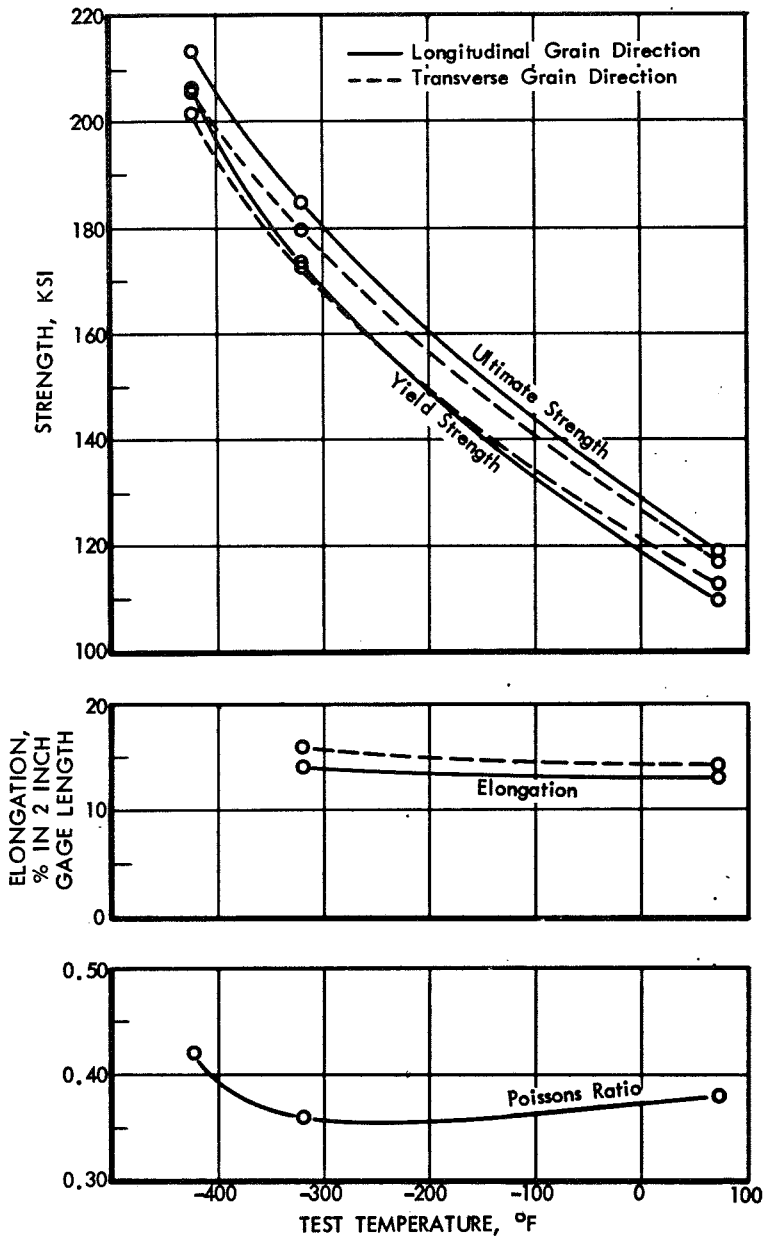


Figure 34: TENSILE PROPERTIES OF 5AI-2.5Sn TITANIUM, 0.040-INCH-THICK BASE METAL

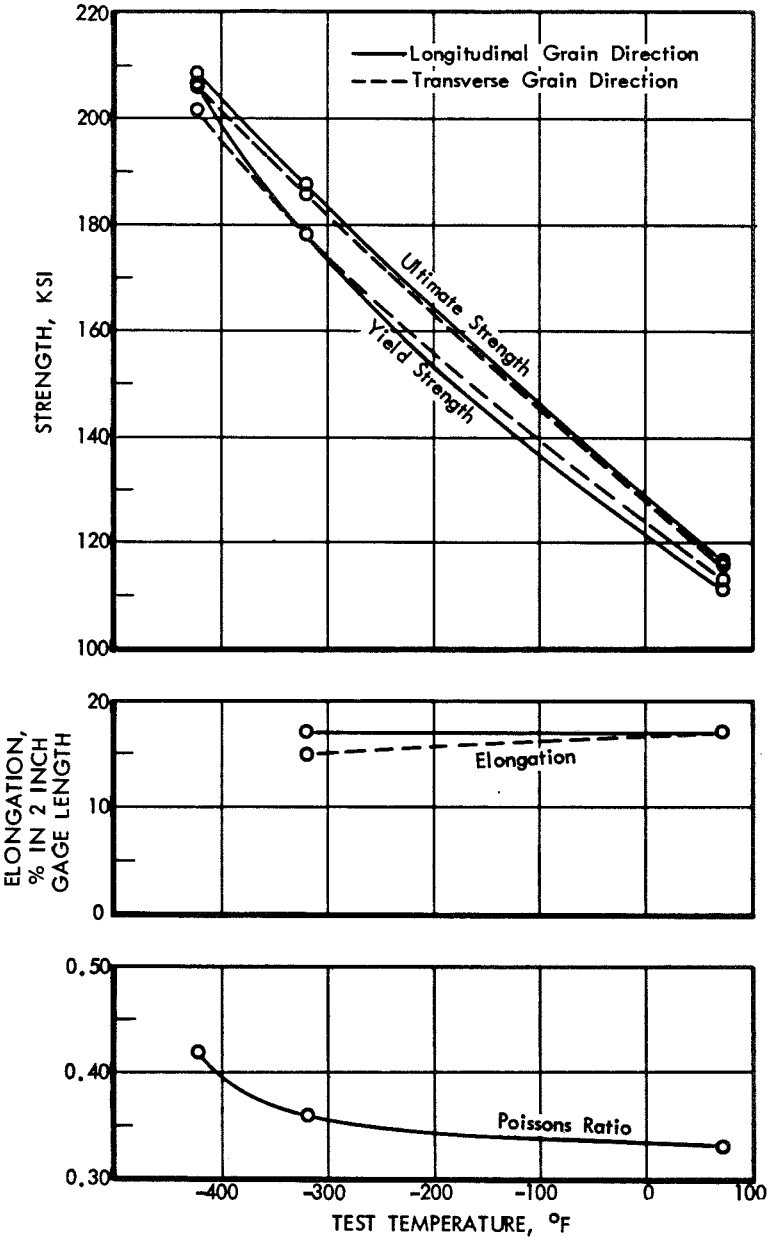


Figure 35: TENSILE PROPERTIES OF 5AI-2.5Sn TITANIUM, 0.200-INCH-THICK BASE METAL

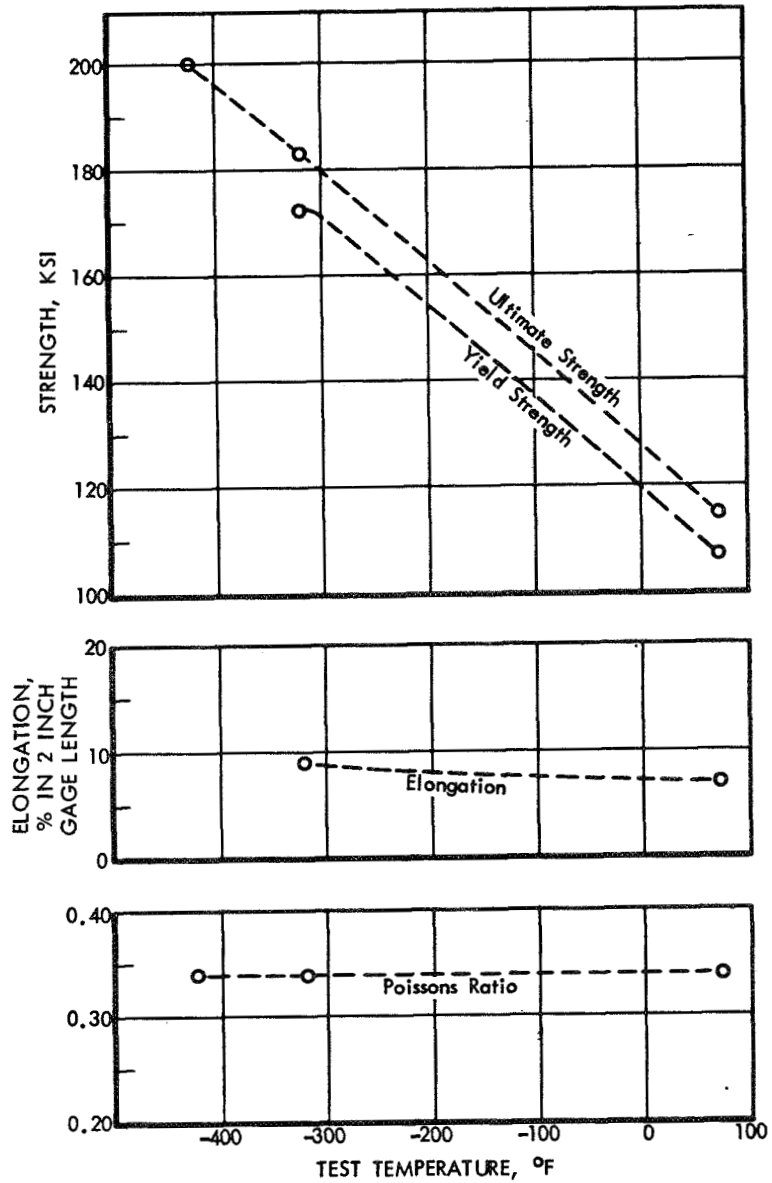


Figure 36: TENSILE PROPERTIES OF 5Al-2.5Sn TITANIUM, 0.040-INCH-THICK WELDMENT

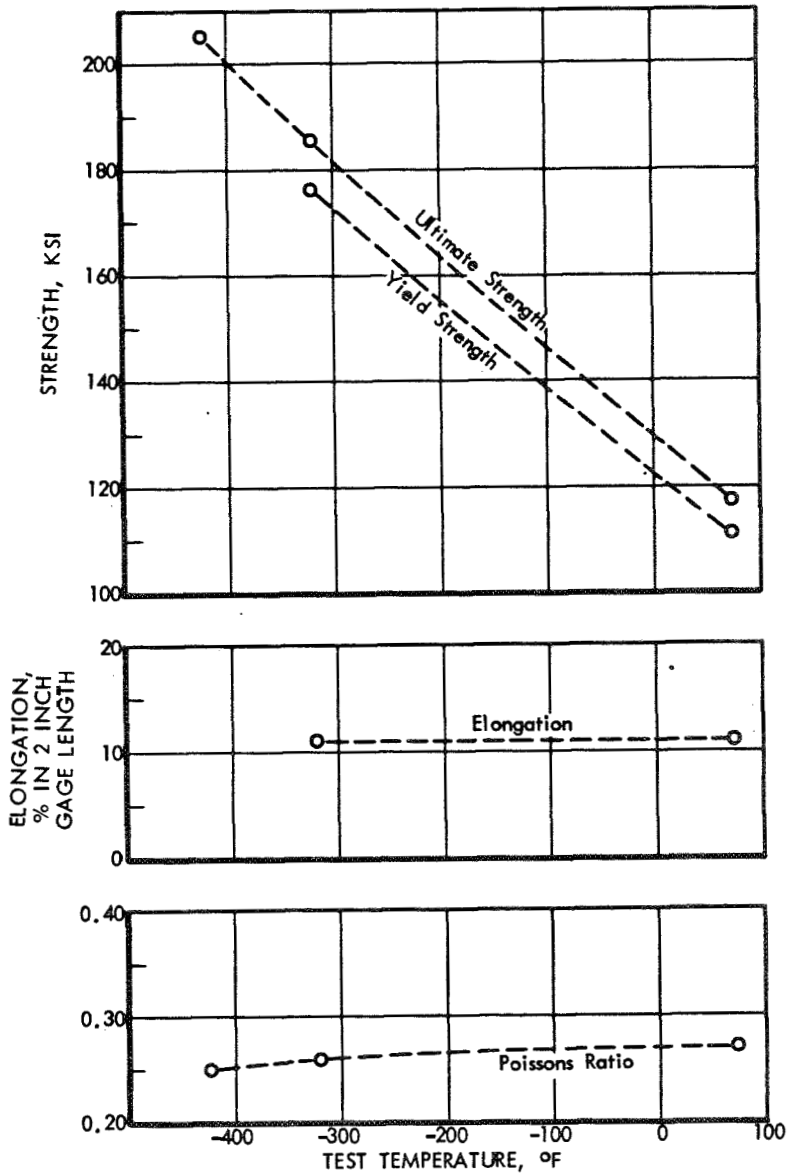


Figure 37: TENSILE PROPERTIES OF 5Al-2.5Sn TITANIUM, 0.200-INCH-THICK WELDMENT

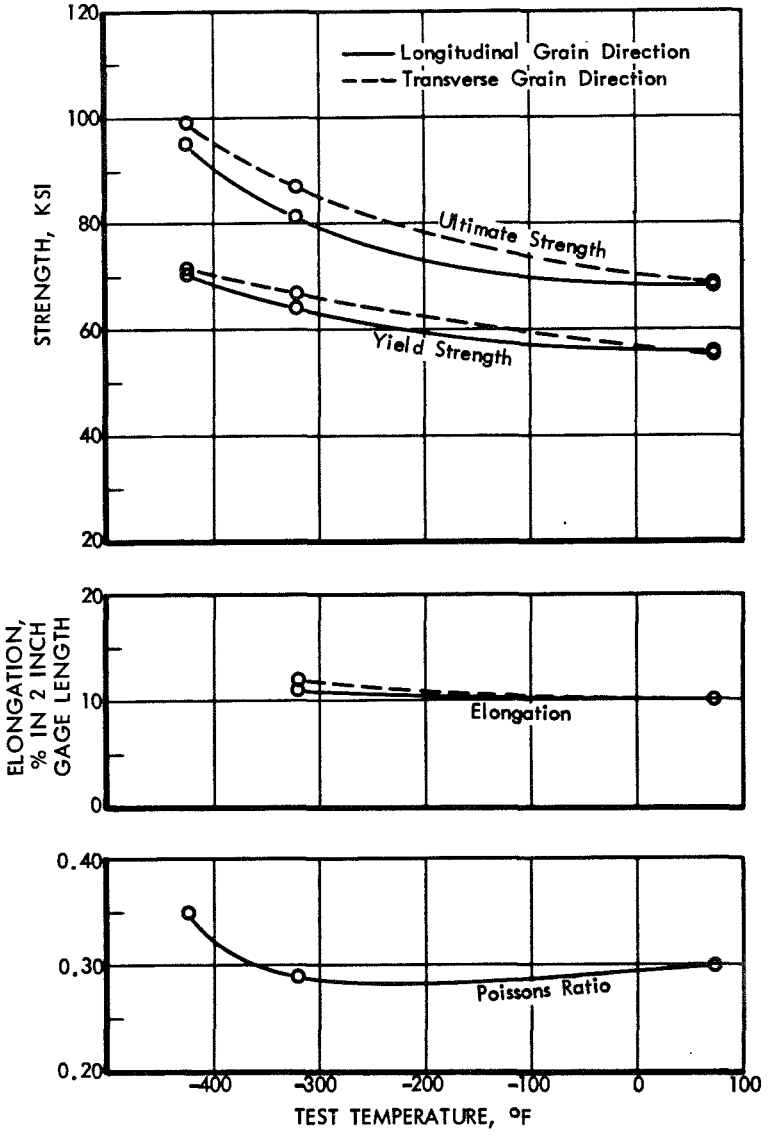


Figure 38: TENSILE PROPERTIES OF 2219-T87 ALUMINUM, 0.125-INCH-THICK BASE METAL

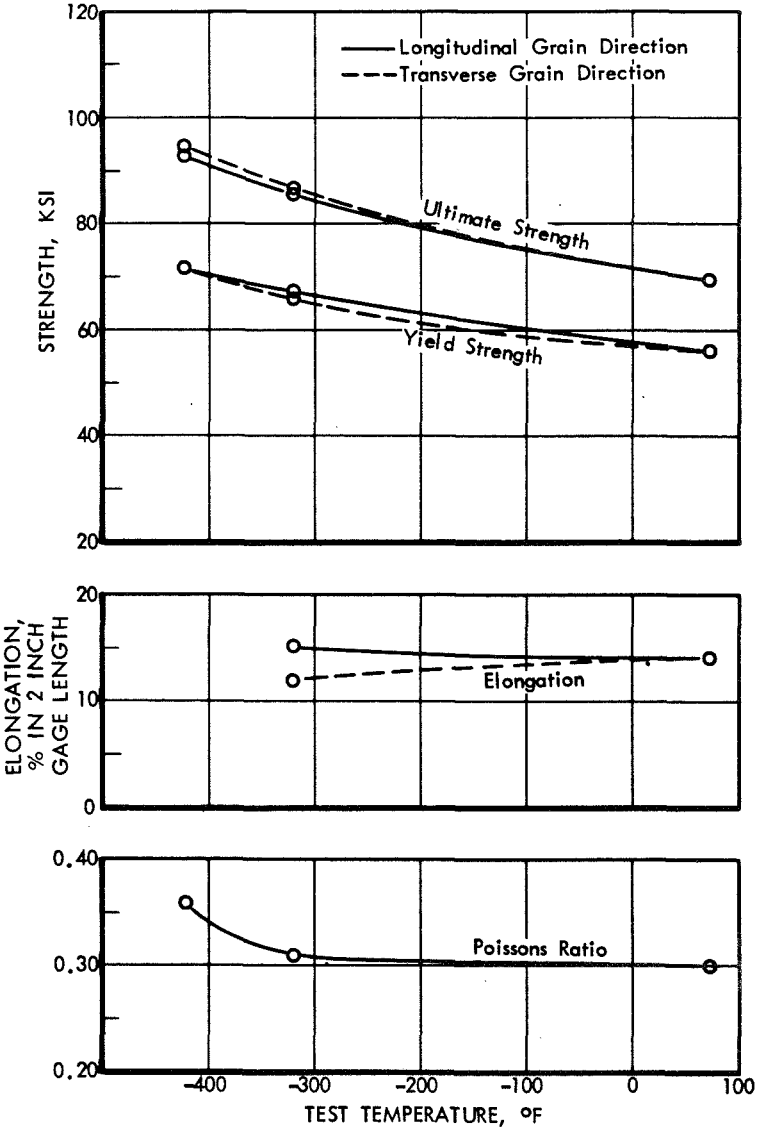


Figure 39: TENSILE PROPERTIES OF 2219-T87 ALUMINUM, 0.625-INCH-THICK BASE METAL

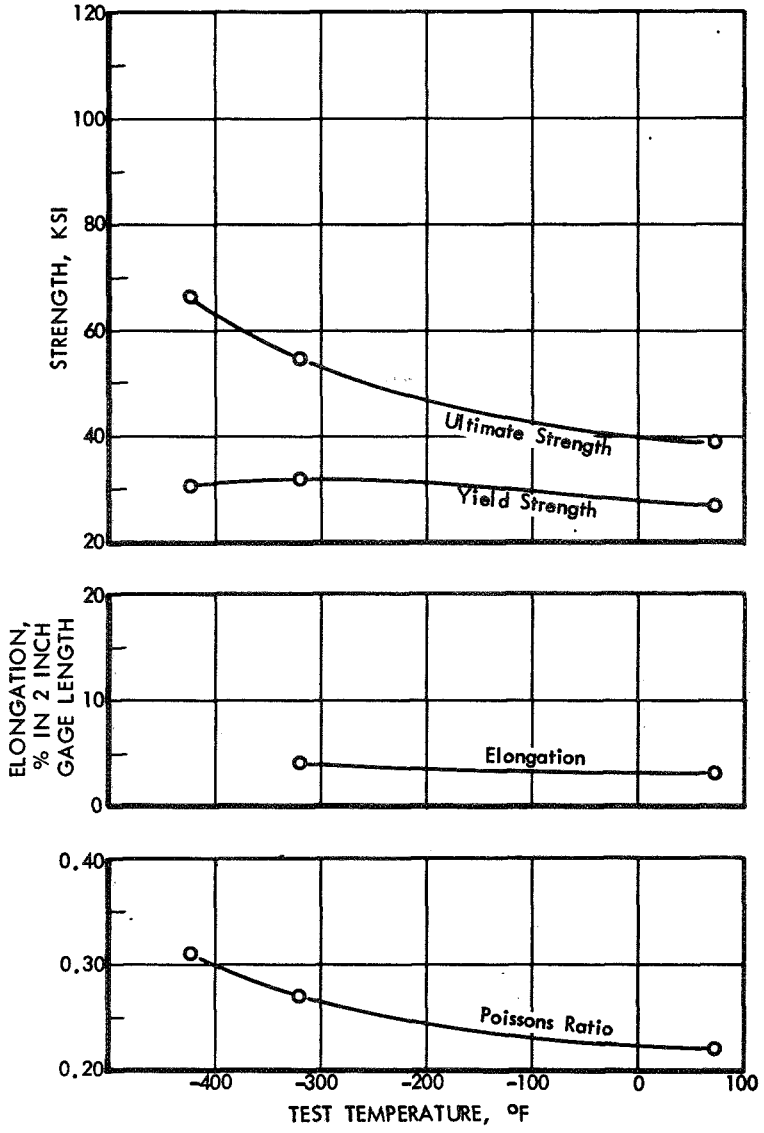


Figure 40: TENSILE PROPERTIES OF 2219 ALUMINUM, 0.125-INCH-THICK WELDMENT

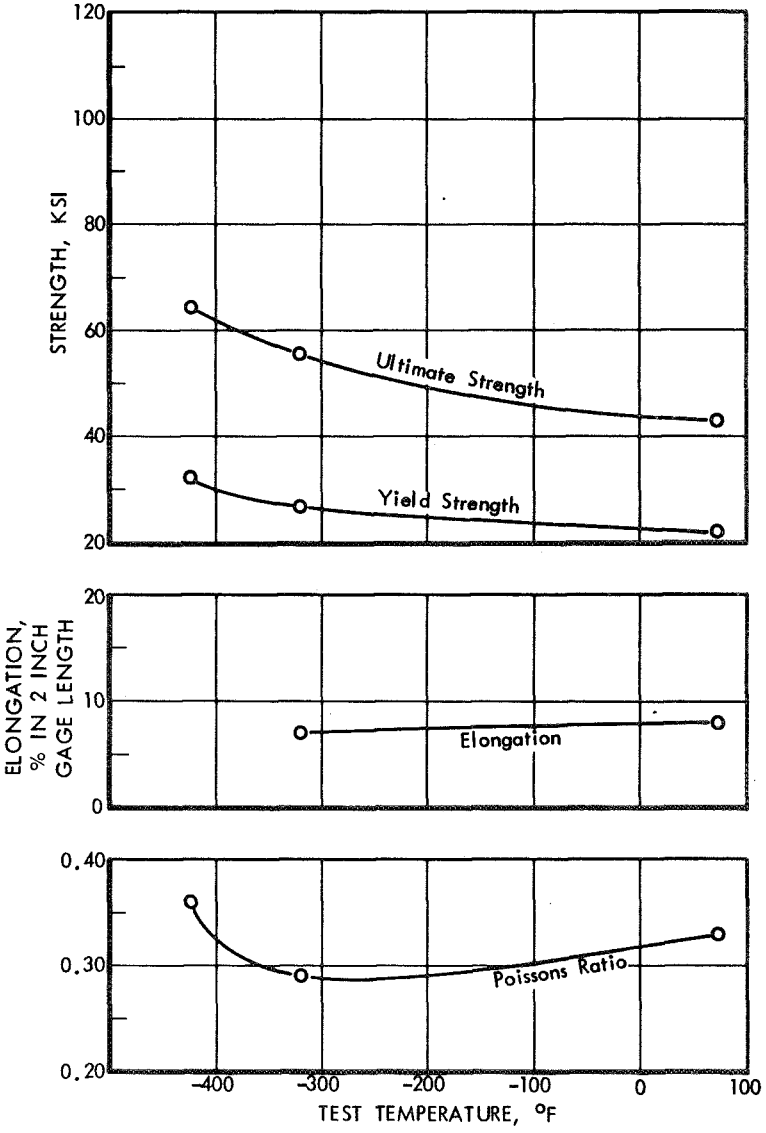


Figure 41: TENSILE PROPERTIES OF 2219 ALUMINUM, 1.00-INCH-THICK WELDMENT

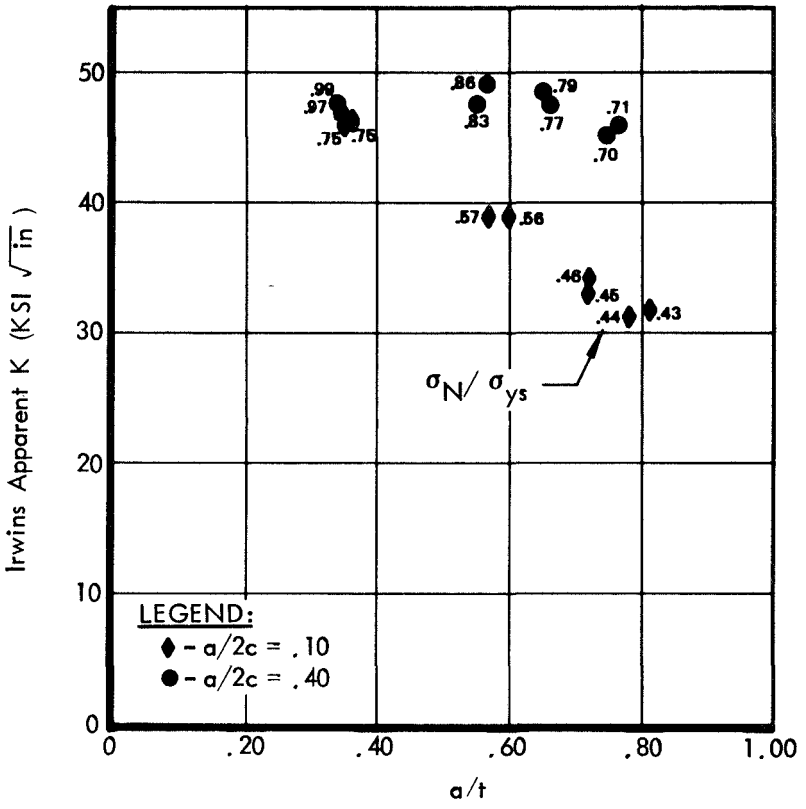


Figure 42: EFFECT OF FLAW DEPTH ON APPARENT K VALUES
(t = 0.625", 2219-T87 Aluminum Base Metal @ -423°F)

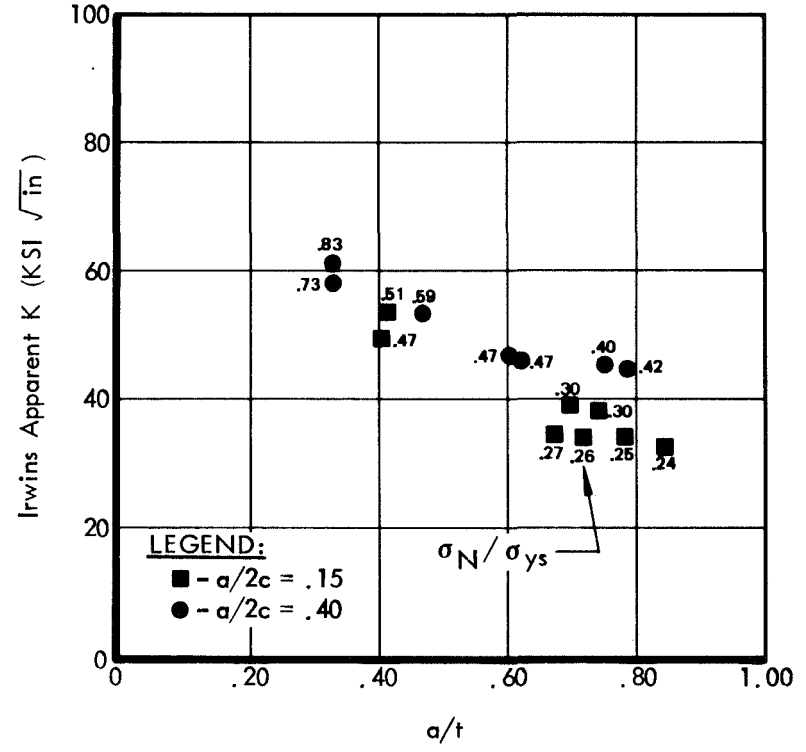


Figure 43: EFFECT OF FLAW DEPTH ON APPARENT K VALUES
(t = 0.200", 5Al-2.5Sn Titanium Base Metal @ -423°F)

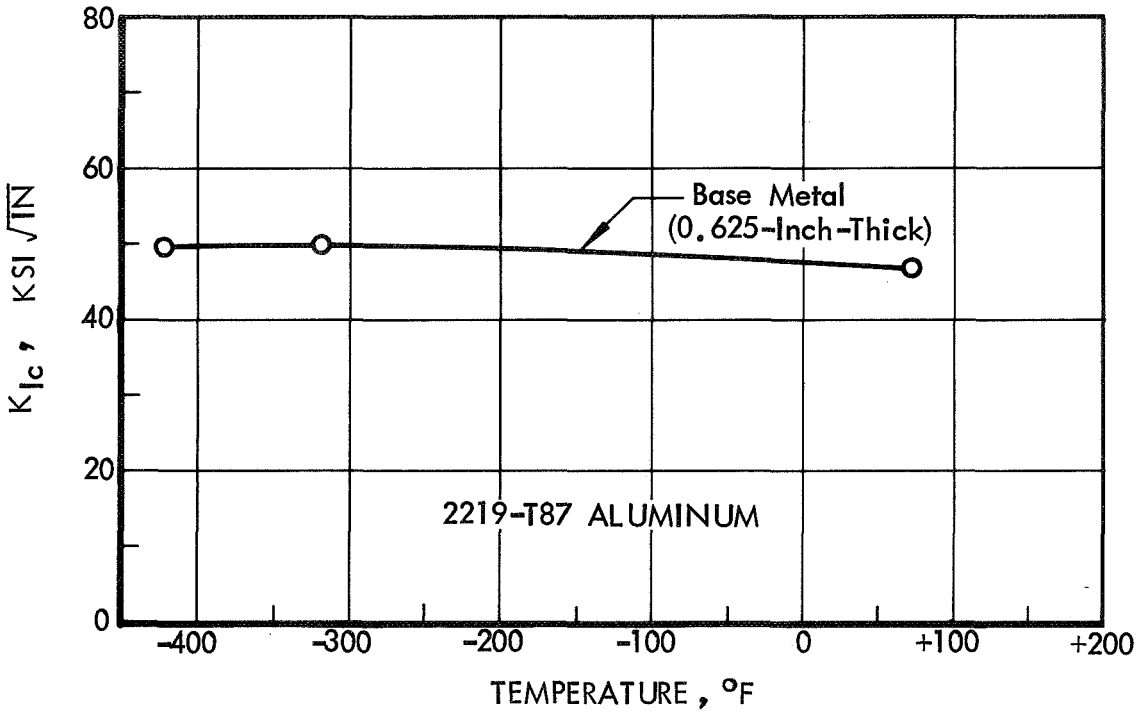


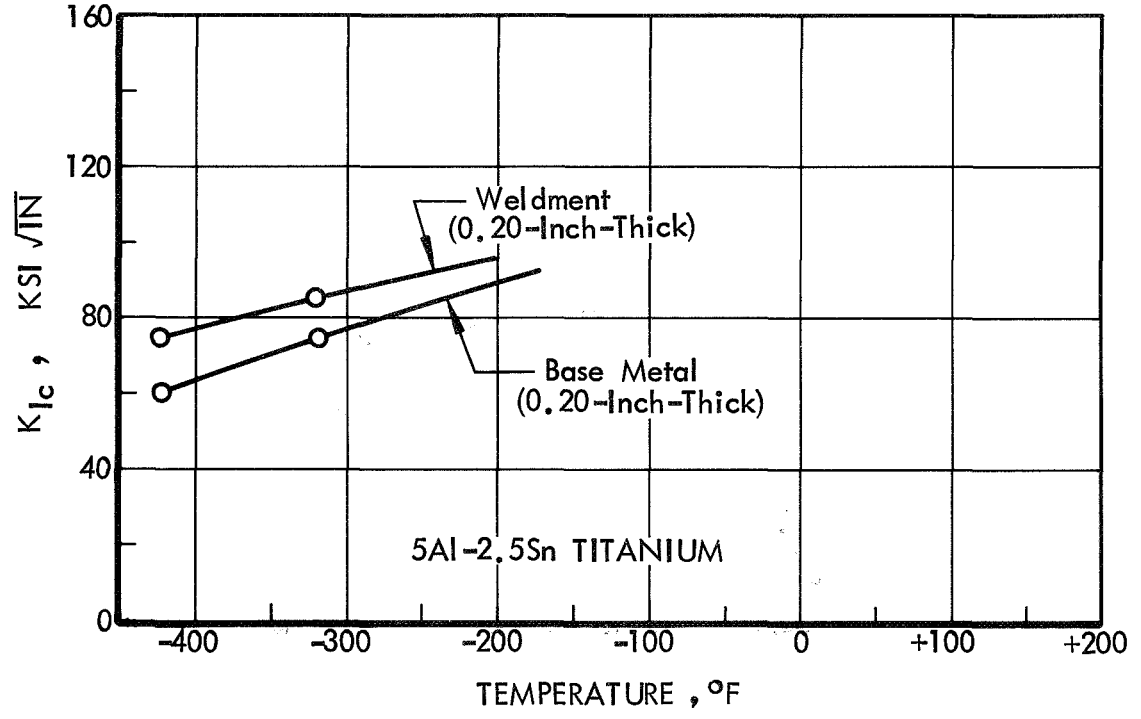


Figure 44 : BASELINE $K_{Ic}$ VALUES AS A FUNCTION OF TEST TEMPERATURE

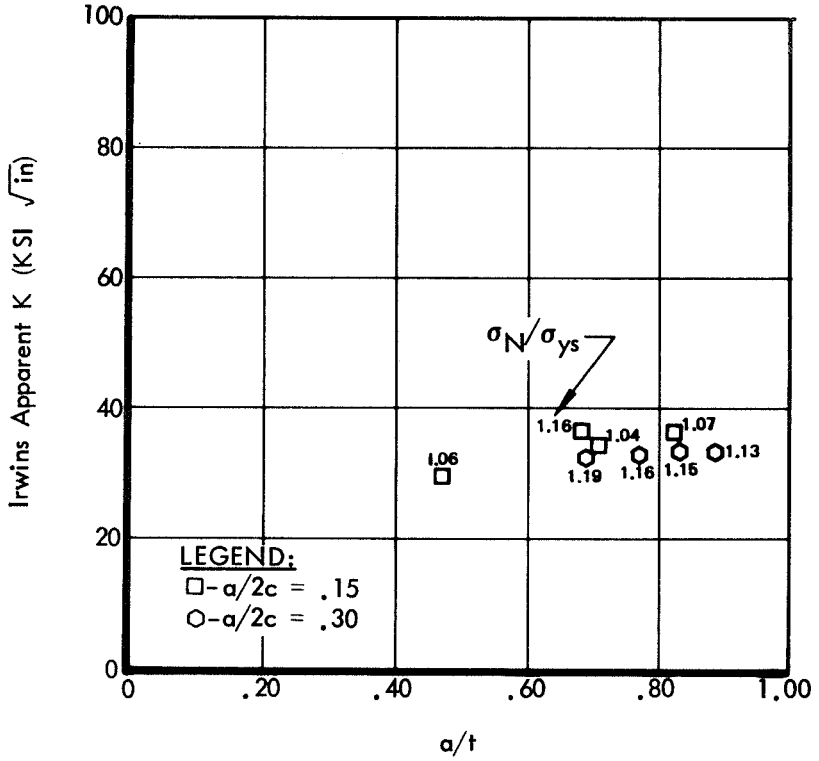


Figure 45: EFFECT OF FLAW DEPTH ON APPARENT K VALUES (t = 1.00", 2219 Aluminum Weld Metal @ R.T.)

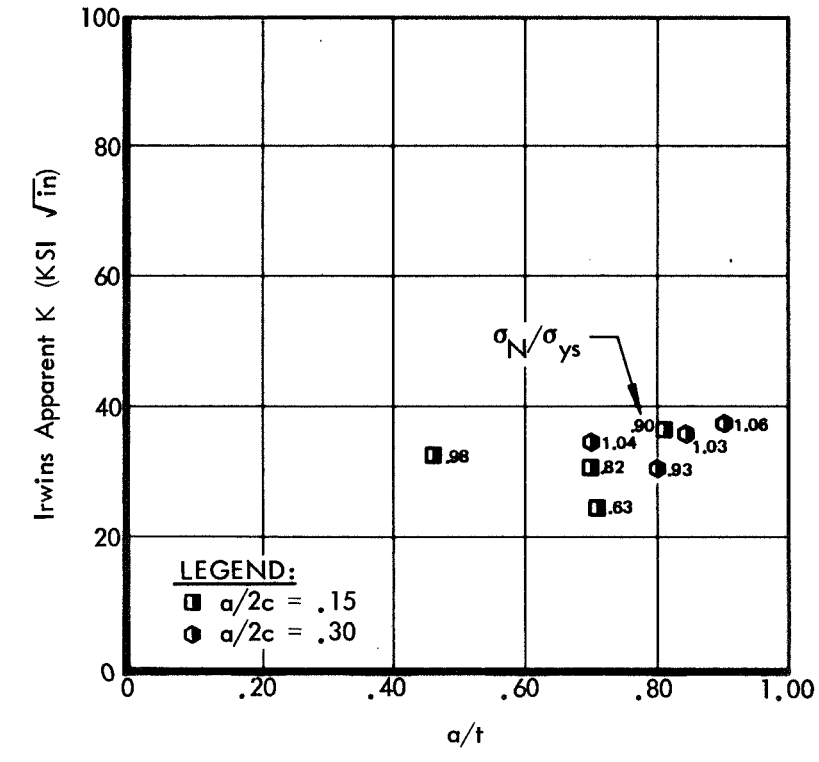


Figure 46: EFFECT OF FLAW DEPTH ON APPARENT K VALUES (t = 1.00", 2219 Aluminum Weld Metal @ -320°F)

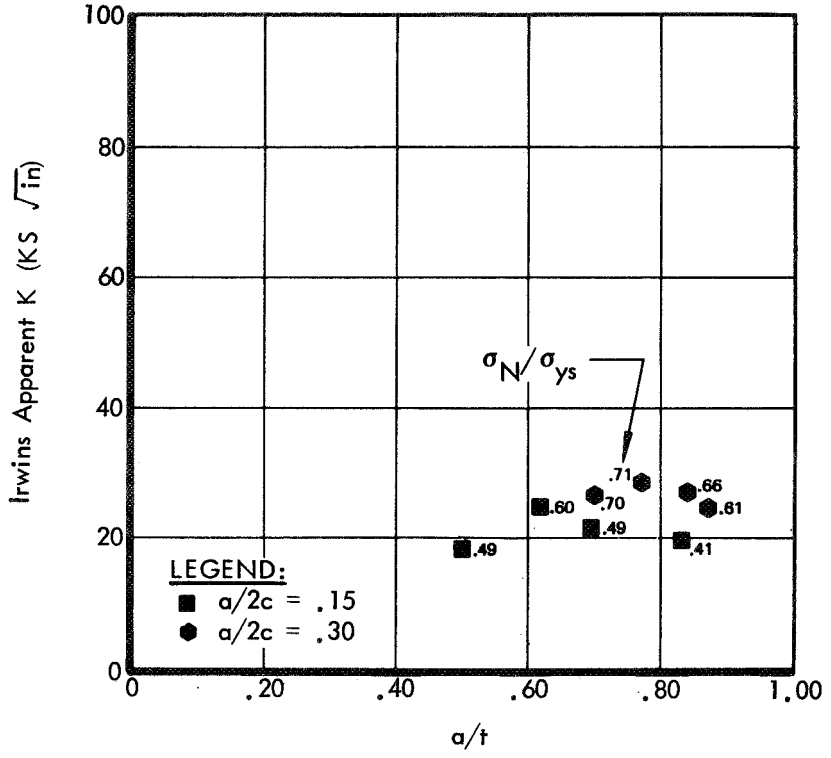


Figure 47: EFFECT OF FLAW DEPTH ON APPARENT K VALUES
(t = 1.00", 2219 Aluminum Weld Metal @ -423°F)

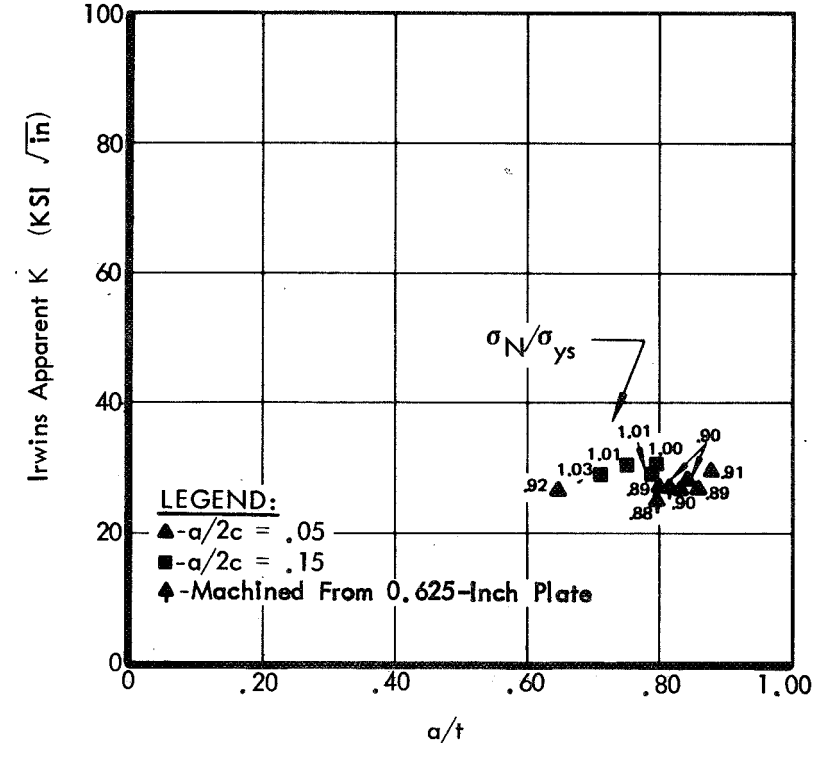


Figure 48: EFFECT OF FLAW DEPTH ON APPARENT K VALUES
(t = 0.063", 2219-T87 Aluminum Base Metal @ -423 °F)

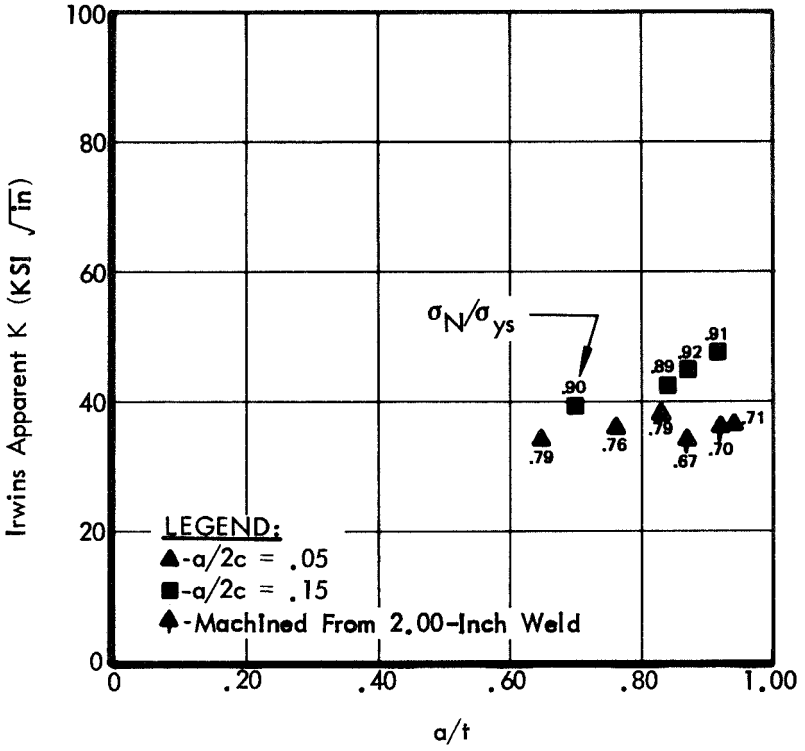


Figure 49: EFFECT OF FLAW DEPTH ON APPARENT K VALUES (t = 0.020", 5A1-2.5Sn Titanium Weld Metal @ -423°F)

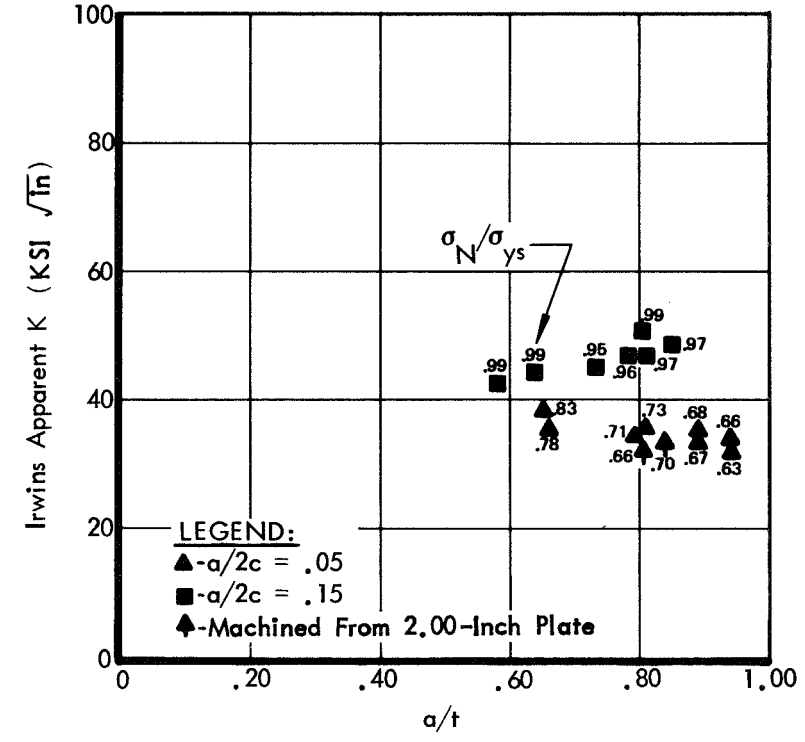


Figure 50: EFFECT OF FLAW DEPTH ON APPARENT K VALUES (t = 0.020", 5A1-2.5Sn Titanium Base Metal @ -423°F)

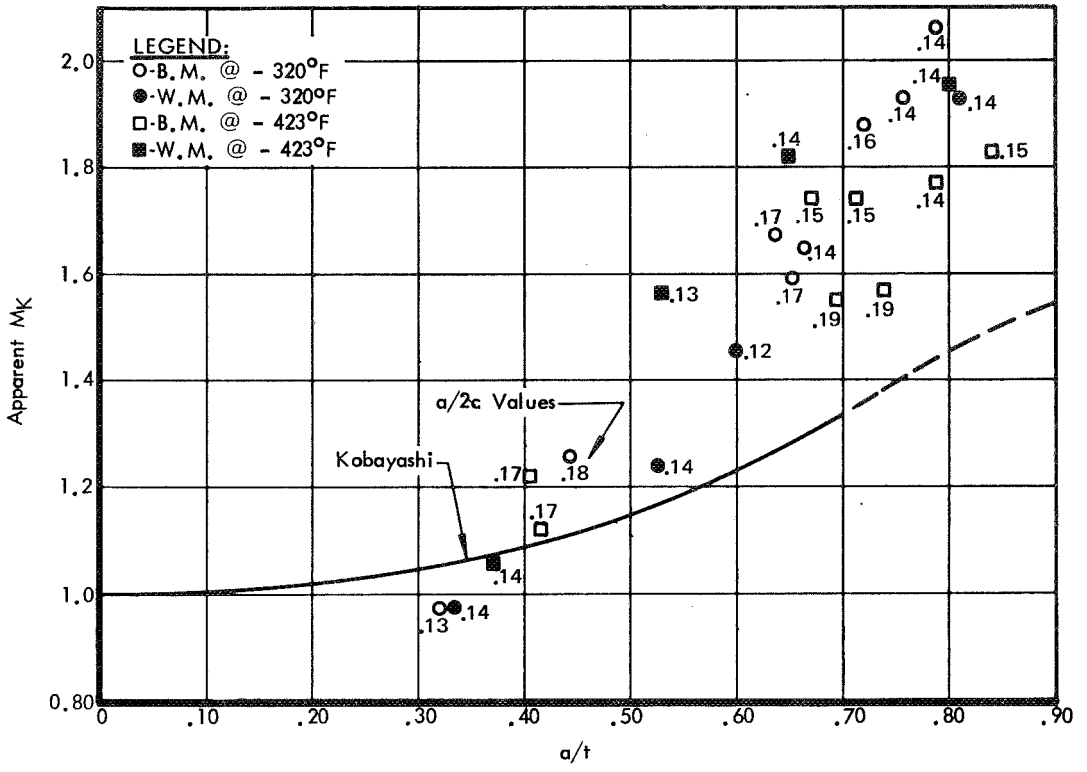


Figure 51: APPARENT MAGNIFICATION - DATA
(t = 0.200", 5Al-2.5Sn Titanium, a/2c = .12 - .19)

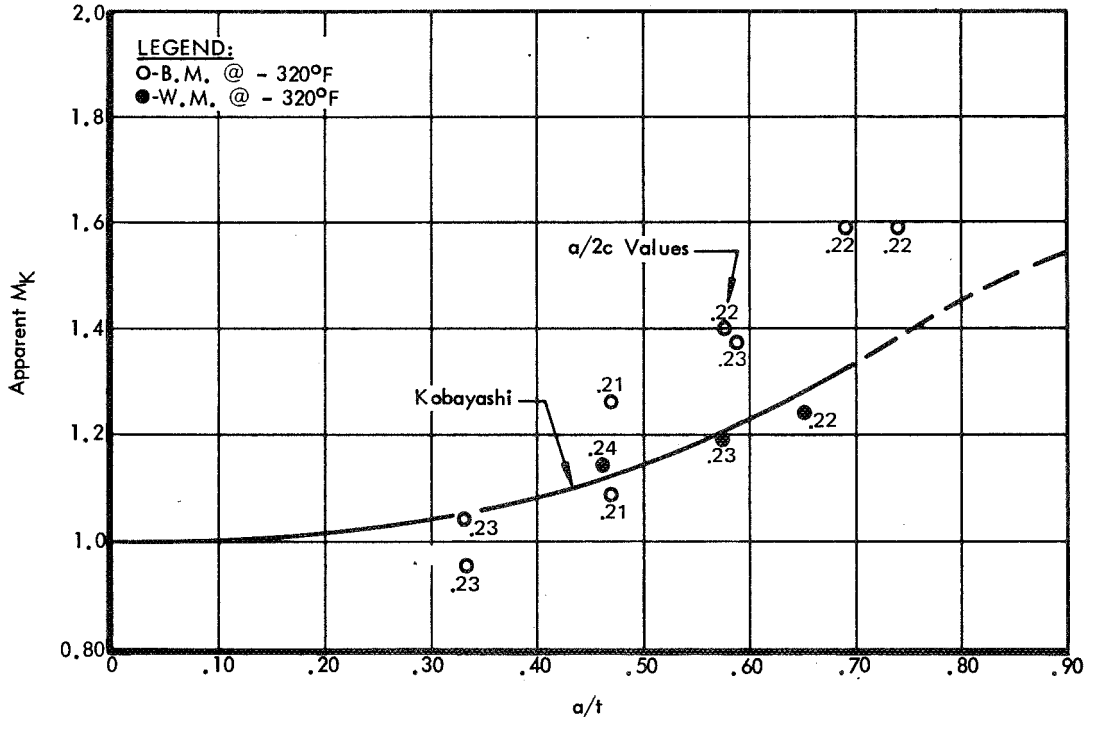


Figure 52: APPARENT MAGNIFICATION - DATA
(t = 0.200", 5Al-2.5Sn Titanium, a/2c = .21 - .24)

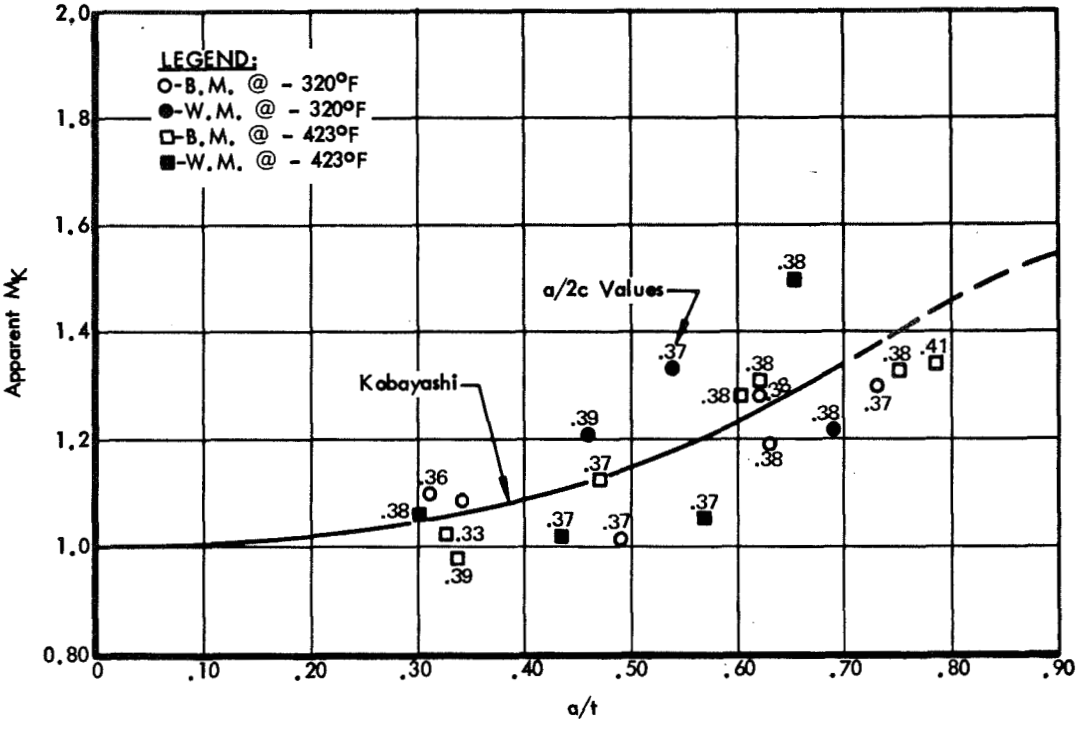


Figure 53: APPARENT MAGNIFICATION - DATA
(t = 0.200", 5Al-2.5Sn Titanium, a/2c = .33 - .41)

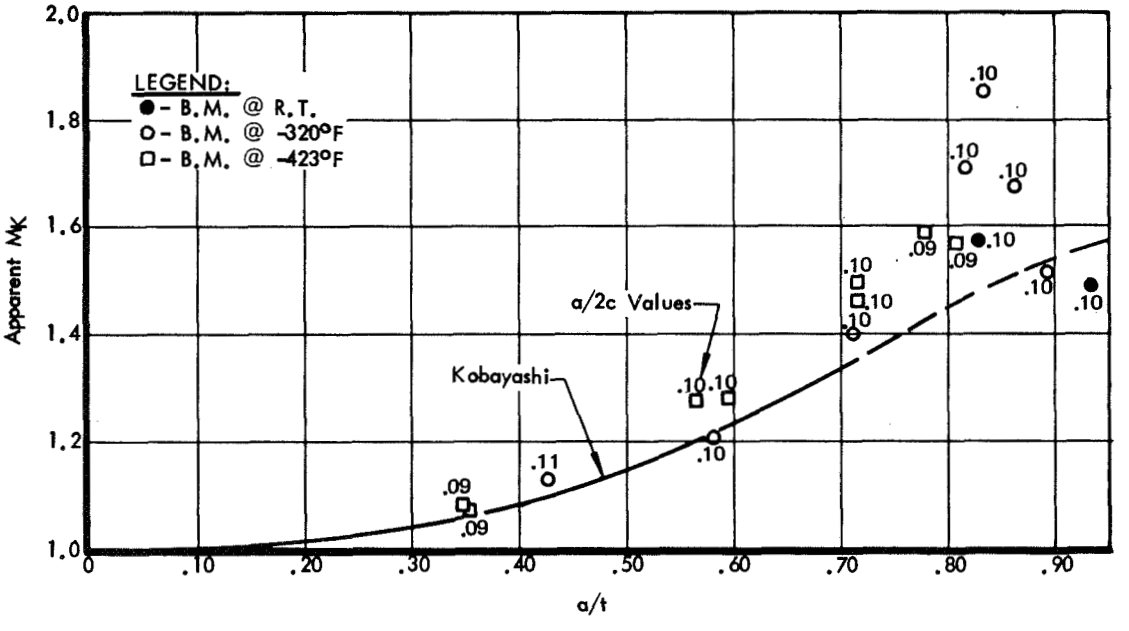


Figure 54: APPARENT MAGNIFICATION - DATA
(t = 0.625", 2219-T87 Aluminum, a/2c = .09 - .11)

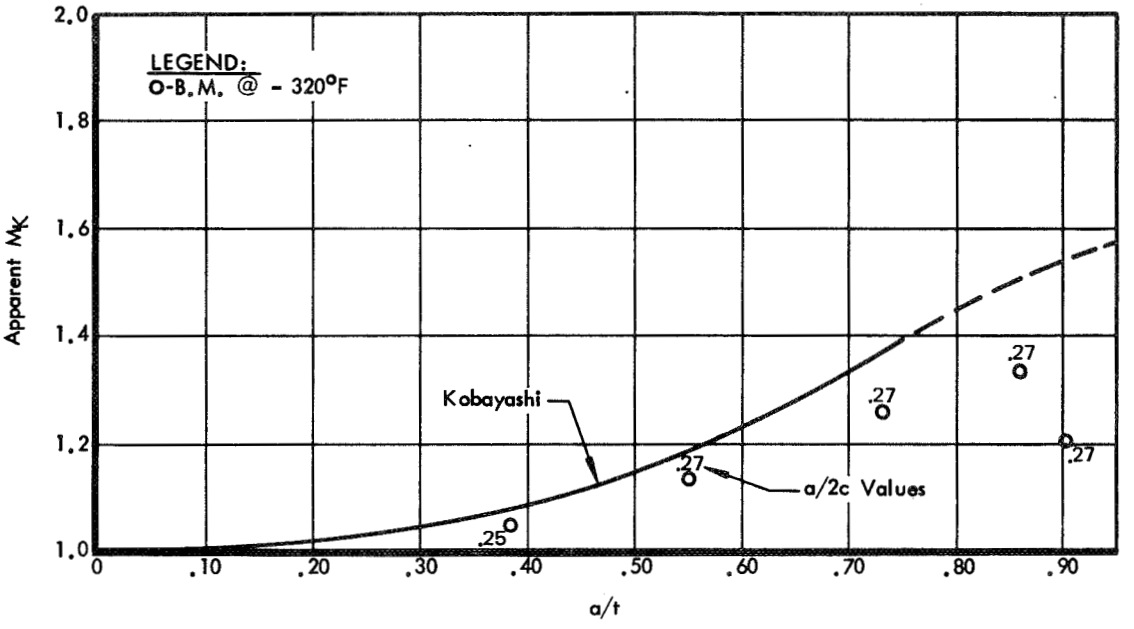


Figure 55: APPARENT MAGNIFICATION - DATA
(t = 0.625", 2219-T87 Aluminum, a/2c = .25 - .27)

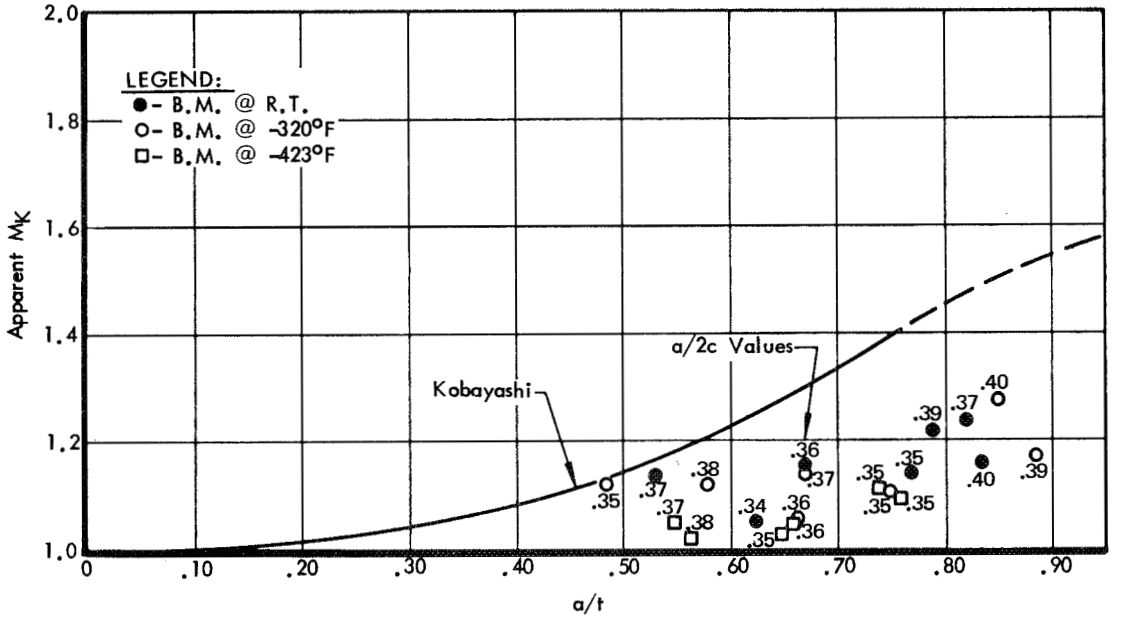


Figure 56: APPARENT MAGNIFICATION - DATA
(t = 0.625", 2219-T87 Aluminum, a/2c = .35 - .40)

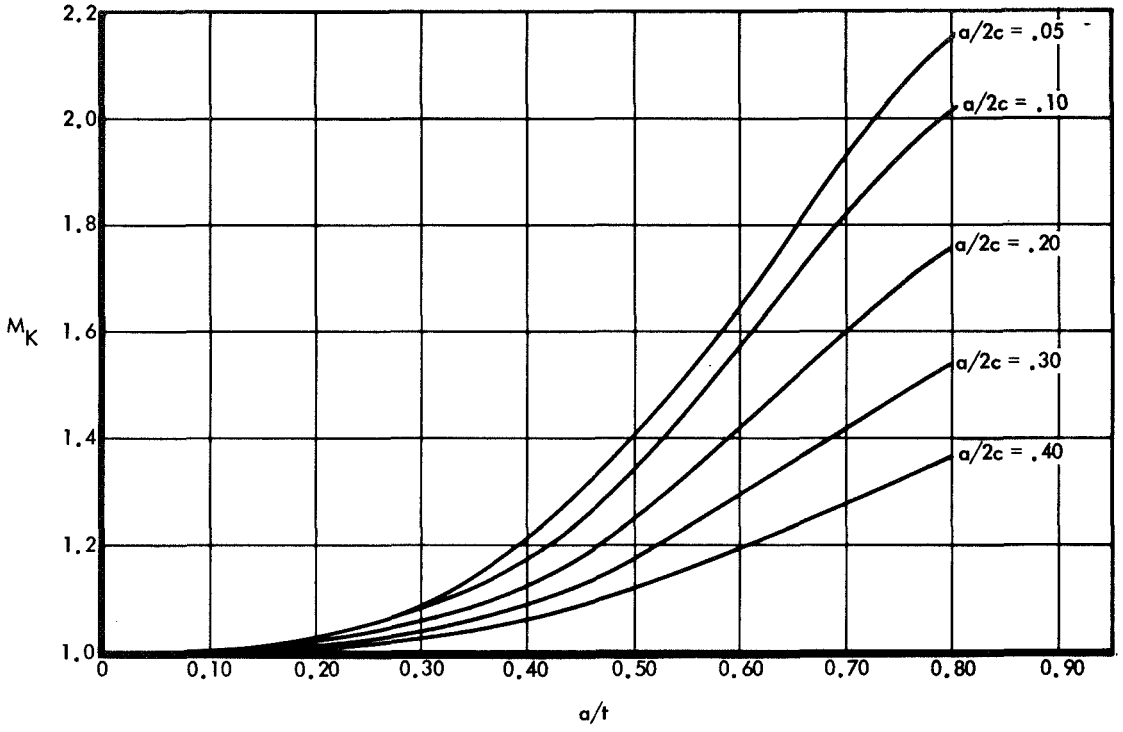


Figure 57: DEEP FLAW MAGNIFICATION CURVES
(t = 0.200", 5Al-2.5Sn Titanium Base Metal
(Transverse) & Weldment @ -320°F & -423°F)

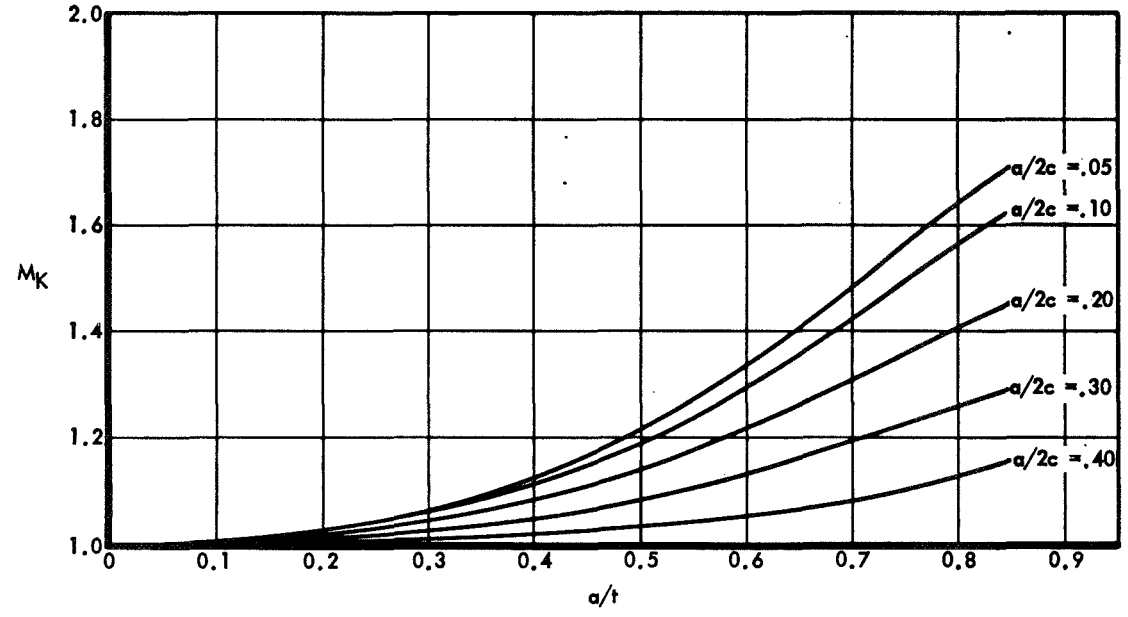


Figure 58: DEEP FLAW MAGNIFICATION CURVES
(t = 0.625", 2219-T87 Aluminum Base Metal,
Longitudinal Grain, @ R.T., -320°F & -423°F)

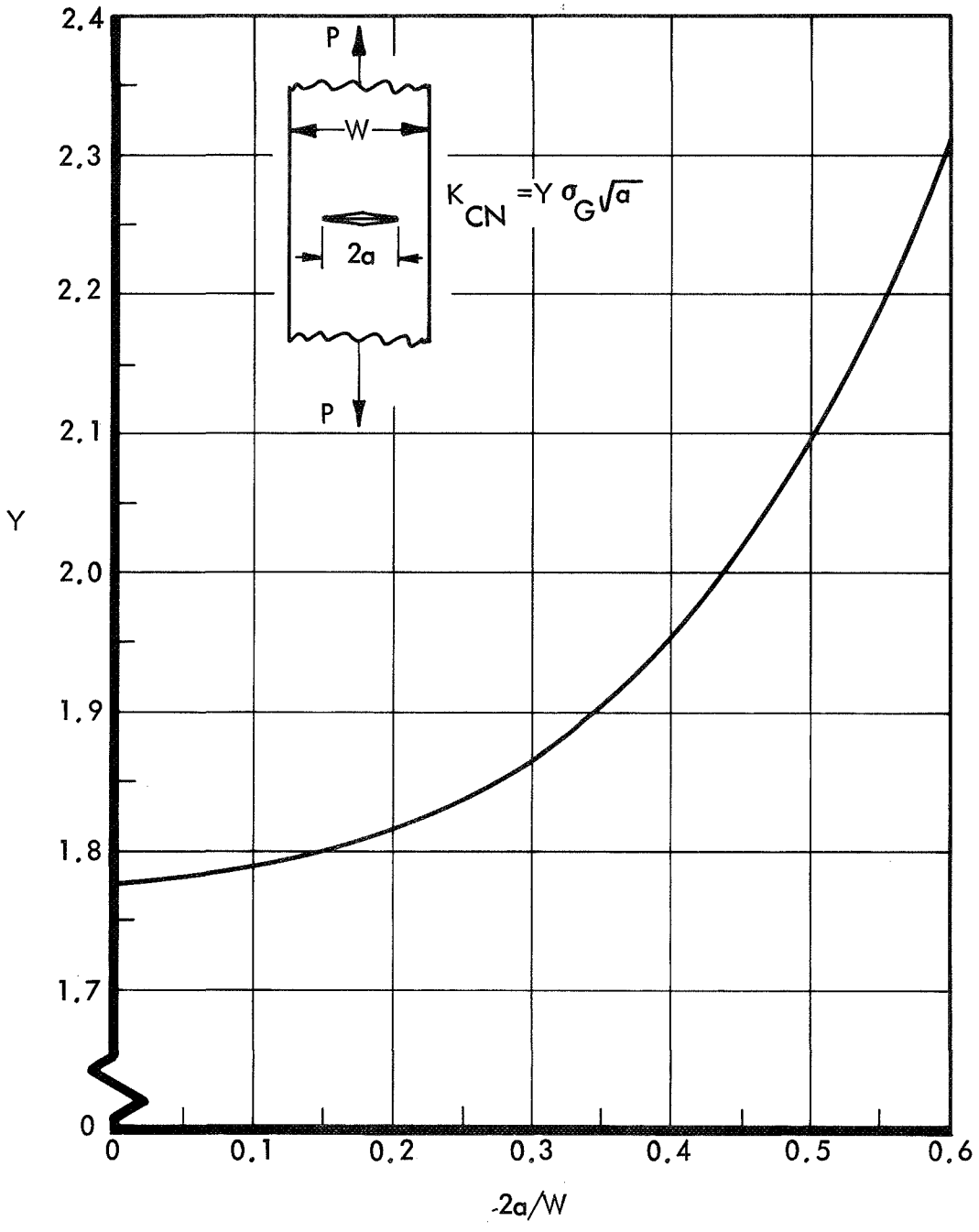


Figure 59: RELATIONSHIP FOR CALCULATING $K_{CN}$ FROM CENTER CRACK SPECIMENS

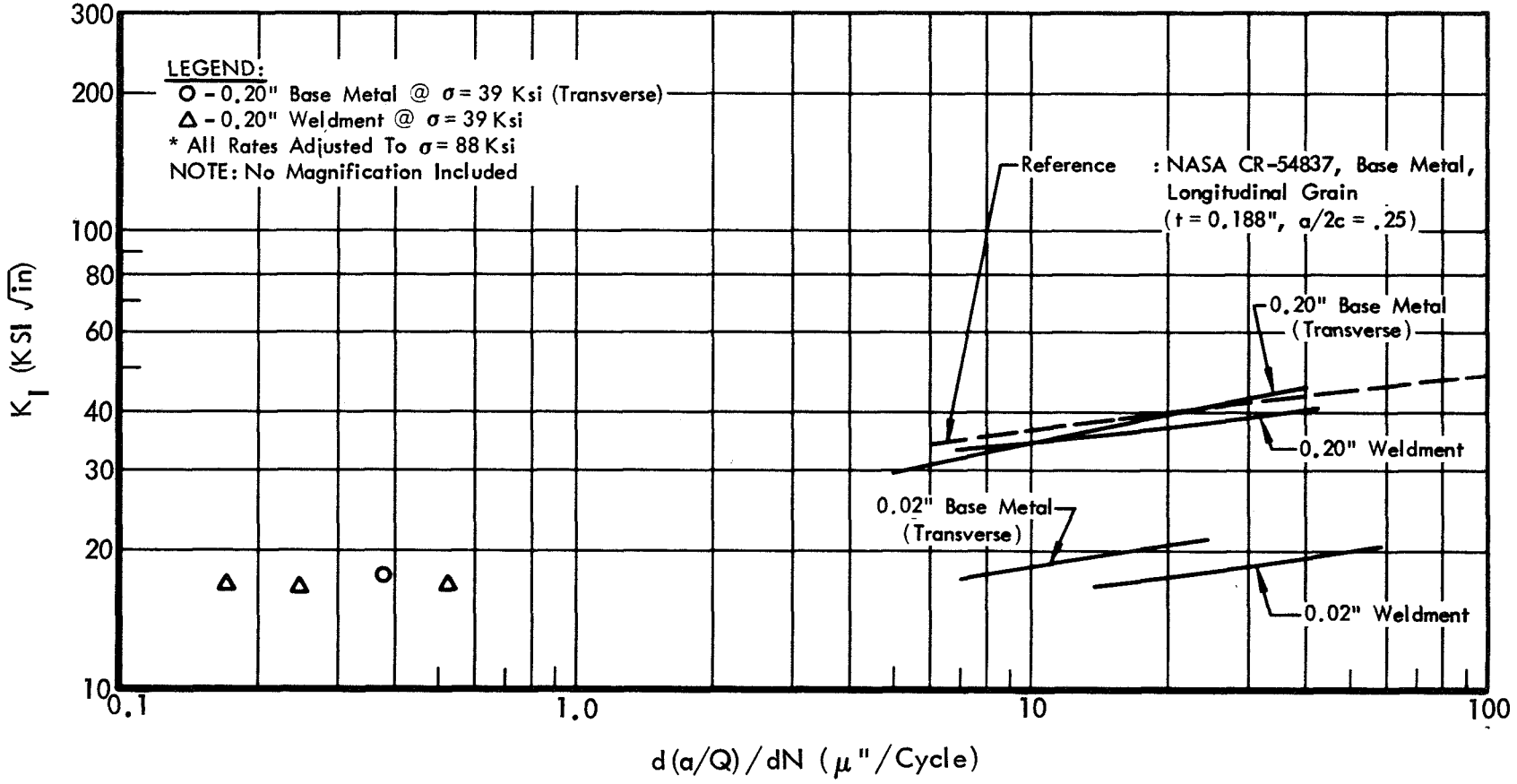


Figure 60: CYCLIC FLAW GROWTH RATES (5Al-2.5Sn Titanium @ R.T.)

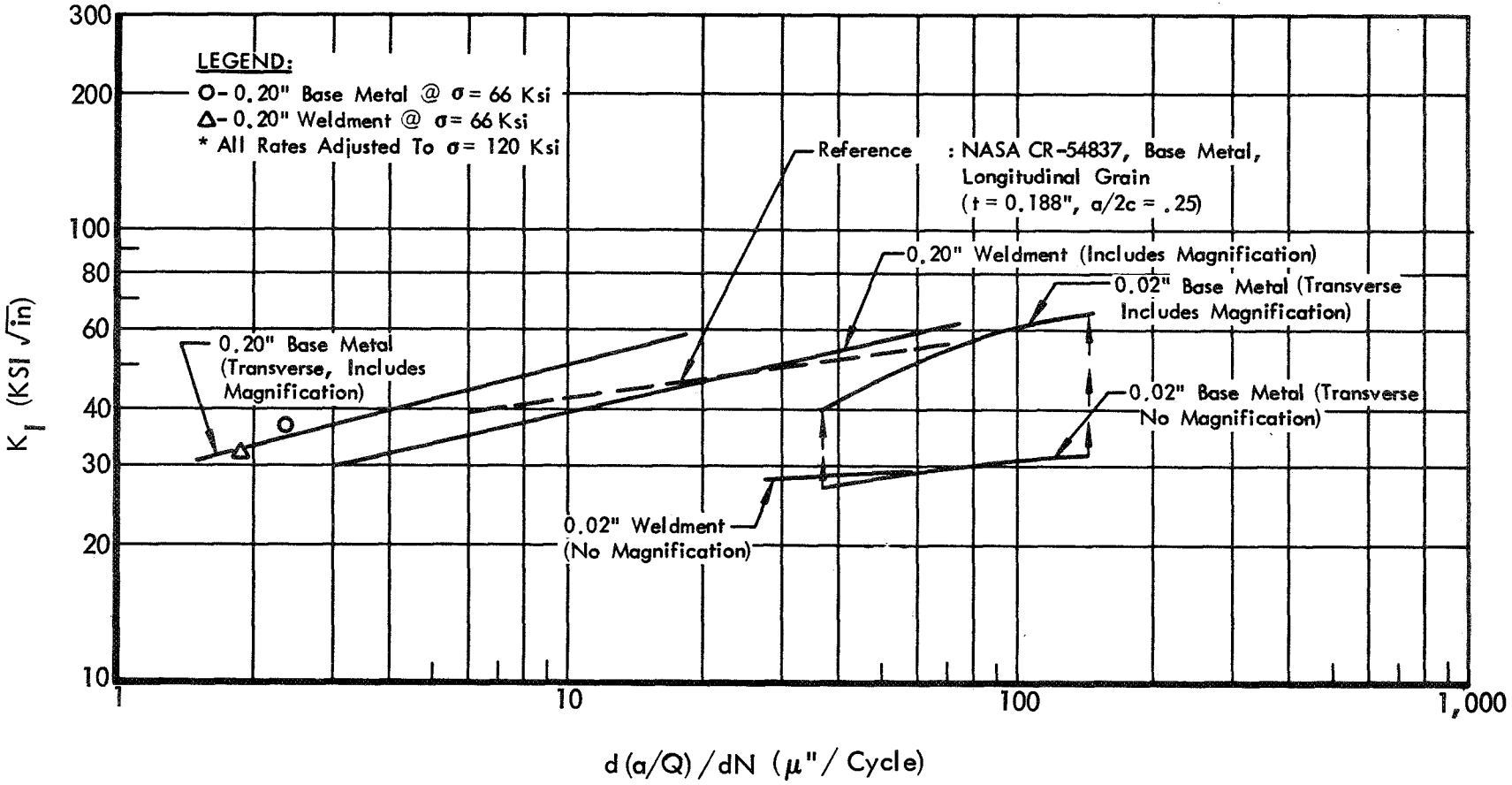


Figure 61: CYCLIC FLAW GROWTH RATES (5Al-2.5Sn Titanium @ -320 °F)

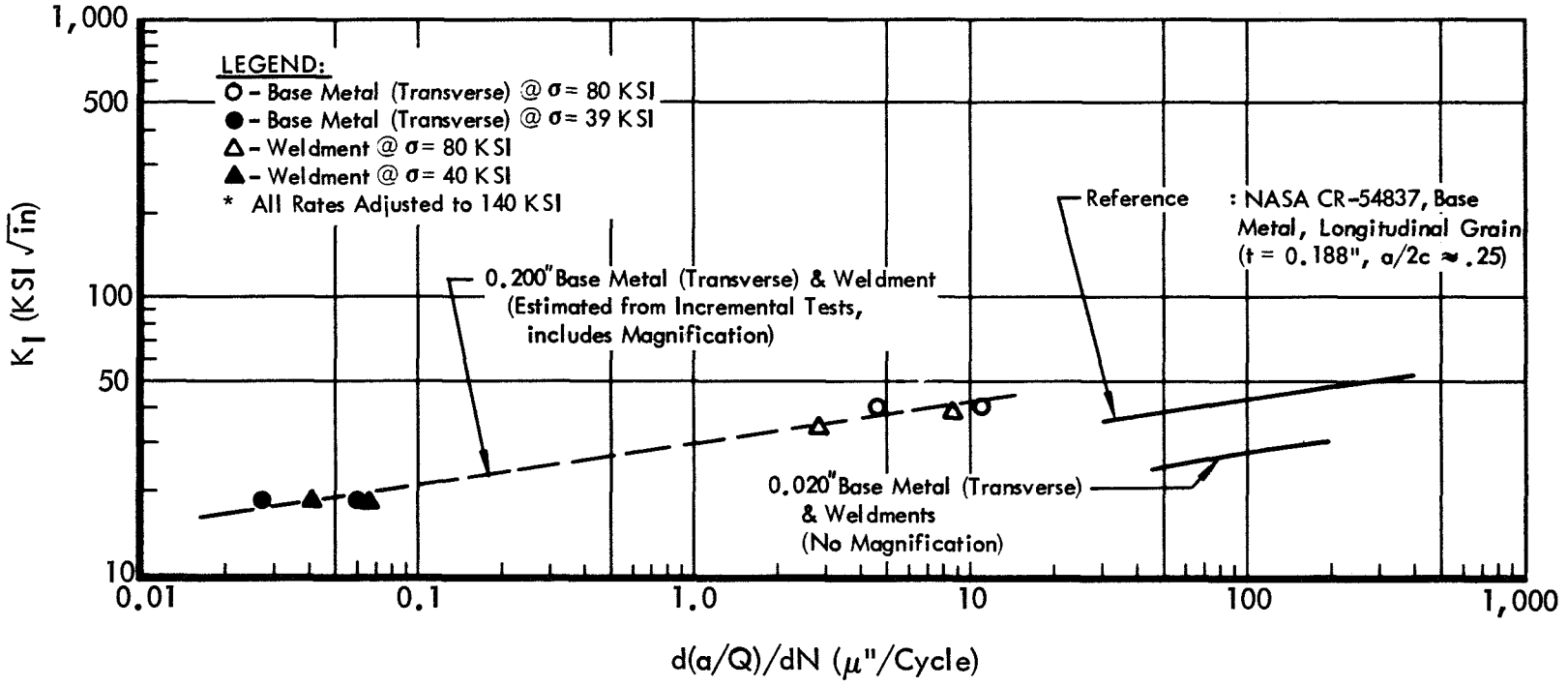


Figure 62: CYCLIC FLAW GROWTH RATES (5Al-2.5Sn Titanium @ -423 °F)

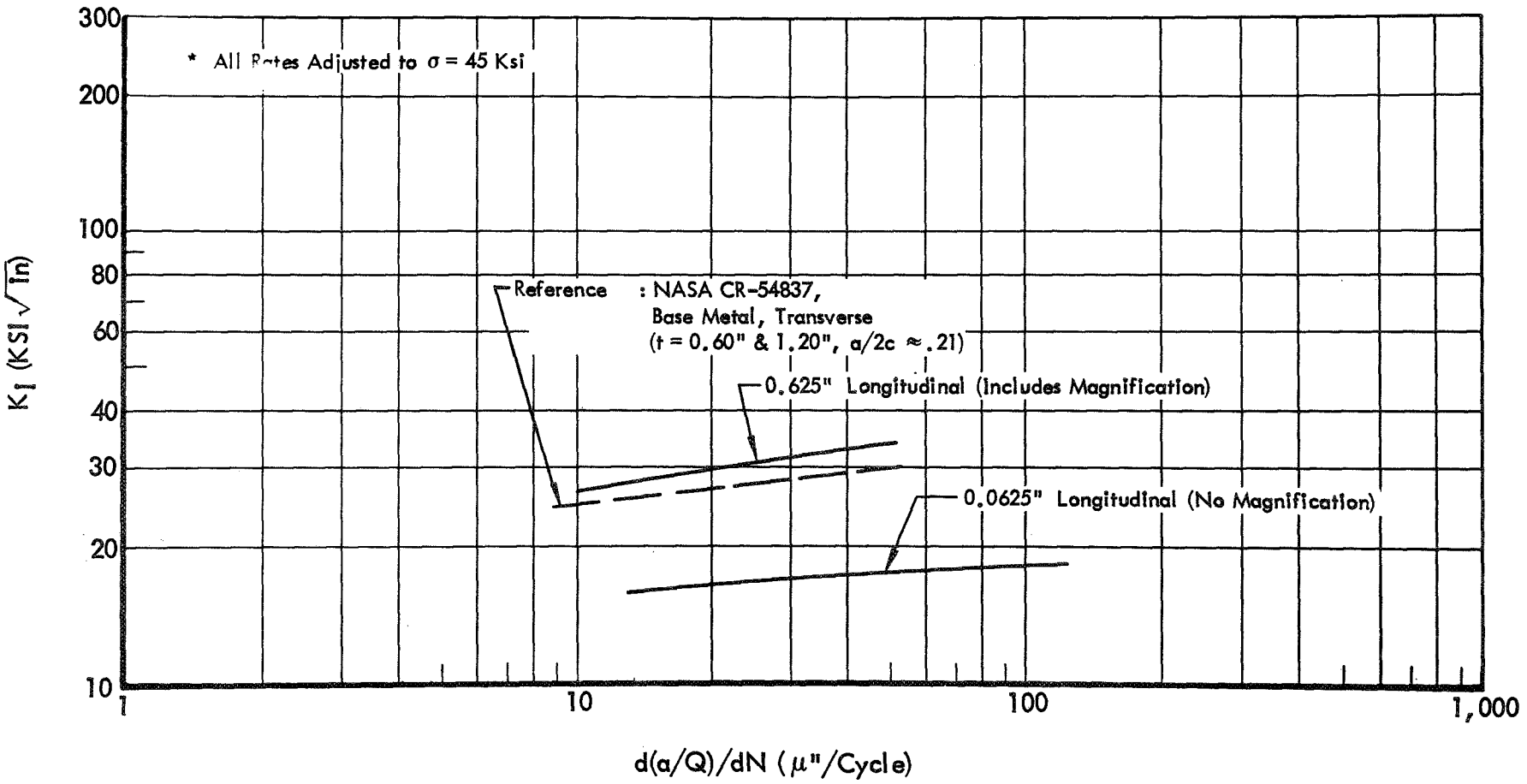


Figure 63: CYCLIC FLAW GROWTH RATES (2219-T87 Aluminum Base Metal @ R.T.*)

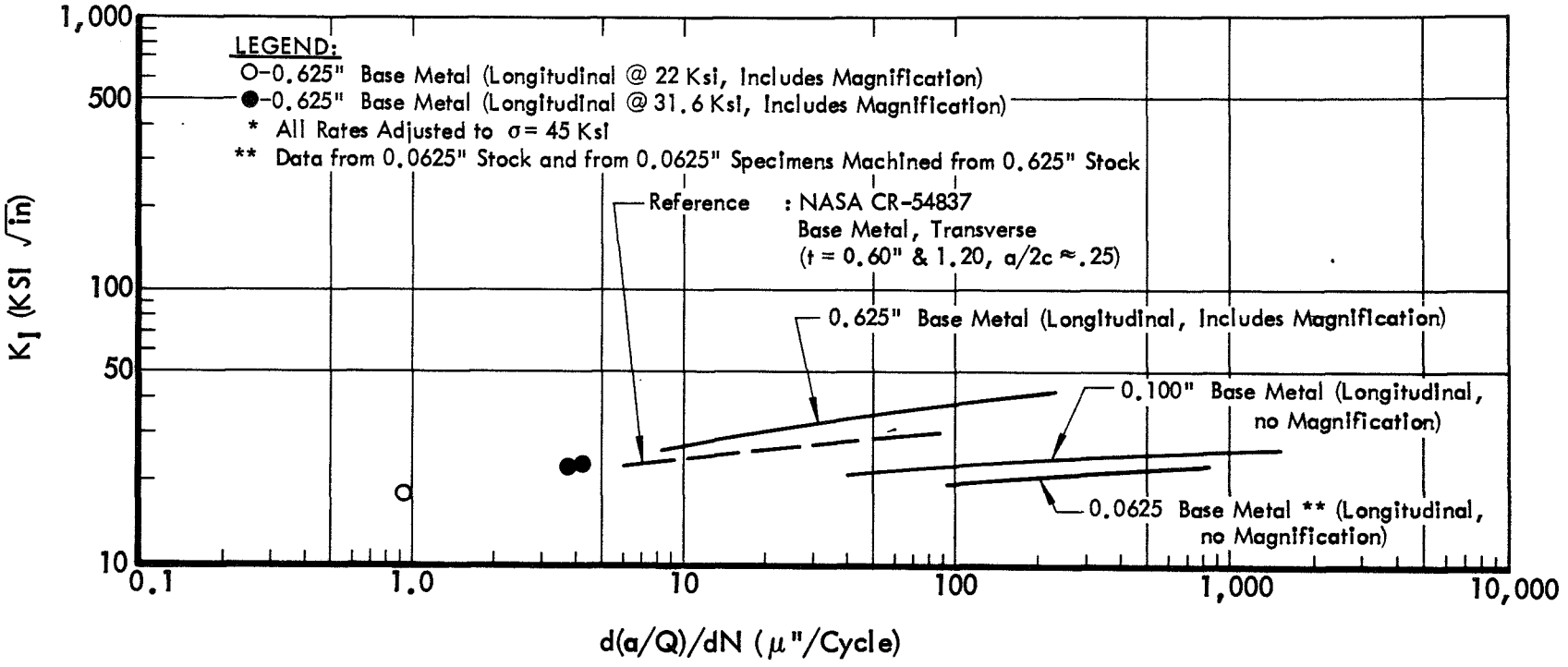


Figure 64: CYCLIC FLAW GROWTH RATES (2219-T87 Aluminum Base Metal @ -320 °F*)

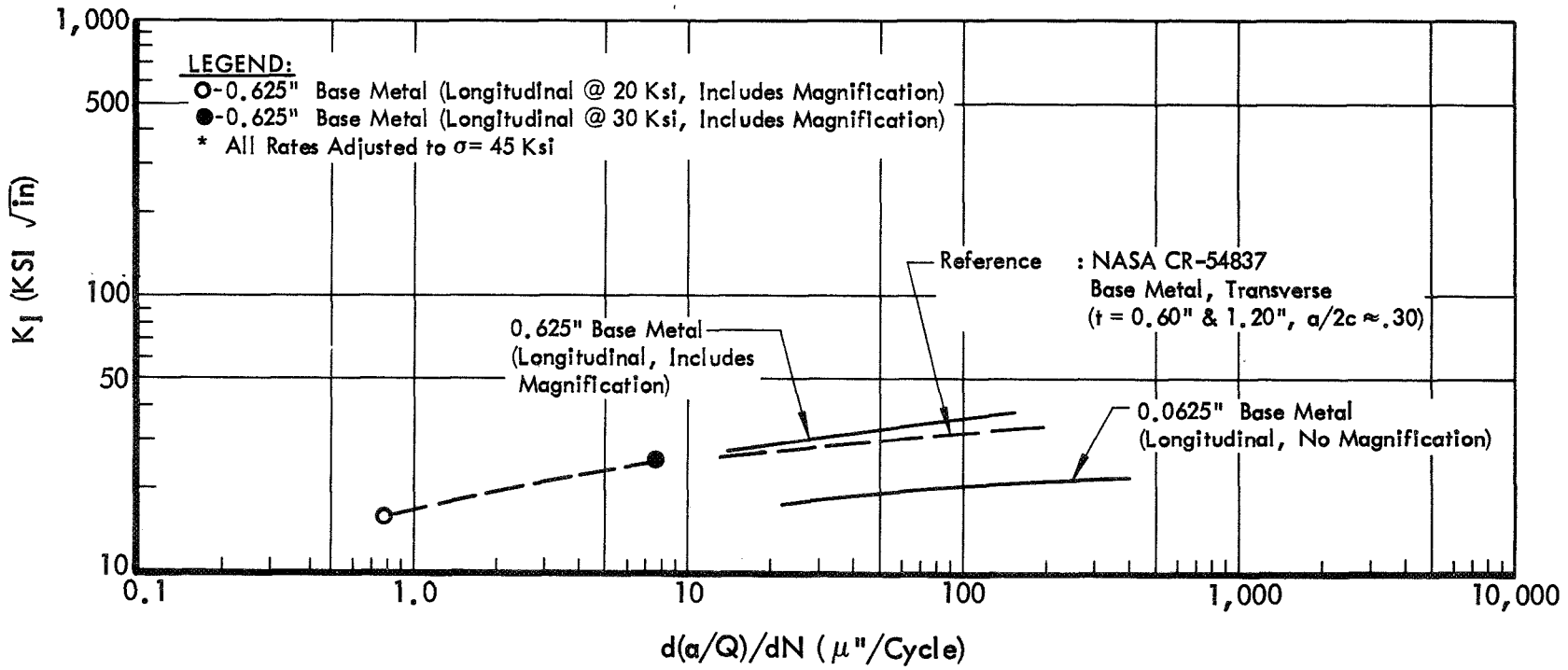


Figure 65: CYCLIC FLAW GROWTH RATES (2219-T87 Aluminum Base Metal @ -423 $^{o}F^{*}$)

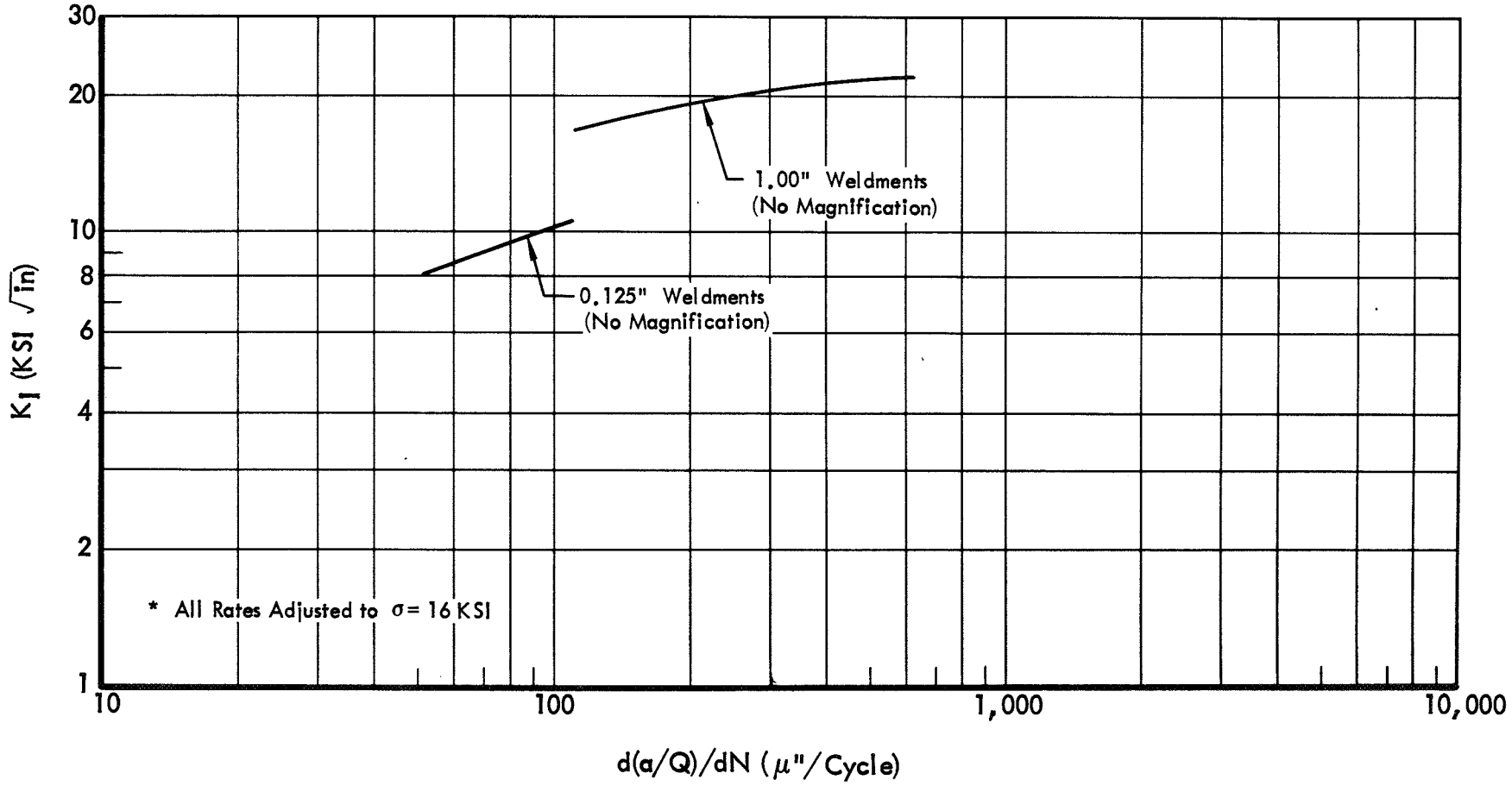


Figure 66: CYCLIC FLAW GROWTH RATES (2219 Aluminum Weldments @ R.T. * )

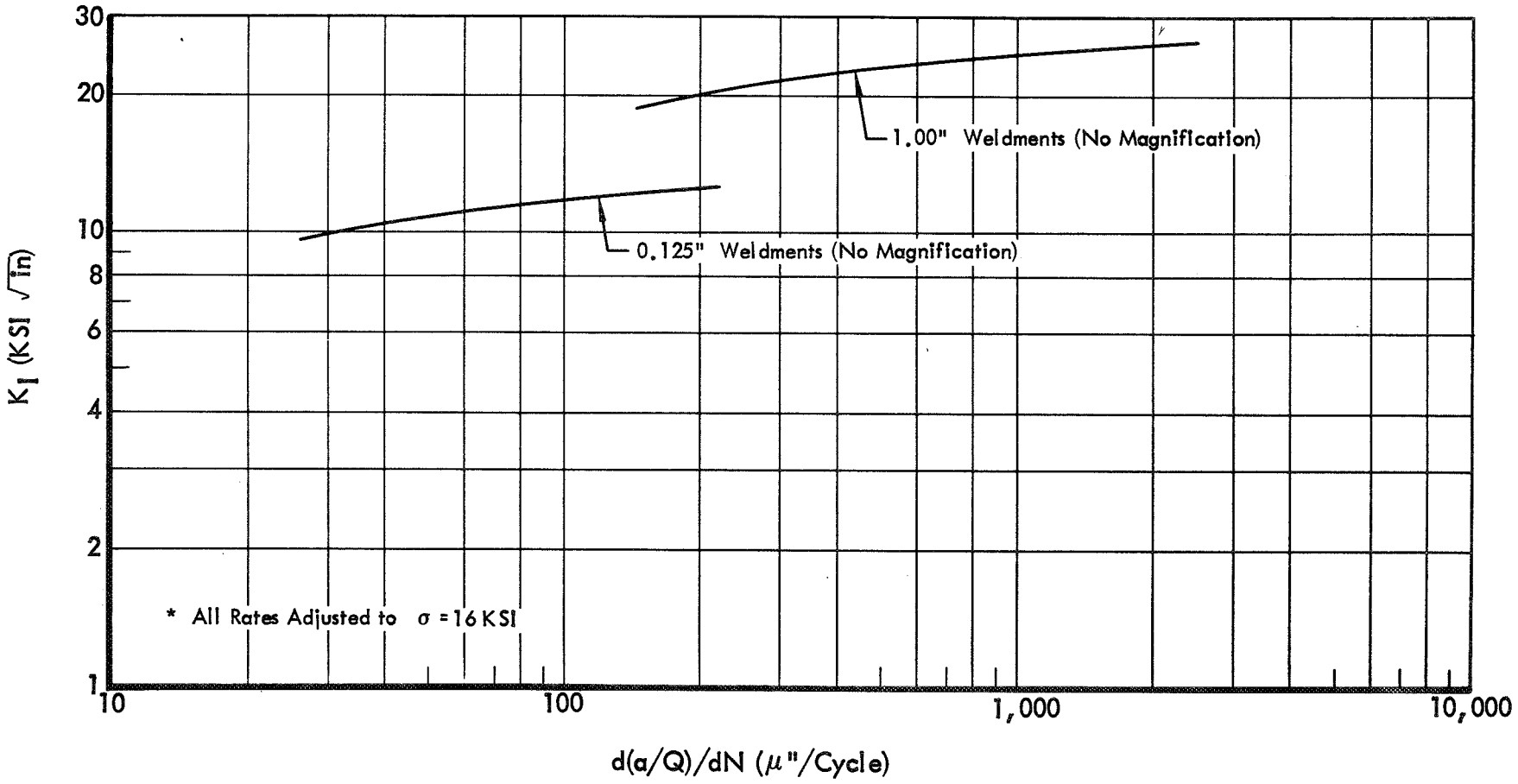


Figure 67: CYCLIC FLAW GROWTH RATES (2219 Aluminum Weldments @ -320 °F *)

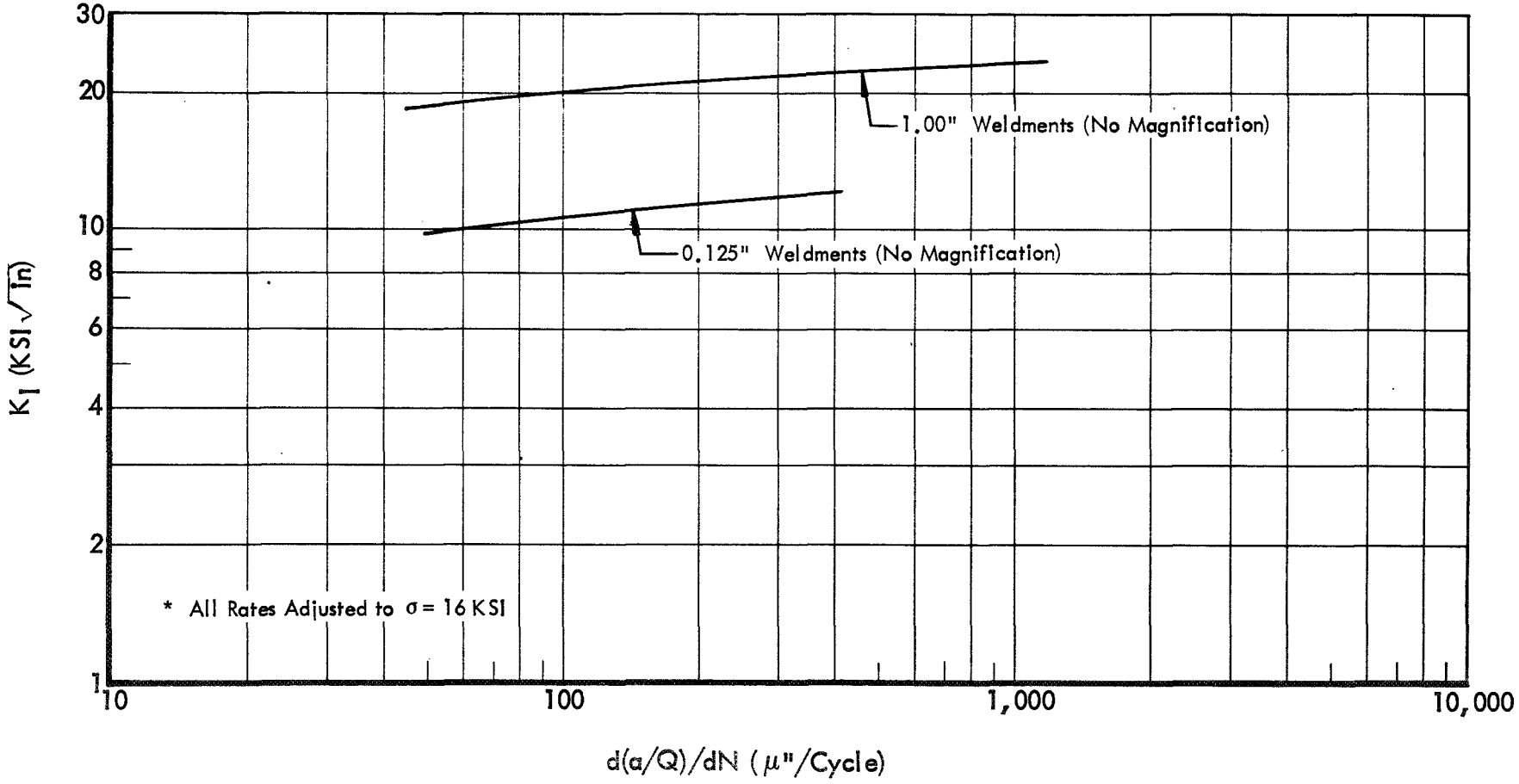


Figure 68: CYCLIC FLAW GROWTH RATES (2219 Aluminum Weldments @ -423 °F *)

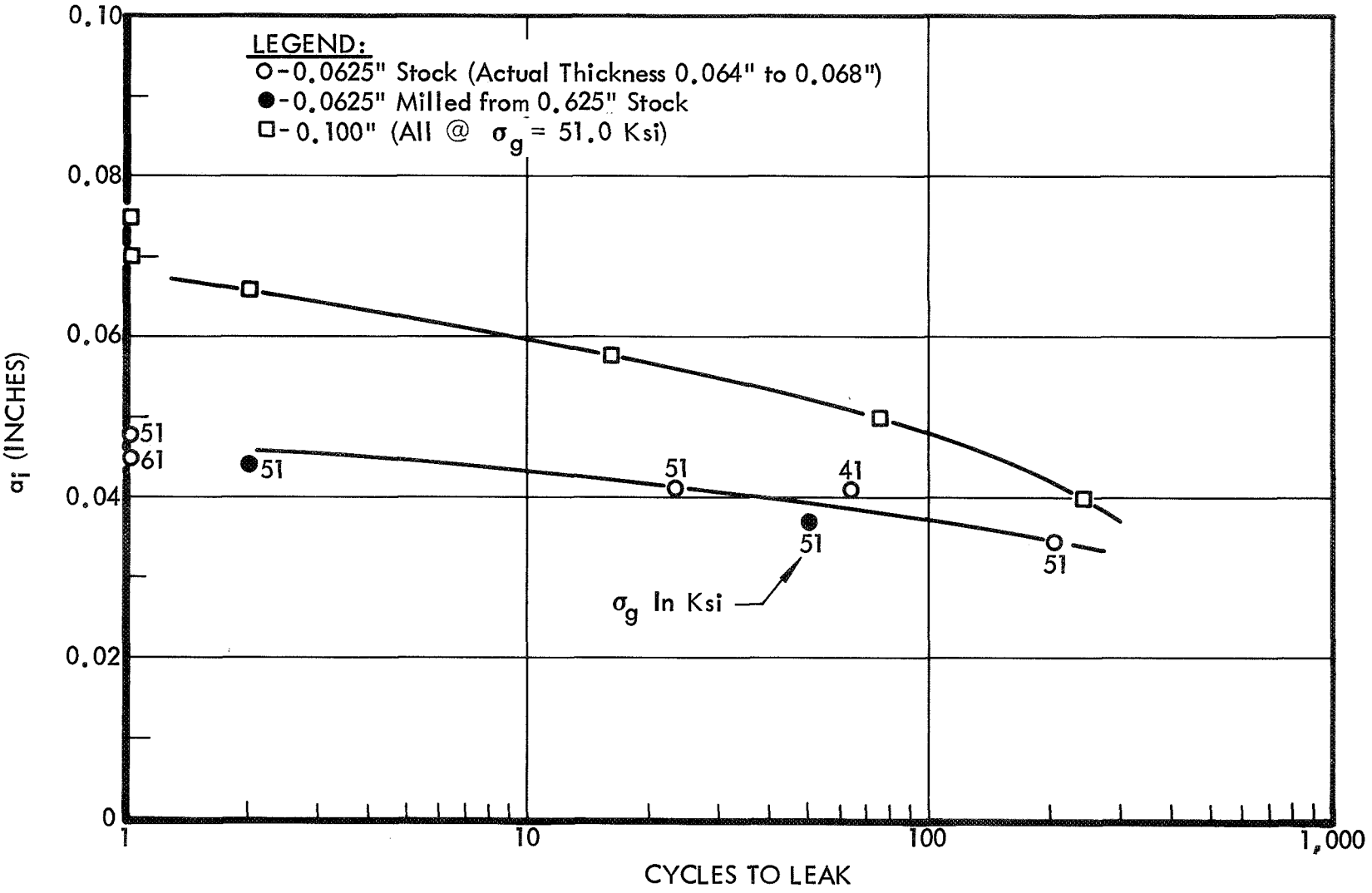


Figure 69: CYCLIC LIFE CURVES( t = 0.063" And 0.100", 2219-T87 Aluminum @ -320 $^{0}$F )

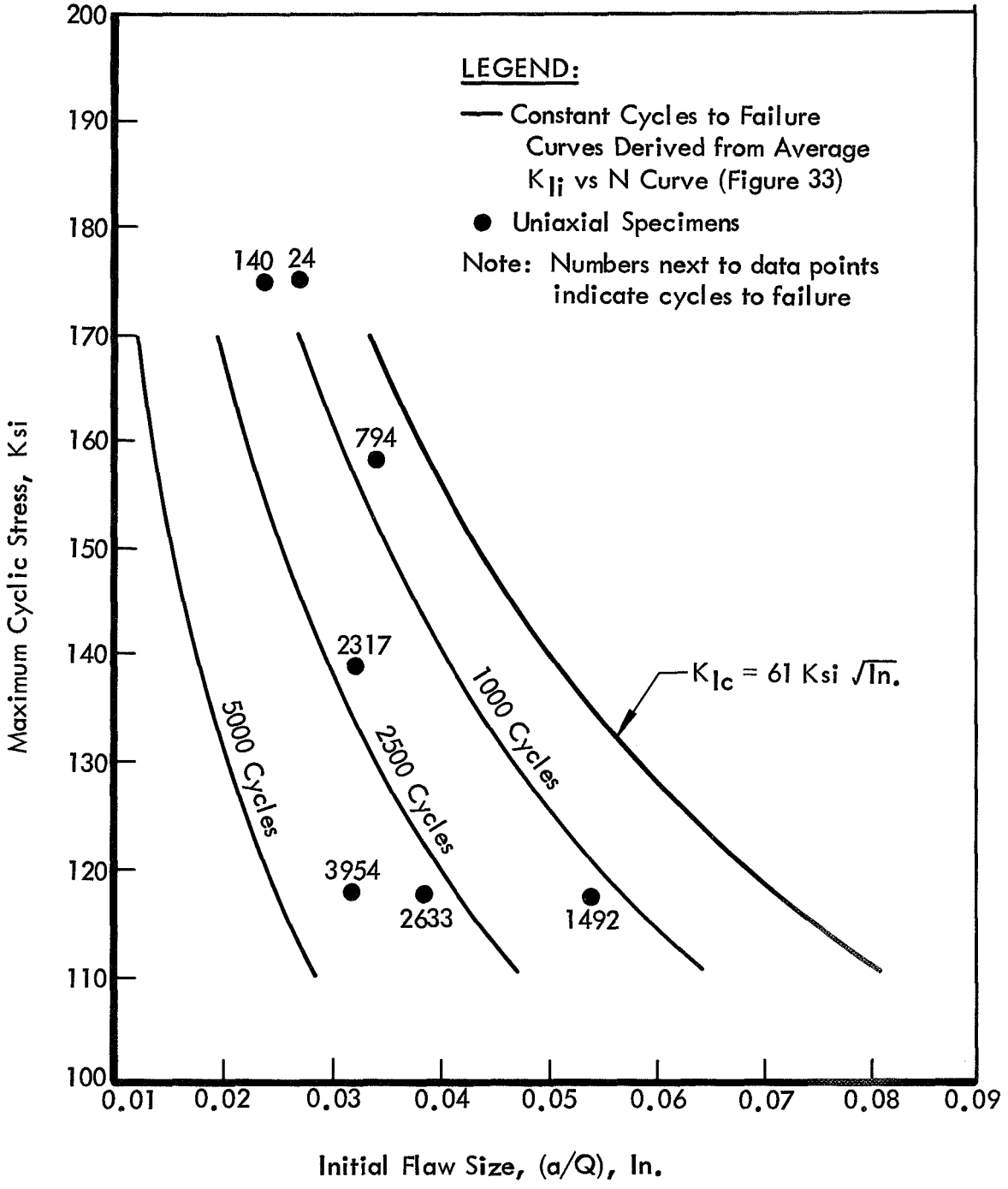


Figure 70: CYCLIC FLAW GROWTH DATA FOR 5Al-2.5Sn (ELI) TITANIUM @ -320 $^{0}$F ( 50-100-50 Load Profile )

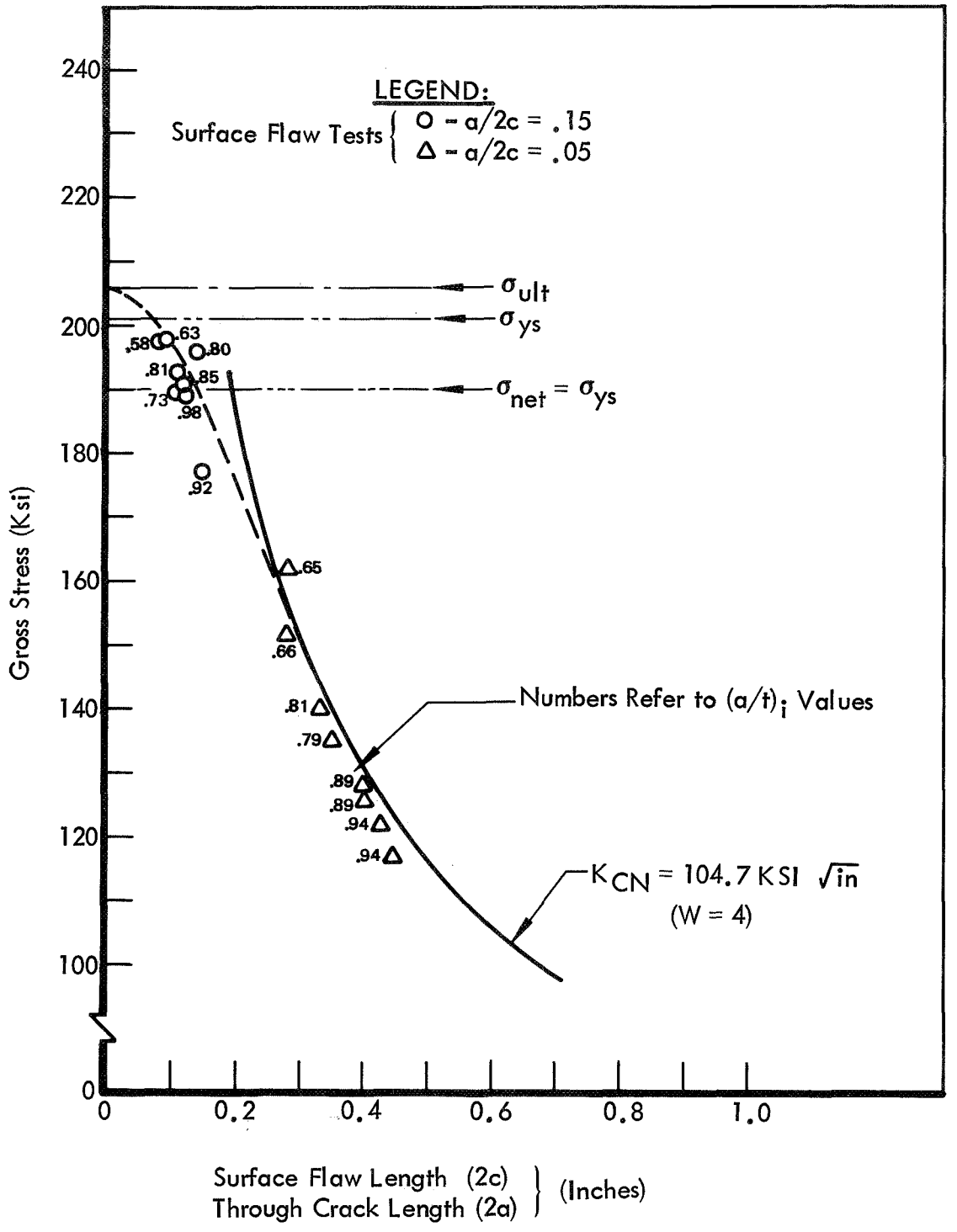


Figure 71: COMPARISON OF SURFACE FLAW & CENTER CRACK DATA
( t = 0.020", 5Al-2.5Sn Titanium Base Metal @ -423 $^{0}$F )

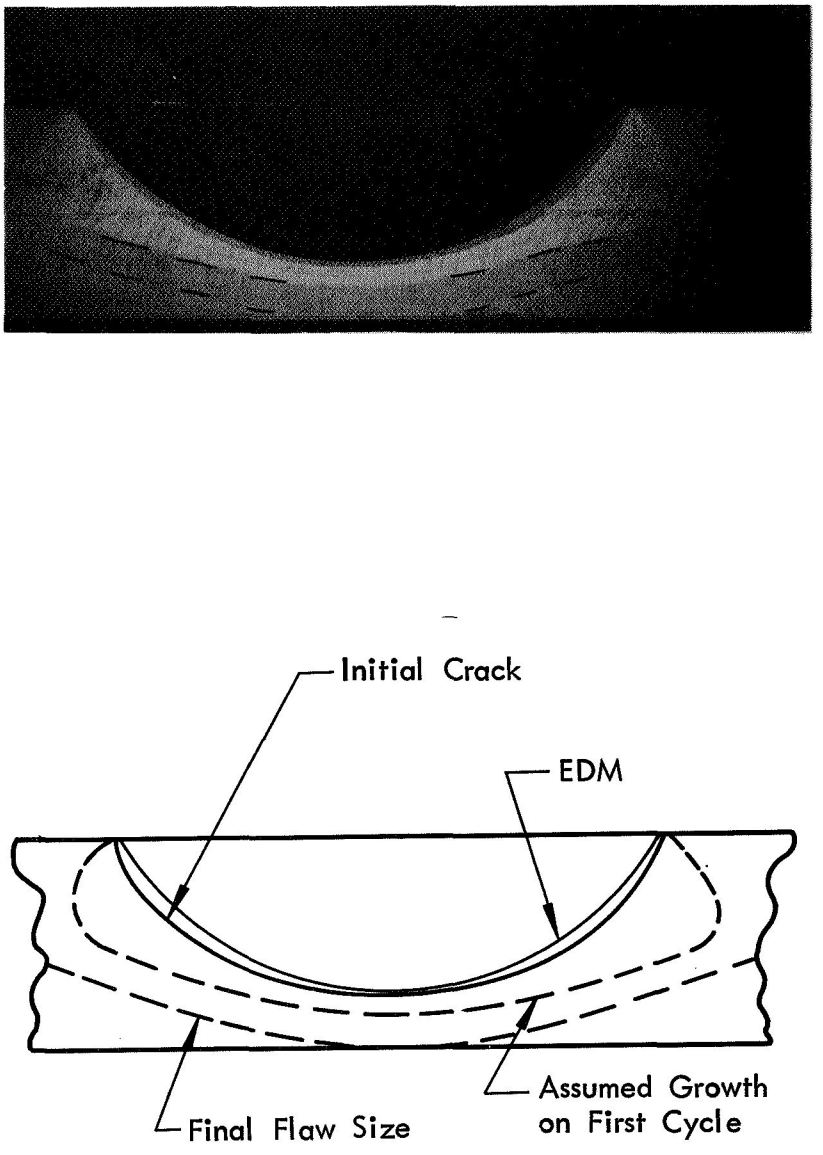


Figure 72: FRACTOGRAPH OF A CYCLIC TEST SPECIMEN (t = 1.00", 2219 Aluminum Weldment @ -320 °F, Specimen No. AWC 80N-5

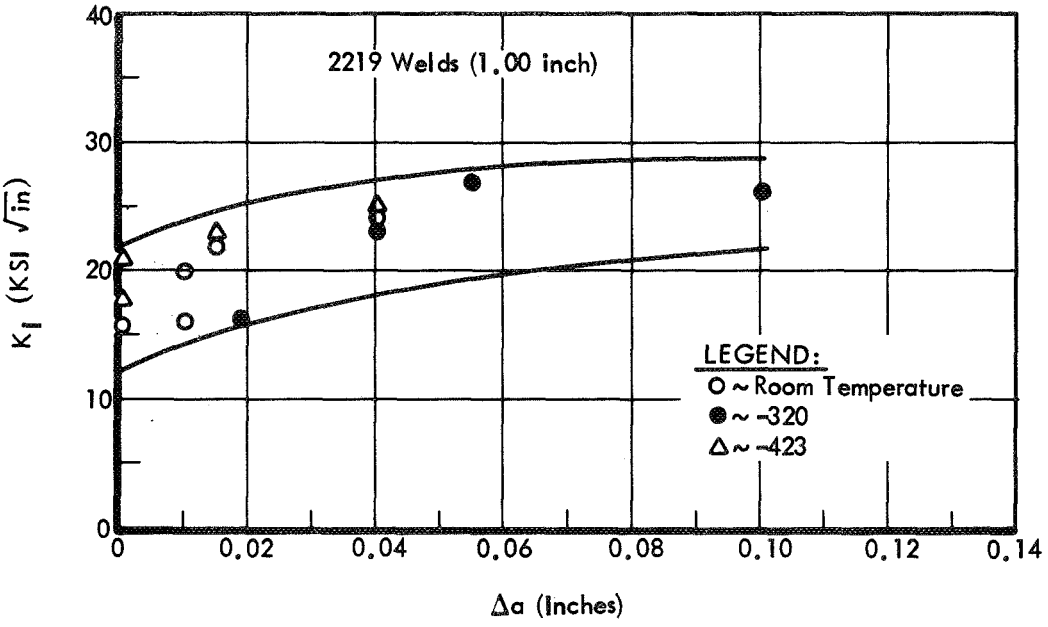


Figure 73: APPARENT FIRST CYCLE GROWTH - 2219 WELDMENTS

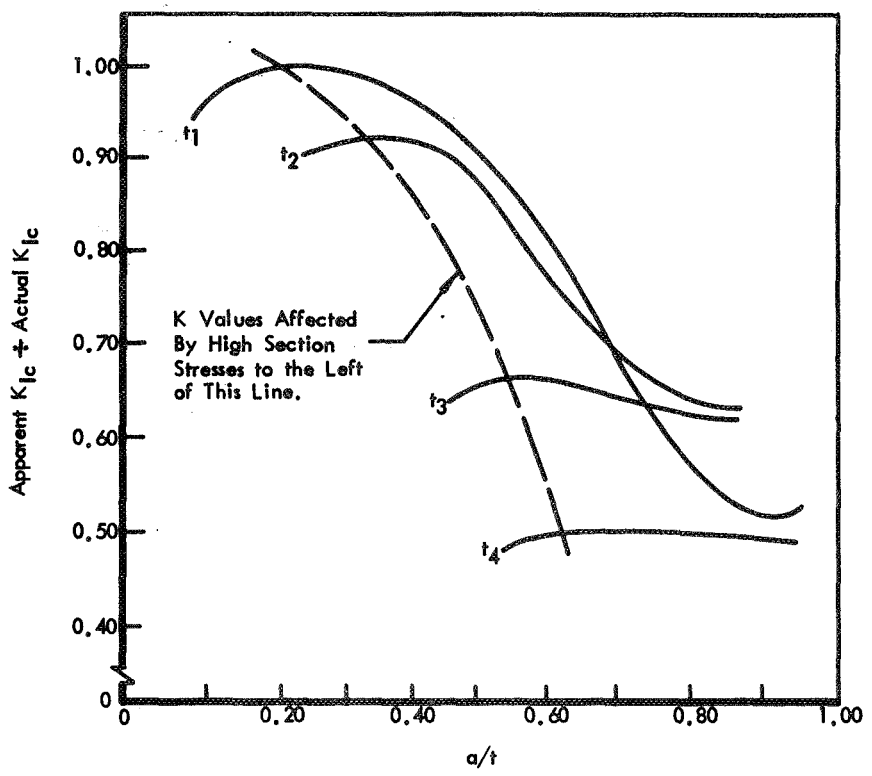


Figure 74: SCHEMATIC OF DEEP FLAW BEHAVIOR

Table 1 : TENSILE PROPERTIES ( t = 0.04", 5Al-2.5Sn Titanium Base Metal )

| SPECIMEN NUMBER | NOMINAL GAGE ~ IN. | MEASURED GAGE ~ IN. | ATMOSPHERE | GRAIN DIRECTION (L = LONGITUDINAL, T = TRANSVERSE) | TEST TEMPERATURE ~ °F | ULTIMATE STRENGTH ~ PSI | YIELD STRENGTH ** ~ PSI | % ELONGATION FOR LENGTH = 4 x DIA. | ELONGATION ~ % PER 2.0 INCHES | REDUCTION IN AREA ~ % | POISSONS RATIO | MODULUS OF ELASTICITY ~ E x $10^{-6}$ PSI |
|---|---|---|---|---|---|---|---|---|---|---|---|---|
| TLR-1 | .04 | .0368 | Air | L | 72 | 117,800 | 108,100 | | 13 | | .38 | 16.6 |
| L-1 | | .0363 | Air | | 72 | 119,200 | 110,400 | | 13 | | | 15.7 |
| | | | | | | 118,500 | 109,200 | Avg. | 13 | | | 16.3 |
| TLN-1 | | .0366 | $LN_2$ | | -320 | 184,100 | 173,200 | | 14 | | .36 | 17.5 |
| L-3 | | .0360 | $LN_2$ | | -320 | 185,100 | 174,000 | | 14 | | | 18.6 |
| | | | | | | 184,600 | 173,600 | Avg. | 14 | | | 17.9 |
| TLH-1 | | .0388 | $LH_2$ | | -423 | 207,200 | 199,400* | | - | | .42 | |
| TLH-2 | | .0358 | $LH_2$ | | -423 | 219,500 | 213,400* | | - | | | |
| | | | | | | 213,300 | 206,400* | Avg. | | | | |
| T-1 | | .0371 | Air | T | 72 | 117,200 | 112,600 | | 14 | | | 15.5 |
| T-2 | | .0372 | Air | | 72 | 116,100 | 111,800 | | 15 | | | 16.0 |
| | | | | | | 116,600 | 112,200 | Avg. | 14 | | | 15.7 |
| T-3 | | .0368 | $LN_2$ | | -320 | 179,300 | 172,500 | | 16 | | | 17.0 |
| T-4 | | .0360 | $LN_2$ | | -320 | 180,000 | 172,800 | | 17 | | | 18.8 |
| | | | | | | 179,600 | 172,500 | Avg. | 16 | | | 17.9 |
| TTH-1 | | .0353 | $LH_2$ | | -423 | 203,300 | 201,100* | | - | | | |
| TTH-2 | | .0372 | $LH_2$ | | -423 | 208,000 | 201,600* | | - | | | |
| | | | | | | 205,600 | 201,300* | Avg. | | | | |

* 0.2% offset yield strength obtained by strain gage

** 0.2% offset yield strength obtained by extensometer on 2.0 gage length

Table 2 : TENSILE PROPERTIES ( t = 0.20", 5Al-2.5Sn Titanium Base Metal***)

| SPECIMEN NUMBER | NOMINAL GAGE ~ IN. | MEASURED GAGE ~ IN. | ATMOSPHERE | GRAIN DIRECTION (L = LONGITUDINAL, T = TRANSVERSE) | TEST TEMPERATURE ~ °F | ULTIMATE STRENGTH ~ PSI | YIELD STRENGTH ** ~ PSI | % ELONGATION FOR LENGTH = 4 x DIA. | ELONGATION ~ % PER 2.0 INCHES | REDUCTION IN AREA ~ % | POISSONS RATIO | MODULUS OF ELASTICITY ~ E x $10^{-6}$ PSI |
|---|---|---|---|---|---|---|---|---|---|---|---|---|
| TLR-1 | .20 | .2165 | Air | L | 72 | 117,000 | 110,300 | | 17 | 40 | .33 | 16.1 |
| TILR-1 | | .2181 | Air | | 72 | 116,200 | 111,600 | | 17 | 42 | | 16.0 |
| | | | | | | 116,600 | 110,900 | Avg. | 17 | 41 | | 16.0 |
| TLN-1 | | .2160 | $LN_2$ | | -320 | 187,400 | 178,200 | | 17 | 21 | .36 | 17.7 |
| TILN-1 | | .2150 | $LN_2$ | | -320 | 187,900 | 178,300 | | 17 | 24 | | 17.4 |
| | | | | | | 187,600 | 178,200 | Avg. | 17 | 22 | | 17.6 |
| TLH-1 | | .2122 | $LH_2$ | | -423 | 208,600 | 206,700* | | - | 19 | .42 | |
| TLH-2 | | .2153 | $LH_2$ | | -423 | 208,100 | 206,200* | | - | 22 | | |
| | | | | | | 208,300 | 206,400* | | | 20 | | |
| TITR-1 | | .2188 | Air | T | 72 | 115,600 | 113,500 | | 17 | 41 | | 15.7 |
| TITR-2 | | .2198 | Air | | 72 | 115,900 | 112,600 | | 17 | 40 | | 15.7 |
| | | | | | | 115,700 | 113,000 | Avg. | 17 | 40 | | 15.7 |
| TITN-1 | | .2205 | $LN_2$ | | -320 | 185,500 | 177,900 | | 15 | 22 | | 18.8 |
| TITN-2 | | .2198 | $LN_2$ | | -320 | 185,600 | 177,900 | | 15 | 22 | | 18.3 |
| | | | | | | 185,500 | 177,900 | Avg. | 15 | 22 | | 18.5 |
| TTH-1 | | .2200 | $LH_2$ | | -423 | 203,400 | 199,800* | | - | 26 | | |
| TTH-2 | | .2190 | $LH_2$ | | -423 | 208,100 | 203,600* | | - | 21 | | |
| | | | | | | 205,700 | 201,700* | | | 23 | | |

* 0.2% Offset yield strength obtained by strain gage

** 0.2% Offset yield strength obtained by extensometer on 2.0 gage length

*** Heat Number G 7622

## Table 3 : TENSILE PROPERTIES ( t = 0.04" & 0.20", 5Al-2.5Sn Titanium Weldment )

| SPECIMEN NUMBER | NOMINAL GAGE ~ IN. | MEASURED GAGE ~ IN. | ATMOSPHERE | GRAIN DIRECTION (L = LONGITUDINAL, T = TRANSVERSE) | TEST TEMPERATURE ~ °F | ULTIMATE STRENGTH ~ PSI | YIELD STRENGTH ** ~ PSI | % ELONGATION FOR LENGTH = 4 x DIA. | ELONGATION ~ % PER 2.0 INCHES | REDUCTION IN AREA ~ % | POISSONS RATIO | MODULUS OF ELASTICITY ~ E x $10^{-6}$ PSI |
|---|---|---|---|---|---|---|---|---|---|---|---|---|
| TWR-1 | .04 | .0335 | Air | T | 75 | 112,500 | 104,800 | | 8 | | 38 | 16.4 |
| TWR-2 | | .0314 | Air | | 75 | 116,500 | 108,900 | | 6 | | 31 | 16.1 |
| | | | | | | 114,500 | 106,800 | Avg. | 7 | | .34 | 16.2 |
| TWN-1 | | .0302 | $LN_2$ | | -320 | 186,200 | 174,000 | | 8 | | .34 | 18.4 |
| TWN-2 | | .0314 | $LN_2$ | | -320 | 181,700 | 171,600 | | 9 | | .34 | 17.1 |
| TWN-3 | | .0330 | $LN_2$ | | -320 | 180,900 | 170,900 | | 10 | | .34 | 18.1 |
| | | | | | | 182,900 | 172,100 | Avg. | 9 | | .34 | 17.8 |
| TWH-1 | | .0313 | $LH_2$ | | -423 | 194,100 | | | | | | |
| TWH-2 | | .0320 | $LH_2$ | | -423 | 205,400 | | | | | .34 | |
| | | | | | | 199,700 | | | | | | |
| TWTR-1A | .20 | .2197 | Air | T | 72 | 116,600 | 110,800 | | 12 | 41 | | 17.9 |
| TWTR-2A | | .2202 | Air | | 72 | 117,600 | 110,900 | | 11 | 37 | .27 | 18.7 |
| | | | | | | 117,100 | 110,800 | Avg. | 11 | 39 | | 18.3 |
| TWTN-1A | | .2210 | $LN_2$ | | -320 | 185,200 | 176,300 | | 12 | 24 | | 18.6 |
| TWTN-2A | | .2203 | $LN_2$ | | -320 | 185,300 | 176,400 | | 10 | 20 | .26 | 19.0 |
| | | | | | | 185,200 | 176,300 | Avg. | 11 | 22 | | 18.8 |
| TWTH-1A | | .2200 | $LH_2$ | | -423 | 202,100 | ▷ | | | | | |
| TWTH-2A | | .2182 | $LH_2$ | | -423 | 208,100 | | | | 21 | .25 | |
| | | | | | | 205,100 | | | | | | |

** 0.2% Offset yield strength obtained by extensometer on 2.0 gage length

▷ Failed Before Reaching Yield Point

*** Heat G 7622

## Table 4 : TENSILE PROPERTIES ( t = 0.125", 2219-T87 Aluminum Base Metal )

| SPECIMEN NUMBER | NOMINAL GAGE ~ IN. | MEASURED GAGE ~ IN. | ATMOSPHERE | GRAIN DIRECTION (L = LONGITUDINAL, T = TRANSVERSE) | TEST TEMPERATURE ~ °F | ULTIMATE STRENGTH ~ PSI | YIELD STRENGTH ** ~ PSI | % ELONGATION FOR LENGTH = 4 x DIA. | ELONGATION ~ % PER 2.0 INCHES | REDUCTION IN AREA ~ % | POISSONS RATIO | MODULUS OF ELASTICITY ~ E x $10^{-6}$ PSI |
|---|---|---|---|---|---|---|---|---|---|---|---|---|
| ALR-1 | .125 | .1242 | Air | L | 72 | 68,200 | 55,900 | | 10 | 35 | .30 | 10.5 |
| AlLR-1 | | .1240 | Air | | 72 | 67,900 | 55,800 | | 11 | 36 | | 10.4 |
| | | | | | | 68,000 | 55,800 | Avg. | 10 | 35 | | 10.5 |
| ALN-1 | | .1242 | $LN_2$ | | -320 | 78,000 | 61,100 | | 12 | 29 | .29 | 11.4 |
| AlLN-1 | | .1235 | $LN_2$ | | -320 | 84,600 | 67,000 | | 11 | 27 | | 10.7 |
| | | | | | | 81,300 | 64,000 | Avg. | 11 | 28 | | 11.2 |
| ALH-1 | | .1245 | $LH_2$ | | -423 | 96,400 | 71,300* | | - | 28 | .35 | 10.9 |
| ALH-2 | | .1240 | $LH_2$ | | -423 | 93,900 | 69,500 | | - | 27 | | 12.1 |
| | | | | | | 95,100 | 70,400* | Avg. | | 27 | | 11.5 |
| AlTR-1 | | .1246 | Air | T | 72 | 68,900 | 55,200 | | 10 | 27 | | 10.5 |
| AlTR-2 | | .1244 | Air | | 72 | 68,500 | 55,200 | | 10 | 25 | | 10.1 |
| | | | | | | 68,700 | 55,200 | Avg. | 10 | 26 | | 10.3 |
| AlTN-1 | | .1245 | $LN_2$ | | -320 | 87,200 | 67,000 | | 13 | 22 | | 12.1 |
| AlTN-2 | | .1244 | $LN_2$ | | -320 | 87,000 | 66,900 | | 12 | 24 | | 11.6 |
| | | | | | | 87,100 | 66,900 | Avg. | 12 | 23 | | 11.8 |
| ATH-1 | | .1247 | $LH_2$ | | -423 | 98,800 | 71,900* | | - | 20 | | 11.2 |
| ATH-2 | | .1248 | $LH_2$ | | -423 | 99,300 | 71,400* | | - | 19 | | 11.0 |
| | | | | | | 99,000 | 71,600* | Avg | | 19 | | 11.1 |

* 0.2% Offset yield strength obtained by strain gage

** 0.2% Offset yield strength obtained by extensometer on 2.0 gage length

Table 5 : TENSILE PROPERTIES ( t = 0.625", 2219-T87 Aluminum Base Metal )

| SPECIMEN NUMBER | NOMINAL GAGE ~ IN. | MEASURED GAGE ~ IN. | ATMOSPHERE | GRAIN DIRECTION (L = LONGITUDINAL, T = TRANSVERSE) | TEST TEMPERATURE ~ °F | ULTIMATE STRENGTH ~ PSI | YIELD STRENGTH ** ~ PSI | % ELONGATION FOR LENGTH = 4 x DIA. | ELONGATION ~ % PER 2.0 INCHES | REDUCTION IN AREA ~ % | POISSONS RATIO | MODULUS OF ELASTICITY ~ E x $10^{-6}$ PSI |
|---|---|---|---|---|---|---|---|---|---|---|---|---|
| ALR-1 | .625 | .6240 | Air | L | 72 | 69,500 | 56,000 | | 14 | 31 | .30 | 11.3 |
| ALR-2 | | .6255 | Air | | 72 | 69,200 | 56,100 | | 14 | 29 | | 9.7 |
| | | | | | | 69,300 | 56,000 | Avg. | 14 | 30 | | 10.5 |
| ALN-1 | | .6268 | $LN_2$ | | -320 | 85,200 | 67,200 | | 15 | 29 | .31 | 12.0 |
| ALN-2 | | .6245 | $LN_2$ | | -320 | 85,900 | 67,000 | | 15 | 29 | | 13.8 |
| | | | | | | 85,500 | 67,100 | Avg. | 15 | 29 | | 12.6 |
| ALH-1 | | .6258 | $LH_2$ | | -423 | 92,100 | 70,300* | | - | 21 | .36 | 10.8 |
| ALH-2 | | .6255 | $LH_2$ | | -423 | 93,800 | 72,700* | | - | 22 | | 9.9 |
| | | | | | | 92,900 | 71,500* | Avg. | | 21 | | 10.3 |
| ATR-1 | | .6266 | Air | T | 72 | 69,300 | 56,000 | | 14 | 31 | | 9.8 |
| ATR-2 | | .6240 | Air | | 72 | 69,300 | 56,100 | | 14 | 29 | | 11.4 |
| | | | | | | 69,300 | 56,000 | Avg. | 14 | 30 | | 10.6 |
| ATN-1 | | .6250 | $LN_2$ | | -320 | 86,800 | 66,100 | | 12 | 19 | | 12.2 |
| ATN-2 | | .6248 | $LN_2$ | | -320 | 86,700 | 65,200 | | 12 | 18 | | 11.0 |
| | | | | | | 86,700 | 65,600 | Avg. | 12 | 18 | | 11.6 |
| ATH-1 | | .6250 | $LH_2$ | | -423 | 94,900 | - | | - | 16 | | 12.4 |
| ATH-2 | | .6250 | $LH_2$ | | -423 | - | 71,400* | | - | 16 | | 11.1 |
| | | | | | | 94,900 | 71,400* | Avg. | | 16 | | 11.7 |

* 0.2% Offset yield strength obtained by strain gage

** 0.2% Offset yield strength obtained by extensometer on 2.0 gage length

Table 6 : TENSILE PROPERTIES ( t = 0.125" & 1.00", 2219 Aluminum Weld Metal

| SPECIMEN NUMBER | NOMINAL GAGE ~ IN. | MEASURED GAGE ~ IN. | ATMOSPHERE | GRAIN DIRECTION (L = LONGITUDINAL, T = TRANSVERSE) | TEST TEMPERATURE ~ °F | ULTIMATE STRENGTH ~ PSI | YIELD STRENGTH ** ~ PSI | % ELONGATION FOR LENGTH = 4 x DIA. | ELONGATION ~ % PER 2.0 INCHES | REDUCTION IN AREA ~ % | POISSONS RATIO | MODULUS OF ELASTICITY ~ E x $10^{-6}$ PSI |
|---|---|---|---|---|---|---|---|---|---|---|---|---|
| AWR-3 | .125 | .1232 | Air | L | 72 | 39,000 | 27,900 | | 3 | 22 | | 9.5 |
| AWR-4 | | .1218 | Air | | 72 | 38,200 | 25,500 | | 3 | 35 | .22 | 8.9 |
| | | | | | | 38,600 | 26,700 | Avg. | 3 | 28 | | 9.2 |
| AWN-3 | | .1228 | $LN_2$ | | -320 | 53,800 | 30,900 | | 4 | 22 | | 10.1 |
| | | .1200 | $LN_2$ | | -320 | 55,000 | 32,500 | | 4 | 25 | .27 | 9.8 |
| | | | | | | 54,400 | 31,700 | Avg. | 4 | 23 | | 10.0 |
| AWH-3 | | .1248 | $LH_2$ | | -423 | 69,700 | 34,200* | | 15 | | | 10.9 |
| | | .1200 | $LH_2$ | | -423 | 62,800 | 26,700* | | | | .31 | 10.6 |
| | | | | | | 66,200 | 30,300* | | | | | 10.7 |
| AWR-1 | 1.00 | 1.006 | Air | L | 72 | 42,900 | 22,100 | | 8 | 19 | | 9.5 |
| AWR-2 | | 1.0142 | Air | | 72 | 42,900 | 21,800 | | 8 | 20 | .33 | 9.4 |
| | | | | | | 42,900 | 21,900 | Avg. | 8 | 19 | | 9.45 |
| AWN-1 | | 1.0175 | $LN_2$ | | -320 | 54,700 | 25,900 | | 7 | 13 | | 10.7 |
| SWN-2 | | 1.0230 | $LN_2$ | | -320 | 56,200 | 27,700 | | 7 | 15 | .29 | 11.4 |
| | | | | | | 55,400 | 26,800 | Avg. | 7 | 14 | | 11.1 |
| AWH-1 | | 1.0090 | $LH_2$ | | -423 | 65,600 | 33,300* | | - | 9 | | 10.4 |
| AWH-2 | | 1.0185 | $LH_2$ | | -423 | 62,600 | 30,900* | | - | 9 | .36 | 9.3 |
| | | | | | | 64,100 | 32,100* | Avg. | | 9 | | 9.8 |

* 0.2% Offset yield strength obtained by strain gage installed on weld metal only

** 0.2% Offset yield strength obtained by extensometer on 2.0 gage length

Table 7: STATIC FRACTURE TOUGHNESS DATA, 0.20 Inch Thick, 5Al-2.5 Sn Titanium Base Metal - Transverse Grain, a/2c = .075, Room Temperature

| SPECIMEN | | | TEST CONDITIONS | | | | FRACTURE DATA | | | | | | |
|---|---|---|---|---|---|---|---|---|---|---|---|---|---|
| Number | Thickness (in) (t) | Width (in) (w) | Temperature (°F) | Environment | Gross Section Stress (Ksi) ($\sigma_G$) | Net Section Stress (Ksi) ($\sigma_N$) | Flaw Depth (in) a | Flaw Length (in) 2c | a/t | a/2c | $\sigma_N/\sigma_{ys}$ | Irwins Apparent K (Ksi $\sqrt{in}$) | Based On Avg. $K_{Ic}$ $M_K$ |
| TB16R-1 | 0.210 | 13.490 | RT | Air | 92.0 | 101.2 | 0.156 | 2.136 | 0.742 | 0.073 | 0.90 | 74.21 | |
| TB16R-2 | 0.209 | 13.490 | RT | Air | 93.0 | 102.5 | 0.161 | 2.128 | 0.770 | 0.076 | 0.91 | 76.17 | |
| TB17R-3 | 0.212 | 13.504 | RT | Air | 92.0 | 101.2 | 0.148 | 2.288 | 0.698 | 0.065 | 0.90 | 72.73 | |
| TB17R-4 | 0.207 | 13.492 | RT | Air | 103.4 | 115.4 | 0.158 | 2.330 | 0.765 | 0.068 | 1.02 | 86.05* | |
| TB18R-5 | 0.221 | 13.506 | RT | Air | 93.0 | 104.7 | 0.180 | 2.380 | 0.814 | 0.076 | 0.93 | 80.54 | |
| TB18R-6 | 0.202 | 13.515 | RT | Air | 91.8 | 103.8 | 0.164 | 2.450 | 0.812 | 0.067 | 0.92 | 76.25* | |
| TB19R-3 | 0.210 | 13.512 | RT | Air | 88.2 | 100.3 | 0.171 | 2.543 | 0.816 | 0.067 | 0.89 | 74.35 | |
| TB19R-4 | 0.213 | 13.510 | RT | Air | 87.9 | 101.3 | 0.194 | 2.500 | 0.910 | 0.078 | 0.90 | 78.25 | |

NOTE: *Made from Heat 303268. Other specimens are from Heat G-7622.

Table 8: STATIC FRACTURE TOUGHNESS DATA, 0.20 Inch Thick, 5Al-2.5 Sn Titanium Base Metal - Transverse Grain, a/2c = .15, Room Temperature

| SPECIMEN | | | TEST CONDITIONS | | | | FRACTURE DATA | | | | | | |
|---|---|---|---|---|---|---|---|---|---|---|---|---|---|
| Number | Thickness (in) (t) | Width (in) (w) | Temperature (°F) | Environment | Gross Section Stress (Ksi) ($\sigma_G$) | Net Section Stress (Ksi) ($\sigma_N$) | Flaw Depth (in) a | Flaw Length (in) 2c | a/t | a/2c | $\sigma_N/\sigma_{ys}$ | Irwins Apparent K (Ksi $\sqrt{in}$) | Based On Avg. $K_{Ic}$ $M_K$ |
| TB18R-4 | 0.209 | 6.998 | RT | Air | 96.9 | 108.7 | 0.169 | 1.180 | 0.809 | 0.143 | 0.96 | 76.55 | |
| TB19R-2 | 0.218 | 7.002 | RT | Air | 95.2 | 107.8 | 0.181 | 1.270 | 0.830 | 0.143 | 0.95 | 77.68 | |
| TB15R-2 | 0.216 | 6.998 | RT | Air | 104.4 | 111.8 | 0.130 | 1.004 | 0.603 | 0.130 | 0.99 | 74.30 | |
| TB15R-1 | 0.220 | 6.998 | RT | Air | 102.7 | 111.6 | 0.164 | 1.006 | 0.746 | 0.163 | 0.99 | 78.91 | |
| TB17R-1 | 0.220 | 7.002 | RT | Air | 99.8 | 110.8 | 0.171 | 1.123 | 0.777 | 0.152 | 0.98 | 78.87 | |
| TB17R-2 | 0.218 | 6.997 | RT | Air | 98.1 | 108.5 | 0.166 | 1.130 | 0.762 | 0.147 | 0.96 | 76.64 | |
| TB18R-1 | 0.213 | 3.259 | RT | Air | 80.6 | 105.7 | 0.175 | 1.180 | 0.822 | 0.148 | 0.94 | 63.00 | |
| TB18R-2 | 0.215 | 4.751 | RT | Air | 86.0 | 102.8 | 0.176 | 1.250 | 0.819 | 0.141 | 0.91 | 68.41 | |
| TB18R-3 | 0.221 | 6.998 | RT | Air | 98.7 | 110.4 | 0.176 | 1.224 | 0.796 | 0.144 | 0.98 | 79.75 | |
| TB18R-9 | 0.221 | 13.500 | RT | Air | 105.9 | 111.8 | 0.170 | 1.190 | 0.769 | 0.143 | 0.99 | 85.20 | |
| TB19R-1 | 0.218 | 7.001 | RT | Air | 97.6 | 107.8 | 0.188 | 1.220 | 0.862 | 0.154 | 0.95 | 80.43 | |

NOTE: All Specimens from Heat G-7622.

Table 9: STATIC FRACTURE TOUGHNESS DATA, 0.20 Inch Thick, 5Al-2.5 Sn Titanium Base Metal - Transverse Grain, a/2c = .15, -320°F

| SPECIMEN | | | TEST CONDITIONS | | | | FRACTURE DATA | | | | | | |
|---|---|---|---|---|---|---|---|---|---|---|---|---|---|
| Number | Thickness (in) (t) | Width (in) (w) | Temperature (°F) | Environment | Gross Section Stress (Ksi) ($\sigma_G$) | Net Section Stress (Ksi) ($\sigma_N$) | Flaw Depth (in) a | Flaw Length (in) 2c | a/t | a/2c | $\sigma_N/\sigma_{ys}$ | Irwins Apparent K (Ksi $\sqrt{in}$) | Based On Avg. $K_{Ic}$ $M_K$ |
| TB08N-5 | 0.214 | 5.990 | -320 | $LN_2$ | 107.9 | 111.4 | 0.095 | 0.520 | 0.443 | 0.183 | 0.68 | 59.44 | 1.262 |
| TB08N-6 | 0.220 | 6.000 | -320 | $LN_2$ | 150.4 | 153.9 | 0.070 | 0.525 | 0.318 | 0.133 | 0.87 | 77.09 | 0.973 |
| TB12N-4 | 0.218 | 6.998 | -320 | $LN_2$ | 71.0 | 75.5 | 0.142 | 0.816 | 0.651 | 0.174 | 0.42 | 47.17 | 1.590 |
| TB12N-5 | 0.217 | 6.996 | -320 | $LN_2$ | 68.2 | 72.6 | 0.138 | 0.801 | 0.636 | 0.172 | 0.41 | 44.70 | 1.678 |
| TB15N-10 | 0.217 | 6.997 | -320 | $LN_2$ | 65.7 | 71.3 | 0.144 | 1.029 | 0.664 | 0.140 | 0.40 | 45.34 | 1.654 |
| TB15N-11 | 0.214 | 6.996 | -320 | $LN_2$ | 56.9 | 62.0 | 0.154 | 0.987 | 0.720 | 0.156 | 0.35 | 39.85 | 1.882 |
| TB18N-8 | 0.216 | 7.004 | -320 | $LN_2$ | 48.9 | 54.7 | 0.170 | 1.194 | 0.787 | 0.142 | 0.31 | 36.38 | 2.062 |
| TB18N-9 | 0.220 | 6.996 | -320 | $LN_2$ | 52.8 | 58.8 | 0.166 | 1.200 | 0.755 | 0.138 | 0.33 | 39.01 | 1.923 |

Table 10: STATIC FRACTURE TOUGHNESS DATA, 0.20 Inch Thick, 5Al-2.5 Sn Titanium Base Metal - Transverse Grain, a/2c = .25, -320°F

| SPECIMEN | | | TEST CONDITIONS | | | | FRACTURE DATA | | | | | | |
|---|---|---|---|---|---|---|---|---|---|---|---|---|---|
| Number | Thickness (in) (t) | Width (in) (w) | Temperature (°F) | Environment | Gross Section Stress (Ksi) ($\sigma_G$) | Net Section Stress (Ksi) ($\sigma_N$) | Flaw Depth (in) a | Flaw Length (in) 2c | a/t | a/2c | $\sigma_N/\sigma_{ys}$ | Irwins Apparent K (Ksi $\sqrt{in}$) | Based On Avg. $K_{Ic}$ $M_K$ |
| TB08N-3 | 0.210 | 4.002 | -320 | $LN_2$ | 168.1 | 171.6 | 0.070 | 0.306 | 0.334 | 0.229 | 0.96 | 78.72 | 0.953 |
| TB08N-4 | 0.211 | 4.001 | -320 | $LN_2$ | 155.5 | 158.7 | 0.070 | 0.306 | 0.333 | 0.229 | 0.89 | 72.01 | 1.042 |
| TB12N-2 | 0.212 | 4.742 | -320 | $LN_2$ | 125.6 | 130.5 | 0.100 | 0.472 | 0.472 | 0.212 | 0.73 | 69.29 | 1.032 |
| TB12N-3 | 0.212 | 4.740 | -320 | $LN_2$ | 108.9 | 113.3 | 0.100 | 0.471 | 0.472 | 0.212 | 0.64 | 59.42 | 1.262 |
| TB15N-8 | 0.219 | 4.750 | -320 | $LN_2$ | 90.1 | 95.6 | 0.129 | 0.571 | 0.589 | 0.226 | 0.54 | 54.50 | 1.376 |
| TB15N-9 | 0.216 | 4.749 | -320 | $LN_2$ | 89.1 | 94.7 | 0.125 | 0.577 | 0.579 | 0.217 | 0.53 | 53.56 | 1.400 |
| TB18N-6 | 0.211 | 4.754 | -320 | $LN_2$ | 70.8 | 77.5 | 0.156 | 0.710 | 0.739 | 0.220 | 0.44 | 47.04 | 1.594 |
| TB18N-7 | 0.220 | 4.753 | -320 | $LN_2$ | 71.8 | 78.1 | 0.152 | 0.692 | 0.691 | 0.220 | 0.44 | 47.11 | 1.592 |

Table 11: STATIC FRACTURE TOUGHNESS DATA, 0.20 Inch Thick, 5Al-2.5 Sn Titanium Base Metal - Transverse Grain, a/2c = .40, -320°F

| SPECIMEN | | | TEST CONDITIONS | | | | FRACTURE DATA | | | | | | |
|---|---|---|---|---|---|---|---|---|---|---|---|---|---|
| Number | Thickness (in) (t) | Width (in) (w) | Temperature (°F) | Environment | Gross Section Stress (Ksi) ($\sigma_G$) | Net Section Stress (Ksi) ($\sigma_N$) | Flaw Depth (in) a | Flaw Length (in) 2c | a/t | a/2c | $\sigma_N/\sigma_{ys}$ | Irwins Apparent K (Ksi $\sqrt{in}$) | Based On Avg. $K_{Ic}$ $M_K$ |
| TB08N-1 | 0.219 | 3.257 | -320 | $LN_2$ | 172.7 | 175.5 | 0.075 | 0.190 | 0.342 | 0.395 | 0.99 | 68.95 | 1.088 |
| TB08N-2 | 0.216 | 2.754 | -320 | $LN_2$ | 174.7 | 177.6 | 0.067 | 0.184 | 0.310 | 0.364 | 1.00 | 68.43 | 1.096 |
| TB12N-6 | 0.218 | 3.244 | -320 | $LN_2$ | 153.9 | 159.3 | 0.107 | 0.286 | 0.490 | 0.374 | 0.90 | 74.29 | 1.010 |
| TB12N-8 | 0.203 | 3.245 | -320 | $LN_2$ | 159.4 | 165.6 | 0.106 | 0.297 | 0.522 | 0.357 | 0.93 | 78.39* | |
| TB15N-7 | 0.219 | 3.251 | -320 | $LN_2$ | 118.0 | 124.8 | 0.138 | 0.362 | 0.629 | 0.381 | 0.70 | 63.02 | 1.190 |
| TB15N-12 | 0.219 | 3.244 | -320 | $LN_2$ | 110.8 | 117.0 | 0.136 | 0.356 | 0.622 | 0.382 | 0.66 | 58.51 | 1.202 |
| TB18N-5 | 0.219 | 3.252 | -320 | $LN_2$ | 100.4 | 111.0 | 0.160 | 0.430 | 0.731 | 0.372 | 0.62 | 57.90 | 1.295 |
| TB18N-4 | 0.203 | 3.248 | -320 | $LN_2$ | 131.2 | 145.0 | 0.172 | 0.470 | 0.847 | 0.366 | 0.82 | 80.05* | |

* Made from Heat 303268. Other Specimens are from Heat G-7622

Table 12: STATIC FRACTURE TOUGHNESS DATA, 0.20 Inch Thick, 5Al-2.5 Sn Titanium Base Metal - Transverse Grain, a/2c = .15, -423°F

| SPECIMEN | | | TEST CONDITIONS | | | | FRACTURE DATA | | | | | | |
|---|---|---|---|---|---|---|---|---|---|---|---|---|---|
| Number | Thickness (in) (t) | Width (in) (w) | Temperature (°F) | Environment | Gross Section Stress (Ksi) ($\sigma_G$) | Net Section Stress (Ksi) ($\sigma_N$) | Flaw Depth (in) a | Flaw Length (in) 2c | a/t | a/2c | $\sigma_N/\sigma_{ys}$ | Irwins Apparent K (Ksi $\sqrt{in}$) | Based On Avg. $K_{Ic}$ $M_K$ |
| TB08H-2 | 0.217 | 5.990 | -423 | $LH_2$ | 100.3 | 103.2 | 0.090 | 0.524 | 0.415 | 0.172 | 0.51 | 53.61 | 1.119 |
| TB08H-3 | 0.222 | 5.995 | -423 | $LH_2$ | 92.5 | 95.3 | 0.090 | 0.515 | 0.406 | 0.175 | 0.47 | 49.13 | 1.221 |
| TB12H-6 | 0.214 | 6.998 | -423 | $LH_2$ | 56.2 | 60.4 | 0.158 | 0.814 | 0.739 | 0.194 | 0.30 | 38.33 | 1.565 |
| TB12H-7 | 0.223 | 6.996 | -423 | $LH_2$ | 57.0 | 61.0 | 0.155 | 0.816 | 0.695 | 0.190 | 0.30 | 38.68 | 1.551 |
| TB15H-6 | 0.220 | 6.996 | -423 | $LH_2$ | 50.1 | 54.1 | 0.147 | 0.985 | 0.670 | 0.149 | 0.27 | 34.40 | 1.744 |
| TB15H-7 | 0.218 | 6.996 | -423 | $LH_2$ | 48.9 | 53.3 | 0.155 | 1.017 | 0.712 | 0.152 | 0.26 | 34.36 | 1.746 |
| TB18H-6 | 0.217 | 7.000 | -423 | $LH_2$ | 45.6 | 50.9 | 0.171 | 1.192 | 0.788 | 0.144 | 0.25 | 33.92 | 1.769 |
| TB18H-7 | 0.214 | 6.995 | -423 | $LH_2$ | 43.3 | 48.7 | 0.180 | 1.190 | 0.842 | 0.151 | 0.24 | 32.78 | 1.880 |

Table 13: STATIC FRACTURE TOUGHNESS DATA, 0.20 Inch Thick, 5Al-2.5 Sn Titanium Base Metal - Transverse Grain, a/2c = .40, -423°F

| SPECIMEN | | | TEST CONDITIONS | | | | FRACTURE DATA | | | | | | |
|---|---|---|---|---|---|---|---|---|---|---|---|---|---|
| Number | Thickness (in) (t) | Width (in) (w) | Temperature (°F) | Environment | Gross Section Stress (Ksi) ($\sigma_G$) | Net Section Stress (Ksi) ($\sigma_N$) | Flaw Depth (in) a | Flaw Length (in) 2c | a/t | a/2c | $\sigma_N/\sigma_{ys}$ | Irwins Apparent K (Ksi $\sqrt{in}$) | Based On Avg. $K_{Ic}$ $M_K$ |
| TB08H-1 | 0.219 | 2.745 | -423 | $LH_2$ | 143.6 | 146.3 | 0.072 | 0.215 | 0.329 | 0.335 | 0.73 | 58.56 | 1.025 |
| TB08H-2 | 0.213 | 2.752 | -423 | $LH_2$ | 164.1 | 167.1 | 0.071 | 0.182 | 0.334 | 0.390 | 0.83 | 61.50 | 0.976 |
| TB12H-4 | 0.205 | 3.249 | -423 | $LH_2$ | 150.9 | 158.4 | 0.107 | 0.300 | 0.523 | 0.357 | 0.79 | 73.45* | |
| TB12H-5 | 0.219 | 3.251 | -423 | $LH_2$ | 114.9 | 118.8 | 0.103 | 0.278 | 0.471 | 0.371 | 0.59 | 53.28 | 1.126 |
| TB15H-4 | 0.219 | 3.242 | -423 | $LH_2$ | 90.4 | 95.6 | 0.132 | 0.350 | 0.602 | 0.377 | 0.47 | 46.78 | 1.283 |
| TB15H-5 | 0.219 | 3.251 | -423 | $LH_2$ | 88.1 | 93.4 | 0.136 | 0.356 | 0.621 | 0.382 | 0.46 | 46.02 | 1.304 |
| TB18H-4 | 0.213 | 3.247 | -423 | $LH_2$ | 73.4 | 79.9 | 0.160 | 0.420 | 0.751 | 0.381 | 0.40 | 45.23 | 1.327 |
| TB18H-5 | 0.219 | 3.257 | -423 | $LH_2$ | 78.7 | 85.6 | 0.172 | 0.420 | 0.785 | 0.410 | 0.42 | 44.80 | 1.339 |

* Heat No. 303268, Other Specimens from Heat G-7622.

Table 14: STATIC FRACTURE TOUGHNESS DATA, 0.20 Inch Thick, 5Al-2.5 Sn Titanium Weld Metal, a/2c = 0.075, Room Temperature

| SPECIMEN | | | TEST CONDITIONS | | | | FRACTURE DATA | | | | | | |
|---|---|---|---|---|---|---|---|---|---|---|---|---|---|
| Number | Thickness (in) (t) | Width (in) (w) | Temperature (°F) | Environment | Gross Section Stress (Ksi) ($\sigma_G$) | Net Section Stress (Ksi) ($\sigma_N$) | Flaw Depth (in) a | Flaw Length (in) 2c | a/t | a/2c | $\sigma_N/\sigma_{ys}$ | Irwins Apparent K (Ksi $\sqrt{in}$) | Based On Avg. $K_{Ic}$ $M_K$ |
| 7TW16R-1 | 0.235 | 10.980 | RT | Air | 89.8 | 98.9 | 0.136 | 2.160 | 0.578 | 0.063 | 0.89 | 68.09 | |
| 7TW17R-2 | 0.221 | 11.000 | RT | Air | 81.2 | 92.1 | 0.152 | 2.340 | 0.689 | 0.065 | 0.83 | 64.10 | |
| 7TW18R-3 | 0.230 | 11.010 | RT | Air | 85.4 | 97.9 | 0.162 | 2.450 | 0.704 | 0.066 | 0.88 | 70.00** | |
| 7TW19R-4 | 0.232 | 11.003 | RT | Air | 81.0 | 95.0 | 0.184 | 2.600 | 0.794 | 0.071 | 0.86 | 70.04 | |

** Made from Heat G-8818. Other Specimens from Heat 293622.

Table 15: STATIC FRACTURE TOUGHNESS DATA, 0.200 Inch Thick, 5Al-2.5 Sn Titanium Weld Metal, a/2c = .15, Room Temperature

| SPECIMEN | | | TEST CONDITIONS | | | | FRACTURE DATA | | | | | | |
|---|---|---|---|---|---|---|---|---|---|---|---|---|---|
| Number | Thickness (in) (t) | Width (in) (w) | Temperature (°F) | Environment | Gross Section Stress (Ksi) ($\sigma_G$) | Net Section Stress (Ksi) ($\sigma_N$) | Flaw Depth (in) a | Flaw Length (in) 2c | a/t | a/2c | $\sigma_N/\sigma_{ys}$ | Irwins Apparent K (Ksi $\sqrt{In}$) | Based On Avg. $K_{Ic}$ $M_K$ |
| ITW15R-1H | 0.214 | 5.749 | RT | Air | 102.4 | 114.1 | 0.153 | 1.036 | 0.715 | 0.148 | 1.03 | 77.54 | |
| ITW17R-1J | 0.213 | 5.748 | RT | Air | 96.9 | 108.8 | 0.147 | 1.126 | 0.690 | 0.131 | 0.98 | 72.56 | |
| ITW18R-1B | 0.210 | 2.756 | RT | Air | 93.1 | 130.7 | 0.159 | 1.185 | 0.757 | 0.134 | 1.18 | 71.79 | |
| ITW18R-2 | 0.223 | 4.006 | RT | Air | 90.9 | 111.6 | 0.162 | 1.203 | 0.728 | 0.135 | 1.01 | 70.48 | |
| ITW18R-31 | 0.215 | 5.744 | RT | Air | 96.0 | 110.4 | 0.160 | 1.216 | 0.744 | 0.132 | 1.00 | 74.81 | |
| ITW18R-4 | 0.214 | 11.002 | RT | Air | 95.1 | 101.4 | 0.155 | 1.200 | 0.724 | 0.129 | 0.92 | 73.01 | |
| ITW19R-1J | 0.213 | 5.748 | RT | Air | 87.8 | 103.6 | 0.172 | 1.348 | 0.806 | 0.128 | 0.94 | 70.30 | |

NOTE: All Specimens from Heat G-7622.

Table 16: STATIC FRACTURE TOUGHNESS DATA, 0.200 Inch Thick, 5Al-2.5 Sn Titanium Weld Metal, a/2c = .15, -320°F

| SPECIMEN | | | TEST CONDITIONS | | | | FRACTURE DATA | | | | | | |
|---|---|---|---|---|---|---|---|---|---|---|---|---|---|
| Number | Thickness (in) (t) | Width (in) (w) | Temperature (°F) | Environment | Gross Section Stress (Ksi) ($\sigma_G$) | Net Section Stress (Ksi) ($\sigma_N$) | Flaw Depth (in) a | Flaw Length (in) 2c | a/t | a/2c | $\sigma_N/\sigma_{ys}$ | Irwins Apparent K (Ksi $\sqrt{In}$) | Based On Avg. $K_{Ic}$ $M_K$ |
| ITW15N-1J | 0.201 | 5.748 | -320 | $LN_2$ | 89.6 | 99.4 | 0.120 | 1.010 | 0.597 | 0.119 | 0.56 | 58.19 | 1.461 |
| ITW08N-1H | 0.212 | 5.748 | -320 | $LN_2$ | 165.9 | 170.3 | 0.071 | 0.525 | 0.334 | 0.135 | 0.97 | 87.04 | 0.977 |
| ITW12N-1 | 0.216 | 5.747 | -320 | $LN_2$ | 109.6 | 116.1 | 0.113 | 0.805 | 0.524 | 0.140 | 0.66 | 68.58 | 1.239 |
| ITW18N-11 | 0.214 | 5.754 | -320 | $LN_2$ | 58.4 | 67.8 | 0.174 | 1.215 | 0.812 | 0.143 | 0.38 | 44.06 | 1.929 |

NOTE: All Specimens from Heat G-7622.

Table 17: STATIC FRACTURE TOUGHNESS DATA, 0.20 Inch Thick, 5Al-2.5 Sn Titanium Weld Metal, a/2c = .25, -320°F

| SPECIMEN | | | TEST CONDITIONS | | | | FRACTURE DATA | | | | | | |
|---|---|---|---|---|---|---|---|---|---|---|---|---|---|
| Number | Thickness (in) (t) | Width (in) (w) | Temperature (°F) | Environment | Gross Section Stress (Ksi) ($\sigma_G$) | Net Section Stress (Ksi) ($\sigma_N$) | Flaw Depth (in) a | Flaw Length (in) 2c | a/t | a/2c | $\sigma_N/\sigma_{ys}$ | Irwins Apparent K (Ksi $\sqrt{in}$) | Based On Avg. $K_{Ic}$ $M_K$ |
| 2TW08N-1 | 0.233 | 3.502 | -320 | $LN_2$ | 184.8 | 188.8 | 0.070 | 0.070 | 0.301 | 0.227 | 1.07 | 87.51 | |
| 2TW12N-2 | 0.237 | 3.999 | -320 | $LN_2$ | 131.9 | 137.7 | 0.110 | 0.460 | 0.464 | 0.239 | 0.78 | 74.40 | 1.142 |
| 2TW15N-3 | 0.236 | 4.000 | -320 | $LN_2$ | 114.3 | 122.9 | 0.136 | 0.593 | 0.576 | 0.229 | 0.70 | 71.66 | 1.186 |
| 2TW18N-4 | 0.236 | 4.000 | -320 | $LN_2$ | 102.7 | 113.0 | 0.154 | 0.695 | 0.652 | 0.222 | 0.64 | 68.64 | 1.238 |

NOTE: All Specimens from Heat 293622.

Table 18: STATIC FRACTURE TOUGHNESS DATA, 0.20 Inch Thick, 5Al-2.5 Sn Titanium Weld Metal, a/2c = .40, -320°F

| SPECIMEN | | | TEST CONDITIONS | | | | FRACTURE DATA | | | | | | |
|---|---|---|---|---|---|---|---|---|---|---|---|---|---|
| Number | Thickness (in) (t) | Width (in) (w) | Temperature (°F) | Environment | Gross Section Stress (Ksi) ($\sigma_G$) | Net Section Stress (Ksi) ($\sigma_N$) | Flaw Depth (in) a | Flaw Length (in) 2c | a/t | a/2c | $\sigma_N/\sigma_{ys}$ | Irwins Apparent K (Ksi $\sqrt{in}$) | Based On Avg. $K_{Ic}$ $M_K$ |
| 4TW08N-1F | 0.227 | 2.752 | -320 | $LN_2$ | 179.7 | 182.6 | 0.069 | 0.181 | 0.305 | 0.381 | 1.04 | 70.16 | |
| 4TW12N-1F | 0.227 | 2.753 | -320 | $LN_2$ | 150.1 | 155.6 | 0.105 | 0.268 | 0.462 | 0.392 | 0.88 | 70.25 | 1.200 |
| 4TW15N-1E | 0.233 | 2.754 | -320 | $LN_2$ | 123.7 | 130.7 | 0.127 | 0.345 | 0.544 | 0.368 | 0.74 | 63.83 | 1.332 |
| 4TW18N-1F | 0.224 | 2.755 | -320 | $LN_2$ | 122.5 | 133.2 | 0.154 | 0.409 | 0.687 | 0.377 | 0.76 | 69.64 | 1.221 |

NOTE: All Specimens from Heat 7909.

Table 19: STATIC FRACTURE TOUGHNESS DATA,
0.200 Inch Thick, 5Al-2.5 Sn Titanium Weld Metal,
a/2c = .15, -423°F

| SPECIMEN | | | TEST CONDITIONS | | | | FRACTURE DATA | | | | | | |
|---|---|---|---|---|---|---|---|---|---|---|---|---|---|
| Number | Thickness (in) (t) | Width (in) (w) | Temperature (°F) | Environment | Gross Section Stress (Ksi) ($\sigma_G$) | Net Section Stress (Ksi) ($\sigma_N$) | Flaw Depth (in) a | Flaw Length (in) 2c | a/t | a/2c | $\sigma_N/\sigma_{ys}$ | Irwins Apparent K (Ksi $\sqrt{in}$) | Based On Avg. $K_{Ic}$ $M_K$ |
| ITW08H-2H | 0.206 | 5.744 | -423 | $LH_2$ | 137.0 | 141.1 | 0.076 | 0.547 | 0.368 | 0.139 | 0.69 | 70.81 | 1.059 |
| ITW12H-21 | 0.211 | 5.749 | -423 | $LH_2$ | 78.2 | 83.1 | 0.112 | 0.830 | 0.530 | 0.135 | 0.41 | 47.86 | 1.567 |
| ITW15H-2J | 0.213 | 5.749 | -423 | $LH_2$ | 61.2 | 67.0 | 0.138 | 1.010 | 0.648 | 0.137 | 0.33 | 41.29 | 1.826 |
| ITW18H-21 | 0.220 | 5.748 | -423 | $LH_2$ | 50.9 | 58.5 | 0.175 | 1.230 | 0.797 | 0.142 | 0.29 | 38.38 | 1.954 |

NOTE: All Specimens Made from Heat Number G-7622.

Table 20: STATIC FRACTURE TOUGHNESS DATA,
0.200 Inch Thick, 5Al-2.5 Sn Titanium Weld Metal,
a/2c = .40, -423°F

| SPECIMEN | | | TEST CONDITIONS | | | | FRACTURE DATA | | | | | | |
|---|---|---|---|---|---|---|---|---|---|---|---|---|---|
| Number | Thickness (in) (t) | Width (in) (w) | Temperature (°F) | Environment | Gross Section Stress (Ksi) ($\sigma_G$) | Net Section Stress (Ksi) ($\sigma_N$) | Flaw Depth (in) a | Flaw Length (in) 2c | a/t | a/2c | $\sigma_N/\sigma_{ys}$ | Irwins Apparent K (Ksi $\sqrt{in}$) | Based On Avg. $K_{Ic}$ $M_K$ |
| 4TW08H-2D | 0.235 | 2.754 | -423 | $LH_2$ | 181.9 | 184.8 | 0.070 | 0.185 | 0.299 | 0.378 | 0.90 | 70.84 | 1.059 |
| 4TW12H-2D | 0.234 | 2.760 | -423 | $LH_2$ | 156.0 | 161.6 | 0.102 | 0.278 | 0.436 | 0.367 | 0.79 | 73.37 | 1.022 |
| 4TW15H-2F | 0.225 | 2.755 | -423 | $LH_2$ | 138.1 | 146.4 | 0.128 | 0.343 | 0.569 | 0.373 | 0.71 | 71.71 | 1.046 |
| 4TW18H-2E | 0.235 | 2.758 | -423 | $LH_2$ | 89.5 | 96.8 | 0.154 | 0.410 | 0.655 | 0.376 | 0.47 | 50.08* | 1.498 |

NOTE: All Specimens Made from Heat Number 7909.

Table 21: STATIC FRACTURE TOUGHNESS DATA,
0.020 Inch Thick, 5Al-2.5 Sn Titanium Base Metal -
Transverse Grain, a/2c = .05, Room Temperature

| SPECIMEN | | | TEST CONDITIONS | | | | FRACTURE DATA | | | | | | |
|---|---|---|---|---|---|---|---|---|---|---|---|---|---|
| Number | Thickness (in) (t) | Width (in) (w) | Temperature (°F) | Environment | Gross Section Stress (Ksi) ($\sigma_G$) | Net Section Stress (Ksi) ($\sigma_N$) | Flaw Depth (in) a | Flaw Length (in) 2c | a/t | a/2c | $\sigma_N/\sigma_{ys}$ | Irwins Apparent K (Ksi $\sqrt{in}$) | Based On Avg. $K_{Ic}$ $M_K$ |
| TB18R-1 | 0.020 | 4.005 | RT | Air | 112.3 | 120.6 | 0.018 | 0.390 | 0.900 | 0.046 | 1.08 | 32.67 | |
| TB18R-2 | 0.020 | 4.003 | RT | Air | 120.7 | 129.6 | 0.018 | 0.390 | 0.900 | 0.046 | 1.16 | 35.11 | |

Table 22: STATIC FRACTURE TOUGHNESS DATA, 0.020 Inch Thick, 5Al-2.5 Sn Titanium Base Metal - Transverse Grain, a/2c = .05, -320°F

| SPECIMEN | | | TEST CONDITIONS | | | | FRACTURE DATA | | | | | | |
|---|---|---|---|---|---|---|---|---|---|---|---|---|---|
| Number | Thickness (in) (t) | Width (in) (w) | Temperature (°F) | Environment | Gross Section Stress (Ksi) ($\sigma_G$) | Net Section Stress (Ksi) ($\sigma_N$) | Flaw Depth (in) a | Flaw Length (in) 2c | a/t | a/2c | $\sigma_N/\sigma_{ys}$ | Irwins Apparent K (Ksi $\sqrt{in}$) | Based On Avg. $K_{Ic}$ $M_K$ |
| TB17N-1 | 0.020 | 3.997 | -320 | $LN_2$ | 171.8 | 181.6 | 0.016 | 0.345 | 0.800 | 0.046 | 1.05 | 47.06 | |
| TB17N-2 | 0.020 | 4.001 | -320 | $LN_2$ | 165.6 | 175.8 | 0.017 | 0.350 | 0.859 | 0.049 | 1.02 | 46.28 | |
| TB15N-1 | 0.020 | 4.002 | -320 | $LN_2$ | 173.0 | 183.0 | 0.018 | 0.305 | 0.914 | 0.059 | 1.06 | 49.92 | |
| TB15N-2 | 0.020 | 4.001 | -320 | $LN_2$ | 170.2 | 180.8 | 0.018 | 0.330 | 0.905 | 0.055 | 1.05 | 49.09 | |
| TB18N-1 | 0.020 | 4.001 | -320 | $LN_2$ | 166.0 | 177.3 | 0.018 | 0.360 | 0.900 | 0.050 | 1.03 | 47.72 | |
| TB18N-2 | 0.020 | 3.998 | -320 | $LN_2$ | 173.7 | 185.6 | 0.018 | 0.360 | 0.909 | 0.050 | 1.08 | 50.42 | |
| TB19N-1 | 0.020 | 3.998 | -320 | $LN_2$ | 166.0 | 179.2 | 0.019 | 0.395 | 0.950 | 0.048 | 1.04 | 49.08 | |
| TB19N-2 | 0.020 | 4.002 | -320 | $LN_2$ | 166.8 | 179.9 | 0.019 | 0.390 | 0.960 | 0.049 | 1.04 | 49.36 | |
| TB15N-5 | 0.018 | 4.002 | -320 | $LN_2$ | 175.7 | 187.3 | 0.018 | 0.325 | 0.984 | 0.055 | 1.09 | 50.83 | |
| TB14N-1* | 0.018 | 3.995 | -320 | $LN_2$ | 162.3 | 171.7 | 0.015 | 0.390 | 0.811 | 0.044 | 0.97 | 42.23 | |
| TB18N-2* | 0.020 | 3.995 | -320 | $LN_2$ | 151.2 | 163.3 | 0.018 | 0.410 | 0.918 | 0.044 | 0.92 | 42.52 | |

* Milled from .20 Inch Thick Plate Heat Number G-7622.

Table 23: STATIC FRACTURE TOUGHNESS DATA, 0.020 Inch Thick, 5Al-2.5 Sn Titanium Base Metal - Transverse Grain, a/2c = .15, -320°F

| SPECIMEN | | | TEST CONDITIONS | | | | FRACTURE DATA | | | | | | |
|---|---|---|---|---|---|---|---|---|---|---|---|---|---|
| Number | Thickness (in) (t) | Width (in) (w) | Temperature (°F) | Environment | Gross Section Stress (Ksi) ($\sigma_G$) | Net Section Stress (Ksi) ($\sigma_N$) | Flaw Depth (in) a | Flaw Length (in) 2c | a/t | a/2c | $\sigma_N/\sigma_{ys}$ | Irwins Apparent K (Ksi $\sqrt{in}$) | Based On Avg. $K_{Ic}$ $M_K$ |
| TB15N-3 | 0.020 | 3.998 | -320 | $LN_2$ | 190.4 | 193.6 | 0.015 | 0.106 | 0.761 | 0.142 | 1.12 | 46.17 | |
| TB15N-4 | 0.019 | 4.001 | -320 | $LN_2$ | 186.3 | 189.3 | 0.015 | 0.105 | 0.777 | 0.143 | 1.10 | 45.11 | |
| TB17N-4 | 0.020 | 3.998 | -320 | $LN_2$ | 187.3 | 190.6 | 0.015 | 0.114 | 0.765 | 0.132 | 1.10 | 45.92 | |
| TB17N-3 | 0.020 | 4.001 | -320 | $LN_2$ | 187.4 | 191.0 | 0.017 | 0.116 | 0.867 | 0.147 | 1.11 | 48.10 | |
| TB18N-3 | 0.020 | 3.997 | -320 | $LN_2$ | 180.6 | 184.3 | 0.018 | 0.126 | 0.882 | 0.143 | 1.07 | 47.90 | |
| TB18N-4 | 0.019 | 4.003 | -320 | $LN_2$ | 186.3 | 190.7 | 0.018 | 0.128 | 0.933 | 0.141 | 1.11 | 49.54 | |
| TB19N-3 | 0.020 | 3.998 | -320 | $LN_2$ | 181.0 | 185.2 | 0.018 | 0.138 | 0.882 | 0.130 | 1.07 | 48.67 | |
| TB19N-4 | 0.021 | 4.002 | -320 | $LN_2$ | 182.0 | 186.7 | 0.019 | 0.140 | 0.918 | 0.136 | 1.08 | 49.99 | |
| TB15N-6 | 0.019 | 4.000 | -320 | $LN_2$ | 190.9 | 194.4 | 0.016 | 0.107 | 0.860 | 0.150 | 1.13 | 47.37 | |
| TB17N-5 | 0.018 | 3.999 | -320 | $LN_2$ | 188.5 | 192.7 | 0.017 | 0.118 | 0.955 | 0.144 | 1.12 | 48.52 | |

Table 24: STATIC FRACTURE TOUGHNESS DATA, 0.020 Inch Thick, 5Al-2.5 Sn Titanium Base Metal - Transverse Grain, a/2c = .05, -423°F

| SPECIMEN | | | TEST CONDITIONS | | | | FRACTURE DATA | | | | | | |
|---|---|---|---|---|---|---|---|---|---|---|---|---|---|
| Number | Thickness (in) (t) | Width (in) (w) | Temperature (°F) | Environment | Gross Section Stress (Ksi) ($\sigma_G$) | Net Section Stress (Ksi) ($\sigma_N$) | Flaw Depth (in) a | Flaw Length (in) 2c | a/t | a/2c | $\sigma_N/\sigma_{ys}$ | Irwins Apparent K (Ksi $\sqrt{in}$) | Based On Avg. $K_{Ic}$ $M_K$ |
| TB12H-1 | 0.020 | 3.999 | -423 | $LH_2$ | 161.7 | 167.7 | 0.013 | 0.280 | 0.647 | 0.046 | 0.83 | 38.13 | |
| TB12H-2 | 0.020 | 4.002 | -423 | $LH_2$ | 151.5 | 157.3 | 0.013 | 0.280 | 0.657 | 0.046 | 0.78 | 35.40 | |
| TB15H-1 | 0.020 | 3.998 | -423 | $LH_2$ | 135.0 | 142.8 | 0.016 | 0.350 | 0.792 | 0.046 | 0.71 | 34.56 | |
| TB15H-2 | 0.020 | 4.000 | -423 | $LH_2$ | 139.6 | 147.2 | 0.016 | 0.330 | 0.812 | 0.049 | 0.73 | 35.81 | |
| TB18H-1 | 0.020 | 3.999 | -423 | $LH_2$ | 125.7 | 135.2 | 0.018 | 0.400 | 0.887 | 0.045 | 0.67 | 33.92 | |
| TB18H-2 | 0.020 | 4.002 | -423 | $LH_2$ | 128.1 | 137.7 | 0.018 | 0.400 | 0.887 | 0.045 | 0.68 | 34.62 | |
| TB19H-1 | 0.020 | 4.003 | -423 | $LH_2$ | 121.8 | 132.0 | 0.019 | 0.425 | 0.936 | 0.045 | 0.66 | 33.68 | |
| TB19H-2 | 0.020 | 4.002 | -423 | $LH_2$ | 116.3 | 126.7 | 0.019 | 0.440 | 0.941 | 0.043 | 0.63 | 32.07 | |
| 2TB15H-1* | 0.020 | 3.997 | -423 | $LH_2$ | 126.7 | 133.9 | 0.016 | 0.340 | 0.804 | 0.047 | 0.66 | 32.27 | |
| 2TB15H-2* | 0.019 | 3.990 | -423 | $LH_2$ | 132.6 | 140.5 | 0.016 | 0.340 | 0.842 | 0.047 | 0.70 | 33.92 | |

* Milled from .20 Inch Thick Plate Heat Number G-7622.

Table 25: STATIC FRACTURE TOUGHNESS DATA, 0.020 Inch Thick, 5Al-2.5 Sn Titanium Base Metal - Transverse Grain, a/2c = .15, -423°F

| SPECIMEN | | | TEST CONDITIONS | | | | FRACTURE DATA | | | | | | |
|---|---|---|---|---|---|---|---|---|---|---|---|---|---|
| Number | Thickness (in) (t) | Width (in) (w) | Temperature (°F) | Environment | Gross Section Stress (Ksi) ($\sigma_G$) | Net Section Stress (Ksi) ($\sigma_N$) | Flaw Depth (in) a | Flaw Length (in) 2c | a/t | a/2c | $\sigma_N/\sigma_{ys}$ | Irwins Apparent K (Ksi $\sqrt{in}$) | Based On Avg. $K_{Ic}$ $M_K$ |
| TB12H-3 | 0.021 | 4.000 | -423 | $LH_2$ | 197.5 | 199.7 | 0.013 | 0.092 | 0.634 | 0.141 | 0.99 | 44.25 | |
| TB12H-4 | 0.021 | 4.001 | -423 | $LH_2$ | 197.6 | 199.6 | 0.012 | 0.084 | 0.580 | 0.143 | 0.99 | 42.47 | |
| TB15H-3 | 0.021 | 4.002 | -423 | $LH_2$ | 189.4 | 192.1 | 0.015 | 0.104 | 0.728 | 0.144 | 0.95 | 45.08 | |
| TB15H-4 | 0.020 | 4.000 | -423 | $LH_2$ | 192.5 | 195.7 | 0.016 | 0.106 | 0.812 | 0.151 | 0.97 | 47.10 | |
| TB17H-3 | 0.021 | 4.002 | -423 | $LH_2$ | 189.8 | 193.3 | 0.016 | 0.118 | 0.777 | 0.136 | 0.96 | 47.11 | |
| TB17H-4 | 0.020 | 3.997 | -423 | $LH_2$ | 190.8 | 194.4 | 0.017 | 0.116 | 0.850 | 0.147 | 0.97 | 48.28 | |
| TB19H-3 | 0.021 | 4.003 | -423 | $LH_2$ | 177.0 | 181.5 | 0.019 | 0.144 | 0.922 | 0.132 | 0.90 | 47.49* | |
| TB19H-4 | 0.021 | 3.997 | -423 | $LH_2$ | 196.0 | 200.2 | 0.017 | 0.136 | 0.802 | 0.125 | 0.99 | 51.01 | |

* Fatigue Sharpening Incomplete.

Table 26: STATIC FRACTURE TOUGHNESS DATA, 0.020 Inch Thick, 5Al-2.5 Sn Titanium Weld Metal, a/2c = .05, Room Temperature

| SPECIMEN | | | TEST CONDITIONS | | | | FRACTURE DATA | | | | | | |
|---|---|---|---|---|---|---|---|---|---|---|---|---|---|
| Number | Thickness (in) (t) | Width (in) (w) | Temperature (°F) | Environment | Gross Section Stress (Ksi) ($\sigma_G$) | Net Section Stress (Ksi) ($\sigma_N$) | Flaw Depth (in) a | Flaw Length (in) 2c | a/t | a/2c | $\sigma_N/\sigma_{ys}$ | Irwins Apparent K (Ksi $\sqrt{in}$) | Based On Avg. $K_{Ic}$ $M_K$ |
| TW18R-1 | 0.020 | 4.019 | RT | Air | 108.5 | 114.1 | 0.016 | 0.320 | 0.784 | 0.050 | 1.07 | 29.69 | |

Table 27: STATIC FRACTURE TOUGHNESS DATA, 0.020 Inch Thick, 5Al-2.5 Sn Titanium Weld Metal, a/2c = .05, -320°F

| SPECIMEN | | | TEST CONDITIONS | | | | FRACTURE DATA | | | | | | |
|---|---|---|---|---|---|---|---|---|---|---|---|---|---|
| Number | Thickness (in) (t) | Width (in) (w) | Temperature (°F) | Environment | Gross Section Stress (Ksi) ($\sigma_G$) | Net Section Stress (Ksi) ($\sigma_N$) | Flaw Depth (in) a | Flaw Length (in) 2c | a/t | a/2c | $\sigma_N/\sigma_{ys}$ | Irwins Apparent K (Ksi $\sqrt{in}$) | Based On Avg. $K_{Ic}$ $M_K$ |
| TW15N-1 | 0.020 | 4.009 | -320 | $LN_2$ | 152.9 | 160.9 | 0.017 | 0.325 | 0.854 | 0.052 | 0.93 | 41.88 | |
| TW17N-1 | 0.019 | 4.019 | -320 | $LN_2$ | 154.1 | 164.1 | 0.017 | 0.350 | 0.885 | 0.049 | 0.95 | 42.37 | |
| TW18N-1 | 0.020 | 4.012 | -320 | $LN_2$ | 155.1 | 165.9 | 0.018 | 0.370 | 0.909 | 0.049 | 0.96 | 43.93 | |
| TW19N-1 | 0.021 | 4.010 | -320 | $LN_2$ | 149.9 | 161.7 | 0.019 | 0.400 | 0.927 | 0.048 | 0.94 | 43.37 | |
| 2TW15N-2* | 0.020 | 4.009 | -320 | $LN_2$ | 148.9 | 153.7 | 0.019 | 0.360 | 0.754 | 0.042 | 0.89 | 38.22 | |
| 2TW18N-2* | 0.021 | 3.992 | -320 | $LN_2$ | 136.2 | 146.2 | 0.018 | 0.400 | 0.874 | 0.045 | 0.83 | 37.70 | |

* Milled from .20 Inch Thick Weld from Plate Heat Number G-7622.

Table 28: STATIC FRACTURE TOUGHNESS DATA, 0.020 Inch Thick, 5Al-2.5 Sn Titanium Weld Metal, a/2c = .15, -320°F

| SPECIMEN | | | TEST CONDITIONS | | | | FRACTURE DATA | | | | | | |
|---|---|---|---|---|---|---|---|---|---|---|---|---|---|
| Number | Thickness (in) (t) | Width (in) (w) | Temperature (°F) | Environment | Gross Section Stress (Ksi) ($\sigma_G$) | Net Section Stress (Ksi) ($\sigma_N$) | Flaw Depth (in) a | Flaw Length (in) 2c | a/t | a/2c | $\sigma_N/\sigma_{ys}$ | Irwins Apparent K (Ksi $\sqrt{in}$) | Based On Avg. $K_{Ic}$ $M_K$ |
| TW15N-3 | 0.019 | 4.009 | -320 | $LN_2$ | 176.4 | 179.2 | 0.015 | 0.106 | 0.781 | 0.142 | 1.04 | 42.78 | |
| TW17N-3 | 0.019 | 4.012 | -320 | $LN_2$ | 169.7 | 173.2 | 0.017 | 0.118 | 0.876 | 0.144 | 1.01 | 43.50 | |
| TW18N-3 | 0.020 | 4.020 | -320 | $LN_2$ | 173.1 | 176.9 | 0.017 | 0.128 | 0.854 | 0.133 | 1.03 | 45.11 | |
| TW19N-3 | 0.021 | 4.022 | -320 | $LN_2$ | 165.5 | 169.6 | 0.019 | 0.135 | 0.922 | 0.141 | 0.99 | 44.78 | |

Table 29: STATIC FRACTURE TOUGHNESS DATA, 0.020 Inch Thick, 5Al-2.5 Sn Titanium Weld Metal, a/2c = .05, -423°F

| SPECIMEN | | | TEST CONDITIONS | | | | FRACTURE DATA | | | | | | |
|---|---|---|---|---|---|---|---|---|---|---|---|---|---|
| Number | Thickness (in) (t) | Width (in) (w) | Temperature (°F) | Environment | Gross Section Stress (Ksi) ($\sigma_G$) | Net Section Stress (Ksi) ($\sigma_N$) | Flaw Depth (in) a | Flaw Length (in) 2c | a/t | a/2c | $\sigma_N/\sigma_{ys}$ | Irwins Apparent K (Ksi $\sqrt{in}$) | Based On Avg. $K_{Ic}$ $M_K$ |
| TW12H-1 | 0.019 | 4.008 | -423 | $LH_2$ | 152.0 | 157.0 | 0.012 | 0.255 | 0.645 | 0.047 | 0.79 | 34.25 | |
| TW15H-1 | 0.019 | 4.010 | -423 | $LH_2$ | 148.3 | 156.9 | 0.016 | 0.340 | 0.829 | 0.047 | 0.74 | 38.46 | |
| TW18H-1A | 0.020 | 4.009 | -423 | $LH_2$ | 144.2 | 151.6 | 0.015 | 0.325 | 0.758 | 0.046 | 0.76 | 36.10 | |
| TW19H-1 | 0.020 | 4.019 | -423 | $LH_2$ | 130.8 | 141.2 | 0.019 | 0.400 | 0.936 | 0.048 | 0.71 | 36.44 | |
| 2TW15H-1* | 0.020 | 3.991 | -423 | $LH_2$ | 129.8 | 138.4 | 0.017 | 0.365 | 0.867 | 0.047 | 0.67 | 34.11 | |
| 2TW15H-2* | 0.020 | 3.995 | -423 | $LH_2$ | 134.8 | 144.2 | 0.018 | 0.360 | 0.923 | 0.050 | 0.70 | 36.52 | |

* *Milled from .20 Inch Thick Weld Heat Number G-7622.*

Table 30: STATIC FRACTURE TOUGHNESS DATA, 0.020 Inch Thick, 5Al-2.5 Sn Titanium Weld Metal, a/2c = .15, -423°F

| SPECIMEN | | | TEST CONDITIONS | | | | FRACTURE DATA | | | | | | |
|---|---|---|---|---|---|---|---|---|---|---|---|---|---|
| Number | Thickness (in) (t) | Width (in) (w) | Temperature (°F) | Environment | Gross Section Stress (Ksi) ($\sigma_G$) | Net Section Stress (Ksi) ($\sigma_N$) | Flaw Depth (in) a | Flaw Length (in) 2c | a/t | a/2c | $\sigma_N/\sigma_{ys}$ | Irwins Apparent K (Ksi $\sqrt{in}$) | Based On Avg. $K_{Ic}$ $M_K$ |
| TW12H-3 | 0.020 | 4.016 | -423 | $LH_2$ | 177.7 | 179.4 | 0.014 | 0.080 | 0.700 | 0.175 | 0.90 | 39.25 | |
| TW15H-3 | 0.020 | 4.004 | -423 | $LH_2$ | 173.7 | 176.8 | 0.017 | 0.105 | 0.842 | 0.162 | 0.89 | 42.70 | |
| TW17H-3 | 0.020 | 4.012 | -423 | $LH_2$ | 180.0 | 183.5 | 0.017 | 0.114 | 0.867 | 0.149 | 0.92 | 45.13 | |
| TW19H-3 | 0.021 | 4.012 | -423 | $LH_2$ | 177.7 | 182.1 | 0.019 | 0.136 | 0.914 | 0.140 | 0.91 | 47.52 | |

Table 31: STATIC FRACTURE TOUGHNESS DATA, 0.625 Inch Thick, 2219-T87 Aluminum Base Metal - Long Grain, a/2c = .10, Room Temperature

| SPECIMEN | | | TEST CONDITIONS | | | | FRACTURE DATA | | | | | | |
|---|---|---|---|---|---|---|---|---|---|---|---|---|---|
| Number | Thickness (in) (t) | Width (in) (w) | Temperature (°F) | Environment | Gross Section Stress (Ksi) ($\sigma_G$) | Net Section Stress (Ksi) ($\sigma_N$) | Flaw Depth (in) a | Flaw Length (in) 2c | a/t | a/2c | $\sigma_N/\sigma_{ys}$ | Irwins Apparent K (Ksi $\sqrt{In}$) | Based On Avg. $K_{Ic}$ $M_K$ |
| AB24R-1A | 0.633 | 9.002 | RT | Air | 61.4 | 66.5 | 0.316 | 2.306 | 0.499 | 0.137 | 1.19 | 68.68* | |
| AB24R-2 | 0.643 | 8.997 | RT | Air | 42.2 | 45.3 | 0.296 | 2.411 | 0.460 | 0.123 | 0.81 | 44.25* | |
| AB36R-1 | 0.630 | 11.000 | RT | Air | 55.6 | 61.8 | 0.370 | 3.570 | 0.588 | 0.104 | 1.10 | 69.58 | |
| AB36R-2 | 0.628 | 10.992 | RT | Air | 53.2 | 59.2 | 0.380 | 3.610 | 0.605 | 0.105 | 1.06 | 66.69* | |
| AB45R-1 | 0.628 | 14.479 | RT | Air | 35.2 | 43.4 | 0.465 | 4.650 | 0.741 | 0.100 | 0.78 | 46.44* | |
| AB45R-2 | 0.627 | 14.474 | RT | Air | 32.0 | 39.4 | 0.472 | 4.510 | 0.753 | 0.105 | 0.70 | 42.04* | |
| AB54R-1 | 0.638 | 22.010 | RT | Air | 21.7 | 24.3 | 0.530 | 5.380 | 0.831 | 0.099 | 0.43 | 29.86 | 1.574 |
| AB54R-2 | 0.627 | 22.005 | RT | Air | 30.7 | 34.5 | 0.535 | 5.395 | 0.853 | 0.099 | 0.62 | 43.06* | |
| AB57R-1 | 0.643 | 22.005 | RT | Air | 21.6 | 26.8 | 0.600 | 5.725 | 0.934 | 0.105 | 0.48 | 31.43 | 1.495 |
| AB57R-2 | 0.628 | 22.003 | RT | Air | 32.0 | 36.5 | 0.555 | 5.940 | 0.884 | 0.093 | 0.65 | 46.09* | |

* Delamination

Table 32: STATIC FRACTURE TOUGHNESS DATA, 0.625 Inch Thick, 2219-T87 Aluminum Base Metal - Long Grain, a/2c = .40, Room Temperature

| SPECIMEN | | | TEST CONDITIONS | | | | FRACTURE DATA | | | | | | |
|---|---|---|---|---|---|---|---|---|---|---|---|---|---|
| Number | Thickness (in) (t) | Width (in) (w) | Temperature (°F) | Environment | Gross Section Stress (Ksi) ($\sigma_G$) | Net Section Stress (Ksi) ($\sigma_N$) | Flaw Depth (in) a | Flaw Length (in) 2c | a/t | a/2c | $\sigma_N/\sigma_{ys}$ | Irwins Apparent K (Ksi $\sqrt{In}$) | Based On Avg. $K_{Ic}$ $M_K$ |
| AB24R-1 | 0.625 | 5.502 | RT | Air | 54.1 | 56.5 | 0.271 | 0.654 | 0.434 | 0.414 | 1.01 | 40.11 | |
| AB24R-2 | 0.641 | 6.748 | RT | Air | 55.0 | 56.5 | 0.239 | 0.601 | 0.373 | 0.398 | 1.01 | 39.11 | |
| AB36R-1 | 0.640 | 5.500 | RT | Air | 48.0 | 51.8 | 0.339 | 0.922 | 0.530 | 0.368 | 0.93 | 41.51 | 1.132 |
| AB36R-2 | 0.626 | 5.504 | RT | Air | 48.6 | 52.6 | 0.362 | 0.961 | 0.578 | 0.377 | 0.94 | 43.03* | |
| AB45R-1 | 0.644 | 6.747 | RT | Air | 42.3 | 46.7 | 0.432 | 1.190 | 0.670 | 0.363 | 0.83 | 41.10 | 1.144 |
| AB45R-2 | 0.624 | 6.749 | RT | Air | 46.9 | 51.1 | 0.390 | 1.150 | 0.625 | 0.339 | 0.91 | 44.86 | 1.048 |
| AB54R-1 | 0.629 | 6.747 | RT | Air | 39.8 | 45.5 | 0.485 | 1.370 | 0.771 | 0.354 | 0.81 | 41.22 | 1.140 |
| AB54R-2 | 0.641 | 6.748 | RT | Air | 35.8 | 41.5 | 0.527 | 1.440 | 0.823 | 0.366 | 0.74 | 37.92 | 1.234 |
| AB57R-1 | 0.672 | 11.995 | RT | Air | 37.2 | 40.0 | 0.530 | 1.343 | 0.789 | 0.395 | 0.71 | 38.36 | 1.225 |
| AB57R-2 | 0.644 | 11.996 | RT | Air | 39.0 | 42.2 | 0.538 | 1.353 | 0.835 | 0.398 | 0.75 | 40.49 | 1.161 |

* Delamination

Table 33: STATIC FRACTURE TOUGHNESS DATA, 0.625 Inch Thick, 2219-T87 Aluminum Base Metal - Long Grain, a/2c = .10, -320°F

| SPECIMEN | | | TEST CONDITIONS | | | | FRACTURE DATA | | | | | | |
|---|---|---|---|---|---|---|---|---|---|---|---|---|---|
| Number | Thickness (in) (t) | Width (in) (w) | Temperature (°F) | Environment | Gross Section Stress (Ksi) ($\sigma_G$) | Net Section Stress (Ksi) ($\sigma_N$) | Flaw Depth (in) a | Flaw Length (in) 2c | a/t | a/2c | $\sigma_N/\sigma_{ys}$ | Irwins Apparent K (Ksi $\sqrt{in}$) | Based On Avg. $K_{Ic}$ $M_K$ |
| AB24N-1 | 0.640 | 8.996 | -320 | $LN_2$ | 45.6 | 50.2 | 0.275 | 2.430 | 0.430 | 0.113 | 0.75 | 45.97* | |
| AB24N-2 | 0.638 | 8.980 | -320 | $LN_2$ | 44.4 | 48.9 | 0.272 | 2.449 | 0.426 | 0.111 | 0.73 | 44.49 | 1.124 |
| AB36N-1 | 0.646 | 10.994 | -320 | $LN_2$ | 38.7 | 45.6 | 0.360 | 3.610 | 0.557 | 0.100 | 0.68 | 44.65* | |
| AB36N-2 | 0.647 | 11.003 | -320 | $LN_2$ | 35.6 | 41.8 | 0.375 | 3.615 | 0.580 | 0.104 | 0.62 | 41.54 | 1.204 |
| AB45N-1 | 0.633 | 14.486 | -320 | $LN_2$ | 28.1 | 34.3 | 0.450 | 4.610 | 0.712 | 0.098 | 0.51 | 35.75 | 1.399 |
| AB45N-2 | 0.627 | 14.484 | -320 | $LN_2$ | 38.5 | 47.3 | 0.445 | 4.645 | 0.710 | 0.096 | 0.70 | 49.56* | |
| AB54N-1 | 0.643 | 22.004 | -320 | $LN_2$ | 21.5 | 25.6 | 0.525 | 5.405 | 0.817 | 0.097 | 0.38 | 29.34 | 1.704 |
| AB54N-2 | 0.639 | 22.005 | -320 | $LN_2$ | 19.7 | 23.5 | 0.533 | 5.385 | 0.834 | 0.099 | 0.35 | 27.00 | 1.852 |
| AB57N-1 | 0.627 | 21.994 | -320 | $LN_2$ | 23.3 | 28.7 | 0.560 | 5.815 | 0.893 | 0.096 | 0.43 | 32.93 | 1.518 |
| AB57N-2 | 0.643 | 21.995 | -320 | $LN_2$ | 21.3 | 26.0 | 0.555 | 5.525 | 0.863 | 0.101 | 0.39 | 29.79 | 1.678 |

* Delamination

Table 34: STATIC FRACTURE TOUGHNESS DATA, 0.625 Inch Thick, 2219-T87 Aluminum Base Metal - Long Grain, a/2c = .25, -320°F

| SPECIMEN | | | TEST CONDITIONS | | | | FRACTURE DATA | | | | | | |
|---|---|---|---|---|---|---|---|---|---|---|---|---|---|
| Number | Thickness (in) (t) | Width (in) (w) | Temperature (°F) | Environment | Gross Section Stress (Ksi) ($\sigma_G$) | Net Section Stress (Ksi) ($\sigma_N$) | Flaw Depth (in) a | Flaw Length (in) 2c | a/t | a/2c | $\sigma_N/\sigma_{ys}$ | Irwins Apparent K (Ksi $\sqrt{in}$) | Based On Avg. $K_{Ic}$ $M_K$ |
| AB24N-1 | 0.643 | 5.497 | -320 | $LN_2$ | 56.7 | 59.8 | 0.247 | 0.971 | 0.384 | 0.254 | 0.89 | 47.67 | 1.049 |
| AB24N-2 | 0.631 | 5.499 | -320 | $LN_2$ | 57.0 | 60.5 | 0.262 | 0.978 | 0.415 | 0.268 | 0.90 | 48.61* | |
| AB36N-3 | 0.638 | 9.003 | -320 | $LN_2$ | 45.6 | 48.8 | 0.351 | 1.303 | 0.550 | 0.269 | 0.73 | 44.06 | 1.135 |
| AB36N-4 | 0.625 | 9.007 | -320 | $LN_2$ | 50.8 | 54.3 | 0.347 | 1.324 | 0.555 | 0.262 | 0.81 | 49.63* | |
| AB45N-3 | 0.642 | 12.004 | -320 | $LN_2$ | 35.9 | 39.1 | 0.470 | 1.750 | 0.732 | 0.269 | 0.58 | 39.67 | 1.260 |
| AB45N-4 | 0.633 | 12.003 | -320 | $LN_2$ | 40.0 | 43.8 | 0.480 | 1.780 | 0.758 | 0.270 | 0.65 | 44.83* | |
| AB54N-3 | 0.626 | 12.009 | -320 | $LN_2$ | 34.5 | 39.4 | 0.565 | 2.070 | 0.903 | 0.273 | 0.59 | 41.53 | 1.204 |
| AB54N-4 | 0.646 | 12.006 | -320 | $LN_2$ | 31.5 | 35.5 | 0.555 | 2.030 | 0.860 | 0.273 | 0.53 | 37.44 | 1.335 |

* Delamination

Table 35: STATIC FRACTURE TOUGHNESS DATA, 0.625 Inch Thick, 2219-T87 Aluminum Base Metal - Long Grain, a/2c = .40, -320°F

| SPECIMEN | | | TEST CONDITIONS | | | | FRACTURE DATA | | | | | | |
|---|---|---|---|---|---|---|---|---|---|---|---|---|---|
| Number | Thickness (in) (t) | Width (in) (w) | Temperature (°F) | Environment | Gross Section Stress (Ksi) ($\sigma_G$) | Net Section Stress (Ksi) ($\sigma_N$) | Flaw Depth (in) a | Flaw Length (in) 2c | a/t | a/2c | $\sigma_N/\sigma_{ys}$ | Irwins Apparent K (Ksi $\sqrt{in}$) | Based On Avg. $K_{Ic}$ $M_K$ |
| AB24N-3 | 0.647 | 5.500 | -320 | $LN_2$ | 61.5 | 63.7 | 0.249 | 0.612 | 0.385 | 0.407 | 0.95 | 43.85 | |
| AB24N-4 | 0.630 | 5.497 | -320 | $LN_2$ | 61.2 | 63.1 | 0.225 | 0.587 | 0.357 | 0.383 | 0.94 | 42.60 | |
| AB36N-1 | 0.641 | 5.498 | -320 | $LN_2$ | 53.4 | 57.0 | 0.311 | 0.889 | 0.485 | 0.350 | 0.85 | 44.86 | 1.115 |
| AB36N-2 | 0.637 | 5.502 | -320 | $LN_2$ | 50.9 | 55.3 | 0.369 | 0.964 | 0.579 | 0.383 | 0.82 | 44.72 | 1.118 |
| AB45N-1 | 0.646 | 6.748 | -320 | $LN_2$ | 45.8 | 50.3 | 0.432 | 1.170 | 0.669 | 0.369 | 0.75 | 43.91 | 1.139 |
| AB45N-2 | 0.632 | 6.748 | -320 | $LN_2$ | 49.3 | 54.1 | 0.417 | 1.165 | 0.660 | 0.358 | 0.81 | 47.24 | 1.058 |
| AB54N-1 | 0.632 | 6.750 | -320 | $LN_2$ | 44.0 | 50.2 | 0.486 | 1.363 | 0.770 | 0.357 | 0.75 | 45.28* | |
| AB54N-2 | 0.630 | 6.753 | -320 | $LN_2$ | 44.3 | 50.2 | 0.472 | 1.370 | 0.749 | 0.345 | 0.75 | 45.55 | 1.098 |
| AB57N-1 | 0.642 | 11.991 | -320 | $LN_2$ | 37.8 | 41.0 | 0.546 | 1.371 | 0.851 | 0.398 | 0.61 | 39.14 | 1.277 |
| AB57N-2 | 0.626 | 12.003 | -320 | $LN_2$ | 40.7 | 44.1 | 0.554 | 1.404 | 0.885 | 0.395 | 0.66 | 42.74 | 1.170 |

* Delamination

Table 36: STATIC FRACTURE TOUGHNESS DATA, 0.625 Inch Thick, 2219-T87 Aluminum Base Metal - Long Grain, a/2c = .10, -423°F

| SPECIMEN | | | TEST CONDITIONS | | | | FRACTURE DATA | | | | | | |
|---|---|---|---|---|---|---|---|---|---|---|---|---|---|
| Number | Thickness (in) (t) | Width (in) (w) | Temperature (°F) | Environment | Gross Section Stress (Ksi) ($\sigma_G$) | Net Section Stress (Ksi) ($\sigma_N$) | Flaw Depth (in) a | Flaw Length (in) 2c | a/t | a/2c | $\sigma_N/\sigma_{ys}$ | Irwins Apparent K (Ksi $\sqrt{in}$) | Based On Avg. $K_{Ic}$ $M_K$ |
| AB24H-1 | 0.644 | 9.000 | -423 | $LH_2$ | 49.7 | 53.8 | 0.225 | 2.425 | 0.349 | 0.093 | 0.75 | 46.29 | 1.080 |
| AB24H-2 | 0.643 | 8.996 | -423 | $LH_2$ | 49.6 | 53.6 | 0.228 | 2.430 | 0.355 | 0.094 | 0.75 | 46.53 | 1.075 |
| AB36H-1 | 0.630 | 11.008 | -423 | $LH_2$ | 33.8 | 40.2 | 0.375 | 3.595 | 0.595 | 0.104 | 0.56 | 39.16 | 1.277 |
| AB36H-2 | 0.630 | 11.005 | -423 | $LH_2$ | 34.5 | 40.6 | 0.355 | 3.610 | 0.564 | 0.098 | 0.57 | 39.15 | 1.277 |
| AB45H-1 | 0.642 | 14.487 | -423 | $LH_2$ | 26.7 | 32.6 | 0.460 | 4.670 | 0.717 | 0.099 | 0.46 | 34.18 | 1.463 |
| AB45H-2 | 0.641 | 14.487 | -423 | $LH_2$ | 26.1 | 31.9 | 0.460 | 4.645 | 0.718 | 0.099 | 0.45 | 33.37 | 1.498 |
| AB54H-1 | 0.641 | 14.489 | -423 | $LH_2$ | 23.5 | 31.3 | 0.500 | 5.375 | 0.780 | 0.093 | 0.44 | 31.42 | 1.591 |
| AB54H-2 | 0.643 | 14.484 | -423 | $LH_2$ | 23.4 | 31.0 | 0.520 | 5.510 | 0.809 | 0.094 | 0.43 | 31.87 | 1.569 |

Table 37: STATIC FRACTURE TOUGHNESS DATA, 0.625 Inch Thick, 2219-T87 Aluminum Base Metal - Long Grain, a/2c = .40, -423°F

| SPECIMEN | | | TEST CONDITIONS | | | | FRACTURE DATA | | | | | | |
|---|---|---|---|---|---|---|---|---|---|---|---|---|---|
| Number | Thickness (in) (t) | Width (in) (w) | Temperature (°F) | Environment | Gross Section Stress (Ksi) ($\sigma_G$) | Net Section Stress (Ksi) ($\sigma_N$) | Flaw Depth (in) a | Flaw Length (in) 2c | a/t | a/2c | $\sigma_N/\sigma_{ys}$ | Irwins Apparent K (Ksi $\sqrt{in}$) | Based On Avg. $K_{Ic}$ $M_K$ |
| AB24H-1 | 0.645 | 5.500 | -423 | $LH_2$ | 67.4 | 69.4 | 0.224 | 0.591 | 0.347 | 0.379 | 0.97 | 47.17 | |
| AB24H-2 | 0.624 | 5.490 | -423 | $LH_2$ | 68.7 | 70.8 | 0.216 | 0.589 | 0.346 | 0.367 | 0.99 | 47.99 | |
| AB36H-1 | 0.647 | 5.497 | -423 | $LH_2$ | 54.7 | 59.1 | 0.355 | 0.956 | 0.549 | 0.371 | 0.83 | 47.77 | 1.047 |
| AB36H-2 | 0.625 | 5.496 | -423 | $LH_2$ | 56.9 | 61.5 | 0.352 | 0.930 | 0.564 | 0.379 | 0.86 | 49.23 | 1.016 |
| AB45H-1 | 0.641 | 6.748 | -423 | $LH_2$ | 49.9 | 54.7 | 0.422 | 1.176 | 0.659 | 0.359 | 0.77 | 47.88 | 1.044 |
| AB45H-2 | 0.633 | 6.750 | -423 | $LH_2$ | 51.2 | 56.3 | 0.410 | 1.161 | 0.648 | 0.353 | 0.79 | 48.81 | 1.024 |
| AB54H-1 | 0.642 | 6.747 | -423 | $LH_2$ | 44.3 | 50.2 | 0.476 | 1.361 | 0.742 | 0.350 | 0.70 | 45.32 | 1.103 |
| AB54H-2 | 0.627 | 6.745 | -423 | $LH_2$ | 44.8 | 51.1 | 0.476 | 1.371 | 0.759 | 0.347 | 0.71 | 45.99 | 1.087 |

Table 38: STATIC FRACTURE TOUGHNESS DATA, 0.063 Inch Thick, 2219-T87 Aluminum Base Metal - Long Grain, a/2c = .05, Room Temperature

| SPECIMEN | | | TEST CONDITIONS | | | | FRACTURE DATA | | | | | | |
|---|---|---|---|---|---|---|---|---|---|---|---|---|---|
| Number | Thickness (in) (t) | Width (in) (w) | Temperature (°F) | Environment | Gross Section Stress (Ksi) ($\sigma_G$) | Net Section Stress (Ksi) ($\sigma_N$) | Flaw Depth (in) a | Flaw Length (in) 2c | a/t | a/2c | $\sigma_N/\sigma_{ys}$ | Irwins Apparent K (Ksi $\sqrt{in}$) | Based On Avg. $K_{Ic}$ $M_K$ |
| AB54-1 | 0.067 | 2.508 | RT | Air | 36.6 | 50.5 | 0.054 | 1.090 | 0.806 | 0.050 | 0.91 | 17.19 | |
| AB54-2 | 0.065 | 2.507 | RT | Air | 35.5 | 50.1 | 0.055 | 1.090 | 0.851 | 0.051 | 0.90 | 16.77 | |
| AB54-3 | 0.064 | 6.757 | RT | Air | 47.4 | 53.4 | 0.056 | 1.070 | 0.875 | 0.052 | 0.96 | 23.45 | |
| AB54-4 | 0.067 | 6.757 | RT | Air | 48.1 | 53.3 | 0.052 | 1.060 | 0.782 | 0.049 | 0.96 | 23.03 | |
| AB54-5 | 0.067 | 12.000 | RT | Air | 48.0 | 50.8 | 0.051 | 1.080 | 0.761 | 0.047 | 0.91 | 22.78 | |
| AB54-6 | 0.066 | 12.010 | RT | Air | 48.8 | 51.5 | 0.051 | 1.079 | 0.779 | 0.048 | 0.92 | 23.31 | |
| AB57R-1A | 0.069 | 6.748 | RT | Air | 44.8 | 50.4 | 0.057 | 1.128 | 0.823 | 0.050 | 0.90 | 22.09 | |
| AB57R-2 | 0.066 | 6.748 | RT | Air | 45.5 | 51.4 | 0.058 | 1.116 | 0.875 | 0.052 | 0.92 | 22.67 | |
| AB47R-1* | 0.069 | 6.746 | RT | Air | 45.7 | 50.2 | 0.050 | 1.006 | 0.730 | 0.050 | 0.89 | 21.20 | |
| AB47R-2* | 0.063 | 6.745 | RT | Air | 46.3 | 50.5 | 0.050 | 0.947 | 0.796 | 0.053 | 0.90 | 21.49 | |

* Milled from 0.625 Inch Thick Plate.

Table 39: STATIC FRACTURE TOUGHNESS DATA, 0.063 Inch Thick, 2219-T87 Aluminum Base Metal - Long Grain, a/2c = .15, Room Temperature

| SPECIMEN | | | TEST CONDITIONS | | | | FRACTURE DATA | | | | | | |
|---|---|---|---|---|---|---|---|---|---|---|---|---|---|
| Number | Thickness (in) (t) | Width (in) (w) | Temperature (°F) | Environment | Gross Section Stress (Ksi) ($\sigma_G$) | Net Section Stress (Ksi) ($\sigma_N$) | Flaw Depth (in) a | Flaw Length (in) 2c | a/t | a/2c | $\sigma_N/\sigma_{ys}$ | Irwins Apparent K (Ksi $\sqrt{In}$) | Based On Avg. $K_{Ic}$ $M_K$ |
| AB54R-1 | 0.067 | 5.501 | RT | Air | 52.6 | 54.8 | 0.056 | 0.336 | 0.836 | 0.167 | 0.98 | 23.72 | |
| AB54R-2 | 0.064 | 5.505 | RT | Air | 53.1 | 55.6 | 0.055 | 0.338 | 0.851 | 0.162 | 1.00 | 23.82 | |
| AB57R-1 | 0.067 | 5.501 | RT | Air | 54.3 | 56.5 | 0.050 | 0.370 | 0.746 | 0.135 | 1.01 | 24.12 | |
| AB57R-2 | 0.065 | 5.501 | RT | Air | 52.2 | 54.8 | 0.053 | 0.379 | 0.807 | 0.139 | 0.98 | 23.49 | |

Table 40: STATIC FRACTURE TOUGHNESS DATA, 0.063 Inch Thick, 2219-T87 Aluminum Base Metal - Long Grain, a/2c = .05, -320°F

| SPECIMEN | | | TEST CONDITIONS | | | | FRACTURE DATA | | | | | | |
|---|---|---|---|---|---|---|---|---|---|---|---|---|---|
| Number | Thickness (in) (t) | Width (in) (w) | Temperature (°F) | Environment | Gross Section Stress (Ksi) ($\sigma_G$) | Net Section Stress (Ksi) ($\sigma_N$) | Flaw Depth (in) a | Flaw Length (in) 2c | a/t | a/2c | $\sigma_N/\sigma_{ys}$ | Irwins Apparent K (Ksi $\sqrt{In}$) | Based On Avg. $K_{Ic}$ $M_K$ |
| AB51N-1 | 0.068 | 6.746 | -320 | $LN_2$ | 55.3 | 61.0 | 0.052 | 1.000 | 0.767 | 0.052 | 0.95 | 26.18 | |
| AB51N-2 | 0.067 | 6.750 | -320 | $LN_2$ | 55.3 | 60.8 | 0.051 | 1.000 | 0.761 | 0.051 | 0.95 | 25.95 | |
| AB54N-2 | 0.065 | 6.745 | -320 | $LN_2$ | 55.9 | 62.6 | 0.055 | 1.032 | 0.846 | 0.053 | 0.98 | 27.25 | |
| AB57N-1 | 0.070 | 6.748 | -320 | $LN_2$ | 53.7 | 60.2 | 0.055 | 1.100 | 0.785 | 0.050 | 0.94 | 26.06 | |
| AB57N-2 | 0.069 | 6.750 | -320 | $LN_2$ | 55.0 | 61.9 | 0.057 | 1.120 | 0.827 | 0.051 | 0.97 | 27.26 | |
| AB54N-1A | 0.068 | 6.757 | -320 | $LN_2$ | 53.1 | 59.2 | 0.051 | 1.060 | 0.748 | 0.048 | 0.93 | 24.80 | |
| AB47N-1 | 0.063 | 6.752 | -320 | $LN_2$ | 56.7 | 61.7 | 0.046 | 0.943 | 0.728 | 0.049 | 0.92 | 25.39 | |
| AB47N-2 | 0.065 | 6.747 | -320 | $LN_2$ | 54.8 | 59.3 | 0.048 | 0.968 | 0.736 | 0.050 | 0.88 | 24.92 | |

Table 41: STATIC FRACTURE TOUGHNESS DATA, 0.063 Inch Thick, 2219-T87 Aluminum Base Metal - Long Grain, a/2c = .15, -320°F

| SPECIMEN | | | TEST CONDITIONS | | | | FRACTURE DATA | | | | | | |
|---|---|---|---|---|---|---|---|---|---|---|---|---|---|
| Number | Thickness (in) (t) | Width (in) (w) | Temperature (°F) | Environment | Gross Section Stress (Ksi) ($\sigma_G$) | Net Section Stress (Ksi) ($\sigma_N$) | Flaw Depth (in) a | Flaw Length (in) 2c | a/t | a/2c | $\sigma_N/\sigma_{ys}$ | Irwins Apparent K (Ksi $\sqrt{in}$) | Based On Avg. $K_{Ic}$ $M_K$ |
| AB54N-1 | 0.068 | 5.501 | -320 | $LN_2$ | 66.8 | 69.1 | 0.047 | 0.340 | 0.696 | 0.138 | 1.08 | 28.76 | |
| AB57N-1 | 0.066 | 5.502 | -320 | $LN_2$ | 63.8 | 66.6 | 0.052 | 0.370 | 0.794 | 0.141 | 1.04 | 28.55 | |
| AB54N-2 | 0.064 | 5.503 | -320 | $LN_2$ | 64.5 | 67.1 | 0.051 | 0.343 | 0.793 | 0.149 | 1.05 | 28.38 | |
| AB57N-2 | 0.064 | 5.504 | -320 | $LN_2$ | 64.0 | 67.0 | 0.057 | 0.369 | 0.888 | 0.155 | 1.05 | 29.53 | |

Table 42: STATIC FRACTURE TOUGHNESS DATA, 0.063 Inch Thick, 2219-T87 Aluminum Base Metal - Long Grain, a/2c = .05, -423°F

| SPECIMEN | | | TEST CONDITIONS | | | | FRACTURE DATA | | | | | | |
|---|---|---|---|---|---|---|---|---|---|---|---|---|---|
| Number | Thickness (in) (t) | Width (in) (w) | Temperature (°F) | Environment | Gross Section Stress (Ksi) ($\sigma_G$) | Net Section Stress (Ksi) ($\sigma_N$) | Flaw Depth (in) a | Flaw Length (in) 2c | a/t | a/2c | $\sigma_N/\sigma_{ys}$ | Irwins Apparent K (Ksi $\sqrt{in}$) | Based On Avg. $K_{Ic}$ $M_K$ |
| AB45H-1 | 0.068 | 6.748 | -423 | $LH_2$ | 60.6 | 64.7 | 0.044 | 0.789 | 0.647 | 0.056 | 0.92 | 26.47 | |
| AB45H-2 | 0.067 | 6.746 | -423 | $LH_2$ | 59.1 | 64.4 | 0.059 | 0.807 | 0.879 | 0.073 | 0.91 | 29.40 | |
| AB54H-1 | 0.065 | 6.750 | -423 | $LH_2$ | 57.1 | 63.6 | 0.054 | 1.025 | 0.835 | 0.053 | 0.90 | 27.42 | |
| AB54H-2 | 0.067 | 6.746 | -423 | $LH_2$ | 56.7 | 63.4 | 0.056 | 1.046 | 0.836 | 0.054 | 0.90 | 27.68 | |
| AB57H-1 | 0.067 | 6.750 | -423 | $LH_2$ | 55.0 | 62.4 | 0.058 | 1.036 | 0.862 | 0.056 | 0.89 | 27.17 | |
| AB57H-2 | 0.068 | 6.749 | -423 | $LH_2$ | 55.8 | 62.8 | 0.055 | 1.106 | 0.803 | 0.049 | 0.89 | 26.90 | |
| AB47H-1* | 0.062 | 6.748 | -423 | $LH_2$ | 57.9 | 62.9 | 0.050 | 0.940 | 0.804 | 0.053 | 0.88 | 26.78 | |
| AB47H-2* | 0.062 | 6.747 | -423 | $LH_2$ | 59.0 | 64.6 | 0.051 | 0.952 | 0.820 | 0.054 | 0.90 | 27.69 | |

* Milled from 0.625 Inch Thick Plate.

Table 43: STATIC FRACTURE TOUGHNESS DATA, 0.063 Inch Thick, 2219-T87 Aluminum Base Metal - Long Grain, a/2c = .15, -423°F

| SPECIMEN | | | TEST CONDITIONS | | | | FRACTURE DATA | | | | | | |
|---|---|---|---|---|---|---|---|---|---|---|---|---|---|
| Number | Thickness (in) (t) | Width (in) (w) | Temperature (°F) | Environment | Gross Section Stress (Ksi) ($\sigma_G$) | Net Section Stress (Ksi) ($\sigma_N$) | Flaw Depth (in) a | Flaw Length (in) 2c | a/t | a/2c | $\sigma_N/\sigma_{ys}$ | Irwins Apparent K (Ksi $\sqrt{in}$) | Based On Avg. $K_{Ic}$ $M_K$ |
| AB54H-1 | 0.067 | 5.498 | -423 | $LH_2$ | 70.30 | 72.8 | 0.047 | 0.321 | 0.707 | 0.146 | 1.03 | 29.93 | |
| AB54H-2 | 0.069 | 5.503 | -423 | $LH_2$ | 68.10 | 70.8 | 0.052 | 0.339 | 0.754 | 0.153 | 1.01 | 30.06 | |
| AB57H-1 | 0.066 | 5.500 | -423 | $LH_2$ | 67.60 | 70.5 | 0.052 | 0.359 | 0.788 | 0.145 | 1.00 | 30.09 | |
| AB57H-2 | 0.064 | 5.502 | -423 | $LH_2$ | 67.70 | 70.8 | 0.050 | 0.376 | 0.780 | 0.133 | 1.01 | 29.94 | |

Table 44: STATIC FRACTURE TOUGHNESS DATA, 1.00 Inch Thick, 2219 Aluminum Weld Metal, a/2c = .15, Room Temperature

| SPECIMEN | | | TEST CONDITIONS | | | | FRACTURE DATA | | | | | | |
|---|---|---|---|---|---|---|---|---|---|---|---|---|---|
| Number | Thickness (in) (t) | Width (in) (w) | Temperature (°F) | Environment | Gross Section Stress (Ksi) ($\sigma_G$) | Net Section Stress (Ksi) ($\sigma_N$) | Flaw Depth (in) a | Flaw Length (in) 2c | a/t | a/2c | $\sigma_N/\sigma_{ys}$ | Irwins Apparent K (Ksi $\sqrt{in}$) | Based On Avg. $K_{Ic}$ $M_K$ |
| 1AW50R-2 | 1.006 | 20.01 | RT | Air | 21.9 | 23.3 | 0.470 | 3.320 | 0.467 | 0.142 | 1.06 | 29.73 | |
| 1AW63R-1 | 1.022 | 24.00 | RT | Air | 22.8 | 25.3 | 0.690 | 4.155 | 0.676 | 0.166 | 1.16 | 36.46 | |
| 1AW75R-2 | 1.017 | 29.99 | RT | Air | 20.7 | 22.8 | 0.725 | 4.995 | 0.713 | 0.145 | 1.04 | 34.36 | |
| 1AW90R-1 | 1.031 | 30.00 | RT | Air | 20.4 | 23.5 | 0.845 | 5.915 | 0.820 | 0.143 | 1.07 | 36.55 | |

Table 45: STATIC FRACTURE TOUGHNESS DATA, 1.00 Inch Thick, 2219 Aluminum Weld Metal, a/2c = .30, Room Temperature

| SPECIMEN | | | TEST CONDITIONS | | | | FRACTURE DATA | | | | | | |
|---|---|---|---|---|---|---|---|---|---|---|---|---|---|
| Number | Thickness (in) (t) | Width (in) (w) | Temperature (°F) | Environment | Gross Section Stress (Ksi) ($\sigma_G$) | Net Section Stress (Ksi) ($\sigma_N$) | Flaw Depth (in) a | Flaw Length (in) 2c | a/t | a/2c | $\sigma_N/\sigma_{ys}$ | Irwins Apparent K (Ksi $\sqrt{in}$) | Based On Avg. $K_{Ic}$ $M_K$ |
| 3AW75R-1 | 1.007 | 13.50 | RT | Air | 23.5 | 26.0 | 0.696 | 2.377 | 0.691 | 0.293 | 1.19 | 32.40 | |
| 3AW83R-1 | 1.005 | 16.02 | RT | Air | 23.1 | 25.5 | 0.773 | 2.533 | 0.769 | 0.305 | 1.16 | 33.07 | |
| 3AW90R-1 | 1.005 | 16.01 | RT | Air | 22.1 | 25.2 | 0.830 | 2.850 | 0.826 | 0.291 | 1.15 | 33.34 | |
| 3AW95R-1 | 1.005 | 16.01 | RT | Air | 21.5 | 24.7 | 0.889 | 3.010 | 0.885 | 0.295 | 1.13 | 33.30 | |

Table 46: STATIC FRACTURE TOUGHNESS DATA, 1.00 Inch Thick, 2219 Aluminum Weld Metal, a/2c = .15, -320°F

| SPECIMEN | | | TEST CONDITIONS | | | | FRACTURE DATA | | | | | | |
|---|---|---|---|---|---|---|---|---|---|---|---|---|---|
| Number | Thickness (in) (t) | Width (in) (w) | Temperature (°F) | Environment | Gross Section Stress (Ksi) ($\sigma_G$) | Net Section Stress (Ksi) ($\sigma_N$) | Flaw Depth (in) a | Flaw Length (in) 2c | a/t | a/2c | $\sigma_N/\sigma_{ys}$ | Irwins Apparent K (Ksi $\sqrt{in}$) | Based On Avg. $K_{Ic}$ $M_K$ |
| 1AW50N-3 | 1.007 | 19.972 | -320 | $LN_2$ | 24.6 | 26.2 | 0.467 | 3.330 | 0.464 | 0.140 | 0.98 | 32.77 | |
| 1AW63N-2 | 1.018 | 24.005 | -320 | $LN_2$ | 19.8 | 22.0 | 0.710 | 4.245 | 0.698 | 0.167 | 0.82 | 30.67 | |
| 1AW75N-3 | 1.037 | 30.020 | -320 | $LN_2$ | 15.4 | 17.0 | 0.735 | 5.035 | 0.709 | 0.146 | 0.63 | 24.31 | |
| 1AW90N-2 | 1.019 | 30.015 | -320 | $LN_2$ | 21.1 | 24.2 | 0.825 | 5.785 | 0.810 | 0.143 | 0.90 | 36.42 | |

Table 47: STATIC FRACTURE TOUGHNESS DATA, 1.00 Inch Thick, 2219 Aluminum Weld Metal, a/2c = .30, -320°F

| SPECIMEN | | | TEST CONDITIONS | | | | FRACTURE DATA | | | | | | |
|---|---|---|---|---|---|---|---|---|---|---|---|---|---|
| Number | Thickness (in) (t) | Width (in) (w) | Temperature (°F) | Environment | Gross Section Stress (Ksi) ($\sigma_G$) | Net Section Stress (Ksi) ($\sigma_N$) | Flaw Depth (in) a | Flaw Length (in) 2c | a/t | a/2c | $\sigma_N/\sigma_{ys}$ | Irwins Apparent K (Ksi $\sqrt{in}$) | Based On Avg. $K_{Ic}$ $M_K$ |
| 3AW75N-2 | 1.007 | 13.49 | -320 | $LN_2$ | 25.3 | 28.0 | 0.703 | 2.374 | 0.698 | 0.296 | 1.04 | 34.63 | |
| 3AW95N-2 | 0.989 | 16.01 | -320 | $LN_2$ | 21.6 | 24.8 | 0.787 | 2.584 | 0.796 | 0.305 | 0.93 | 30.44 | |
| 3AW90N-2 | 1.008 | 16.00 | -320 | $LN_2$ | 24.4 | 27.6 | 0.841 | 2.832 | 0.834 | 0.297 | 1.03 | 36.33 | |
| 3AW83N-2 | 1.000 | 16.01 | -320 | $LN_2$ | 24.6 | 28.3 | 0.898 | 3.022 | 0.898 | 0.297 | 1.06 | 37.87 | |

Table 48: STATIC FRACTURE TOUGHNESS DATA, 1.00 Inch Thick, 2219 Aluminum Weld Metal, a/2c = .15, -423°F

| SPECIMEN | | | TEST CONDITIONS | | | | FRACTURE DATA | | | | | | |
|---|---|---|---|---|---|---|---|---|---|---|---|---|---|
| Number | Thickness (in) (t) | Width (in) (w) | Temperature (°F) | Environment | Gross Section Stress (Ksi) ($\sigma_G$) | Net Section Stress (Ksi) ($\sigma_N$) | Flaw Depth (in) a | Flaw Length (in) 2c | a/t | a/2c | $\sigma_N/\sigma_{ys}$ | Irwins Apparent K (Ksi $\sqrt{in}$) | Based On Avg. $K_{Ic}$ $M_K$ |
| 1AW50H-4 | 1.002 | 16.01 | -423 | $LH_2$ | 14.3 | 15.6 | 0.500 | 3.355 | 0.499 | 0.149 | 0.49 | 18.34 | |
| 1AW63H-3 | 1.010 | 20.01 | -423 | $LH_2$ | 17.3 | 19.3 | 0.620 | 4.165 | 0.614 | 0.149 | 0.60 | 24.93 | |
| 1AW75H-4 | 1.016 | 24.01 | -423 | $LH_2$ | 14.3 | 15.8 | 0.700 | 4.215 | 0.689 | 0.166 | 0.49 | 21.34 | |
| 1AW90H-3 | 1.010 | 30.00 | -423 | $LH_2$ | 11.6 | 13.3 | 0.840 | 5.970 | 0.832 | 0.141 | 0.41 | 19.32 | |

Table 49: STATIC FRACTURE TOUGHNESS DATA,
1.00 Inch Thick, 2219 Aluminum Weld Metal,
a/2c = .30, -423°F

| SPECIMEN | | | TEST CONDITIONS | | | | FRACTURE DATA | | | | | | |
|---|---|---|---|---|---|---|---|---|---|---|---|---|---|
| Number | Thickness (in) (t) | Width (in) (w) | Temperature (°F) | Environment | Gross Section Stress (Ksi) ($\sigma_G$) | Net Section Stress (Ksi) ($\sigma_N$) | Flaw Depth (in) a | Flaw Length (in) 2c | a/t | a/2c | $\sigma_N/\sigma_{ys}$ | Irwins Apparent K (Ksi $\sqrt{in}$) | Based On Avg. $K_{Ic}$ $M_K$ |
| 3AW75H-3 | 1.014 | 13.472 | -423 | $LH_2$ | 20.2 | 22.4 | 0.710 | 2.335 | 0.701 | 0.304 | 0.70 | 26.60 | |
| 3AW83H-3 | 1.007 | 16.011 | -423 | $LH_2$ | 20.7 | 22.9 | 0.775 | 2.490 | 0.770 | 0.311 | 0.71 | 28.29 | |
| 3AW90H-3 | 0.998 | 15.998 | -423 | $LH_2$ | 18.8 | 21.2 | 0.835 | 2.895 | 0.837 | 0.288 | 0.66 | 27.21 | |
| 3AW95H-3 | 1.000 | 16.009 | -423 | $LH_2$ | 17.0 | 19.6 | 0.870 | 2.985 | 0.870 | 0.292 | 0.61 | 24.92 | |

Table 50: STATIC FRACTURE TOUGHNESS DATA,
0.125 Inch Thick, 2219 Aluminum Weld Metal,
a/2c = .05, Room Temperature

| SPECIMEN | | | TEST CONDITIONS | | | | FRACTURE DATA | | | | | | |
|---|---|---|---|---|---|---|---|---|---|---|---|---|---|
| Number | Thickness (in) (t) | Width (in) (w) | Temperature (°F) | Environment | Gross Section Stress (Ksi) ($\sigma_G$) | Net Section Stress (Ksi) ($\sigma_N$) | Flaw Depth (in) a | Flaw Length (in) 2c | a/t | a/2c | $\sigma_N/\sigma_{ys}$ | Irwins Apparent K (Ksi $\sqrt{in}$) | Based On Avg. $K_{Ic}$ $M_K$ |
| 5AW50R-1 | 0.122 | 6.015 | RT | Air | 32.8 | 34.8 | 0.056 | 0.970 | 0.460 | 0.058 | 1.30 | 16.71 | |
| 5AW75R-1 | 0.119 | 7.507 | RT | Air | 27.3 | 30.4 | 0.088 | 1.430 | 0.737 | 0.062 | 1.14 | 17.39 | |
| 5AW94R-3 | 0.124 | 9.520 | RT | Air | 26.4 | 30.3 | 0.097 | 1.990 | 0.785 | 0.049 | 1.13 | 17.75 | |
| 5AW113R-1 | 0.123 | 11.986 | RT | Air | 30.2 | 34.3 | 0.099 | 2.300 | 0.804 | 0.043 | 1.28 | 20.64 | |

Table 51: STATIC FRACTURE TOUGHNESS DATA,
0.125 Inch Thick, 2219 Aluminum Weld Metal,
a/2c = .15, Room Temperature

| SPECIMEN | | | TEST CONDITIONS | | | | FRACTURE DATA | | | | | | |
|---|---|---|---|---|---|---|---|---|---|---|---|---|---|
| Number | Thickness (in) (t) | Width (in) (w) | Temperature (°F) | Environment | Gross Section Stress (Ksi) ($\sigma_G$) | Net Section Stress (Ksi) ($\sigma_N$) | Flaw Depth (in) a | Flaw Length (in) 2c | a/t | a/2c | $\sigma_N/\sigma_{ys}$ | Irwins Apparent K (Ksi $\sqrt{in}$) | Based On Avg. $K_{Ic}$ $M_K$ |
| 1AW50R-1 | 0.125 | 3.753 | RT | Air | 31.7 | 32.6 | 0.047 | 0.341 | 0.375 | 0.138 | 1.22 | 13.66 | |
| 1AW75R-1 | 0.123 | 3.754 | RT | Air | 29.6 | 31.3 | 0.063 | 0.496 | 0.514 | 0.127 | 1.17 | 14.94 | |
| 1AW94R-1 | 0.122 | 3.750 | RT | Air | 30.4 | 33.3 | 0.082 | 0.629 | 0.672 | 0.130 | 1.25 | 17.45 | |
| 1AW113R-1 | 0.122 | 3.746 | RT | Air | 26.5 | 30.6 | 0.101 | 0.733 | 0.828 | 0.138 | 1.15 | 16.71 | |

Table 52: STATIC FRACTURE TOUGHNESS DATA, 0.125 Inch Thick, 2219 Aluminum Weld Metal, a/2c = .05, -320°F

| SPECIMEN | | | TEST CONDITIONS | | | | FRACTURE DATA | | | | | | |
|---|---|---|---|---|---|---|---|---|---|---|---|---|---|
| Number | Thickness (in) (t) | Width (in) (w) | Temperature (°F) | Environment | Gross Section Stress (Ksi) ($\sigma_G$) | Net Section Stress (Ksi) ($\sigma_N$) | Flaw Depth (in) a | Flaw Length (in) 2c | a/t | a/2c | $\sigma_N/\sigma_{ys}$ | Irwins Apparent K (Ksi $\sqrt{in}$) | Based On Avg. $K_{Ic}$ $M_K$ |
| 5AW50N-2 | 0.122 | 6.004 | -320 | $LN_2$ | 36.5 | 38.1 | 0.044 | 0.982 | 0.361 | 0.045 | 1.20 | 16.61 | |
| 5AW75N-2 | 0.121 | 7.508 | -320 | $LN_2$ | 34.5 | 38.4 | 0.087 | 1.400 | 0.772 | 0.062 | 1.21 | 21.84 | |
| 5AW94N-2 | 0.123 | 9.513 | -320 | $LN_2$ | 33.2 | 36.9 | 0.081 | 1.865 | 0.661 | 0.043 | 1.16 | 20.52 | |
| 5AW113N-2 | 0.122 | 11.988 | -320 | $LN_2$ | 34.0 | 39.1 | 0.100 | 2.250 | 0.823 | 0.044 | 1.23 | 23.34 | |

Table 53: STATIC FRACTUE TOUGHNESS DATA, 0.125 Inch Thick, 2219 Aluminum Weld Metal, a/2c = .15, -320°F

| SPECIMEN | | | TEST CONDITIONS | | | | FRACTURE DATA | | | | | | |
|---|---|---|---|---|---|---|---|---|---|---|---|---|---|
| Number | Thickness (in) (t) | Width (in) (w) | Temperature (°F) | Environment | Gross Section Stress (Ksi) ($\sigma_G$) | Net Section Stress (Ksi) ($\sigma_N$) | Flaw Depth (in) a | Flaw Length (in) 2c | a/t | a/2c | $\sigma_N/\sigma_{ys}$ | Irwins Apparent K (Ksi $\sqrt{in}$) | Based On Avg. $K_{Ic}$ $M_K$ |
| 1AW50N-2 | 0.123 | 3.754 | -320 | $LN_2$ | 39.9 | 41.0 | 0.046 | 0.344 | 0.374 | 0.134 | 1.29 | 17.09 | |
| 1AW75N-2 | 0.123 | 3.754 | -320 | $LN_2$ | 36.1 | 38.6 | 0.078 | 0.488 | 0.634 | 0.160 | 1.22 | 19.54 | |
| 1AW94N-2 | 0.123 | 3.749 | -320 | $LN_2$ | 34.4 | 37.9 | 0.086 | 0.631 | 0.699 | 0.136 | 1.20 | 20.09 | |
| 1AW113N-2 | 0.125 | 3.746 | -320 | $LN_2$ | 33.3 | 37.9 | 0.094 | 0.747 | 0.752 | 0.126 | 1.20 | 20.56 | |

Table 54: STATIC FRACTURE TOUGHNESS DATA,
0.125 Inch Thick, 2219 Aluminum Weld Metal,
a/2c = .05, -423°F

| SPECIMEN | | | TEST CONDITIONS | | | | FRACTURE DATA | | | | | | |
|---|---|---|---|---|---|---|---|---|---|---|---|---|---|
| Number | Thickness (in) (t) | Width (in) (w) | Temperature (°F) | Environment | Gross Section Stress (Ksi) ($\sigma_G$) | Net Section Stress (Ksi) ($\sigma_N$) | Flaw Depth (in) a | Flaw Length (in) 2c | a/t | a/2c | $\sigma_N/\sigma_{ys}$ | Irwins Apparent K (Ksi $\sqrt{in}$) | Based On Avg. $K_{Ic}$ $M_K$ |
| 5AW50H-3 | 0.126 | 5.994 | -423 | $LH_2$ | 43.9 | 46.6 | 0.052 | 1.065 | 0.413 | 0.049 | 1.53 | 21.67 | |
| 5AW75H-3 | 0.123 | 7.508 | -423 | $LH_2$ | 33.2 | 36.6 | 0.070 | 1.455 | 0.571 | 0.048 | 1.20 | 19.03 | |
| 5AW94H-3 | 0.122 | 9.480 | -423 | $LH_2$ | 34.2 | 38.2 | 0.075 | 1.900 | 0.615 | 0.040 | 1.26 | 20.38 | |
| 5AW113H-3 | 0.123 | 11.995 | -423 | $LH_2$ | 32.7 | 37.7 | 0.105 | 2.465 | 0.852 | 0.043 | 1.24 | 23.02 | |

Table 55: STATIC FRACTURE TOUGHNESS DATA,
0.125 Inch Thick, 2219 Aluminum Weld Metal,
a/2c = .15, -423°F

| SPECIMEN | | | TEST CONDITIONS | | | | FRACTURE DATA | | | | | | |
|---|---|---|---|---|---|---|---|---|---|---|---|---|---|
| Number | Thickness (in) (t) | Width (in) (w) | Temperature (°F) | Environment | Gross Section Stress (Ksi) ($\sigma_G$) | Net Section Stress (Ksi) ($\sigma_N$) | Flaw Depth (in) a | Flaw Length (in) 2c | a/t | a/2c | $\sigma_N/\sigma_{ys}$ | Irwins Apparent K (Ksi $\sqrt{in}$) | Based On Avg. $K_{Ic}$ $M_K$ |
| 1AW50H-3 | 0.125 | 3.751 | -423 | $LH_2$ | 40.3 | 41.4 | 0.042 | 0.310 | 0.336 | 0.136 | 1.36 | 16.46 | |
| 1AW75H-3 | 0.124 | 3.757 | -423 | $LH_2$ | 37.1 | 39.5 | 0.070 | 0.495 | 0.567 | 0.141 | 1.30 | 19.44 | |
| 1AW94H-3 | 0.125 | 3.749 | -423 | $LH_2$ | 37.2 | 40.7 | 0.080 | 0.625 | 0.643 | 0.128 | 1.34 | 21.14 | |
| 1AW113H-3A | 0.123 | 3.748 | -423 | $LH_2$ | 35.9 | 41.2 | 0.097 | 0.770 | 0.792 | 0.126 | 1.36 | 22.51 | |

Table 56 : STATIC FRACTURE TOUGHNESS DATA - CENTER CRACKED PANELS
(t = 0.020", 5Al-2.5Sn Titanium Base Metal, Transverse Grain)

| SPECIMEN NUMBER | THICKNESS ~ IN. | WIDTH ~ IN. | CRACK LENGTH ~ IN. | TEST TEMPERATURE ~ °F | TEST ENVIRONMENT | GROSS AREA FAILURE STRESS - KSI | $K^*_{CN}$ | TYPE FRACTURE |
|---|---|---|---|---|---|---|---|---|
| TBCR-2 | .0192 | 30.00 | 15.02 | RT | Air | 32.3 | 185.4 | Full Shear |
| TBCN-1 | .0218 | 8.00 | 4.03 | -320°F | $LN_2$ | 78.0 | 232.3 | Full Shear |
| TBCH-1 | .0208 | 8.001 | 3.93 | -423°F | $LH_2$ | 35.9 | 104.7 | Full Shear |

* Calculated using an expression recommended by Brown and Srawley in the ASTM Special Technical Publication No. 410

Table 57 : STATIC FRACTURE TOUGHNESS DATA - CENTER CRACKED PANELS
(t = 0.20", 5Al-2.5Sn Titanium Base Metal, Transverse Grain)

| SPECIMEN NUMBER | THICKNESS ~ IN. | WIDTH ~ IN. | CRACK LENGTH ~ IN. | TEST TEMPERATURE ~ °F | TEST ENVIRONMENT | GROSS AREA FAILURE STRESS - KSI | $K^*_{CN}$ | TYPE FRACTURE |
|---|---|---|---|---|---|---|---|---|
| TBCR-1 | .218 | 29.985 | 15.05 | RT | Air | 38.4 | 220.8 | Full Shear |
| TBCN-2 | .216 | 8.008 | 4.05 | -320°F | $LN_2$ | 19.4 | 58.0 | Flat |
| TBCH-2 | .216 | 8.010 | 4.00 | -423°F | $LH_2$ | 18.6 | 55.0 | Flat |

* Calculated using an expression recommended by Brown and Srawley in the ASTM Special Technical Publication No. 410

NOTE: All Specimens from Heat No. G-7622

Table 58 : STATIC FRACTURE TOUGHNESS DATA - CENTER CRACKED PANELS
(t = 0.020", 5Al-2.5Sn Titanium Weldment)

| SPECIMEN NUMBER | THICKNESS ~ IN. | WIDTH ~ IN. | CRACK LENGTH ** ~ IN. | TEST TEMPERATURE ~ °F | TEST ENVIRONMENT | GROSS AREA FAILURE STRESS ~ KSI | $K^*_{CN}$ | TYPE FRACTURE |
|---|---|---|---|---|---|---|---|---|
| TWCR-1 | .0198 | 29.99 | 14.82 | RT | Air | 25.8 | 146.2 | Full Shear |
| TWCN-1 | .0197 | 8.010 | 4.01 | -320°F | $LN_2$ | 47.5 | 141.0 | Full Shear |
| TWCH | .0208 | 8.001 | 4.08 | -423°F | $LH_2$ | 39.9 | 120.1 | Full Shear |

* Calculated using an expression recommended by Brown and Srawley in the ASTM Special Technical Publication No. 410

** Flaw in Center of Weld

Table 59 : STATIC FRACTURE TOUGHNESS DATA - CENTER CRACKED PANELS
(t = 0.20", 5Al-2.5Sn Titanium Weldment)

| SPECIMEN NUMBER | THICKNESS ~ IN. | WIDTH ~ IN. | CRACK LENGTH ** ~ IN. | TEST TEMPERATURE ~ °F | TEST ENVIRONMENT | GROSS AREA FAILURE STRESS ~ KSI | $K^*_{CN}$ | TYPE FRACTURE |
|---|---|---|---|---|---|---|---|---|
| TWCR-2 | .2172 | 30.00 | 15.13 | RT | Air | 30.8 | 177.9 | Full Shear |
| TWCN | .2165 | 8.012 | 4.02 | -320°F | $LN_2$ | 25.7 | 76.3 | Flat |
| TWCH | .2145 | 8.011 | 3.92 | -423°F | $LH_2$ | 25.6 | 74.4 | Flat |

* Calculated using an expression recommended by Brown and Srawley in the ASTM Special Technical Publication No. 410

** Flaws in Center of Weld

NOTE: All Specimens from Heat No. G-8818

Table 60 : STATIC FRACTURE TOUGHNESS DATA - CENTER CRACKED PANELS
($t = 0.063$", 2219-T87 Aluminum Base Metal, Long Grain)

| SPECIMEN NUMBER | THICKNESS ~ IN. | WIDTH ~ IN. | CRACK LENGTH ~ IN. | TEST TEMPERATURE ~ °F | TEST ENVIRONMENT | GROSS AREA FAILURE STRESS ~ KSI | $K^*_{CN}$ | TYPE FRACTURE |
|---|---|---|---|---|---|---|---|---|
| ABCR-1 | .0679 | 15.97 | 7.98 | RT | Air | 16.6 | 69.5 | Full Shear |
| ABCN-2 | .0670 | 15.97 | 7.98 | -320°F | $LN_2$ | 20.9 | 87.5 | Full Shear |
| ABCH-3 | .0702 | 12.00 | 6.00 | -423°F | $LH_2$ | 18.9 | 68.6 | Full Shear |

* Calculated using an expression recommended by Brown and Srawley in the ASTM Special Technical Publication No. 410

Table 61 : STATIC FRACTURE TOUGHNESS DATA - CENTER CRACKED PANELS
($t = 0.625$", 2219-T87 Aluminum Base Metal, Long Grain)

| SPECIMEN NUMBER | THICKNESS ~ IN. | WIDTH ~ IN. | CRACK LENGTH ~ IN. | TEST TEMPERATURE ~ °F | TEST ENVIRONMENT | GROSS AREA FAILURE STRESS ~ KSI | $K^*_{CN}$ | TYPE FRACTURE |
|---|---|---|---|---|---|---|---|---|
| ABCR-1 | .6275 | 16.00 | 8.00 | RT | Air | 15.1 | 63.2 | Mixed Mode |
| ABCN-1 | .6355 | 16.00 | 8.06 | -320°F | $LN_2$ | 13.1 | 55.1 | Flat |
| ABCH-1 | .6265 | 12.02 | 6.01 | -423°F | $LH_2$ | 15.6 | 56.6 | Flat |

* Calculated using an expression recommended by Brown and Srawley in the ASTM Special Technical Publication No. 410

Table 62 : STATIC FRACTURE TOUGHNESS DATA - CENTER CRACKED PANELS
(t = 0.125", 2219 Aluminum Weld Metal)

| SPECIMEN NUMBER | THICKNESS ~ IN. | WIDTH ~ IN. | CRACK LENGTH ** ~ IN. | TEST TEMPERATURE ~ °F | TEST ENVIRONMENT | GROSS AREA FAILURE STRESS - KSI | $K_{CN}^{*}$ | TYPE FRACTURE |
|---|---|---|---|---|---|---|---|---|
| AWCR-2 | .1240 | 36.00 | 18.10 | RT | Air | 11.06 | 69.9 | Full Shear |
| AWCN-2 | .1240 | 35.94 | 18.02 | -320°F | $LN_2$ | 11.23 | 70.6 | Mixed Mode |
| AWCH-2 | .1240 | 30.00 | 15.10 | -423°F | $LH_2$ | 10.67 | 61.6 | Mixed Mode |

* Calculated using an expression recommended by Brown and Srawley in the ASTM Special Technical Publication No. 410

** Flaws in Center of Weld

Table 63 : STATIC FRACTURE TOUGHNESS DATA - CENTER CRACKED PANELS
(t = 1.00", 2219 Aluminum Weld Metal)

| SPECIMEN NUMBER | THICKNESS ~ IN. | WIDTH ~ IN. | CRACK LENGTH ** ~ IN. | TEST TEMPERATURE ~ °F | TEST ENVIRONMENT | GROSS AREA FAILURE STRESS - KSI | $K_{CN}^{*}$ | TYPE FRACTURE |
|---|---|---|---|---|---|---|---|---|
| AWCR-1 | .9850 | 36.00 | 18.415 | RT | Air | 9.1 | 58.5 | Flat |
| AWCN-1 | 1.0075 | 36.03 | 18.270 | -320°F | $LN_2$ | 7.9 | 50.1 | Flat |
| AWCH-4 | 1.0083 | 12.01 | 6.190 | -423°F | $LH_2$ | 8.5 | 35.8 | Flat |

* Calculated using an expression recommended by Brown and Srawley in the ASTM Special Technical Publication No. 410

** Flaws in Center of Weld

Table 64: CYCLIC FRACTURE DATA, 0.20 Inch Thick, 5Al-2.5 Sn Titanium Base Metal - Transverse Grain, a/2c = .40, Room Temperature

| SPECIMEN | | | TEST CONDITIONS | | | CYCLE TEST DATA | | | | | |
|---|---|---|---|---|---|---|---|---|---|---|---|
| Number | Thickness (in) (t) | Width (in) (w) | Temperature (°F) | Environment | Gross Section Stress (Ksi) ($\sigma_G$) | Initial Flaw Depth (in) $a_i$ | Initial Flaw Length (in) $2c_i$ | $(a/t)_i$ | $(a/2c)_i$ | Irwins Apparent $K_i$ (Ksi $\sqrt{in}$) | Cycles to Breakthrough |
| TBC08R-1 | 0.201 | 2.749 | RT | Air | 85.0 | 0.073 | 0.196 | 0.364 | 0.372 | 33.58 | 2337 |
| TBC10R-2 | 0.204 | 2.747 | RT | Air | 39.0 | 0.088 | 0.236 | 0.432 | 0.373 | 16.48 | 3000* |
| TBC10R-3 | 0.200 | 2.747 | RT | Air | 85.0 | 0.090 | 0.248 | 0.450 | 0.363 | 37.69 | 1546 |
| TBC10R-4 | 0.199 | 2.748 | RT | Air | 39.0 | 0.086 | 0.240 | 0.432 | 0.358 | 16.54 | 6000* |
| TBC12R-5 | 0.200 | 2.749 | RT | Air | 85.0 | 0.106 | 0.286 | 0.524 | 0.371 | 40.55 | 1130 |

* Specimens Marked and Failed after Indicated Number of Cycles.
Flaw Information after Indicated Number of Cycles Given Below:

| SPECIMEN | $\sigma_G$ | $a_f$ | $2c_f$ | $(a/t)_f$ | $(a/2c)_f$ | $K_f$ |
|---|---|---|---|---|---|---|
| TBC10R-2 | 39.0 | 0.095 | 0.255 | 0.466 | 0.373 | 17.13 |
| TBC10R-4 | 39.0 | 0.107 | 0.299 | 0.537 | 0.358 | 18.46 |

NOTE: All Specimens from Heat 303268.

Table 65: CYCLIC FRACTURE DATA, 0.20 Inch Thick, 5Al-2.5 Sn Titanium Base Metal - Transverse Grain, a/2c = .40, -320°F

| SPECIMEN | | | TEST CONDITIONS | | | CYCLE TEST DATA | | | | | |
|---|---|---|---|---|---|---|---|---|---|---|---|
| Number | Thickness (in) (t) | Width (in) (w) | Temperature (°F) | Environment | Gross Section Stress (Ksi) ($\sigma_G$) | Initial Flaw Depth (in) $a_i$ | Initial Flaw Length (in) $2c_i$ | $(a/t)_i$ | $(a/2c)_i$ | Irwins Apparent $K_i$ (Ksi $\sqrt{in}$) | Cycles to Failure |
| TBC08N-1 | 0.203 | 2.747 | -320 | $LN_2$ | 108.0 | 0.075 | 0.205 | 0.370 | 0.366 | 43.06 | 1964 |
| TBC10N-2 | 0.196 | 2.748 | -320 | $LN_2$ | 66.0 | 0.086 | 0.237 | 0.439 | 0.363 | 27.89 | 3000* |
| TBC10N-3 | 0.202 | 2.746 | -320 | $LN_2$ | 66.0 | 0.091 | 0.242 | 0.451 | 0.376 | 28.29 | 4130 |
| TBC10N-4 | 0.200 | 2.747 | -320 | $LN_2$ | 108.0 | 0.090 | 0.243 | 0.450 | 0.370 | 46.94 | 756 |
| TBC12N-5 | 0.199 | 2.747 | -320 | $LN_2$ | 108.0 | 0.105 | 0.284 | 0.529 | 0.370 | 50.74 | 530 |

* Specimen Marked and Failed after Indicated Number of Cycles.
Flaw Information after Indicated Number of Cycles Given Below:

| SPECIMEN | $\sigma_G$ | $a_f$ | $2c_f$ | $(a/t)_f$ | $(a/2c)_f$ | $K_f$ |
|---|---|---|---|---|---|---|
| TBC10N-2 | 66.0 | 0.130 | 0.351 | 0.664 | 0.370 | 34.02 |
| | | | | | | |

NOTE: All Specimens from Heat 303268

Table 66: CYCLIC FRACTURE DATA, 0.20 Inch Thick, 5Al-2.5 Sn Titanium Base Metal - Transverse Grain, a/2c = .40, -423°F

| SPECIMEN | | | TEST CONDITIONS | | | CYCLE TEST DATA | | | | | |
|---|---|---|---|---|---|---|---|---|---|---|---|
| Number | Thickness (in) (t) | Width (in) (w) | Temperature (°F) | Environment | Gross Section Stress (Ksi) ($\sigma_G$) | Initial Flaw Depth (in) $a_i$ | Initial Flaw Length (in) $2c_i$ | $(a/t)_i$ | $(a/2c)_i$ | Irwins Apparent $K_i$ (Ksi $\sqrt{in}$) | Cycles to Failure |
| TBC08H-1 | 0.200 | 2.747 | -423 | $LH_2$ | 80.0 | 0.072 | 0.198 | 0.360 | 0.364 | 30.95 | 1688** |
| TBC10H-2 | 0.194 | 2.748 | -423 | $LH_2$ | 39.9 | 0.086 | 0.238 | 0.443 | 0.361 | 16.79 | 3000* |
| TBC10H-3 | 0.202 | 2.744 | -423 | $LH_2$ | 80.0 | 0.086 | 0.248 | 0.425 | 0.347 | 34.44 | 1188 |
| TBC10H-4 | 0.205 | 2.746 | -423 | $LH_2$ | 40.0 | 0.086 | 0.244 | 0.419 | 0.353 | 16.99 | 4500* |
| TBC12H-5 | 0.200 | 2.747 | -423 | $LH_2$ | 80.0 | 0.105 | 0.290 | 0.525 | 0.362 | 37.43 | 922 |

* Specimens Marked and Failed after Indicated Number of Cycles.
Flaw Information after Indicated Number of Cycles Given Below:
** Failed in Grip Holes.

| SPECIMEN | $\sigma_G$ | $a_f$ | $2c_f$ | $(a/t)_f$ | $(a/2c)_f$ | $K_f$ |
|---|---|---|---|---|---|---|
| TBC10H-2 | 39.9 | 0.093 | 0.250 | 0.479 | 0.372 | 17.27 |
| TBC10H-4 | 40.0 | 0.091 | 0.250 | 0.443 | 0.364 | 17.27 |
| TBC08H-1 | 80.0 | 0.130 | 0.310 | 0.649 | 0.493 | 39.40 |

NOTE: All Specimens from Heat 303268.

Table 67: CYCLIC FRACTURE DATA, 0.20 Inch Thick, 5Al-2.5 Sn Titanium Weld Metal, a/2c = .040, Room Temperature

| SPECIMEN | | | TEST CONDITIONS | | | CYCLE TEST DATA | | | | | |
|---|---|---|---|---|---|---|---|---|---|---|---|
| Number | Thickness (in) (t) | Width (in) (w) | Temperature (°F) | Environment | Gross Section Stress (Ksi) ($\sigma_G$) | Initial Flaw Depth (in) $a_i$ | Initial Flaw Length (in) $2c_i$ | $(a/t)_i$ | $(a/2c)_i$ | Irwins Apparent $K_i$ (Ksi $\sqrt{in}$) | Cycles to Breakthrough |
| TWC08-R1G | 0.234 | 2.749 | RT | Air | 85.0 | 0.071 | 0.196 | 0.304 | 0.362 | 33.55 | 2808 |
| TWC10-R2E | 0.229 | 2.747 | RT | Air | 39.0 | 0.089 | 0.245 | 0.389 | 0.363 | 16.75 | 2000* |
| TWC10-R3D | 0.230 | 2.748 | RT | Air | 85.0 | 0.087 | 0.233 | 0.378 | 0.373 | 36.67 | 2055 |
| TWC10-R4FA | 0.222 | 2.747 | RT | Air | 39.0 | 0.087 | 0.236 | 0.392 | 0.369 | 16.46 | 1500* |
| TWC12-R5E | 0.233 | 2.750 | RT | Air | 85.0 | 0.104 | 0.281 | 0.446 | 0.370 | 40.24 | 1790 |

* Specimen Marked and Failed after Indicated Number of Cycles.
Flaw Information after Indicated Number of Cycles Given Below:

| SPECIMEN | $\sigma_G$ | $a_f$ | $2c_f$ | $(a/t)_f$ | $(a/2c)_f$ | $K_f$ |
|---|---|---|---|---|---|---|
| TWC10-R2E | 39.0 | 0.096 | 0.251 | 0.419 | 0.383 | 17.04 |
| TWC10-R4FA | 39.0 | 0.095 | 0.256 | 0.428 | 0.371 | 17.16 |

NOTE: All Specimens from Heat 7909.

Table 68: CYCLIC FRACTURE DATA,
0.20 Inch Thick, 5Al-2.5 Sn Titanium Weld Metal,
$a/2c = .40$, -320°F

| SPECIMEN | | | TEST CONDITIONS | | | CYCLE TEST DATA | | | | | |
|---|---|---|---|---|---|---|---|---|---|---|---|
| Number | Thickness (in) (t) | Width (in) (w) | Temperature (°F) | Environment | Gross Section Stress (Ksi) ($\sigma_G$) | Initial Flaw Depth (in) $a_i$ | Initial Flaw Length (in) $2c_i$ | $(a/t)_i$ | $(a/2c)_i$ | Irwins Apparent $K_i$ (Ksi $\sqrt{in}$) | Cycles to Failure |
| TWC08N-1 | 0.227 | 2.747 | -320 | $LN_2$ | 108.0 | 0.071 | 0.195 | 0.312 | 0.364 | 42.00 | 1004 |
| TWC10N-2 | 0.232 | 2.747 | -320 | $LN_2$ | 66.0 | 0.090 | 0.235 | 0.389 | 0.383 | 27.93 | 2700 |
| TWC10N-3 | 0.229 | 2.746 | -320 | $LN_2$ | 108.0 | 0.084 | 0.240 | 0.368 | 0.350 | 46.39 | 276 |
| TWC10N-4 | 0.232 | 2.748 | -320 | $LN_2$ | 66.0 | 0.090 | 0.235 | 0.389 | 0.383 | 27.04 | 2000* |
| TWC12N-5 | 0.231 | 2.747 | -320 | $LN_2$ | 108.0 | 0.104 | 0.205 | 0.450 | 0.366 | 50.71 | 573 |

* Specimen Marked and Failed after Indicated Number of Cycles.
Flaw Information after Indicated Number of Cycles Given Below.

| SPECIMEN | $\sigma_G$ | $a_f$ | $2c_f$ | $(a/t)_f$ | $(a/2c)_f$ | $K_f$ |
|---|---|---|---|---|---|---|
| TWC10N-4 | 66.0 | 0.120 | 0.294 | 0.518 | 0.408 | 31.40 |
| | | | | | | |

NOTE: All Specimens from Heat 7909.

Table 69: CYCLIC FRACTURE DATA,
0.20 Inch Thick, 5Al-2.5 Sn Titanium Weld Metal,
$a/2c = .40$, -423°F

| SPECIMEN | | | TEST CONDITIONS | | | CYCLE TEST DATA | | | | | |
|---|---|---|---|---|---|---|---|---|---|---|---|
| Number | Thickness (in) (t) | Width (in) (w) | Temperature (°F) | Environment | Gross Section Stress (ksi) ($\sigma_G$) | Initial Flaw Depth (in) $a_i$ | Initial Flaw Length (in) $2c_i$ | $(a/t)_i$ | $(a/2c)_i$ | Irwins Apparent $K_i$ (Ksi $\sqrt{in}$) | Cycles to Failure |
| TWC08H-1G | 0.222 | 2.747 | -423 | $LH_2$ | 80.0 | 0.072 | 0.199 | 0.324 | 0.362 | 31.00 | 1344** |
| TWC10H-2F | 0.226 | 2.746 | -423 | $LH_2$ | 40.0 | 0.086 | 0.240 | 0.380 | 0.358 | 16.89 | 2000* |
| TWC10H-3G | 0.226 | 2.747 | -423 | $LH_2$ | 80.0 | 0.087 | 0.234 | 0.385 | 0.372 | 33.71 | 521 |
| TWC10H-4G | 0.226 | 2.748 | -423 | $LH_2$ | 40.0 | 0.087 | 0.246 | 0.386 | 0.354 | 17.07 | 3500* |
| TWC12H-5G | 0.222 | 2.747 | -423 | $LH_2$ | 81.8 | 0.103 | 0.278 | 0.464 | 0.371 | 37.57 | 178 |

* Specimen Marked and Failed after Indicated Number of Cycles.
Flaw Information after Indicated Number of Cycles Given Below
** Last 20 Cycles were run at a Stress of 81.0 KSI.

| SPECIMEN | $\sigma_G$ | $a_f$ | $2c_f$ | $(a/t)_f$ | $(a/2c)_f$ | $K_f$ |
|---|---|---|---|---|---|---|
| TWC10H-2F | 40.0 | 0.095 | 0.244 | 0.420 | 0.389 | 17.18 |
| TWC10H-4G | 40.0 | 0.096 | 0.251 | 0.426 | 0.383 | 17.39 |

Table 70: CYCLIC FRACTURE DATA,
0.020 Inch Thick, 5Al-2.5 Sn Titanium Base Metal -
Transverse Grain, a/2c = .05, Room Temperature

| SPECIMEN | | | TEST CONDITIONS | | | CYCLE TEST DATA | | | | | |
|---|---|---|---|---|---|---|---|---|---|---|---|
| Number | Thickness (in) (t) | Width (in) (w) | Temperature (°F) | Environment | Gross Section Stress (Ksi) ($\sigma_G$) | Initial Flaw Depth (in) $a_i$ | Initial Flaw Length (in) $2c_i$ | $(a/t)_i$ | $(a/2c)_i$ | Irwins Apparent $K_i$ (Ksi $\sqrt{in}$) | Cycles to Breakthrough |
| TBCR-1 | .020 | 4.002 | RT | Air | 83.3 | 0.011 | 0.202 | 0.564 | 0.055 | 17.90 | 325 |
| TBCR-2 | .019 | 4.000 | RT | Air | 83.3 | 0.013 | 0.220 | 0.703 | 0.059 | 19.41 | 267 |
| TBCR-3 | .019 | 4.000 | RT | Air | 83.3 | 0.012 | 0.212 | 0.632 | 0.057 | 18.67 | 445 |
| TBCR-4 | .020 | 4.000 | RT | Air | 83.3 | 0.014 | 0.208 | 0.707 | 0.067 | 20.03 | 168 |
| TBCR-5 | .020 | 4.002 | RT | Air | 83.3 | 0.015 | 0.200 | 0.758 | 0.075 | 20.61 | 175 |

Table 71: CYCLIC FRACTURE DATA,
0.020 Inch Thick, 5Al-2.5 Sn Titanium Base Metal -
Transverse Grain, a/2c = .05, -320°F

| SPECIMEN | | | TEST CONDITIONS | | | CYCLE TEST DATA | | | | | |
|---|---|---|---|---|---|---|---|---|---|---|---|
| Number | Thickness (in) (t) | Width (in) (w) | Temperature (°F) | Environment | Gross Section Stress (Ksi) ($\sigma_G$) | Initial Flaw Depth (in) $a_i$ | Initial Flaw Length (in) $2c_i$ | $(a/t)_i$ | $(a/2c)_i$ | Irwins Apparent $K_i$ (Ksi $\sqrt{in}$) | Cycles to Breakthrough |
| TBCN-1 | 0.019 | 4.000 | -320 | $LN_2$ | 128.3 | 0.014 | 0.226 | 0.722 | 0.062 | 30.83 | 23 |
| TBCN-2 | 0.019 | 3.999 | -320 | $LN_2$ | 128.3 | 0.012 | 0.224 | 0.628 | 0.054 | 28.70 | 49 |
| TBCN-3 | 0.019 | 4.000 | -320 | $LN_2$ | 128.3 | 0.015 | 0.224 | 0.790 | 0.067 | 31.81 | 12 |
| TBCN-4 | 0.020 | 4.002 | -320 | $LN_2$ | 128.3 | 0.017 | 0.206 | 0.872 | 0.083 | 33.45 | 10 |
| TBCN-5 | 0.020 | 3.999 | -320 | $LN_2$ | 128.3 | 0.014 | 0.222 | 0.700 | 0.063 | 30.83 | 46 |

Table 72: CYCLIC FRACTURE DATA,
0.020 Inch Thick, 5Al-2.5 Sn Titanium Base Metal -
Transverse Grain, a/2c = .05, -423°F

| SPECIMEN | | | TEST CONDITIONS | | | CYCLE TEST DATA | | | | | |
|---|---|---|---|---|---|---|---|---|---|---|---|
| Number | Thickness (in) (t) | Width (in) (w) | Temperature (°F) | Environment | Gross Section Stress (Ksi) ($\sigma_G$) | Initial Flaw Depth (in) $a_i$ | Initial Flaw Length (in) $2c_i$ | $(a/t)_i$ | $(a/2c)_i$ | Irwins Apparent $K_i$ (Ksi $\sqrt{in}$) | Cycles to Failure |
| TBCH-1 | 0.020 | 4.000 | -423 | $LH_2$ | 146.8 | 0.013 | 0.218 | 0.667 | 0.060 | 33.99 | 5 |
| TBCH-2 | 0.019 | 3.999 | -423 | $LH_2$ | 146.8 | 0.013 | 0.250 | 0.677 | 0.052 | 34.15 | 3 |
| TBCH-3 | 0.020 | 3.995 | -423 | $LH_2$ | 130.3 | 0.013 | 0.230 | 0.657 | 0.057 | 29.84 | 12 |
| TBCH-4 | 0.020 | 4.000 | -423 | $LH_2$ | 130.4 | 0.015 | 0.236 | 0.769 | 0.064 | 31.94 | 16 |
| TBCH-5 | 0.021 | 4.001 | -423 | $LH_2$ | 130.6 | 0.015 | 0.220 | 0.732 | 0.068 | 31.90 | 29 |

Table 73: CYCLIC FRACTURE DATA,
0.020 Inch Thick, 5Al-2.5 Sn Titanium Weld Metal,
a/2c = .05, Room Temperature

| SPECIMEN | | | TEST CONDITIONS | | | CYCLE TEST DATA | | | | | |
|---|---|---|---|---|---|---|---|---|---|---|---|
| Number | Thickness (in) (t) | Width (in) (w) | Temperature (°F) | Environment | Gross Section Stress (Ksi) ($\sigma_G$) | Initial Flaw Depth (in) $a_i$ | Initial Flaw Length (in) $2c_i$ | $(a/t)_i$ | $(a/2c)_i$ | Irwins Apparent $K_i$ (Ksi $\sqrt{in}$) | Cycles to Breakthrough |
| TWCR-19 | 0.019 | 4.015 | RT | Air | 83.3 | 0.012 | 0.206 | 0.635 | 0.058 | 18.71 | 100 |
| TWCR-20 | 0.020 | 4.016 | RT | Air | 81.8 | 0.014 | 0.228 | 0.707 | 0.061 | 19.76 | 59 |
| TWCR-21 | 0.020 | 4.008 | RT | Air | 81.8 | 0.014 | 0.206 | 0.686 | 0.068 | 19.67 | 59 |
| TWCR-22 | 0.019 | 4.008 | RT | Air | 81.0 | 0.011 | 0.202 | 0.567 | 0.055 | 17.39 | 141 |
| TWCR-25 | 0.020 | 4.007 | RT | Air | 81.8 | 0.010 | 0.200 | 0.495 | 0.050 | 16.81 | 241 |

Table 74: CYCLIC FRACTURE DATA,
0.020 Inch Thick, 5Al-2.5 Sn Titanium Weld Metal,
$a/2c = .05$, -320°F

| SPECIMEN | | | TEST CONDITIONS | | | CYCLE TEST DATA | | | | | |
|---|---|---|---|---|---|---|---|---|---|---|---|
| Number | Thickness (in) (t) | Width (in) (w) | Temperature (°F) | Environment | Gross Section Stress (Ksi) ($\sigma_G$) | Initial Flaw Depth (in) $a_i$ | Initial Flaw Length $2c_i$ | $(a/t)_i$ | $(a/2c)_i$ | Irwins Apparent $K_i$ (Ksi $\sqrt{in}$) | Cycles to Breakthrough |
| TWCN-26 | 0.020 | 4.017 | -320 | $LN_2$ | 130.6 | 0.013 | 0.198 | 0.667 | 0.066 | 30.27 | 10 |
| TWCN-27 | 0.020 | 4.022 | -320 | $LN_2$ | 130.6 | 0.012 | 0.212 | 0.606 | 0.057 | 29.26 | 45 |
| TWCN-29 | 0.019 | 4.007 | -320 | $LN_2$ | 130.6 | 0.012 | 0.206 | 0.625 | 0.058 | 29.23 | 10 |
| TWCN-30 | 0.020 | 4.006 | -320 | $LN_2$ | 130.6 | 0.012 | 0.202 | 0.603 | 0.059 | 29.21 | 23 |
| TWCN-37 | 0.020 | 4.023 | -320 | $LN_2$ | 130.6 | 0.014 | 0.200 | 0.701 | 0.070 | 31.32 | 53 |

Table 75: CYCLIC FRACTURE DATA,
0.020 Inch Thick, 5Al-2.5 Sn Titanium Weld Metal,
$a/2c = .05$, -423°F

| SPECIMEN | | | TEST CONDITIONS | | | CYCLE TEST DATA | | | | | |
|---|---|---|---|---|---|---|---|---|---|---|---|
| Number | Thickness (in) (t) | Width (in) (w) | Temperature (°F) | Environment | Gross Section Stress (Ksi) ($\sigma_G$) | Initial Flaw Depth (in) $a_i$ | Initial Flaw Length $2c_i$ | $(a/t)_i$ | $(a/2c)_i$ | Irwins Apparent $K_i$ (Ksi $\sqrt{in}$) | Cycles to Breakthrough |
| TWCH-31 | 0.020 | 4.007 | -423 | $LH_2$ | 130.6 | 0.010 | 0.188 | 0.500 | 0.053 | 26.31 | 82 |
| TWCH-32 | 0.017 | 4.007 | -423 | $LH_2$ | 130.7 | 0.010 | 0.184 | 0.575 | 0.054 | 26.32 | 37 |
| TWCH-33 | 0.020 | 4.006 | -423 | $LH_2$ | 130.5 | 0.010 | 0.208 | 0.510 | 0.048 | 26.36 | 25 |
| TWCH-34 | 0.020 | 4.011 | -423 | $LH_2$ | 130.7 | 0.014 | 0.210 | 0.686 | 0.067 | 30.90 | 12 |
| TWCH-35 | 0.020 | 4.009 | -423 | $LH_2$ | 130.6 | 0.012 | 0.202 | 0.612 | 0.059 | 28.72 | 17 |

Table 76: CYCLIC FRACTURE DATA,
0.625 Inch Thick, 2219-T87 Aluminum Base Metal -
Long Grain, a/2c = .40, Room Temperature

| SPECIMEN | | | TEST CONDITIONS | | | CYCLE TEST DATA | | | | | |
|---|---|---|---|---|---|---|---|---|---|---|---|
| Number | Thickness (in) (t) | Width (in) (w) | Temperature (°F) | Environment | Gross Section Stress (Ksi) ($\sigma_G$) | Initial Flaw Depth (in) $a_i$ | Initial Flaw Length (in) $2c_i$ | $(a/t)_i$ | $(a/2c)_i$ | Irwins Apparent $K_i$ (Ksi $\sqrt{in}$) | Cycles to Failure |
| ABC25R-1 | 0.645 | 6.743 | RT | Air | 36.0 | 0.230 | 0.569 | 0.357 | 0.404 | 24.16 | 2927 |
| ABC31R-2 | 0.627 | 6.743 | RT | Air | 31.0 | 0.286 | 0.724 | 0.456 | 0.395 | 23.30 | 3909 |
| ABC31R-3 | 0.638 | 6.742 | RT | Air | 41.0 | 0.278 | 0.740 | 0.436 | 0.376 | 31.44 | 1013 |
| ABC31R-4 | 0.636 | 6.744 | RT | Air | 36.0 | 0.282 | 0.743 | 0.443 | 0.380 | 27.49 | 2737 |
| ABC38R-5 | 0.643 | 6.744 | RT | Air | 36.0 | 0.350 | 0.875 | 0.545 | 0.400 | 29.95 | 798 |

Table 77: CYCLIC FRACTURE DATA,
0.625 Inch Thick, 2219-T87 Aluminum Base Metal -
Long Grain, a/2c = .40, -320°F

| SPECIMEN | | | TEST CONDITIONS | | | CYCLE TEST DATA | | | | | |
|---|---|---|---|---|---|---|---|---|---|---|---|
| Number | Thickness (in) (t) | Width (in) (w) | Temperature (°F) | Environment | Gross Section Stress (Ksi) ($\sigma_G$) | Initial Flaw Depth (in) $a_i$ | Initial Flaw Length (in) $2c_i$ | $(a/t)_i$ | $(a/2c)_i$ | Irwins Apparent $K_i$ (Ksi $\sqrt{in}$) | Cycles to Failure |
| ABC25N-1 | 0.642 | 6.740 | -320 | $LN_2$ | 43.0 | 0.232 | 0.577 | 0.361 | 0.402 | 29.05 | 1774 |
| ABC31N-2 | 0.624 | 6.748 | -320 | $LN_2$ | 48.0 | 0.311 | 0.769 | 0.499 | 0.404 | 37.66 | 585 |
| ABC31N-3 | 0.644 | 6.744 | -320 | $LN_2$ | 43.0 | 0.290 | 0.761 | 0.450 | 0.381 | 33.24 | 977 |
| ABC31N-4 | 0.642 | 6.736 | -320 | $LN_2$ | 38.0 | 0.276 | 0.742 | 0.430 | 0.372 | 28.79 | 1723 |
| ABC38N-5 | 0.630 | 6.743 | -320 | $LN_2$ | 43.0 | 0.345 | 0.882 | 0.547 | 0.391 | 35.85 | 925 |
| A-1 | 0.638 | 6.752 | -320 | $LN_2$ | 31.6 | 0.246 | 0.608 | 0.386 | 0.405 | 21.70 | 1000* |
| A-2 | 0.637 | 6.746 | -320 | $LN_2$ | 31.6 | 0.243 | 0.611 | 0.382 | 0.398 | 21.73 | 3000* |
| A-3 | 0.631 | 6.747 | -320 | $LN_2$ | 22.0 | 0.298 | 0.762 | 0.472 | 0.391 | 16.77 | 6000* |

* Specimens Marked and Failed after Indicated Number of Cycles.
Flaw Information after Indicated Number of Cycles Given Below.

| SPECIMEN | $\sigma_G$ | $a_f$ | $2c_f$ | $(a/t)_f$ | $(a/2c)_f$ | $K_f$ |
|---|---|---|---|---|---|---|
| A-1 | 31.6 | 0.263 | 0.644 | 0.412 | 0.408 | 22.35 |
| A-2 | 31.6 | 0.295 | 0.735 | 0.463 | 0.401 | 23.85 |
| A-3 | 22.0 | 0.345 | 0.878 | 0.547 | 0.393 | 18.01 |

Table 78: CYCLIC FRACTURE DATA, 0.625 Inch Thick, 2219-T87 Aluminum Base Metal - Long Grain, a/2c = .40, -423°F

| SPECIMEN | | | TEST CONDITIONS | | | CYCLE TEST DATA | | | | | |
|---|---|---|---|---|---|---|---|---|---|---|---|
| Number | Thickness (in) (t) | Width (in) (w) | Temperature (°F) | Environment | Gross Section Stress (Ksi) ($\sigma_G$) | Net Section Stress (Ksi) $a_i$ | $2c_i$ | $(a/t)_i$ | $(a/2c)_i$ | Irwins Apparent $K_f$ | Cycles to Failure |
| ABC25H-1 | 0.625 | 6.756 | -423 | $LH_2$ | 43.0 | 0.229 | 0.578 | 0.367 | 0.396 | 28.97 | 1373 |
| ABC31H-2 | 0.629 | 6.744 | -423 | $LH_2$ | 20.0 | 0.274 | 0.750 | 0.436 | 0.365 | 15.00 | 3000* |
| ABC31H-3 | 0.635 | 6.745 | -423 | $LH_2$ | 43.0 | 0.284 | 0.740 | 0.447 | 0.384 | 32.70 | 504 |
| ABC31H-4 | 0.646 | 6.676 | -423 | $LH_2$ | 30.0 | 0.296 | 0.760 | 0.458 | 0.389 | 22.91 | 2000* |
| ABC38H-5 | 0.631 | 6.747 | -423 | $LH_2$ | 43.0 | 0.342 | 0.875 | 0.542 | 0.391 | 35.61 | 315 |

* Specimens Marked and Failed after Indicated Number of Cycles. Flaw Information after Indicated Number of Cycles Given Below.

| SPECIMEN | $\sigma_G$ | $a_f$ | $2c_f$ | $(a/t)_f$ | $(a/2c)_f$ | $K_f$ |
|---|---|---|---|---|---|---|
| ABC31H-2 | 20.0 | 0.310 | 0.801 | 0.493 | 0.387 | 15.59 |
| ABC31H-4 | 30.0 | 0.360 | 0.930 | 0.558 | 0.387 | 25.33 |

Table 79: CYCLIC FRACTURE DATA, 0.063 Inch Thick, 2219-T87 Aluminum Base Metal - Long Grain, a/2c = .05, Room Temperature

| SPECIMEN | | | TEST CONDITIONS | | | CYCLE TEST DATA | | | | | |
|---|---|---|---|---|---|---|---|---|---|---|---|
| Number | Thickness (in) (t) | Width (in) (w) | Temperature (°F) | Environment | Gross Section Stress (Ksi) ($\sigma_G$) | Initial Flaw Depth (in) $a_i$ | Initial Flaw Length (in) $2c_i$ | $(a/t)_i$ | $(a/2c)_i$ | Irwins Apparent $K_i$ (Ksi $\sqrt{in}$) | Cycles to Breakthrough |
| ABC30R-1A | 0.067 | 6.748 | RT | Air | 42.0 | 0.031 | 0.553 | 0.462 | 0.056 | 15.94 | 370 |
| ABC39R-3 | 0.062 | 6.753 | RT | Air | 32.0 | 0.044 | 0.822 | 0.706 | 0.054 | 14.49 | 106 |
| ABC39R-2 | 0.066 | 6.749 | RT | Air | 42.0 | 0.038 | 0.800 | 0.579 | 0.048 | 16.81 | 241 |
| ABC39R-4 | 0.068 | 6.756 | RT | Air | 52.0 | 0.042 | 0.800 | 0.622 | 0.053 | 22.64 | 22 |
| ABC48R-5 | 0.061 | 6.750 | RT | Air | 42.0 | 0.046 | 0.967 | 0.758 | 0.048 | 19.52 | 8 |

Table 80: CYCLIC FRACTURE DATA, 0.063 Inch Thick, 2219-T87 Aluminum Base Metal - Long Grain, a/2c = .05, -320°F

| SPECIMEN | | | TEST CONDITIONS | | | CYCLE TEST DATA | | | | | |
|---|---|---|---|---|---|---|---|---|---|---|---|
| Number | Thickness (in) (t) | Width (in) (w) | Temperature (°F) | Environment | Gross Section Stress (Ksi) ($\sigma_G$) | Initial Flaw Depth (in) $a_i$ | Initial Flaw Length (in) $2c_i$ | $(a/t)_i$ | $(a/2c)_i$ | Irwins Apparent $K_i$ (Ksi $\sqrt{in}$) | Cycles to Breakthrough |
| ABC30N-1A | 0.068 | 6.748 | -320 | $LN_2$ | 51.0 | 0.038 | 0.610 | 0.559 | 0.062 | 20.40 | 205 |
| ABC39N-2 | 0.067 | 6.759 | -320 | $LN_2$ | 41.0 | 0.040 | 0.747 | 0.595 | 0.053 | 21.04 | 23 |
| ABC39N-3 | 0.069 | 6.756 | -320 | $LN_2$ | 61.0 | 0.045 | 0.830 | 0.650 | 0.054 | 27.60 | 1 |
| ABC39N-3A | 0.065 | 6.755 | -320 | $LN_2$ | 51.0 | 0.040 | 0.795 | 0.614 | 0.050 | 16.51 | 63 |
| ABC48N-5 | 0.064 | 6.751 | -320 | $LN_2$ | 51.0 | 0.045 | 0.955 | 0.704 | 0.047 | 22.40 | 1 |
| ABC35N-1 | 0.063 | 6.755 | -320 | $LN_2$ | 51.0 | 0.037 | 0.690 | 0.589 | 0.054 | 20.00 | 50* |
| ABC38N-2 | 0.062 | 6.752 | -320 | $LN_2$ | 51.0 | 0.044 | 0.790 | 0.714 | 0.056 | 21.80 | 2* |

* Specimens Milled from 0.625 Inch Thick Plate.

Table 81: CYCLIC FRACTURE DATA, 0.100 Inch Thick, 2219-T87 Aluminum Base Metal - Long Grain, a/2c = .05, -320°F

| SPECIMEN | | | TEST CONDITIONS | | | CYCLE TEST DATA | | | | | |
|---|---|---|---|---|---|---|---|---|---|---|---|
| Number | Thickness (in) (t) | Width (in) (w) | Temperature (°F) | Environment | Gross Section Stress (Ksi) ($\sigma_G$) | Initial Flaw Depth (in) $a_i$ | Initial Flaw Length (in) $2c_i$ | $(a/t)_i$ | $(a/2c)_i$ | Irwins Apparent $K_i$ (Ksi $\sqrt{in}$) | Cycles to Breakthrough |
| ABC40N-1 | 0.101 | 6.755 | -320 | $LN_2$ | 51.0 | 0.040 | 0.855 | 0.398 | 0.047 | | 240 |
| ABC50N-2 | 0.100 | 6.754 | -320 | $LN_2$ | 51.0 | 0.050 | 1.040 | 0.501 | 0.048 | | 75 |
| ABC60N-3 | 1.101 | 6.757 | -320 | $LN_2$ | 51.0 | 0.058 | 1.240 | 0.574 | 0.047 | | 16 |
| ABC65N-6 | 0.100 | 6.754 | -320 | $LN_2$ | 51.0 | 0.066 | 1.420 | 0.657 | 0.047 | | 2 |
| ABC70N-4 | 0.100 | 6.758 | -320 | $LN_2$ | 51.0 | 0.070 | 1.420 | 0.700 | 0.049 | | 1 |
| ABC80N-5 | 0.100 | 6.760 | -320 | $LN_2$ | 51.0 | 0.075 | 1.560 | 0.700 | 0.048 | | 1 |

Table 82: CYCLIC FRACTURE DATA,
0.063 Inch Thick, 2219-T87 Aluminum Base Metal -
Long Grain, a/2c = .05, -423 °F

| SPECIMEN | | | TEST CONDITIONS | | | CYCLE TEST DATA | | | | | |
|---|---|---|---|---|---|---|---|---|---|---|---|
| Number | Thickness (in) (t) | Width (in) (w) | Temperature (°F) | Environment | Gross Section Stress (Ksi) ($\sigma_G$) | Initial Flaw Depth (in) $a_i$ | Initial Flaw Length (in) $2c_i$ | $(a/t)_i$ | $(a/2c)_i$ | Irwins Apparent $K_i$ (Ksi $\sqrt{in}$) | Cycles to Breakthrough |
| ABC30H-1 | 0.065 | 6.744 | -423 | $LH_2$ | 49.3 | 0.029 | 0.633 | 0.445 | 0.046 | 17.10 | 398 |
| ABC39H-2 | 0.068 | 6.757 | -423 | $LH_2$ | 40.0 | 0.043 | 0.805 | 0.631 | 0.053 | 16.51 | 162 |
| ABC39H-3 | 0.065 | 6.749 | -423 | $LH_2$ | 50.0 | 0.050 | 0.800 | 0.770 | 0.063 | 22.59 | 8 |
| ABC39H-4 | 0.067 | 6.750 | -423 | $LH_2$ | 55.0 | 0.045 | 0.795 | 0.676 | 0.057 | 23.96 | 5 |
| ABC48H-5 | 0.068 | 6.751 | -423 | $LH_2$ | 50.0 | 0.047 | 0.980 | 0.695 | 0.048 | 22.09 | 4 |

Table 83: CYCLIC FRACTURE DATA,
1.00 Inch Thick, 2219 Aluminum Weld Metal,
a/2c = .30, Room Temperature

| SPECIMEN | | | TEST CONDITIONS | | | CYCLE TEST DATA | | | | | |
|---|---|---|---|---|---|---|---|---|---|---|---|
| Number | Thickness (in) (t) | Width (in) (w) | Temperature (°F) | Environment | Gross Section Stress (Ksi) ($\sigma_G$) | Initial Flaw Depth (in) $a_i$ | Initial Flaw Length (in) $2c_i$ | $(a/t)_i$ | $(a/2c)_i$ | Irwins Apparent $K_i$ (Ksi $\sqrt{in}$) | Cycles to Breakthrough |
| AWC50R-1 | 1.003 | 16.005 | RT | Air | 16.0 | 0.510 | 1.630 | 0.509 | 0.313 | 17.84 | 846 |
| AWC65R-2 | 1.001 | 16.011 | RT | Air | 19.0 | 0.630 | 2.090 | 0.629 | 0.301 | 24.22 | 230 |
| AWC65R-3 | 0.999 | 16.007 | RT | Air | 13.0 | 0.660 | 2.080 | 0.661 | 0.317 | 16.21 | 2095 |
| AWC65R-4 | 0.995 | 16.009 | RT | Air | 16.0 | 0.634 | 2.090 | 0.637 | 0.303 | 20.10 | 420 |
| AWC80R-5 | 0.997 | 16.008 | RT | Air | 16.0 | 0.765 | 2.565 | 0.767 | 0.298 | 22.21 | 203 |

Table 84: CYCLIC FRACTURE DATA,
1.00 Inch Thick, 2219 Aluminum Weld Metal,
a/2c = .30, -320 °F

| SPECIMEN | | | TEST CONDITIONS | | | CYCLE TEST DATA | | | | | |
|---|---|---|---|---|---|---|---|---|---|---|---|
| Number | Thickness (in) (t) | Width (in) (w) | Temperature (°F) | Environment | Gross Section Stress (Ksi) ($\sigma_G$) | Initial Flaw Depth (in) $a_i$ | Initial Flaw Length (in) $2c_i$ | $(a/t)_i$ | $(a/2c)_i$ | Irwins Apparent $K_i$ (Ksi $\sqrt{in}$) | Cycles to Breakthrough |
| AWC50N-1 | 0.988 | 16.007 | -320 | $LN_2$ | 21.0 | 0.500 | 1.615 | 0.506 | 0.310 | 23.39 | 416 |
| AWC65N-2 | 0.988 | 16.008 | -320 | $LN_2$ | 13.0 | 0.640 | 2.070 | 0.648 | 0.309 | 15.98 | 3206 |
| AWC65N-3 | 1.000 | 16.008 | -320 | $LN_2$ | 19.0 | 0.625 | 2.080 | 0.625 | 0.301 | 23.73 | 139 |
| AWC65N-4 | 0.991 | 16.012 | -320 | $LN_2$ | 22.0 | 0.652 | 2.075 | 0.658 | 0.314 | 27.95 | 21 |
| AWC80N-5 | 0.996 | 16.013 | -320 | $LN_2$ | 19.0 | 0.750 | 2.560 | 0.753 | 0.293 | 26.21 | 56 |

Table 85: CYCLIC FRACTURE DATA,
1.00 Inch Thick, 2219 Aluminum Weld Metal,
a/2c = .30, -423 °F

| SPECIMEN | | | TEST CONDITIONS | | | CYCLE TEST DATA | | | | | |
|---|---|---|---|---|---|---|---|---|---|---|---|
| Number | Thickness (in) (t) | Width (in) (w) | Temperature (°F) | Environment | Gross Section Stress (Ksi) ($\sigma_G$) | Initial Flaw Depth (in) $a_i$ | Initial Flaw Length (in) $2c_i$ | $(a/t)_i$ | $(a/2c)_i$ | Irwins Apparent $K_i$ (Ksi $\sqrt{in}$) | Cycles to Breakthrough |
| AWC50H-1 | 1.003 | 16.005 | -423 | $LH_2$ | 17.00 | 0.482 | 1.615 | 0.481 | 0.299 | 18.38 | 1195 |
| AWC65H-2 | 1.000 | 16.010 | -423 | $LH_2$ | 13.00 | 0.635 | 2.080 | 0.635 | 0.305 | 15.90 | 3089 |
| AWC65H-3 | 0.998 | 16.012 | -423 | $LH_2$ | 17.00 | 0.600 | 2.080 | 0.601 | 0.289 | 20.73 | 822 |
| AWC65H-4 | 1.001 | 16.008 | -423 | $LH_2$ | 20.00 | 0.645 | 2.080 | 0.644 | 0.310 | 24.86 | 148 |
| AWC80H-5 | 1.006 | 16.010 | -423 | $LH_2$ | 16.90 | 0.755 | 2.550 | 0.751 | 0.296 | 22.92 | 60 |

Table 86: CYCLIC FRACTURE DATA,
0.125 Inch Thick, 2219 Aluminum Weld Metal,
a/2c = .05, Room Temperature

| SPECIMEN | | | TEST CONDITIONS | | | CYCLE TEST DATA | | | | | |
|---|---|---|---|---|---|---|---|---|---|---|---|
| Number | Thickness (in) (t) | Width (in) (w) | Temperature (°F) | Environment | Gross Section Stress (Ksi) ($\sigma_G$) | Initial Flaw Depth (in) $a_i$ | Initial Flaw Length (in) $2c_i$ | $(a/t)_i$ | $(a/2c)_i$ | Irwins Apparent $K_i$ (Ksi $\sqrt{in}$) | Cycles to Breakthrough |
| AWC62R-1 | 0.121 | 11.985 | RT | Air | 17.0 | 0.066 | 1.285 | 0.544 | 0.051 | 8.79 | 545 |
| AWC81R-2 | 0.125 | 11.992 | RT | Air | 14.0 | 0.080 | 1.680 | 0.641 | 0.048 | 7.87 | 561 |
| AWC81R-3 | 0.126 | 11.998 | RT | Air | 17.0 | 0.090 | 1.689 | 0.714 | 0.053 | 10.25 | 217 |
| AWC81R-4 | 0.133 | 12.000 | RT | Air | 21.0 | 0.082 | 1.630 | 0.619 | 0.050 | 12.41 | 33 |
| AWC100R-5 | 0.121 | 11.999 | RT | Air | 17.0 | 0.091 | 2.060 | 0.752 | 0.044 | 10.35 | 92 |

Table 87: CYCLIC FRACTURE DATA,
0.125 Inch Thick, 2219 Aluminum Weld Metal,
a/2c = .05, -320 °F

| SPECIMEN | | | TEST CONDITIONS | | | CYCLE TEST DATA | | | | | |
|---|---|---|---|---|---|---|---|---|---|---|---|
| Number | Thickness (in) (t) | Width (in) (w) | Temperature (°F) | Environment | Gross Section Stress (Ksi) ($\sigma_G$) | Initial Flaw Depth (in) $a_i$ | Initial Flaw Length (in) $2c_i$ | $(a/t)_i$ | $(a/2c)_i$ | Irwins Apparent $K_i$ (Ksi $\sqrt{in}$) | Cycles to Breakthrough |
| AWC62N-1 | 0.119 | 11.810 | -320 | $LN_2$ | 20.0 | 0.056 | 1.275 | 0.473 | 0.044 | 9.55 | 637 |
| AWC81N-2 | 0.125 | 11.850 | -320 | $LN_2$ | 17.0 | 0.080 | 1.630 | 0.643 | 0.049 | 9.56 | 669 |
| AWC81N-3 | 0.125 | 12.000 | -320 | $LN_2$ | 20.0 | 0.071 | 1.643 | 0.570 | 0.043 | 10.75 | 1072 |
| AWC81N-4 | 0.124 | 11.910 | -320 | $LN_2$ | 25.0 | 0.077 | 1.645 | 0.624 | 0.047 | 14.34 | 12 |
| AWC100N-5 | 0.126 | 11.989 | -320 | $LN_2$ | 20.0 | 0.098 | 2.090 | 0.780 | 0.047 | 12.61 | 11 |

Table 88: CYCLIC FRACTURE DATA,
0.125 Inch Thick, 2219 Aluminum Weld Metal,
$a/2c = .05$, -423 °F

| SPECIMEN | | | TEST CONDITIONS | | | CYCLE TEST DATA | | | | | |
|---|---|---|---|---|---|---|---|---|---|---|---|
| Number | Thickness (in) (t) | Width (in) (w) | Temperature (°F) | Environment | Gross Section Stress (Ksi) ($\sigma_G$) | Initial Flaw Depth (in) $a_i$ | Initial Flaw Length (in) $2c_i$ | $(a/t)_i$ | $(a/2c)_i$ | Irwins Apparent $K_i$ (Ksi $\sqrt{in}$) | Cycles to Breakthrough |
| AWC62H-1 | 0.125 | 11.990 | -423 | $LH_2$ | 20.0 | 0.062 | 1.280 | 0.494 | 0.048 | 10.06 | 348 |
| AWC81H-2 | 0.125 | 11.996 | -423 | $LH_2$ | 17.1 | 0.093 | 1.630 | 0.746 | 0.057 | 10.29 | 156 |
| AWC81H-3 | 0.122 | 11.998 | -423 | $LH_2$ | 20.0 | 0.082 | 1.630 | 0.675 | 0.050 | 11.56 | 68 |
| AWC81H-4 | 0.122 | 11.990 | -423 | $LH_2$ | 25.0 | 0.087 | 1.680 | 0.713 | 0.052 | 15.30 | 15 |
| AWC100H-5 | 0.123 | 11.988 | -423 | $LH_2$ | 20.0 | 0.098 | 1.980 | 0.797 | 0.050 | 12.65 | 47 |

DISTRIBUTION LIST FOR FINAL REPORT NASA CR-72606

CONTRACT NAS3-10290

INVESTIGATION OF DEEP FLAWS IN THIN WALL TANKS

The Boeing Company
Seattle, Washington

| Report Copies R | D | Recipient | Designee |
|---|---|---|---|
| | | National Aeronautics & Space Administration<br>Lewis Research Center<br>21000 Brookpark Road<br>Cleveland, Ohio 44135 | |
| 1 | | Attn: Contracting Officer, MS 500-313 | |
| 5 | | Liquid Rocket Technology Branch, MS 500-209 | |
| 1 | | Technical Report Control Office, MS 5-5 | |
| 1 | | Technology Utilization Office, MS 3-16 | |
| 2 | | AFSC Liaison Office, MS 4-1 | |
| 2 | | Library | |
| 1 | | Office of Reliability & Quality Assurance, MS 500-111 | |
| 1 | | D. L. Nored, Chief, LRTB, MS 500-209 | |
| 3 | | G. T. Smith | Project Manager, MS 500-209 |
| 1 | | W. F. Brown, MS 105-1 | |
| 1 | | R. H. Kemp, MS 49-1 | |
| 1 | | J. E. Srawley, MS 105-1 | |
| 1 | | J. G. Kennard, MS 3-14 | |
| 1 | | G. T. Smith, MS 500-209 | |
| 2 | | Chief, Liquid Experimental Engineering, RPX<br>Office of Advanced Research & Technology<br>NASA Headquarters<br>Washington, D.C. 20546 | |
| 2 | | Chief, Liquid Propulsion Technology, RPL<br>Office of Advanced Research & Technology<br>NASA Headquarters<br>Washington, D.C. 20546 | |
| 1 | | Director, Launch Vehicles & Propulsion, SV<br>Office of Space Science & Applications<br>NASA Headquarters<br>Washington, D.C. 20546 | |

| Report Copies R D | Recipient | Designee |
|---|---|---|
| 1 | Chief, Environmental Factors & Herodynamics<br>Code RV-1<br>Office of Advanced Research & Technology<br>NASA Headquarters<br>Washington, D.C. 20546 | |
| 1 | Chief, Space Vehicles Structures<br>Office of Advanced Research & Technology<br>NASA Headquarters<br>Washington, D.C. 20546 | |
| 1 | Director, Advanced Manned Missions, MT<br>Office of Manned Space Flight<br>NASA Headquarters<br>Washington, D.C. 20546 | |
| 6 | NASA Scientific & Technical Information Facility<br>P.O. Box 33<br>College Park, Maryland 20740 | |
| 1 | Director, Technology Utilization Division<br>Office of Technology Utilization<br>NASA Headquarters<br>Washington, D.C. 20546 | |
| 1 | National Aeronautics & Space Administration<br>Ames Research Center<br>Moffett Field, California 94035<br>Attn: Library | |
| 1 | National Aeronautics & Space Administration<br>Flight Research Center<br>P.O. Box 273<br>Edwards, California 93523<br>Attn: Library | |
| 1 | National Aeronautics & Space Administration<br>Goddard Space Flight Center<br>Greenbelt, Maryland 20771<br>Attn: Library | |

| Report Copies R | Report Copies D | Recipient | Designee |
|---|---|---|---|
| 1 | | National Aeronautics & Space Administration<br>John F. Kennedy Space Center<br>Cocoa Beach, Florida 32931<br>Attn: Library | |
| 1 | | National Aeronautics & Space Administration<br>Langley Research Center<br>Langley Station<br>Hampton, Virginia 23365<br>Attn: Library | |
| 1 | | National Aeronautics & Space Administration<br>Manned Spacecraft Center<br>Houston, Texas 77001<br>Attn: Library | |
| 1 | | National Aeronautics & Space Administration<br>George C. Marshall Space Flight Center<br>Huntsville, Alabama 35812<br>Attn: Library | |
| 1 | 1 | Jet Propulsion Laboratory<br>4800 Oak Grove Drive<br>Pasadena, California 91103<br>Attn: Library | R. Boundy |
| 1 | | Defense Documentation Center<br>Cameron Station<br>Building 5<br>5010 Duke Street<br>Alexandria, Virginia 22314<br>Attn: TISIA | |
| 1 | | Office of the Director of Defense<br>Research & Engineering<br>Washington, D.C. 20301<br>Attn: Office of Asst. Dir. (Chem. Technology) | |
| 1 | | RID (RINP)<br>Bolling Air Force Base<br>Washington, D.C. 20332 | |

| Report Copies R | D | Recipient | Designee |
|---|---|---|---|
| 1 | | Arnold Engineering Development Center<br>Air Force Systems Command<br>Tullahoma, Tennessee 37389<br>Attn: Library | |
| 1 | | Advanced Research Projects Agency<br>Washington, D.C. 20525<br>Attn: Library | |
| 1 | | Aeronautical Systems Division<br>Air Force Systems Command<br>Wright-Patterson Air Force Base,<br>Dayton, Ohio<br>Attn: Library | |
| 1 | | Air Force Missile Test Center<br>Patrick Air Force Base, Florida<br>Attn: Library | |
| 1 | | Air Force Systems Command<br>Andrews Air Force Base<br>Washington, D.C. 20332<br>Attn: Library | |
| 1 | | Air Force FTC (FTAT-2)<br>Edwards Air Force Base, California 93523<br>Attn: Library | |
| 1 | | Air Force Office of Scientific Research<br>Washington, D.C. 20333<br>Attn: Library | SREP, Dr. J.F. Mast |
| 1 | | Space & Missile Systems Organization<br>Air Force Unit Post Office<br>Los Angeles, California 90045 | |
| 1 | | U. S. Air Force<br>Washington, D.C.<br>Attn: Library | |

| Report Copies R | D | Recipient | Designee |
|---|---|---|---|
| 1 | | U. S. Army Missile Command<br>Redstone Scientific Information Center<br>Redstone Arsenal, Alabama 35808<br>Attn: Document Section | |
| 1 | | Bureau of Naval Weapons<br>Department of the Navy<br>Washington, D.C.<br>Attn: Library | |
| 1 | | Commander<br>U. S. Naval Weapons Center<br>China Lake, California 93557<br>Attn: Library | |
| 1 | 1 | Director (Code 6180)<br>U. S. Naval Research Laboratory<br>Washington, D.C. 20390<br>Attn: Library | J. M. Krafft |
| 1 | | Picatinny Arsenal<br>Dover, New Jersey 07801<br>Attn: Library | |
| 1 | | Aerojet-General Corporation<br>P.O. Box 296<br>Azusa, California 91703<br>Attn: Library | |
| 1 | | Aerojet-General Corporation<br>9200 East Flair Drive<br>El Monte, California 91734<br>Attn: Library | |
| 1 | | Aerojet-General Corporation<br>11711 South Woodruff Avenue<br>Downey, California 90241<br>Attn: Library | |
| 1 | 1 | Aerojet-General Corporation<br>P.O. Box 15847<br>Sacramento, California 95803<br>Attn: Technical Library 2484-2015A | C. E. Hartbower |

| Report Copies R | D | Recipient | Designee |
|---|---|---|---|
| 1 | | Aeronutronic Division of Philco Ford Corp.<br>Ford Road<br>Newport Beach, California 92663<br>Attn: Technical Information Department | |
| 1 | | Aerospace Corporation<br>2400 E. El Segundo Blvd.<br>Los Angeles, California 90045<br>Attn: Library-Documents | |
| 1 | | ARO, Incorporated<br>Arnold Engineering Development Center<br>Arnold AF Station, Tennessee 37389<br>Attn: Library | |
| 1 | | Battelle Memorial Institute<br>505 King Avenue<br>Columbus, Ohio 43201<br>Attn: Report Library, Room 6A | |
| 1 | | Beech Aircraft Corporation<br>Boulder Facility<br>Box 631<br>Boulder, Colorado<br>Attn: Library | |
| 1 | 1 | Bell Aerosystems, Inc.<br>Box 1<br>Buffalo, New York 14205<br>Attn: Library | T. Reinhardt |
| 1 | 1 | Boeing Company<br>Space Division<br>P.O. Box 868<br>Seattle, Washington 98124<br>Attn: Library | C. F. Tiffany |
| 1 | | Boeing Company<br>P.O. Box 1680<br>Huntsville, Alabama 35801 | |

| Report Copies R | D | Recipient | Designee |
|---|---|---|---|
| 1 | 1 | IIT Research Institute | C. K. Hersh |
| | 1 | Technology Center<br>Chicago, Illinois 60616<br>Attn: Library | K. E. Hofer |
| 1 | | Ling-Temco-Vought Corporation<br>P. O. Box 5907<br>Dallas, Texas 75222<br>Attn: Library | |
| 1 | | Lockheed Missiles and Space Company<br>P.O. Box 504<br>Sunnyvale, California 94087<br>Attn: Library | |
| 1 | | Lockheed-California Company<br>10445 Glen Oaks Blvd.,<br>Pacoima, California<br>Attn: Library | |
| 1 | | Lockheed Propulsion Company<br>P.O. Box 111<br>Redlands, California 92374<br>Attn: Library, Thackwell | |
| 1 | | Marquardt Corporation<br>16555 Saticoy Street<br>Box 2013 - South Annex<br>Van Nuys, California 91409 | |
| 1 | 1 | Martin-Marietta Corporation (Baltimore Division)<br>Baltimore, Maryland 21203<br>Attn: Library | J. Calathes |
| 1 | 1 | Denver Division | R. D. Keys |
| | 1 | Martin-Marietta Corporation<br>P.O. Box 179<br>Denver, Colorado 80201<br>Attn: Library | F. R. Schwartzberg |

| Report Copies R | D | Recipient | Designee |
|---|---|---|---|
| 1 | 1 | Chemical Propulsion Information Agency<br>Applied Physics Laboratory<br>8621 Georgia Avenue<br>Silver Spring, Maryland 20910 | T. Reedy |
| 1 | | Chrysler Corporation<br>Space Division<br>New Orleans, Louisiana<br>Attn: Librarian | |
| 1 | 1 | Syracuse University Research Institute<br>Department of Metalurgy<br>Syracuse, New York | V. Walss |
| 1 | | Curtiss-Wright Corporation<br>Wright Aeronautical Division<br>Attn: Library | |
| 1 | 1 | General Dynamics/Convair | W. Witzel |
| | 1 | P.O. Box 1128<br>San Diego, California 92112<br>Attn: Library | J. Christian |
| 1 | | Missiles and Space Systems Center<br>General Electric Company<br>Valley Forge Space Technology Center<br>P.O. Box 855<br>Philadelphia, Pa. 190101<br>Attn: Library | |
| 1 | | Grumman Aircraft Engineering Corporation<br>Bethpage, Long Island, New York<br>Attn: Library | |
| 1 | | Hercules Powder Company<br>Allegheny Ballistics Laboratory<br>P.O. Box 210<br>Cumberland, Maryland 21501<br>Attn: Library | |

| Report Copies R | D | Recipient | Designee |
|---|---|---|---|
| 1 | 1 | Western Division | R. Rawe |
| | 1 | McDonnell Douglas Aircraft Company, Inc.<br>3000 Ocean Park Blvd.<br>Santa Monica, California 90406<br>Attn: Library | B. V. Whiteson |
| 1 | | McDonnell Douglas Aircraft Corporation<br>P.O. Box 516<br>Lambert Field, Missouri 63166<br>Attn: Library | |
| 1 | | Rocketdyne Division<br>North American Rockwell Inc.<br>6633 Canoga Avenue<br>Canoga Park, California 9134<br>Attn: Library, Department 596-306 | |
| 1 | | Space & Information Systems Division<br>North American Rockwell<br>12214 Lakewood Blvd.<br>Downey, California<br>Attn: Library | |
| 1 | | Northrop Space Laboratories<br>3401 West Broadway<br>Hawthorne, California<br>Attn: Library | |
| 1 | | Purdue University<br>Lafayette, Indiana 47907<br>Attn: Library (Technical) | |
| 1 | | Rocket Research Corporation<br>Willow Road at 116th Street<br>Redmond, Washington 98052<br>Attn: Library | |
| 1 | | Stanford Research Institute<br>333 Ravenswood Avenue<br>Menlo Park, California 94025<br>Attn: Library | |

| Report Copies R | D | Recipient | Designee |
|---|---|---|---|
| 1 | | TRW Systems Inc.<br>1 Space Park<br>Redondo Beach, California 90278<br>Attn: STL Tech. Lib. Doc. Acquisitions | |
| 1 | | TRW Incorporated<br>23555 Euclid Avenue<br>Cleveland, Ohio 44117 | E.A. Steigerwald |
| 1 | | United Aircraft Corporation<br>United Technology Center<br>P.O. Box 358<br>Sunnyvale, California 94038<br>Attn: Library | |
| 1 | | Wright-Patterson Air Force Base, Ohio 45433<br>Attn: AFML (MAAE) | |
| 1 | | Wright-Patterson Air Force Base, Ohio 45433<br>Attn: AFML (MAAM) | |
| 1 | | Department of the Army<br>U.S. Army Material Command<br>Washington, D.C. 20315<br>Attn: AMCRD-RC | |
| 1 | | Commander<br>U.S. Naval Ordnance Laboratory<br>White Oak<br>Silver Spring, Maryland 20910<br>Attn: Library | |
| 1 | | Commanding Officer<br>U.S. Naval Weapons Laboratory<br>Dehlgren, Virginia 22448<br>Attn: Technical Library | |
| 1 | 1 | Colorado State University<br>Fort Collins, Colorado 80521<br>Attn: Library | F. W. Smith |

| Report Copies R | D | Recipient | Designee |
|---|---|---|---|
| 1 | 1 | Brown University<br>Providence, R. I. 02912<br>Attn: Library | J. R. Rice |
| 1 | | California Institute of Technology<br>1201 E. California Blvd.<br>Pasedena, California<br>Attn: Security Officer | |
| 1 | 1 | General Electric Company<br>Apollo Support Department<br>P.O. Box 2500<br>Daytona Beach, Florida 32015<br>Attn: Library | C. Day |
| 1 | 1 | Carnegie Institute of Technology<br>Department of Civil Engineering<br>Pittsburgh, Pennsylvania<br>Attn: Library | R. B. Anderson |
| 1 | 1 | Frankford Arsenal<br>Philadelphia, Pennsylvania 19137<br>Attn: 1320, Library | C. Carman |
| 1 | 1 | Cornell University<br>Department of Materials Science & Engineering<br>Ithaca, New York 14850<br>Attn: Library | H. H. Johnson |
| 1 | | Director<br>Special Projects Office<br>Department of the Navy<br>Washington, D.C. 20360 | |
| 1 | 1 | Sandia Corporation<br>P.O. Box 969<br>Livermore, California 94550<br>Attn: Technical Library | H. Lucas |
| 1 | 1 | Sandia Corporation | H. E. Montgomery |
| | 1 | Sandia Base | B. R. Allen |
| | 1 | Albuquerque, New Mexico<br>Attn: Library | W. Herrmann |

| Report Copies R | D | Recipient | Designee |
|---|---|---|---|
| 1 | 1 | Brunswick Corporation<br>Defense Products Division<br>P.O. Box 4594<br>43000 Industrial Avenue<br>Lincoln, Nebraska<br>Attn: Library | J. Carter |
| 1 | 1 | General Dynamics<br>P.O. Box 748<br>Fort Worth, Texas 76101<br>Attn: Library | D.E. Westerheide |
| 1 | 1 | Institution of Aerospace Studies<br>University of Toronto<br>Toronto 5, Ontario<br>Attn: Library | Dr. I.I. Glass |